MANCHESTER 1824
The University of Manchester

Essays on Option Implied Information

A thesis submitted to The University of Manchester for the degree of
Doctor of Philosophy
in the Faculty of Humanities

2022

Liangyi Mu

Alliance Manchester Business School

Accounting and Finance Division

Contents

This thesis contains 33,804 words including title page, tables, and footnotes.

Abstract

This thesis aims to understanding the option implied information, including political event risk, after-hours option trading, and Ross recovered probability. It consists of three essays.

The first essay shows that the option market can ex ante detect and quantify the effects of political event risk. Focussing on the 2016 UK referendum on EU membership, we find that the Risk-Neutral Distribution extracted from GBPUSD futures options whose expiry spans the referendum date becomes bimodal and the Implied Volatility curve exhibits an unusual W-shape. To the contrary, the corresponding effects for FTSE100 are found to be very limited. The large swings in expectations regarding the event outcome during the referendum night allow us to observe the counterfactual and validate the ex ante information revealed in the option market.

The second essay documents the trading characteristics of the option market in extended trading hours and explores the intraday intertemporal decisions of liquidity and informed traders. The option market exhibits low liquidity, low trading activities, high transaction costs, and a high probability of informed trading in extended trading hours. However, the introduction of extended trading hours enhances market quality by decreasing the quoted and effective bid-ask spreads in the following regular trading hours with decreased adverse selection costs. Moreover, option prices in extended trading hours are informative for the following regular trading hours in terms of index level and realized volatility.

The third essay presents the importance of an interest rate condition in Ross recovery. The term structure of interest rates explains the differences between approaches that follow the original Ross recovery theorem. A flat term structure of interest rates results in a Ross recovered probability distribution identical to the risk-neutral probability distribution in Ross recovery. After considering interest rates with a market example, empirical evidence still shows Ross recovered probabilities are close to the risk-neutral probabilities. We propose new estimation approaches to reflect the requirements in Ross recovery without imposing additional assumptions. Ross recovery with a short transition period implies a nonnegative matrix root for the transition matrix with a long transition period. Different least squares estimations are not equivalent when there is no unique and exact fitting with the market spot state prices. A sparse spot state price surface probably results in a relatively stable pricing kernel in Ross recovery. By taking into account the implicit requirements in Ross recovery, we propose a recovery estimation labeled Ross Power with a multi-period interest rate condition. This approach provides insights into the relationship among Ross recovered, generalized recovered, and risk-neutral probabilities.

Declaration of originality

I hereby confirm that no portion of the work referred to in the thesis has been submitted in support of an application for another degree or qualification of this or any other university or other institute of learning.

Copyright statement

i The author of this thesis (including any appendices and/or schedules to this thesis) owns certain copyright or related rights in it (the "Copyright") and s/he has given The University of Manchester certain rights to use such Copyright, including for administrative purposes.

ii Copies of this thesis, either in full or in extracts and whether in hard or electronic copy, may be made *only* in accordance with the Copyright, Designs and Patents Act 1988 (as amended) and regulations issued under it or, where appropriate, in accordance with licensing agreements which the University has from time to time. This page must form part of any such copies made.

iii The ownership of certain Copyright, patents, designs, trademarks and other intellectual property (the "Intellectual Property") and any reproductions of copyright works in the thesis, for example graphs and tables ("Reproductions"), which may be described in this thesis, may not be owned by the author and may be owned by third parties. Such Intellectual Property and Reproductions cannot and must not be made available for use without the prior written permission of the owner(s) of the relevant Intellectual Property and/or Reproductions.

iv Further information on the conditions under which disclosure, publication and commercialisation of this thesis, the Copyright and any Intellectual Property and/or Reproductions described in it may take place is available in the University IP Policy (see http://documents.manchester.ac.uk/DocuInfo.aspx?DocID=24420), in any relevant Thesis restriction declarations deposited in the University Library, The University Library's regulations (see http://www.library.manchester.ac.uk/about/regulations/) and in The University's policy on Presentation of Theses.

Acknowledgements

I would acknowledge all people who supported and accompanied me during my PhD study. First and foremost, I am deeply thankful to my supervisors Dr. Yoichi Otsubo and Prof. Alexandros Kostakis for their continuous advice. I am proud to be Yoichi's first PhD student. Without their encouragement and inspiration, it would be impossible for me to complete this thesis.

I would like to thank the faculty members of accounting and finance division at Alliance Manchester Business School for the great suggestions, Prof. Kevin Aretz, Prof. Michael Bowe, Prof. Ian Garrett, Prof. Hening Liu, Dr. Olga Kolokolova, Dr. Yifan Li, Dr. Stefan Petry, Dr. Alex Taylor, and other faculty members. I also thank the participants from many seminars, workshops, and conferences for valuable comments and suggestions for my thesis chapters.

Moreover, I would like to thank my PhD colleagues, Dr. Adnan Gazi, Dr. Xinyu Cui, Dr. Xiangshang Cai, Dr. Jiaxu Jin, Dr. Lavinia Rognone, Francisco Pinto Avalos, Samia Marium, Mohammad Dehghani, Yi Zhang, Yue Ye, Ruisheng Zhao, Tianshu Ma, Siqi Liu, Eghbal Rahimikia, Tiancheng Yu, Lijie Yu, Yiyuan Sun, Mengqian Chen, Jiayu Jin, Mo Hao, who together made my PhD study enjoyable.

I want to thank all support from my friends during the Covid-19 pandemic. My partner, Xinzhu Yu, took care of me when I had coronavirus. I simply couldn't have done this without you.

I would give my special thanks to my parents, Mr. Huoran Mu and Ms. Zhengmao Li, and other family members for their love and endless support. I want to thank my grandpa, Mr. Wende Mu, for inspiring me when I was little.

Chapter 1

Introduction

1.1. Background and motivation

Risk-neutral probability distributions, or Arrow Debreu prices, can be extracted from a cross-section of options and provide the present values for any future cash flows. It describes the market's expectations about future economy states considering both asset prices and risk preferences. Changes in risk-neutral probabilities reflect changes in the expected future asset prices and/or changes in the risk preferences. Since the breakthrough work of Breeden and Litzenberger (1978), both parametric and non-parametric risk-neutral estimation methods have been well developed in the literature (see Figlewski, 2018; Jackwerth, 2004 for an overview). Therefore, option implied risk-neutral probability distribution may be a useful tool to ex ante identify the impact of exogenous events such as the 2016 referendum on EU membership status of the UK.

Option implied information, including option implied volatility, option implied higher moments, and option implied risk-neutral probability distribution is usually risk-neutral estimated. Recovering risk-neutral probabilities to physical probabilities relies on the assumptions of the representative investor's utility function. Recent literature provides an alternative by considering non-parametric recovery methods. Ross (2015) proposes a recovery theorem trying to recover the physical probabilities and the risk preference at the same time solely based on a snapshot of the option price surface. However, Borovička, Hansen, and Scheinkman (2016) prove Ross recovered probabilities are long term risk-neutral probabilities instead of physical probabilities. A growing literature is still working on the understanding of Ross recovery theorem. Moreover, the option market is still under development as technology advances. The change in the structure of the option market provides a laboratory to examine whether market structure changes improve market quality. Segmented option markets are becoming a integrated nationwide option market in the US (Battalio, Hatch, and Jennings, 2004; Mayhew, 2002). Liquidity in the option market is improving by market structure changes, such as designated market maker (Anand and Weaver, 2006; Mayhew, 2002) and make-take structure (Anand, Hua, and McCormick, 2016). Therefore, it is interesting to examine how recent structure changes in the option market, such as the introduction of extended trading hours for S&P 500 options, affect market quality.

This thesis applies a variety of option implied information methods and analyzes the equity and currency option market with political risk, extended trading hours market quality, and Ross recovered probability.

1.2. Thesis Overview and Contributions

Political events exert a significant impact on financial markets. Turmoil in financial markets, including currencies, bonds, and stocks, caused by political uncertainty may hurt economic activity and increase political costs (Bernhard and Leblang, 2006). Electoral probability during political process impacts equity prices and interest rate (Fowler, 2006; Snowberg, Wolfers, and Zitzewitz, 2007). Political uncertainty is priced into the option market with a political risk premium (Kelly, Pástor, and Veronesi, 2016).

In 2016, the Leave outcome of the UK referendum on EU membership (Brexit referendum) surprised the financial markets. Before the Brexit referendum, the poll by YouGov indicates a marginal victory for a Remain outcome. However, GBPUSD and FTSE 100 dropped from previous day peak to the bottom after the referendum day as -12% and -8.7% with a result of a Leave outcome. In the first essay, we focus on Brexit referendum as there is much uncertainty before the referendum date. We extract non-parametric risk-neutral distribution (Figlewski, 2010), Implied Volatility skew (Xing, Zhang, and Zhao, 2010)/ slope (Kelly, Pástor, and Veronesi, 2016), and implied event probability (Borochin and Golec, 2016) from the option market. Empirical evidence from GBPUSD and FTSE 100 index options confirms option markets can ex ante detect the political event risk in the Brexit referendum and it can also distinguish the differential impacts on different assets.

This essay contributes to the literature on the option implied information and political event risk. The option market ex ante detects and quantifies the political event impacts across financial markets. Risk-neutral distributions spanning the Brexit referendum from the GBPUSD option market are bimodal, indicating a precise high political risk in GBPUSD market. While risk-neutral distributions from the FTSE100 are unimodal, indicating limited political risk in the equity market, ex ante estimations from the option market are consistent with the outcome after the Brexit referendum.

In 2015, CBOE introduced extended trading hours into S&P 500 index options. In the second essay, we examine the market quality and price informativeness during the newly introduced extended trading hours in the option market. The market quality of the option market in the regular trading hours is enhanced after the introduction of extended trading hours with decreased quoted and effective bid-ask spreads and adverse selection costs. Option prices in extended trading hours update timely and are informative for the following regular trading hours in terms of index level and realized volatility.

This essay contributes to the literature on after-hours financial markets. Continuing the analysis of after-hours stock market (Barclay and Hendershott, 2003, 2004; Chen, Yu, and Zivot, 2012; Jiang, Likitapiwat, and Mcinish, 2012; Tsai, 2010) and futures market (Dungey, Fakhrutdinova, and Goodhart, 2009), we use the opportunity of introducing the extended trading hours option market as a quasi-experiment for market design, providing novel empirical evidence of enhanced market quality and informative option prices despite of extreme illiquidity in extended trading hours.

In the third essay, we intend to recover the option implied risk-neutral probability to Ross (2015) recovered probability with the term structure of interest rates. Following a similar non-parametric approach as Figlewski (2010), we extract the risk-neutral probability surface from a cross-section of option prices. Based on the Ross (2015) recovery theorem and the yield curve (Martin and Ross, 2019), we propose a precise approach for Ross recovery estimation which correctly reflects the term structure of interest rates in the recovered probability. Moreover, we present some empirical application difficulties in Ross recovery, including the selection of transition period and the density of the state price surface.

This essay contributes to the literature on the estimation method of Ross recovery and the understanding of Ross recovered probability. Previous Ross recovery empirical applications,

such as (Audrino, Huitema, and Ludwig, 2021; Jackwerth and Menner, 2020; Ross, 2015), omit an important interest rate condition. This essay links the term structure of interest rates and the Ross recovery estimation, providing an accurate estimation process for Ross recovery. This essay also contributes to the understanding of Ross recovered and risk-neutral probabilities. When the term structure of interest rates is flat, Ross recovered probability is the same as risk-neutral probability. Under a market term structure, Ross recovered probability is still close to risk-neutral probability, indicating little additional information from Ross recovery.

1.3. Thesis Structure

The thesis structure follows the format accepted by the Manchester Accounting and Finance Group, Alliance Manchester Business School. The chapters are incorporated into a format suitable for submission and publication in peer-reviewed academic journals. This thesis is structured around three essays containing original research in chapters 2, 3, and 4. The chapters are self-contained, i.e. each chapter has a separate literature review, answers unique and original questions, and employs distinct analysis with different data sets. Footnotes are independent and are numbered from the beginning of each chapter. The equations, tables, figures, page numbers, titles, and subtitles have a sequential order throughout the thesis.

The thesis continues as follows. Chapter 2 detects political event risk in the option market using the Brexit referendum as an example. Chapter 3 explores market quality and price informativeness around the introduction of extended trading hours in the option market. Chapter 4 brings some omitted conditions in previous literature for the empirical application of the Ross recovery theorem. Chapter 5 concludes.

References

Anand, A., Hua, J., and McCormick, T. (2016) Make-take structure and market quality: Evidence from the U.S. options markets. *Management Science* 62.11, pp. 3271–3290.

Anand, A. and Weaver, D. G. (2006) The value of the specialist: Empirical evidence from the CBOE. *Journal of Financial Markets* 9.2, pp. 100–118.

Audrino, F., Huitema, R., and Ludwig, M. (2021) An Empirical Implementation of the Ross Recovery Theorem as a Prediction Device. *Journal of Financial Econometrics* 19.2, pp. 291–312.

Barclay, M. J. and Hendershott, T. (2003) Price Discovery and Trading After Hours. *Review of Financial Studies* 16.4, pp. 1041–1073.

Barclay, M. J. and Hendershott, T. (2004) Liquidity Externalities and Adverse Selection: Evidence from Trading after Hours. *Journal of Finance* 59.2, pp. 681–710.

Battalio, R., Hatch, B., and Jennings, R. (2004) Toward a National Market System for U.S. Exchange–listed Equity Options. *Journal of Finance* 59.2, pp. 933–962.

Bernhard, W. and Leblang, D. (2006) *Democratic Processes and Financial Markets: Pricing Politics*. Cambridge University Press.

Borochin, P. and Golec, J. (2016) Using options to measure the full value-effect of an event: Application to Obamacare. *Journal of Financial Economics* 120.1, pp. 169–193.

Borovička, J., Hansen, L. P., and Scheinkman, J. A. (2016) Misspecified Recovery. *Journal of Finance* 71.6, pp. 2493–2544.

Breeden, D. T. and Litzenberger, R. H. (1978) Prices of State-Contingent Claims Implicit in Option Prices. *Journal of Business* 51.4, pp. 621–651.

Chen, C.-H., Yu, W.-C., and Zivot, E. (2012) Predicting stock volatility using after-hours information: Evidence from the NASDAQ actively traded stocks. *International Journal of Forecasting* 28.2, pp. 366–383.

Dungey, M., Fakhrutdinova, L., and Goodhart, C. (2009) After-hours trading in equity futures markets. *Journal of Futures Markets* 29.2, pp. 114–136.

Figlewski, S. (2010) Estimating the Implied Risk-Neutral Density for the US Market Portfolio. *Volatility and Time Series Econometrics*. Oxford: Oxford University Press.

Figlewski, S. (2018) Risk-Neutral Densities: A Review. *Annual Review of Financial Economics* 10.1, pp. 329–359.

Fowler, J. H. (2006) Elections and markets: The effect of partisanship, policy risk, and electoral margins on the economy. *Journal of Politics* 68.1, pp. 89–103.

Jackwerth, J. C. (2004) *Option-implied Risk-neutral Distributions and Risk Aversion*. Charlotteville: Research Foundation of AIMR.

Jackwerth, J. C. and Menner, M. (2020) Does the Ross recovery theorem work empirically? *Journal of Financial Economics* 137.3, pp. 723–739.

Jiang, C. X., Likitapiwat, T., and Mcinish, T. H. (2012) Information Content of Earnings Announcements: Evidence from After-Hours Trading. *Journal of Financial and Quantitative Analysis* 47.6, pp. 1303–1330.

Kelly, B., Pástor, Ľ., and Veronesi, P. (2016) The Price of Political Uncertainty: Theory and Evidence from the Option Market. *Journal of Finance* 71.5, pp. 2417–2480.

Martin, I. W. R. and Ross, S. A. (2019) Notes on the yield curve. *Journal of Financial Economics* 134.3, pp. 689–702.

Mayhew, S. (2002) Competition, Market Structure, and Bid-Ask Spreads in Stock Option Markets. *Journal of Finance* 57.2, pp. 931–958.

Ross, S. (2015) The Recovery Theorem. *Journal of Finance* 70.2, pp. 615–648.

Snowberg, E., Wolfers, J., and Zitzewitz, E. (2007) Partisan Impacts on the Economy: Evidence from Prediction Markets and Close Elections. *The Quarterly Journal of Economics* 122.2, pp. 807–829.

Tsai, I.-C. (2010) Order imbalances from after-hours trading. *Applied Financial Economics* 20.12, pp. 983–987.

Xing, Y., Zhang, X., and Zhao, R. (2010) What Does the Individual Option Volatility Smirk Tell Us About Future Equity Returns? *Journal of Financial and Quantitative Analysis* 45.3, pp. 641–662.

Chapter 2

Detecting Political Event Risk in the Option Market

2.1. Introduction

Political events can exert a significant impact on financial markets (see Bernhard and Leblang, 2006; Fowler, 2006; Snowberg, Wolfers, and Zitzewitz, 2007; Kelly, Pástor, and Veronesi, 2016). Hence, there is a growing interest in identifying the effects of electoral outcomes on asset prices and volatility. To the extent that an election or referendum outcome can lead to a dramatic shift in the macroeconomic environment, the institutional framework, or government policy, such a political process can give rise to *event risk*.[1] This type of risk naturally affects asset pricing, portfolio choice, and risk management practices.[2]

Equally importantly, *ex ante* identification and quantification of political event risk could affect voters' decision making. This is particularly true for a polarised event where, in the absence of an objective measure of the economic impact of its outcomes in real time, the opposite sides of the campaign typically make sharply contradictory predictions. Wolfers and Zitzewitz (2016, p. 3) argue that a "shortcoming of traditional [political] event studies is that they are retrospective: we usually learn about the expected effects of an event afterwards, but not in time to affect any policy or political decision involved". Our study addresses this shortcoming, showing how the option market can *ex ante* identify the existence and measure the effects of political event risk on asset prices and volatility.

We examine the referendum that took place in the United Kingdom (UK) on 23rd June 2016, asking the electorate whether the UK should remain a member of or leave the European Union (EU). Table 2.1 contains a chronology of the key political events leading to this referendum.

-Table 2.1 here-

This referendum provides an ideal laboratory to assess the ability of options to detect and quantify political event risk. It is a single upcoming event with two possible outcomes that may or may not have distinct effects across different assets. Moreover, the event date is fixed and publicly known well in advance, so its timing is strictly exogenous to the short-term fluctuations in asset prices just before the referendum. Hence, there is no uncertainty over whether and when this event will occur, but only with respect to the outcome and its impact. In fact, there was substantial disagreement between the opposite sides of the campaign with respect to the economic impact of a Leave outcome (henceforth also termed as "Brexit")[3], leading to contradictory predictions.[4]

[1]Following Liu, Longstaff, and Pan (2003) (p. 231), we define event risk as "the risk of a major event precipitating a sudden large shock to security prices and volatilities".

[2]There is a voluminous literature on the implications of event or "jump" risk. See, inter alia, the seminal contributions of Merton (1976), Jorion (1988), Bates (1996, 2000), Duffie, Pan, and Singleton (2000), and Liu, Longstaff, and Pan (2003). The implications of political event risk have recently attracted significant interest among practitioners (see, for example, Clark and Amen, 2017; Putnam et al., 2018; Baker, Gillberg, and Thomas, 2018).

[3]Technically, this referendum outcome did not constitute an immediate change in the EU membership status of the UK. Legally, it was a non-binding mandate from the electorate to the Government and Parliament to trigger the rather prolonged process of the UK leaving the EU, which involved a number of subsequent negotiation rounds, agreements, and ratifications. Nevertheless, at that time, a Leave vote outcome was perceived as a strong democratic mandate that would initiate this process, which is commonly referred to as "Brexit".

[4]Proponents of Brexit were reassuring that such an outcome would not have a significant adverse long-term

Uncertainty regarding the outcome of the referendum and the large swings in the outcome probabilities observed after voting ended render this event an ideal setup for identification purposes. Opinion polls indicated a marginal result in the run up to the referendum. However, following the assassination of the Member of Parliament (MP) Jo Cox on 16th June 2016, a Remain victory was anticipated by the media and the betting market. This anticipation was reinforced as soon as voting ended. Nevertheless, the first official results revealed that the Leave vote performed more strongly than expected. A similar trend was observed throughout the night, albeit with geographical variations, leading to a "surprise" Leave victory with 51.9% of the vote. These large swings in expectations reveal the counterfactual and provide a unique opportunity to validate the ability of the option market to ex ante detect and quantify political event risk.

This "surprising" result was followed by sharp movements in asset prices. GBPUSD dropped from the peak of \$1.50 on the night of 23rd June to the trough of \$1.32 in the early morning of 24th June, i.e., a sharp fall of -12%. The FTSE100 Index opened with a drop of -8.7% relative to the previous day's close, but this drop was contained to -3.2% by the end of the trading day. Interestingly, FTSE100 actually rose by 2.6% and 6.1% by the end of June and July 2016, respectively. To the contrary, GBPUSD continued to trade consistently below \$1.35 until the end of July. Hence, whereas the Brexit outcome has been a major source of event risk for GBPUSD, this is not true for FTSE100, at least from the viewpoint of a domestic investor. Motivated by this observation, we examine not only whether the option market can detect and quantifiy political event risk when there is, but also whether it can signal the absence of significant event risk when there is not. In other words, we ask whether the option market can distinguish the potentially differential effects of the same political event across different assets.

Options are well suited to detect political event risk. First, option prices inherently embed forward-looking information (see Jackwerth, 2004, for an overview). Second, options come with different expiries, allowing us to isolate the effects of a political event on the underlying asset. Comparing the information embedded in options whose expiry spans the event with the corresponding information in similar options that expire before the event, we can identify the effects of the latter on the underlying asset. Third, options come with different strikes, enabling us to measure the counterfactual, even if this is not subsequently realized. The availability of option prices across a range of strikes can yield the entire Risk-Neutral Distribution (RND) of the underlying asset price (see Breeden and Litzenberger, 1978), providing information about the range of possible outcomes and their probabilities. In this study, we utilise options on GBPUSD futures traded at Chicago Mercantile Exchange (CME) and options on the FTSE100 Index traded at the Intercontinental Exchange (ICE) to extract the corresponding RNDs.[5] To this end, we follow the non-parametric methodology of Figlewski (2010), which allows us to

effect on the UK economy, other than a short-term increase in market volatility. To the contrary, the government's official position was that Brexit would have dramatic economic consequences, including a sharp fall in the sterling pound as well as a large drop in share and house prices, triggering an immediate recession (see Treasury, 2016).

[5]We focus on GBPUSD rather than GBPEUR because Brexit could also have a direct effect on the Eurozone economy, blurring the direction of impact of such an outcome on the latter exchange rate. Moreover, we focus on the FTSE100 Index, as there were no actively traded options on any other UK equity index.

flexibly recover the underlying RND without imposing strict parametric assumptions.

Our analysis yields a number of interesting results. First, we compare the RNDs extracted from GBPUSD options on the same trading day but with different expiries, revealing a dramatic shift in the RNDs for options with expiry spanning the referendum date. These RNDs are strongly negatively skewed and exhibit much larger dispersion, as compared to the relatively symmetric RNDs extracted from options that expire before the referendum. Hence, political event risk with respect to GBPUSD can be clearly detected well in advance of the event. To the contrary, this effect is much less pronounced when we compare the corresponding RNDs extracted from FTSE100 options.

Second, in the run up to the referendum, we uncover consistently bimodal GBPUSD RNDs. Their distinct modes correspond to the range of values that the option market assigns to GBPUSD in each of the two referendum outcomes. In particular, the left mode of these RNDs lies between \$1.31-\$1.35, but with substantial dispersion around it, revealing that the option market anticipates a large drop in GBPUSD in the event of a Leave outcome. In contrast, the right mode lies in the region of \$1.50-\$1.53, with much lower dispersion. As a result, GBPUSD RNDs signal that the full effect of Brexit (relative to a Remain outcome) lies in the approximate range of 15¢ -19¢ . On the other hand, the RNDs extracted from FTSE100 options remain clearly unimodal, featuring only a moderate increase in its negative skewenss.

Third, we find that the effect of political event risk is only temporary. In particular, the GBPUSD RND reverts to its usual, relatively symmetric, and unimodal shape immediately after the uncertainty regarding the outcome of the referendum is resolved. This finding confirms that the shift in the shape of the RND in the pre-event period can be entirely attributed to event risk.

We obtain similarly interesting results when we examine the corresponding Implied Volatility (IV) curves. In addition to an overall increase in volatility, we find that the IV curve becomes negatively sloped and concave for GBPUSD options with expiry spanning the referendum. In contrast, it features the typical (for currency options) convex and relatively symmetric smile when the expiry does not span this event. This unusual concave shape is another ex ante manifestation of event risk for the underlying asset. To the contrary, we find only a limited impact on the shape of the IV curve for FTSE100 options.

We also exploit the large swings in outcome probabilities during the referendum night. Using over-the-counter (OTC) options, we extract GBPUSD RNDs and their corresponding moments at the 10-minute frequency. This analysis reveals that the option market immediately incorporates information from actual voting results, as these high frequency RNDs reflect the continuously updated beliefs of market participants regarding the event outcome as well as the price and volatility of GBPUSD. In fact, comparing real-time option-implied information with the corresponding event probabilities implied by betting odds, we show that the Remain outcome is associated with a GBPUSD futures price around \$1.52 and a low volatility level (circa 15% p.a.), whereas the Leave outcome is associated with a futures price around \$1.34 and a high volatility level (circa 25% p.a.). These findings provide strong validation of the two modes appearing in the GBPUSD RNDs in the run up to the referendum and confirm the ability of the option market to quantify the effect of political event risk.

A number of prior studies have attempted to identify the impact of political event outcomes on asset prices. Most commonly, these studies estimate this impact by regressing changes in asset prices on changes in prediction market- or betting odds-implied probabilities during the pre-event period (see, inter Herron, 2000; Knight, 2007; Coulomb and Sangnier, 2014). However, such estimates may be affected by reverse causality or other omitted factors (see Snowberg, Wolfers, and Zitzewitz, 2007, for a critique).

To sidestep these issues, other studies have utilised short windows during which a sharp exogenous shock to the probability of the event outcome is observed (see, for example, Slemrod and Greimel, 1999; Snowberg, Wolfers, and Zitzewitz, 2007; Wolfers and Zitzewitz, 2016). These studies typically extrapolate the relationship estimated during this short window to assess the full impact of the political event outcome. Naturally, the validity of this approach depends on the possibility to identify a large political shock and the accuracy of this extrapolation. Wolfers and Zitzewitz (2018) discuss the limitations regarding the external validity of these event studies. In contrast, utilizing option-implied information allows us to ex ante identify political event risk without relying on the occurrence of large political shocks. This is because options come with different strikes, which allow us to measure the full impact of the counterfactual, even if this is not subsequently realized.

Only a few prior studies have examined the informational content of option prices for political events. Most notably, Leahy and Thomas (1996) report a multi-modal RND extracted from options on Canadian dollar futures prior to the 1995 Quebec sovereignty referendum. Gemmill and Saflekos (2000) examine the RNDs extracted from FTSE100 options around three UK parliamentary elections, providing mixed evidence and concluding that RNDs do not have much forecasting power with respect to post-election outcomes. However, both of these studies impose the ad hoc assumption that the RND is a mixture of three or two lognormal distributions, respectively, which may undermine parameter identification and stability. To the contrary, the non-parametric approach of Figlewski (2010) allows us to more accurately capture the true shape of the RND. In addition, Coutant, Jondeau, and Rockinger (2001), using a variety of methods, show that the RND extracted from interest rate futures options anticipated the 1997 French snap election a few days before its official announcement.

Our study is closely related to Hanke, Poulsen, and Weissensteiner (2018), who also utilise information from GBPUSD options prior to the Brexit referendum, but their focus is on exchange rate forecasting. Hanke, Poulsen, and Weissensteiner (2018) combine betting odds-implied event probabilities with a mixture of two lognormal densities estimated from option prices to extract a blended density. However, they utilise OTC option data with only 5 strikes, which naturally hinders them from fully recovering the true shape of the RND and the IV curve. In contrast, we use a much wider range of strikes from options traded at CME, which allow us to extract a bimodal RND for GBPUSD and to reveal a concave IV curve in the presence of event risk, relying *solely* on information embedded in option prices. Hence, we demonstrate the ability of the option market to ex ante detect and quantify the impact of political event risk without resorting to betting odds that may not be always available.

Ferreira, Gong, and Gozluklu (2022) also examine the Brexit referendum using information from opinion polls as well as from option and betting markets. Different from our study,

their focus is on risk-adjusting implied probabilities. They find that markets could have signalled more accurately the actual referendum result under the assumption of a risk-seeking representative agent and speculative trading triggered by this binary political event.

The rest of the study is organised as follows. Section 2.2 describes the data and methodologies employed to extract RNDs and option-implied event probabilities, respectively. Section 2.3 contains the main results of the study using daily options, whereas Section 2.4 illustrates the price discovery process during the referendum night. Section 2.5 extracts option-implied event probabilities, latent state prices and volatilities, Section 2.6 presents some further results, and Section 2.7 concludes.

2.2. Data and Methodology

2.2.1. Data

We use daily option data on the GBPUSD futures contract traded at CME. These are European-style options with traded quarterly expiries in March, June, September, and December plus two serial months. Their last trading day is on the second Friday prior to the third Wednesday of the expiry month and they are physically settled into futures. Each futures contract amounts to £ 62,500. Their trading hours are Sunday 5pm to Friday 4pm (Central Time, CT) with a 60-minute break each day beginning at 4pm (CT). Options are quoted in US$ per British pound increment, with a tick size of 0.0001 (i.e., $6.25). We use option data with expiries on 3rd June, 8th July, and 5th August 2016. Daily settlement option and futures prices are sourced from CME Datamine.

We also use daily option data on the FTSE100 Index traded at the ICE. These are European-style options and serial month expiries are traded for up to two years. Their last trading day is on the third Friday of the expiry month and they are cash settled. Their trading hours are from 8am to 4.50pm (London time). Since quarterly FTSE100 futures (March, June, September, December) expire on the same date as the options, the European-style FTSE100 option contract can be actually regarded as an option on the futures. For serial months, when the futures contract is not traded, we utilise the futures price implied by put-call parity. Options are quoted in index points, with a tick size of 0.5, and each contract is valued at £ 10 per index point. We use options with expiries on 17th June, 15th July, and 19th August 2016. The source of FTSE100 option data is Refinitiv DataScope.

We further utilise intraday GBPUSD option data around the referendum day. In particular, we source the implied volatility surfaces computed from over-the-counter (OTC) options and provided by Bloomberg. More specifically, Bloomberg provides the following information: $i)$ at-the-money implied volatility (σ_{ATM}), $ii)$ risk reversals for 10-delta $(\sigma_{RR10\Delta})$ and 25-delta $(\sigma_{RR25\Delta})$ options, and $iii)$ butterfly spreads for 10-delta $(\sigma_{BF10\Delta})$ and 25-delta $(\sigma_{BF25\Delta})$ options. Following Beber, Breedon, and Buraschi (2010), this information can be used to compute the following 5 implied volatilies in the delta space:

$$\sigma_{50\Delta Call} = \sigma_{ATM} \tag{2.1}$$

$$\sigma_{10\Delta Call} = \sigma_{ATM} + \sigma_{BF10\Delta} + (1/2)\sigma_{RR10\Delta} \tag{2.2}$$

$$\sigma_{10\Delta Put} = \sigma_{ATM} + \sigma_{BF10\Delta} - (1/2)\sigma_{RR10\Delta} \tag{2.3}$$

$$\sigma_{25\Delta Call} = \sigma_{ATM} + \sigma_{BF25\Delta} + (1/2)\sigma_{RR25\Delta} \tag{2.4}$$

$$\sigma_{25\Delta Put} = \sigma_{ATM} + \sigma_{BF25\Delta} - (1/2)\sigma_{RR25\Delta} \tag{2.5}$$

We focus on 1-month maturity options and we extract these implied volatilies at the 10-minute frequency on the 23rd and 24th June 2016. These implied volatilities are sourced from Bloomberg using the following conventions: $i)$ the underlying asset is the spot exchange rate (with USD as domestic and GBP as foreign currency), $ii)$ ATM strike is defined so as to ensure a delta-neutral straddle, $iii)$ forward deltas are used, without adjustment for the option premium. Forward rates are also sourced from Bloomberg.

In addition, we source the US$ risk-free rate from OptionMetrics and we interpolate using a cubic spline to match the horizon of option expiry. Moreover, we use LIBOR as proxy for the risk-free rate for FTSE100 options. This is sourced from Refinitiv DatasScope, and we interpolate again using a cubic spline to match the horizon of option expiry. We also use the probability of a Leave outcome implied by betting odds. The entire time series of this probability has been provided by Betfair, which is the largest Internet betting exchange.

2.2.2. Methodology

A. Extracting Risk-Neutral Distributions

We follow an approach similar to the non-parametric methodology proposed by Figlewski (2010) to extract RNDs from option prices. This approach involves a number of steps. First, we use daily settlement prices of OTM and ATM put and call options and convert them to IVs using Black (1976) formula. In-the-money options are typically thinly traded and their prices reflect their intrinsic value, so they are discarded. Moreover, we discard extremely deep OTM options. In particular, we discard GBPUSD options with price less than 0.001$ per British pound increment and FTSE100 options with price less than 1 index point.

Table 2.2 reports descriptive statistics for the options we use in our analysis after applying the above filters. We obtain a large number of OTM and ATM options that enable us to extract the corresponding RNDs. We should stress that we use settlement prices rather than traded prices. Settlement prices are thought to reflect the aggregate view of sophisticated market participants, so they are expected to be more informative than traded prices. For GBPUSD options, trading volume and open interest information from CME is not relevant, as currency option trading predominantly takes place OTC. On the other hand, FTSE100 options exhibit significant trading volume and open interest, which is reported in Table 2.2. Nevertheless, we still use settlement prices due to their superior informativeness.

-Table 2.2 here-

Second, we blend the IVs of puts and calls whose strike price X lies within 2% of the underlying futures price into a single point as follows: $IV_{blend}(X) = aIV_{put}(X) + (1 - a)IV_{call}(X)$, where $a = (X_{high} - X)/(X_{high} - X_{low})$. This practice avoids creating an artificial jump in the IV curve at the ATM region, which may arise from ATM puts potentially trading at higher IV relative to ATM calls.

In the third step, we interpolate across the computed implied volatilities, fitting a quintic spline using *spaps* in MATLAB. A quintic spline ensures that the third derivative of the IV curve (and option price function) is continuous, leading to a well-behaved RND. This step yields the smoothest IV curve in the strike space subject to an upper bound (tolerance level) for the sum of weighted squared errors between the computed and fitted IVs. In the spirit of Bliss and Panigirtzoglou (2002, 2004), the quintic spline minimizes the following objective function:

$$\rho \sum_{i=1}^{N} w_i \left[IV\left(X_i\right) - \widehat{IV}\left(X_i, \Theta\right) \right]^2 + \int_{-\infty}^{\infty} S^{(3)}(x;\Theta)^2 dx, \tag{2.6}$$

where w_i is the weight applied to the squared fitted implied volatility error of option i, $IV\left(X_i\right)$ is the computed implied volatility for strike X_i, $\widehat{IV}\left(X_i, \Theta\right)$ is the corresponding fitted implied volatility, which is a function of the parameters Θ that define the quintic spline $S(x;\Theta)$, and ρ is a smoothing parameter that is optimally selected to ensure that the sum of squared implied volatility errors does not exceed a given tolerance level.[6] We extract daily RNDs using equal weights and setting the tolerance level equal to $\sum_{i=1}^{N} \left(\widetilde{V}_i \text{ x } Tick \right)^2$, where $\widetilde{V}_i$ is the vega of option i and $Tick$ is the option tick size.[7]

The fourth step involves converting the smoothed IV curve back to call prices using again the Black formula. This yields a set of densely and equally spaced option prices. Fifth, using this set of prices, we can recover the RND function, $f(X)$, based on the standard result of Breeden and Litzenberger (1978). In particular, given call option prices for a continuum of strikes, the density function can be computed as:

$$f(X) = e^{rT} \frac{\partial^2 C}{\partial X^2}. \tag{2.7}$$

In the absence of a continuum of strikes, we approximate $f(X)$ using finite differences:

$$f(X_i) \approx e^{rT} \frac{C_{i+1} - 2C_i + C_{i-1}}{(\Delta X)^2}, \tag{2.8}$$

[6] In particular, parameter ρ controls the tradeoff between the goodness-of-fit and the smoothness of the spline function, with the latter captured by its integrated squared third derivative. Setting a low tolerance level ensures that the spline fits well the actual implied volatility points at the expense of smoothness. To the contrary, setting a high tolerance level yields a rather smooth spline that may not fit well all implied volatility points.

[7] We use this rather low tolerance level to ensure that the fitted implied volatilities do not considerably deviate from the actual ones. This choice of tolerance level implicitly acknowledges that the "true" option price may lie within one tick size from the observed one. Translated into volatility terms, this choice acknowledges that the "true" implied volatility may lie within the range of $\widetilde{V}_i$ x $Tick$ relative to the observed one.

whereas the cumulative density function, $F(X)$, is given by:

$$F\left(X_i\right) \approx e^{rT}\left[\frac{C_{i+1}-C_{i-1}}{X_{i+1}-X_{i-1}}\right]+1. \tag{2.9}$$

The previous steps yield the central part of the RND, from the second lowest to the second highest strikes. To complete the density, we need to append its tails. To this end, following Birru and Figlewski (2012), we utilise the Generalized Extreme Value (GEV) distribution and connect each of the right and left tails with the central part of the RND at two points (strikes). This distributional choice follows from the Fisher-Tippett Theorem stating that the GEV distribution is a natural candidate for modelling the tails of an unknown density.

The functional form of the GEV distribution is given by:

$$G(x)=\exp\left[-\left(1+\xi\left(\frac{x-\mu}{\sigma}\right)\right)^{-1/\xi}\right], \tag{2.10}$$

where ξ controls the tail shape, μ the location, and σ the scale of the distribution. The values of these three distributional parameters are selected for each tail separately to satisfy the following three constraints: $i)$ the total probability mass in the fitted tail must equal the missing tail probability, $ii)$ the density of the GEV tail must be equal to the central RND at the first connection point; and $iii)$ the density of the GEV tail must be equal to the central RND at the second connection point, which is further out in the tail. In particular, to append the right tail, the connection points we use are the highest strike of the central RND, which corresponds to the distribution percentile α_R, and the strike that is closest to the percentile $\alpha_R - 3\%$. For the left tail, we use the lowest strike of the central RND, which corresponds to the distribution percentile α_L, and the strike that is closest to the percentile $\alpha_L + 3\%$.

To extract RNDs from high frequency option data provided by Bloomberg, we adjust the above procedure as follows. Following Reiswich and Wystup (2010), we use the relationship below to convert the provided 5-point IV curve from the delta space to the strike space:

$$X_i = f e^{-\Phi N^{-1}\left(\Phi\Delta_i^f\right)\sigma\sqrt{\tau}+(1/2)\sigma^2\tau}, \tag{2.11}$$

where f is the forward rate, $\Phi = 1\ (-1)$ for a call (put) option, N^{-1} is the inverse of the normal cdf, and Δ_i^f is the forward delta of option i. Since we are equipped with the implied volatility-strike surface, we directly fit the smoothing spline as in the third step of the above procedure. However, here we set the tolerance level equal to zero, since there are only 5 IV points available. Moreover, in the fourth step, we convert implied volatilities to option prices using the Garman and Kohlhagen (1983) formula (see Reiswich and Wystup, 2010). The rest of the procedure remains the same.

B. Option-Implied Event Probabilities

We further utilise option prices to extract information regarding the ex ante probability for each of the two potential referendum outcomes as well as the corresponding latent GBPUSD futures price and volatility. To this end, we follow the methodology proposed by Borochin

and Golec (2016).[8]

In particular, the current GBPUSD futures price, F_0, can be regarded as a probability-weighted average of the price F_n, which would prevail in the event of a Remain outcome, and the corresponding price $F_n - V_e$, which would prevail in the event of a Leave outcome:

$$F_0 = p_e \left(F_n - V_e\right) + \left(1 - p_e\right) F_n = F_n - p_e V_e, \tag{2.12}$$

where p_e is the ex ante probability of a Leave outcome, and V_e denotes the full price effect due to a Leave outcome.[9] It should be noted that p_e is a risk-neutral probability. However, since we use a very short event window prior to the referendum, its evolution could be interpreted similarly to the evolution of the corresponding physical probability.

Similarly, the current price $O(X_i)$ of option i with strike X_i, whose expiry spans the referendum date, can be regarded as a probability-weighted average of the theoretical Black price $O^B(F_n, \sigma_n, X_i)$ that would prevail in the event of a Remain outcome and the corresponding price $O^B(F_n - V_e, \sigma_e, X_i)$ that would prevail in the event of a Leave outcome:

$$O(X_i) = p_e O^B(F_n - V_e, \sigma_e, X_i) + \left(1 - p_e\right) O^B(F_n, \sigma_n, X_i), \text{ for } i = 1, 2, ..., N, \tag{2.13}$$

where σ_e (σ_n) denotes the volatility in the event of a Leave (Remain) outcome. This relationship holds for both call and put options.

We can re-write equation (2.12) as:

$$p_e = \frac{F_n - F_0}{V_e}, \tag{2.14}$$

and substitute this expression into the system of equations in (2.13). The latter is an overidentified system of $N > 4$ equations that can be used to estimate the vector of 4 unknown parameters, $\theta = \{F_n, V_e, \sigma_e, \sigma_n\}$, and compute p_e. In particular, we estimate θ by minimising the following sum of squared errors:

$$SSE = \sum_{i=1}^{N} \left(O(X_i, \theta) - O^M(X_i)\right)^2, \tag{2.15}$$

where $O(X_i, \theta)$ is the option price for stike X_i determined by the parameter values in θ, as in equation (2.13), and $O^M(X_i)$ denotes the corresponding observable market price. We minimize this multivariate non-linear objective function using *lsqnonlin* in MATLAB.

We estimate the set of unknown parameters in θ and compute p_e on a daily basis in the run up to the referendum using daily settlement prices of CME options on GBPUSD futures that expire on 8th July 2016. Different from Borochin and Golec (2016), we utilise all available OTM and ATM calls and puts. Since this political event may cause a substantial movement in the underlying asset's price, it is helpful to utilise information from option prices across

[8]This approach is more restrictive than the one by Figlewski (2010) to extract RNDs, since it implicitly imposes the assumption of mixed lognormality. This is because option prices in each event outcome are assumed to be determined by the relevant Black-Scholes formula or the binomial model.

[9]We can ignore potential discounting effects because the time horizon of the event is quite short.

moneyness levels. We have also found that this approach yields more stable estimates than using only near-the-money options.

2.3. Main Results

2.3.1. Early Detection of Political Event Risk

Early detection that a political event may be the source of risk for the underlying asset can be provided by comparing the RND extracted from options whose expiry spans the event date with the corresponding RND from options whose expiry does not span this date. In particular, major shifts in the RNDs extracted on the same trading day for adjacent expiries can be attributed to a horizon effect and the event occurring between these two expiries. Figure 2.1 presents this comparison for options on GBPUSD futures (Panel A) and FTSE100 (Panel B). Figure 2.1 illustrates these RNDs computed on 17th May 2016 as a means of example to show that political event risk can be detected quite early, but very similar patterns are found on other trading days and they are available upon request.

-Figure 2.1 here-

Panel A shows that the RNDs extracted from options on GBPUSD futures expiring on 8th July and 5th August, i.e., after the referendum, are dramatically different from the corresponding RND computed from options with expiry on 3rd June, i.e., before the referendum.[10] In particular, the RNDs with a post-referendum expiry exhibit a mode shift to the right, much larger dispersion, and fatter tails. Equally importantly, the latter RNDs become strongly negatively skewed, whereas the RND from options with expiry not spanning the referendum is relatively symmetric. Most characteristically, the RNDs from options expiring after the referendum assign a non-negligible probability to GBPUSD futures values below \$1.34, even though these are essentially zero-probability values under the RND extracted from options expiring before the referendum. Interestingly, the shape of the RNDs from options with post-referendum expiries is very similar, and hence there seems to be no substantial horizon effect between them. In sum, this remarkable shift in the shape of RNDs from options whose expiry spans the referendum provides a clear indication that this political event is a major source of risk for GBPUSD futures.

Panel B illustrates the corresponding effect on the RNDs extracted from options on FTSE100. Here, the effect of political event risk is much less pronounced. The RND from options expiring before the referendum is already negatively skewed, as it is typically the case for equity index options, and it becomes more disperse and more negatively skewed for options expiring after the referendum. Hence, this political event increases the probability of large drops in FTSE100, but its effect is substantially less pronounced in comparison to the corresponding effect on the GBPUSD RND.

[10]The Kolmogorov-Smirnov test rejects the null hypothesis that the RND extracted from options expiring on 8th July is equal to the RND extracted from options expiring on 3rd June with a p-value$<$0.001. Similarly, it rejects the corresponding null hypothesis of equality between the RNDs extracted from options expiring on 5th August and 3rd June with a p-value$<$0.001.

Motivated by the previous evidence, it is interesting to see how political event risk is manifested in the IV curve. Figure 2.2 illustrates the corresponding IV curves for options on GBPUSD futures (Panels A&B) as well as for options on FTSE100 (Panels C&D). As with the above presented RNDs, these IV curves are computed on 17th May 2016 as a means of example, but very similar patterns are found on other trading days, which are available upon request. Panel A shows the IV curve for options expiring on 3rd June, i.e., before the referendum. This curve resembles an "IV smile", which is typically encountered for exchange rate options (see Hull, 2009, p. 391). This shape reveals that both OTM puts and OTM calls exhibit substantially higher implied volatility relative to ATM options. In fact, this pattern is reflected in the relatively symmetric RND extracted for this expiry, as illustrated in Panel A of Figure 2.1.

-Figure 2.2 here-

To the contrary, the IV curve becomes slightly concave when options expiring after the referendum are considered. In particular, Panel B of Figure 2.2 shows this concave IV curve for options on GBPUSD futures with expiry on 8th July.[11] Apart from the overall increase in the level of implied volatility relative to Panel A, this shape reflects two additional features. First, the implied volatility of OTM puts is substantially higher than the implied volatility of both ATM options and OTM calls, giving rise to a negatively sloped curve; this feature is reflected into a highly negatively skewed RND for this expiry, as illustrated in Panel A of Figure 2.1. Second, the rate by which the implied volatility of OTM puts drops as we approach the ATM region is rather slow, creating this concave shape. In other words, both deep OTM puts and nearer-the-money puts are relatively very expensive, reflecting the willingness of investors to pay a high price to be protected against a sharp drop in GBPUSD futures. This is another clear indication of event risk arising due to the forthcoming referendum.

Panel C illustrates the IV curve for options on FTSE100 expiring prior to the referendum (17th June). The shape of this curve resembles a "smirk" and it is typical for equity index options, with deep OTM puts being substantially more expensive than both ATM options and OTM calls (see Hull, 2009, p. 394). This typical IV curve is reflected into a moderately negatively skewed RND, as illustrated in Panel B of Figure 2.1. Panel D of Figure 2.2 illustrates the corresponding IV curve computed from options with expiry spanning the referendum (15th July). We report again a slightly convex "smirk", which is similar to the one presented in Panel C. Even though the level of implied volatility is overall higher for options expiring after the referendum, it seems that this event does not dramatically affect the shape of the IV curve.

2.3.2. Effects of Political Event Risk

The above analysis shows that political event risk can be detected quite early by examining the RND and IV curve of options with expiries spanning the event date. To identify more accurately the effects of political event risk, we now focus on RNDs and IV curves around

[11] Interestingly, Hull (2009, p. 400) shows that a concave IV curve can be a reflection of a bimodal RND for the underlying asset.

the referendum date from options with the same expiry. Specifically, Figure 2.3 illustrates the RNDs extracted from options on GBPUSD futures (Panel A) and FTSE100 (Panel B) on 23rd June at settlement, i.e., prior to the polls closing, as well as on 24th June, i.e., after the referendum result is known.

-Figure 2.3 here-

Panel A reveals the most striking effect of political event risk. The GBPUSD RND extracted on 23rd June clearly exhibits bimodality.[12] The shape of the RND essentially shows that the option market assigns a distinct range of GBPUSD futures values associated with each of the two referendum outcomes. The two distinct modes of the RND correspond to GBPUSD futures values of \$1.34 and \$1.53, respectively. Given that the underlying was trading around \$1.48 at CME option settlement on 23rd June, this is a clear indication that the option market was pricing a potential sharp drop in the exchange rate due to the referendum.

A related question is whether the effect of political event risk is permanent or temporary. If the effect of the political event is temporary, the RND and IV curve would revert to their standard shapes once the uncertainty surrounding this event is resolved; otherwise, if this political event causes a structural shift in the RND, this bimodal shape would persist. Panel A shows that the GBPUSD RND extracted on 24th June becomes unimodal and relatively symmetric, a shape similar to the one reported in Panel A of Figure 2.1 for options whose expiry does not span the referendum date. Since the RND reverts back to its standard shape immediately after the resolution of uncertainty surrounding the political event, we can conclude that the effect of the latter is only temporary.

Another interesting observation is that the GBPUSD RND extracted on 24th June exhibits its unique mode at \$1.38, providing ex post identification of the two modes observed in the bimodal RND extracted on 23rd June. The left mode (\$1.34) can be associated with a Leave outcome, whereas the right mode (\$1.53) can be associated with a Remain outcome. Moreover, the shift of the biggest RND mode from \$1.53 on 23rd June to \$1.38 on 24th June, which corresponds to a percentage decrease of -9.8%, provides an ex post justification for characterizing the referendum as a source of political event risk for GBPUSD.

Panel B presents the corresponding RNDs from options on FTSE100. We clearly observe unimodality in the RND extracted at settlement on 23rd June, so the option market does not assign a distinct mode to each of the two referendum outcomes. The effect of this political event on FTSE100 is manifested via a strongly negatively skewed RND. This effect is again found to be temporary, since the RND extracted on 24th June reverts back to its standard shape of a moderately negatively skewed distribution (see, e.g., Panel B of Figure 2.1). Moreover, the mode of the RND shifts from 6,621 on 23rd June to 6,382 on the following day, which corresponds to a drop of only -3.6%. This relatively smaller effect reveals that, in fact, the referendum did not pose a substantial event risk for FTSE100.

A plausible explanation for the absence of substantial event risk for FTSE100 lies with the geographic revenue exposure of its constituent stocks. In addition to the largest UK companies,

[12]The Hartigan and Hartigan (1985) test formally rejects the null of unimodality with a p-value$<$0.001.

this Index comprises a number of multinational companies which hold assets overseas and whose income is predominantly earned in foreign currency.[13] As a result, for "global" firms, the depreciation of sterling pound would actually increase in GBP terms the value of their overseas assets and income, and hence the value of their equity. This effect could offset the potentially sharp drop in equity values for "domestic" firms triggered by the adverse UK macroeconomic outlook due to a Leave victory.

Validating this conjecture, on the first trading day after the referendum, we indeed observe markedly heterogeneous share price reactions according to firms' geographic revenue exposure. To illustrate this heterogeneous response, CBOE's BATS constructed two UK indices based on the proportion of firms' domestic-to-total revenues.[14] On the one hand, Brexit High 50 Index, which comprises the 50 firms in the BATS UK 100 Index that derive the largest portion of their revenues from the UK market, experienced a sharp drop of -11.8% on 24th June. On the other hand, Brexit Low 50 Index, which comprises the 50 firms in the BATS UK 100 Index that derive the lowest portion of their revenues from the UK market, actually rose by 1.1% on the same day. Providing a characteristic example, the biggest FTSE100 winner was the Africa-based gold-mining company Randgold, whose share price rose by 14.2% on 24th June, whereas the biggest loser was the UK residential developer, Taylor Wimpey, whose share price dropped by -29.3%.

To examine further this heterogeneous effect, we extract the RNDs for four companies with substantially different geographic exposure. In particular, Figure SA.1 in the Supplementary Appendix illustrates the RNDs for AstraZeneca (AZN) and GlaxoSmithKline (GSK) around the referendum date. These two pharmaceutical companies are characteristic examples of "global" firms and they are constituents of the Brexit Low 50 Index. On the other hand, Figure SA.2 in the Supplementary Appendix illustrates the corresponding RNDs for British Telecom (BT) and Sainsbury's (SBRY), which are examples of "domestic" firms and they are constituents of the Brexit High 50 Index.[15]

Figure SA.1 confirms the absence of substantial event risk for AZN and GSK, as their RNDs are unimodal and only slightly negatively skewed prior to the referendum. Moreover, the shape of these RNDs remains very similar right after the referendum. In fact, their modes shift to the right, since the corresponding share prices actually rose on the 24th June.

To the contrary, one can detect the effect of the referendum on the RNDs of BT and SBRY presented in Figure SA.2. Most interestingly, we document a bimodal RND for BT on 23rd June, indicating that the option market priced a possible large drop in its share price. In fact, BT's share price decreased from 439.7p on 23rd June to 383.85p on 24th June due to the

[13] FTSE Russell characterises a company as "global" ("domestic") if its Global Sales Ratio is greater (lower) than 80% (20%). Using this criterion, they report that 60% of FTSE100 firms are predominantly global, whereas only 10% of FTSE100 firms are considered purely domestic. For more details, see https://hub.ipe.com/download?ac=76863.

[14] For more details, see http://www.cboe.com/resources/general/BatsBrexit5050-Product-Overview-1.pdf

[15] Option price data for these companies are sourced from Refinitiv DataScope. These are American-style options with expiry on 15th July, 2016. We extract RNDs following the non-parametric methodology of Figlewski (2010). Since these are American-style options, we convert option prices to implied volatilities using the Cox-Ross-Rubinstein binomial tree model via the MATLAB function *opstockbycrr*. Moreover, when fitting the IV curve via *spaps*, we have assigned a higher (lower) weight to observations with relatively high (low) open interest.

Leave outcome and its RND reverted back to a unimodal and slightly negatively skewed shape. Regarding SBRY, we find that event risk is manifested via a strongly negatively skewed RND on 23rd June. Again, its share price experienced a substantial drop on 24th June and its RND reverted to a much more symmetric shape.

Figure 2.4 illustrates the corresponding effects on the IV curves of GBPUSD and FTSE100. Panel A presents the IV curve for options on GBPUSD futures at settlement on 23rd June, revealing a rather unusual shape. The IV curve exhibits an overall negative slope, with OTM puts trading at substantially higher volatility relative to both ATM options and OTM calls. Implied volatility decreases as the strike increases but the rate of decrease varies at different strike regions. In fact, the IV curve switches from convex to concave and back to convex, with the first inflection point appearing around the $1.34 strike. This unusual W-shape reveals that the option market assigns relatively high prices for OTM puts with strikes between $1.34-$1.38. Actually, this feature is the underlying source of bimodality in the RND illustrated in Panel A of Figure 2.3.

-Figure 2.4 here-

Panel B of Figure 2.4 shows that the IV curve for options on GBPUSD futures reverts back to a standard "smile" on 24th June (see also Panel A of Figure 2.2). In other words, once the uncertainty surrounding this political event is resolved, the IV curve becomes again convex. This shape is consistent with the unimodal and relatively symmetric RND presented in Panel B of Figure 2.4. In addition, the overall level of implied volatility is now substantially lower.

Panels C and D of Figure 2.4 repeat this analysis for the FTSE100 IV curve. Panel C shows that, prior to the referendum, the IV curve exhibits a negative slope, with OTM puts trading at substantially higher implied volatility relative to both ATM options and OTM calls. This feature is consistent with the strongly negatively skewed RND presented in Panel B of Figure 2.3. There is also some evidence of local concavity in the IV curve, but this is much less clear relative to the corresponding patterns in the GBPUSD IV curve.

Panel D of Figure 2.4 shows that the shape of the FTSE100 IV curve is not dramatically different on 24th June. In particular, there is no substantial reduction in the level of volatility and the curve is still characterised by a negative slope. However, this slope now seems to be less steep, explaining why the corresponding RND on 24th June is less negatively skewed than the RND on the previous day (see Panel B of Figure 2.3). In sum, the IV curve seems to revert back to its standard shape (see Panel C of Figure 2.2), and hence we conclude that the effect due to the referendum is only temporary and much less pronounced.

2.3.3. Bimodality vs. Unimodality and Risk-Neutral Moments

One of the most striking effects of political event risk is the emergence of bimodality in the GBPUSD RND (see Panel A of Figure 2.3). We examine here how consistent this feature is in the run up to the referendum. Panels A and B of Figure 2.5 plot GBPUSD RNDs on various trading days prior to the referendum. We find that these RNDs exhibit clear bimodality already on 10th June, revealing that the option market is consistently pricing a possible large drop in

GBPUSD.[16] The left mode of these bimodal distributions lies between \$1.31-\$1.35, revealing the option market's anticipation of the exchange rate in the event of a Leave outcome. To the contrary, the right mode of the RND, which is associated with a Remain outcome, lies in the region of \$1.50-\$1.53. The distance between the two modes provides a rough approximation of the full impact of a Leave outcome (relative to Remain), which is 15¢ -19¢ .

-Figure 2.5 here-

On the other hand, Panels C and D of Figure 2.5 provide no evidence of bimodality in the FTSE100 RND prior to the referendum. The main effect of this event is manifested in terms of a fatter left tail. The consistent unimodality of FTSE100 RNDs in the run up to the referendum provides further evidence that the event risk for FTSE100 is much more limited relative to the corresponding event risk for GBPUSD.

Motivated by the above analysis, we further examine in more detail how this event risk and the subsequent resolution of uncertainty are reflected by the evolution of Risk-Neutral moments computed from the corresponding RND. Figure 2.6 presents the evolution of Risk-Neutral Volatility (RNV) from 9th May until 5th July.

-Figure 2.6 here-

Panel A of Figure 2.6 shows that the GBPUSD RNV computed from options whose expiry spans the referendum date is substantially higher relative to the RNV from options expiring before the referendum. In fact, the RNV computed from options expiring on 8th July is almost twice as high as the RNV from options expiring on 3rd June. We also observe an upward trend in RNV during the last three weeks before the referendum, which reaches a peak of 30.8% p.a. on 22nd June. In contrast, RNV is substantially reduced immediately after the referendum; the resolution of uncertainty surrounding this political event halves the RNV to 15.9% p.a. on 29th June. Panel B of Figure 2.6 illustrates the corresponding effects on FTSE100 RNV. Whereas the RNV computed from options expiring after the referendum is overall higher than the RNV from options expiring before the referendum, the effect is much less pronounced in this case.

Figure 2.7 presents the corresponding time-variation in Risk-Neutral Skewness (RNS). Panel A shows that the GBPUSD RNS computed from options expiring after the referendum is substantially more negative than the RNS for options expiring before the referendum. This difference arises due to the political event risk that is manifested as a fat left tail or, even more clearly, as a second left mode in the RND (see Panel A of Figures 2.1 and 2.3). RNS remains consistently negative in the run up to the referendum but sharply increases towards zero in the aftermath of this event, as the RND reverts to its standard, relatively symmetric shape for currency options (see Panel A of Figure 2.3).

-Figure 2.7 here-

[16] In all cases of visually bimodal RNDs, the Hartigan and Hartigan (1985) test formally rejects the null hypothesis of unimodality.

To the contrary, Panel B of Figure 2.7 shows that the FTSE100 RNS is not substantially different when comparing options expiring before and after the referendum. RNS takes substantially negative values throughout the period and across expiries, as it is common for equity index options, reflecting the RND shape in Panel B of Figure 2.1 and the IV smirk in Panels C and D of Figure 2.2. Moreover, we observe no notable upward trend in RNS right after the referendum.

We have identified bimodality in the GBPUSD RND as the primary manifestation of political event risk. To examine further this feature, we compute the following Bimodality Coefficient (BC) combining the skewness and kurtosis of a given RND:[17]

$$BC = \frac{Skewness^2 + 1}{Kurtosis}. \tag{2.16}$$

Panel A of Figure 2.8 presents the evolution of BC for GBPUSD RNDs. First, we find that the BC for RNDs from options whose expiry spans the referendum date is substantially higher than the one from options expiring before the referendum. Second, we observe an upward trend in the last week before the referendum. Third, BC values exhibit a sharp drop immediately after the referendum.

-Figure 2.8 here-

Panel B of Figure 2.8 presents the corresponding BC values for FTSE100 RNDs. The relatively high BC values reported here are due to the negative skewness featured by the unimodal FTSE100 RNDs (see Panel B of Figures 2.1 and 3). Interestingly, the BC values for RNDs extracted from options expiring on 15th July or 19th August are not substantially higher than the ones for options expiring before the referendum. We also observe an increase in BC in the days just before the referendum, reflecting the decrease in RNS that is observed in the corresponding RND (see Panel B of Figure 2.7). However, we find no dramatic decrease in BC in the aftermath of the referendum, as FTSE100 RNDs remain negatively skewed (see Panel B of Figure 2.3).

2.4. Price Discovery in the Option Market

Having documented the effects of political event risk on GBPUSD options in the previous Section, we examine here their manifestation during the announcement of the referendum results. This referendum provides a unique setup to capture these effects, offering a validation test for the option market expectations. This is because a complete reversal of the anticipated referendum outcome occurred during the vote counting process. In particular, an almost certain Remain victory right after the polls closed at 22:00 British Summer Time (BST) gave way to a Leave victory in the early hours of the following day.[18] Hence, this referendum provides a rare

[17] The value of this coefficient can be compared with the benchmark value of 0.555, which is the BC value of a uniform distribution. Higher values indicate bimodality, whereas lower values indicate unimodality. Nevertheless, it should be noted that high BC values can also result from heavily skewed unimodal distributions.

[18] All subsequent times are expressed in British Summer Time.

opportunity to observe the counterfactual using information from high frequency option prices. Table 2.3 outlines the key political events during the night of 23rd and the early morning of 24th June 2016.

-Table 2.3 here-

Figure 2.9 provides an overview of GBPUSD RNDs during the referendum night. First, it presents the RND extracted from CME options at 20:00 (settlement) on 23rd June. As mentioned above, this RND is bimodal, reflecting the effect of each of the two referendum outcomes. Second, Figure 2.9 illustrates the RND extracted from OTC options at 23:00. By that time, on the basis of opinion polls, it is widely anticipated that the Remain side has won, with leading figures of the Leave campaign conceding their defeat. As a result, the GBPUSD RND is clearly unimodal with a large concentration of probability mass around the mode at \$1.53. The RND is still negatively skewed, but the probability mass below \$1.35 is very low. Third, this Figure also illustrates the RND extracted at 05:30 on 24th June, when the final result is announced with a clear victory for the Leave side. The GBPUSD RND takes a strikingly different shape. The mode of the RND shifts to \$1.38, a reduction of 15¢ relative to the mode of the corresponding RND at 23:00. Moreover, the RND is now much more disperse, leptokurtic, and strongly negatively skewed with a substantial probability mass below \$1.33.

-Figure 2.9 here-

The availability of high frequency OTC option data allows us to examine more closely how GBPUSD RNDs respond to the announcement of the key results outlined in Table 2.3. In particular, Figure 2.10 presents twelve RNDs at different stages of the referendum night. Specifically, Panel A illustrates how the bimodal RND extracted from CME options at 20:00 (settlement) turns into a negatively skewed but unimodal RND by 22:30, when leading figures of the Leave side, including MEP Farage, concede defeat on the basis of private polls as well as the YouGov poll conducted on the same day.

-Figure 2.10 here-

Panel B shows the dramatic shifts in the RND as a response to unanticipated actual voting results. The surprisingly tight result from Newcastle at 23:59, an area expected to be won by the Remain side with a wide margin, causes a substantial shift of the RND to the left. In particular, the unimodal RND at 23:30, exhibiting a large concentration of probability mass around the mode at \$1.53, shifts to the left at 00:10, with a mode at \$1.47. By 01:00, a number of further results are announced and early indications of results from other areas are communicated by the media. On the one hand, the result from Sunderland confirms a clear pattern that Leave would perform very strongly in North England, whereas on the other hand, there are indications that Remain would gain a very large share of votes in London. As a result, even though the RND exhibits a mode at \$1.50 at 01:00, it becomes very disperse, reflecting the fact that the referendum result is a coin toss.

Panel C presents the corresponding RNDs at 02:00, 03:30, and 04:00, respectively, when actual results from across the country gradually indicate that Leave will most likely win, and

that the outperformance of Remain in London is not sufficient to offset the outperformance of Leave in other places. In fact, Panel C illustrates a gradual shift of the RNDs to the left. All RNDs are clearly unimodal and negatively skewed, with the mode shifting from \$1.47 at 02:00 to \$1.44 at 03:30, and \$1.41 at 04:00. This gradual shift reveals how the option market updates its beliefs regarding the referendum outcome.

Panel D illustrates the GBPUSD RND at 04:40, when it becomes certain that the Leave side will be victorious. The RND is clearly unimodal but quite disperse, with the mode shifted to \$1.39. To sum up, the mode of the RND shifts from \$1.53 at 23:30 (see Panel B) to \$1.39 at 04:40, i.e., a reduction of 14¢ in 5 hours, as the anticipation of a Remain victory gives way to the certainty of a Leave victory. The RND becomes less disperse at 05:30, and its mode is at \$1.38. Last but not least, it is interesting to observe that the option market continues reacting to events even after the announcement of the referendum result. Whereas PM Cameron announces at 08:22 that he will reisgn, the Bank of England Governor makes a public statement right after, to reassure the market that the central bank is ready to provide liquidity and take further policy actions to support the economy. Responding to this announcement, the RND extracted at 08:50 shifts to the right and becomes more symmetric, with its mode at \$1.42.

An alternative way to show how the option market responds to the events unfolding during the referendum night is to show the evolution of the GBPUSD futures price and RNV together with the probability of Leave victory implied from betting odds. Panel A of Figure 2.11 presents the evolution of the futures price (left axis) together with the odds-implied probability of Leave victory (right axis) from 22:00 on 23rd June until 05:50 on 24th June. The overall picture in Panel A is consistent with the sequence of events outlined in Table 2.3. When voting ends at 22:00, the probability of Leave victory is near 10%, whereas the GBPUSD futures is traded at around \$1.50. This near certainty of a Remain victory is questioned at midnight, leading to a sharp increase in the probability of Leave victory to more than 30% and a sharp drop in the futures price to \$1.45.

-Figure 2.11 here-

As the results come in favourably for Leave, the probability of its victory exceeds 50% at 02:00 for the first time and the futures contract trades at \$1.42. There is a temporary reversal of the upward trend for the probability of Leave victory around 02:30, when Remain gains a bigger than anticipated vote share in a London borough (Wandsworth). However, as it gradually becomes clear that the outperformance of Remain in London is not sufficient to offset the outperformance of Leave in other places, the probability of Leave victory continues its upward trend, with the latter becoming a certainty at around 04:40, when BBC calls the referendum for Leave. At the same time, the GBPUSD futures price continues its downward trend, trading at a low of \$1.33 at 05:20.

This sequence of events provides us the rare opportunity to observe the counterfactual and identify the impact of each of the referendum outcomes on GBPUSD futures. Specifically, we observe a sharp drop of 17¢ , from \$1.50 at 22:40 to \$1.33 at 05:20. Hence, Panel A of Figure 2.11 provides ex post validation of the two modes appearing in the bimodal GBPUSD RNDs

before the referendum (see Panels A & B of Figure 2.5), confirming the ability of the option market to ex ante identify the effects of political event risk.

Panel B of Figure 2.11 illustrates the evolution of GBPUSD RNV (left axis) together with the odds-implied probability of Leave victory (right axis). When Remain is almost certain to win at 22:00, RNV fluctuates around 15% p.a.. But as the probability of Leave victory begins its upward trend, especially after midnight, RNV follows in tandem. Specifically, when the probability of Leave victory stands at 63% at 02:10, RNV is equal to 23.5%. It actually reaches a peak of 32.5% p.a. at 04:10, when the probability of Leave victory exceeds 90% and a sharp drop in the futures price takes place. Interestingly, we also observe a de-escalation of RNV towards 25% p.a., once the uncertainty regarding the referendum outcome is resolved after 05:00 and the futures price is stabilised.

The evolution of RNV during the referendum night is consistent with the corresponding shapes and dispersion of the RNDs illustrated in Figure 2.10. Moreover, we can clearly identify two distinct states in RNV; a low state around 15% p.a. associated with a Remain victory and a high state around 25% p.a. associated with a Leave victory. In sum, high frequency option prices allow us to identify the effect of this political event not only with respect to the GBPUSD futures price but also with respect to its volatility.

2.5. Option-Implied Event Probability, State Price and Volatility

The analysis in Section 4 demonstrates that each of the referendum outcomes can be associated with a distinct state of GBPUSD futures price and volatility. Motivated by this evidence, in this Section we follow the approach suggested by Borochin and Golec (2016), as described in Section 2.2.2, to ex ante identify the option-implied GBPUSD futures price and volatility that would prevail in the case of a Remain or a Leave outcome, respectively. This approach also allows us to extract the corresponding option-implied probabilities with respect to the referendum outcome.

Figure 2.12 presents the option-implied probability, p_e, of Leave victory from 9th May until 23rd June, computed on a daily basis using CME options on GBPUSD futures. We also plot the time series of the corresponding probability implied by betting odds from Betfair. Overall, we observe that the two time series move in a similar direction in the run up to the referendum. In particular, we observe an upward trend in both the option-implied and the betting odds-implied probability of a Leave outcome during the week prior to the murder of the pro-Remain MP Jo Cox on 16th June. In the aftermath of this event, with official campaigning from both sides suspended, there is a sharp drop in both probabilities.

-Figure 2.12 here-

Furthermore, the option-implied probability series is quite volatile, showing that the outcome of this political event was very uncertain and that the option market continuously updated its beliefs as the events unfolded. Most interestingly, the option-implied probability of

Leave victory exceeds 50% on 15th and 16th June. Hence, despite the widespread belief among media and political circles that Remain would win, the option market indicates Leave victory as the most likely outcome one week before the referendum; the peak of the betting-odds probability series is 41.2% on 14th June. Even in the aftermath of the murder of MP Cox, the option-implied probability of a Leave outcome remains high and it is equal to 27.2% on the day of the referendum. To the contrary, the corresponding probability implied by Betfair odds is only 10.6%. In sum, this analysis shows that the option market is not only able to detect political event risk, but it can also quantify the probability of the event's outcome in an informative manner.[19]

Figure 2.13 illustrates the option-implied GBPUSD futures price (Panel A) and volatility (Panel B) estimates associated with each of the two referendum outcomes. These are again extracted on a daily basis from CME options from 9th May until 23rd June. In Panel A, we observe that the GBPUSD futures price associated with a Remain outcome, F_n, fluctuates around \$1.50 throughout the examined period, with \$1.52 prevailing at settlement on the referendum day.[20] This range of values is consistent with the right mode of the ex ante GBPUSD RNDs illustrated in Figures 2.3 and 2.5. The futures price associated with a Leave outcome, $F_n - V_e$, fluctuates in the range \$1.31-\$1.39, which is again consistent with the left mode of the corresponding RNDs before the referendum as well as the prevailing RND once the Leave victory becomes certainty (see Panel D of Figure 2.10).[21]

-Figure 2.13 here-

This analysis also allows us to ex ante quantify the full price effect, V_e, of a Leave outcome relative to Remain. This is given by the difference between the two latent futures prices. In particular, we find that this wedge takes values between 12¢ -18¢ during the examined period, and it is equal to 13.4¢ at settlement on 23rd June. Again, these estimates are very similar to the difference between the values of the two modes of the GBPUSD RNDs in the run up to the referendum. Interestingly, the high frequency analysis presented in Section 4 confirms these estimates.

Panel A of Figure 2.13 also illustrates the actual futures price, F_0, during the examined period. In line with equation (2.12), F_0 fluctuates between the latent prices associated with each of the two referendum outcomes according to the corresponding option-implied probabilities. In particular, as the probability p_e of a Leave outcome increases during the week before the

[19]We have also examined whether there is a lead-lag relationship between the betting and the option market during the sample period analyzed in this Section. To this end, we conduct a Granger-causality analysis. Specifically, we estimate a bivariate VAR model consisted of the betting-odds implied probability of a Leave outcome and the corresponding option-implied probability. The VAR lag length is selected on the basis of the Akaike Information Criterion. We find evidence of bi-directional Granger-causality. In particular, we can reject at the 5% level the null hypothesis that the betting-odds implied probability does not Granger-cause the option-implied probability. We can also reject at the 5% level the null hypothesis that the option-implied probability does not Granger-cause the betting-odds implied probability. We thank an anonymous referee for suggesting this analysis.

[20]The standard deviation of the option-implied futures prices associated with a Remain outcome during the examined period is 1.3¢ .

[21]The standard deviation of the option-implied futures prices associated with a Leave outcome during this period is 2.4¢ .

assassination of MP Cox, the futures trades consistently below \$1.45, with F_0 equal to \$1.42 on 15th June. To the contrary, the sharp reduction in p_e right after the assassination is associated with a large increase in F_0, which reaches \$1.48 on the referendum day.

Panel B of Figure 2.13 shows the evolution of the option-implied volatility estimates for each of the two referendum outcomes. For comparison, it also plots the annualized realized volatility of GBPUSD futures, estimated on a daily basis from intraday 1-min log returns.[22] A Remain outcome is characterised by a low level of volatility, fluctuating between 10-15% p.a. during the last two weeks before the referendum.[23] To the contrary, the volatility estimate associated with a Leave outcome is much higher and volatile itself. In fact, it fluctuates in the region of 25-35% p.a., reaching a peak of 36% p.a. on 22nd & 23rd June.[24] Interestingly, these ex ante estimates of volatility for each of the two outcomes are validated by the high frequency analysis presented in Section 4. Hence, we conclude that the option market can identify remarkably well not only the value but also the volatility of the underlying asset associated with each of the two potential outcomes of this political event.

2.6. Further Results

2.6.1. Risk-adjusted Distributions

Throughout the study, we extract risk-neutral distributions and probabilities from option prices without performing any risk-adjustment. Arguably, the existence of a risk premium could potentially affect the interpretation of our results. Whereas it is obvious that a risk-adjustment would be necessary to compute the physical density for FTSE100, which is an equity index and is expected to carry a risk premium, it is not clear to what extent this adjustment is appropriate for GBPUSD. Hanke, Poulsen, and Weissensteiner (2018, p. 2678) provide an insightful discussion on whether GBPUSD carries a premium or not. In sum, they argue that as long as the interest rate differential is close to zero, which holds true for GBPUSD during the examined period, then the exchange rate would be almost drift-free under the real-world probability measure and the risk premium would be near zero.

Nevertheless, an important question for our analysis is whether the shape of the RNDs for GBPUSD futures and FTSE100 Index would be substantially modified if we used a risk-adjusted distribution. Most characteristically, it is natural to ask whether the bimodality we uncover in the GBPUSD RND prior to the referendum reflects bimodality in the physical density or this is an artefact of risk-neutrality.

To address these potential concerns, we perform a risk-adjustment to convert the GBPUSD and FTSE100 RNDs into physical ones. To this end, we follow the standard approach of

[22] We use the futures contract expiring in September because according to the CME rulebook, this is the nearest quarterly futures contract that serves as the underlying for GBPUSD options that expire on 8th July. We compute these intraday returns using mid-quotes from the corresponding CME GBPUSD futures BBO data.

[23] The standard deviation of the option-implied volatility associated with a Remain outcome during the examined period is 1.8% p.a.

[24] The standard deviation of the volatility associated with a Leave outcome during the examined period is 5.2% p.a.

Bliss and Panigirtzoglou (2004), as recently implemented in Jackwerth and Menner (2020). Specifically, we assume a power utility function for the representative agent and we compute physical probabilities, $p(S_T)$, using the relationship:

$$p(S_T) = \frac{\frac{q(S_T)}{U'(S_T)}}{\int \frac{q(x)}{U'(x)} dx}, \tag{2.17}$$

where $U'(S_T) = S_T^{-\gamma}$ denotes the marginal utility function with degree of relative risk aversion γ, S_T is the underlying asset price at expiry T, and $q(S_T)$ is the risk-neutral probability.

To examine how the shape of the physical density would change for different levels of risk aversion, we perform this risk-adjustment using different values of γ. Figure SA.3 in the Supplementary Appendix illustrates the corresponding physical densities computed on 23rd June 2016, together with the RND for GBPUSD futures (Panel A) and the FTSE100 Index (Panel B), respectively.

Given the discussion in Hanke, Poulsen, and Weissensteiner (2018), we illustrate the physical density for GBPUSD futures using a low ($\gamma = 1$) as well as a moderate ($\gamma = 3$) degree of risk aversion. We find that this risk-adjustment has only a minor effect on the shape of the physical density. Most importantly, we find that the physical density remains bimodal with its modes located very close to the corresponding modes of the RND. To this end, we argue that our main conclusions regarding the detection and quantification of political event risk are not affected by the fact that we rely on RNDs.

For FTSE100, we illustrate the physical density using risk aversion coefficients ($\gamma = 2$ and $\gamma = 4$) that are similar in magnitude to the ones employed for equity indices in prior studies (see Bliss and Panigirtzoglou, 2004; Jackwerth and Menner, 2020). Again, we find that the shape of the physical density is very similar to the risk-neutral one. The physical density is clearly unimodal and strongly negatively skewed, and hence the conclusions derived in our main analysis from the corresponding RND remain intact.

2.6.2. Alternative Measures of Tail Risk

Our main analysis examines the effect of the Brexit referendum on the shape of RNDs and the evolution of the corresponding risk-neutral moments. To a large extent, these characteristics reflect the price of protection in the option market against a possible sharp drop in the underlying asset values due to this political event. Following the suggestion of an anonymous referee, we examine here alternative measures of tail risk.

First, we estimate the *Slope* of the IV curve, in the spirit of Kelly, Pástor, and Veronesi (2016). Specifically, on each trading day, we regress the implied volatilities of OTM puts on their deltas, including an intercept. We only include delta values that lie in the range of $(-0.5, -0.1)$. The corresponding slope coefficient estimate yields the *Slope* measure on a given trading day for the corresponding option expiry date. Figure SA.4 in the Supplementary Appendix illustrates the evolution of the *Slope* measure for GBPUSD (Panel A) and the FTSE100 Index (Panel B), respectively.

Second, in the spirit of Xing, Zhang, and Zhao (2010), we compute the *SKEW* of the IV

curve as another measure that captures the expensiveness of OTM puts. *SKEW* is defined as the difference between the annualized implied volatilities of a deep OTM put and an ATM call. For the deep OTM put, we choose the put with delta closest to -0.25. For the ATM call, we select the call with delta closest to 0.5. Figure SA.5 in the Supplementary Appendix presents the evolution of the *SKEW* measure for GBPUSD (Panel A) and the FTSE100 Index (Panel B), respectively.

Both of these measures reveal patterns that are similar to the evolution of RNS, as illustrated in Figure 2.7. For GBPUSD, we observe that on a given trading day, *Slope* and *SKEW* are substantially higher when computed from options expiring after rather than before the referendum. In addition, the values of these measures remain consistently high in the run up to the referendum but sharply decrease towards zero right after this event. On the other hand, the corresponding effects for FTSE100 are less pronounced when comparing options expiring before and after the referendum. Whereas we observe a spike in *Slope* and *SKEW* just before the referendum date, there is no clear downward trend in the aftermath of this event.

2.6.3. Risk-Neutral Distribution for EuroStoxx50

Arguably, this political event could also affect the Eurozone economy since Brexit could undermine the integrity of the European Union and its single market. Hence, it is interesting to examine whether this event risk was priced in the options of a major European stock index. To this end, we extract RNDs from options on EuroStoxx50 Index, which is consisted of European stocks with the largest capitalisation. These are European-style options and we source the relevant price data from Refinitiv DataScope. Figure SA.6 in the Supplementary Appendix illustrates the RNDs extracted on 23rd and 24th June, respectively, from options expiring on 15th July 2016.

We observe that the RND of EuroStoxx50 extracted on 23rd June is clearly unimodal. The main manifestation of event risk is a strongly negatively skewed RND, similar to the effect observed for FTSE100 prior to the referendum (see Panel B of Figure 2.3). This effect disappears in the aftermath of the referendum, as the RND reverts back to its standard shape of a slightly negatively skewed distribution. Interestingly, whereas the EuroStoxx50 Index experienced a substantial drop from 3,037 on 23rd June to 2,776 on 24th June, it fully recovered its losses by the option expiry date, closing at 2,958 on 15th July. Hence, similar to FTSE100, this provides an ex post confirmation that the referendum did not pose a substantial event risk for EuroStoxx50.

2.7. Conclusions

There is a growing interest in understanding the information signalled by financial markets with respect to polarised political events. Among other consequences, the outcome of such events can lead to sharp movements in asset prices and volatility, with adverse implications for financial stability and social welfare. However, the opposite sides of the campaign usually make contradictory predictions regarding these effects, causing confusion among voters before

the event and regret afterwards. Hence, a main challenge is to measure the potential impact of these outcomes *before* the event takes place, so that voters can make an informed political decision.

This study examines the UK referendum on EU membership in June, 2016. We show that the option market can ex ante detect and quantify the event risk arising due to this referendum. Most characteristically, the RNDs extracted from GBPUSD futures options, whose expiry spanned the referendum date, became bimodal. In the run up to the referendum, the left mode of these RNDs lied between \$1.31-\$1.35, revealing that the option market anticipated a large drop in the exchange rate in the event of a Leave outcome. In contrast, the right mode of these RNDs lied in the region of \$1.50-1.53. Hence, one could infer from the option market that the full effect of a Leave victory on GBPUSD was approximately 15¢ -19¢ .

This referendum also provides a strong validation test for option market expectations, because the large swings in outcome probabilities during the vote counting process offer us the rare opportunity to observe the counterfactual. Using high frequency option and futures prices during the referendum night, we confirm the ability of the option market to ex ante identify the effects of each outcome.

We also extract option-implied event probabilities. Despite the widespread belief that the Remain side would win, we find that the option market indicated Leave victory as the most likely outcome prior to the murder of MP Cox, one week before the referendum. Therefore, we show that option prices allow us to extract meaningful event probabilities, providing a good alternative to betting odds-implied probabilities.

Last but not least, we show that the option market not only can detect political event risk when there is, but it can also indicate the absence of such risk when there is not. In particular, we show that the effects on the corresponding RNDs and IV curves computed from FTSE100 options are very limited. The RNDs remain clearly unimodal, featuring only a moderate increase in negative skewness. Interestingly, whereas the Leave victory led to a sharp and permanent drop in GBPUSD, the effect on FTSE100 was much less pronounced on the first post-event trading day and it was subsequently reversed, with the index trading by the end of June higher than its pre-referendum close. Hence, we conclude that the option market can distinguish the potentially differential effects of the same political event across different assets.

References

Baker, M., Gillberg, T., and Thomas, S. (2018) Trading Events: Smiles, Frowns and Moustaches–the Many Faces of the Options Market. *SSRN*.

Bates, D. S. (1996) Jumps and stochastic volatility: Exchange rate processes implicit in deutsche mark options. *Review of Financial Studies* 9.1, pp. 69–107.

Bates, D. S. (2000) Post-'87 crash fears in the S&P 500 futures option market. *Journal of Econometrics* 94.1, pp. 181–238.

Beber, A., Breedon, F., and Buraschi, A. (2010) Differences in beliefs and currency risk premiums. *Journal of Financial Economics* 98.3, pp. 415–438.

Bernhard, W. and Leblang, D. (2006) *Democratic Processes and Financial Markets: Pricing Politics*. Cambridge University Press.

Birru, J. and Figlewski, S. (2012) Anatomy of a meltdown: The risk neutral density for the S&P 500 in the fall of 2008. *Journal of Financial Markets* 15.2, pp. 151–180.

Black, F. (1976) The pricing of commodity contracts. *Journal of Financial Economics* 3.1, pp. 167–179.

Bliss, R. R. and Panigirtzoglou, N. (2002) Testing the stability of implied probability density functions. *Journal of Banking and Finance* 26.2, pp. 381–422.

Bliss, R. R. and Panigirtzoglou, N. (2004) Option-Implied Risk Aversion Estimates. *Journal of Finance* 59.1, pp. 407–446.

Borochin, P. and Golec, J. (2016) Using options to measure the full value-effect of an event: Application to Obamacare. *Journal of Financial Economics* 120.1, pp. 169–193.

Breeden, D. T. and Litzenberger, R. H. (1978) Prices of State-Contingent Claims Implicit in Option Prices. *Journal of Business* 51.4, pp. 621–651.

Clark, I. J. and Amen, S. (2017) Implied distributions from GBPUSD risk-reversals and implication for brexit scenarios. *Risks* 5.3, p. 35.

Coulomb, R. and Sangnier, M. (2014) The impact of political majorities on firm value: Do electoral promises or friendship connections matter? *Journal of Public Economics* 115 (C), pp. 158–170.

Coutant, S., Jondeau, E., and Rockinger, M. (2001) Reading PIBOR futures options smiles: The 1997 snap election. *Journal of Banking and Finance* 25.11, pp. 1957–1987.

Duffie, D., Pan, J., and Singleton, K. (2000) Transform Analysis and Asset Pricing for Affine Jump-diffusions. *Econometrica* 68.6, pp. 1343–1376.

Ferreira, A. L., Gong, Y., and Gozluklu, A. E. (2022) Risk-Corrected Probabilities of a Binary Event. *SSRN*.

Figlewski, S. (2010) Estimating the Implied Risk-Neutral Density for the US Market Portfolio. *Volatility and Time Series Econometrics*. Oxford: Oxford University Press.

Fowler, J. H. (2006) Elections and markets: The effect of partisanship, policy risk, and electoral margins on the economy. *Journal of Politics* 68.1, pp. 89–103.

Garman, M. B. and Kohlhagen, S. W. (1983) Foreign currency option values. *Journal of International Money and Finance* 2.3, pp. 231–237.

Gemmill, G. and Saflekos, A. (2000) How Useful are Implied Distributions?: Evidence from Stock Index Options. *Journal of Derivatives* 7.3, pp. 83–91.

Hanke, M., Poulsen, R., and Weissensteiner, A. (2018) Event-Related Exchange-Rate Forecasts Combining Information from Betting Quotes and Option Prices. *Journal of Financial and Quantitative Analysis* 53.6, pp. 2663–2683.

Hartigan, J. A. and Hartigan, P. M. (1985) The Dip Test of Unimodality. *The Annals of Statistics* 13.1, pp. 70–84.

Herron, M. C. (2000) Estimating the Economic Impact of Political Party Competition in the 1992 British Election. *American Journal of Political Science* 44.2, pp. 326–337.

Hull, J. (2009) *Options, Futures and Other Derivatives*. 7th ed. Upper Saddle River, N.J: Pearson Prentice Hall.

Jackwerth, J. C. (2004) *Option-implied Risk-neutral Distributions and Risk Aversion*. Charlotteville: Research Foundation of AIMR.

Jackwerth, J. C. and Menner, M. (2020) Does the Ross recovery theorem work empirically? *Journal of Financial Economics* 137.3, pp. 723–739.

Jorion, P. (1988) On Jump Processes in the Foreign Exchange and Stock Markets. *Review of Financial Studies* 1.4, pp. 427–445.

Kelly, B., Pástor, Ľ., and Veronesi, P. (2016) The Price of Political Uncertainty: Theory and Evidence from the Option Market. *Journal of Finance* 71.5, pp. 2417–2480.

Knight, B. (2007) Are policy platforms capitalized into equity prices? Evidence from the Bush/Gore 2000 Presidential Election. *Journal of Public Economics* 91.1, pp. 389–409.

Leahy, M. P. and Thomas, C. P. (1996) The Sovereignty Option : The Quebec Referendum and Market Views on the Canadian Dollar. *International Finance Discussion Papers* 1996.555, pp. 1–34.

Liu, J., Longstaff, F. A., and Pan, J. (2003) Dynamic Asset Allocation with Event Risk. *Journal of Finance* 58.1, pp. 231–259.

Merton, R. C. (1976) Option pricing when underlying stock returns are discontinuous. *Journal of Financial Economics* 3.1, pp. 125–144.

Putnam, B., McDannel, G., Ayikara, M., and Peyyalamitta, L. S. (2018) Describing the dynamic nature of transactions costs during political event risk episodes. *High Frequency* 1.1, pp. 6–20.

Reiswich, D. and Wystup, U. (2010) A guide to FX options quoting conventions. *Journal of Derivatives* 18.2, pp. 58–68.

Slemrod, J. and Greimel, T. (1999) Did Steve Forbes scare the US municipal bond market? *Journal of Public Economics* 74.1, pp. 81–96.

Snowberg, E., Wolfers, J., and Zitzewitz, E. (2007) Partisan Impacts on the Economy: Evidence from Prediction Markets and Close Elections. *The Quarterly Journal of Economics* 122.2, pp. 807–829.

Treasury, H. M. (2016) HM Treasury analysis: the immediate economic impact of leaving the EU: CM 9292. UK Parliament 2016-2017.

Wolfers, J. and Zitzewitz, E. (2016) What do financial markets think of the 2016 election. *Washington, DC: The Brookings Institution*.

Wolfers, J. and Zitzewitz, E. (2018) The “Standard Error” of Event Studies: Lessons from the 2016 Election. *AEA Papers and Proceedings* 108, pp. 584–589.

Xing, Y., Zhang, X., and Zhao, R. (2010) What Does the Individual Option Volatility Smirk Tell Us About Future Equity Returns? *Journal of Financial and Quantitative Analysis* 45.3, pp. 641–662.

Figure 2.1:
This Figure shows Risk-Neutral Distributions (RNDs) extracted on 17th May 2016 from options with expiry spanning as well as options with expiry not spanning the Brexit Referendum date (23rd June, 2016). In Panel A, RNDs are extracted from options on GBPUSD futures with expiries on 3rd June (blue), 8th July (red), and 5th August 2016 (green). In Panel B, RNDs are extracted from options on FTSE100 Index with expiries on 17th June (blue), 15th July (red), and 19th August 2016 (green).

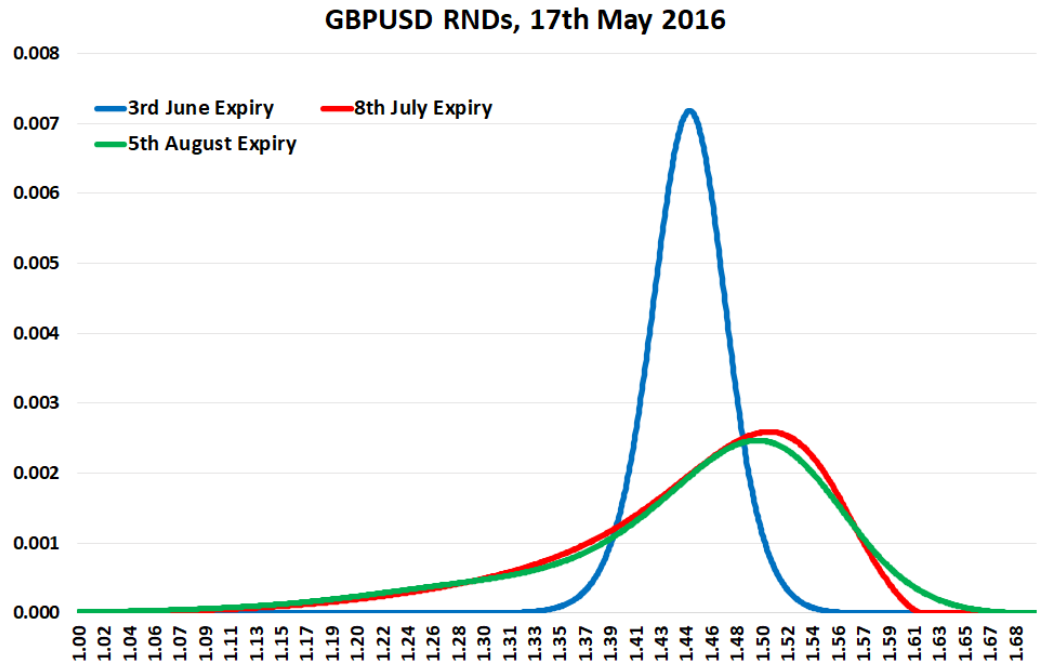

Panel A

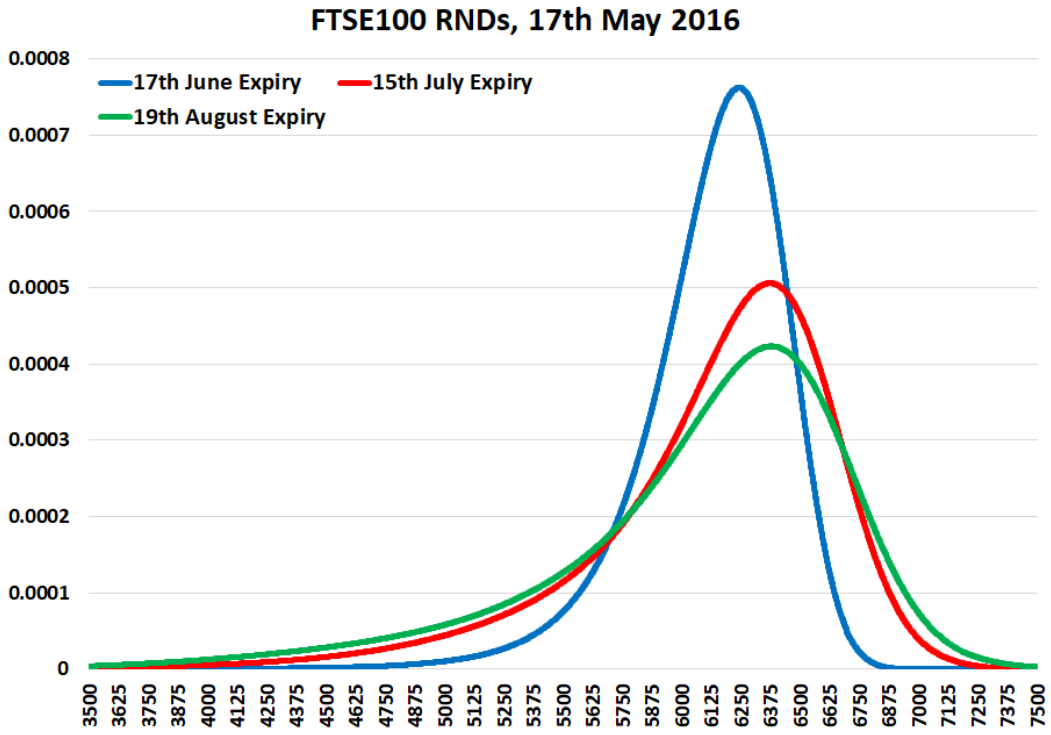

Panel B

Figure 2.2:
This Figure shows Implied Volatility (IV) curves extracted on 17th May 2016 from options with expiry spanning as well as options with expiry not spanning the Brexit Referendum date (23rd June, 2016). Panels A and B show the IV curves extracted from options on GBPUSD futures with expiry on 3rd June (Panel A) and 8th July 2016 (Panel B). Panels C and D show the IV curves extracted from options on FTSE100 Index with expiry on 17th June (Panel A) and 15th July 2016 (Panel B). In all Panels, black dots represent the IVs (p.a.) computed from observable option prices, whereas the coloured curves depict the fitted implied volatilities according to the spline methodology presented in Section 2.2. The corresponding at-the-money (ATM) point is indicated in all Panels.

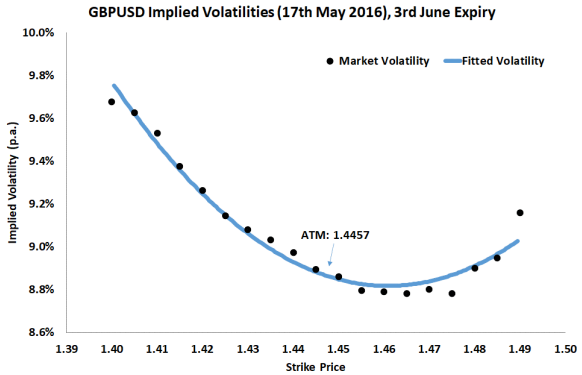

Panel A

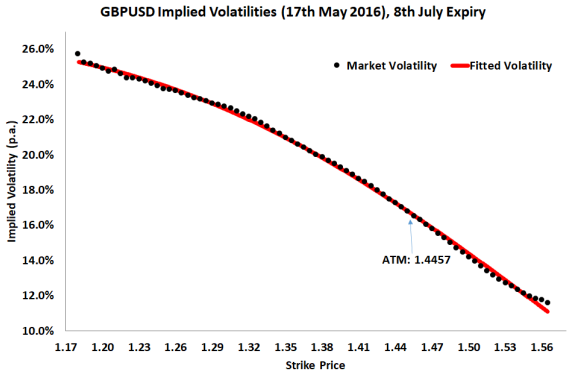

Panel B

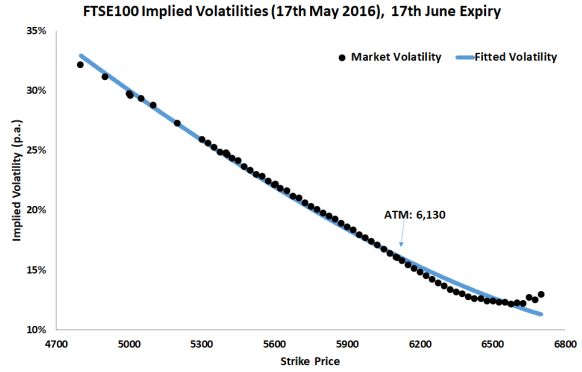

Panel C

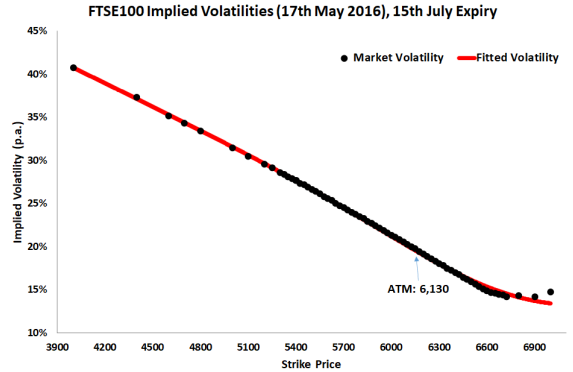

Panel D

Figure 2.3:
This Figure shows Risk-Neutral Distributions (RNDs) extracted around the Brexit Referendum date (23rd June, 2016) from options with same expiry. In Panel A, RNDs are extracted on 23rd June (blue) and 24th June 2016 (red) from options on GBPUSD futures with expiry on 8th July 2016. In Panel B, RNDs are extracted on 23rd June (blue) and 24th June 2016 (red) from options on FTSE100 Index with expiry on 15th July 2016. In both Panels, the mode(s) of the RNDs are indicated.

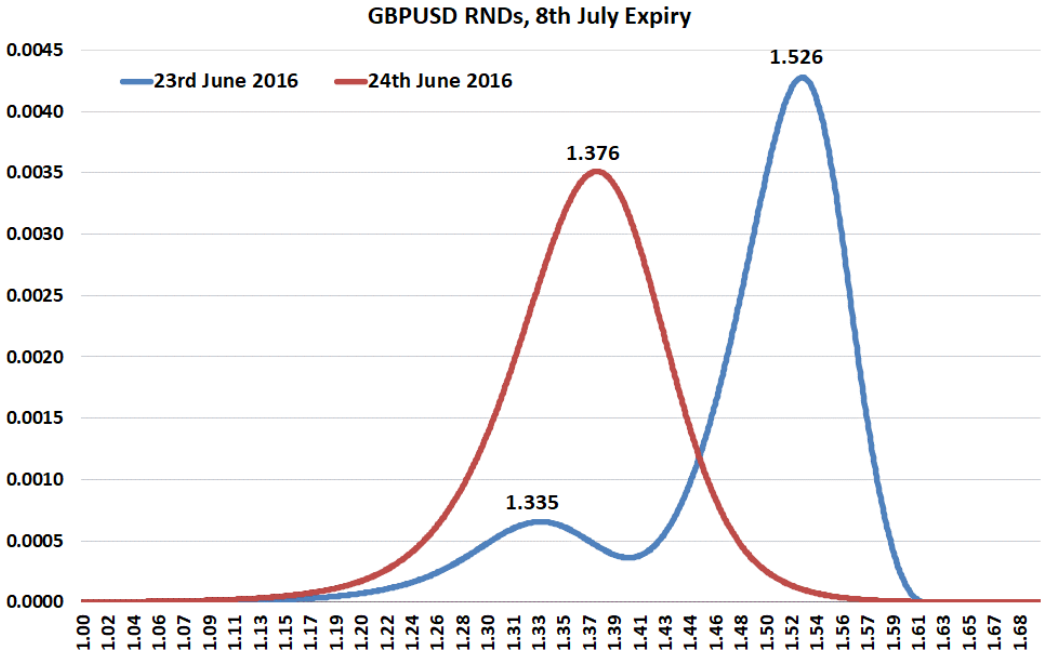

Panel A

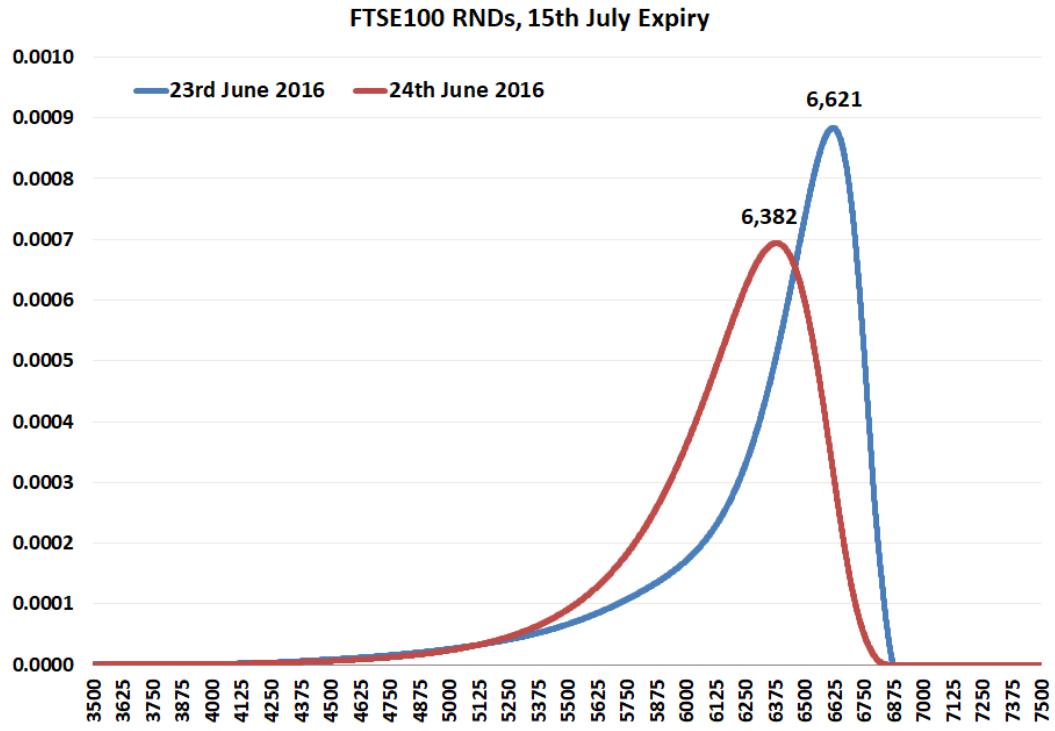

Panel B

Figure 2.4:
This Figure shows Implied Volatility (IV) curves extracted around the Brexit Referendum date (23rd June, 2016) from options with same expiry. Panels A and B show the IV curves extracted on 23rd June (Panel A) and 24th June 2016 (Panel B) from options on GBPUSD futures with expiry on 8th July 2016. Panels C and D show the IV curves extracted on 23rd June (Panel C) and 24th June 2016 (Panel D) from options on FTSE100 Index with expiry on 15th July 2016. In all Panels, black dots represent the IVs (p.a.) computed from observable option prices, whereas the coloured curves depict the fitted implied volatilities according to the spline methodology presented in Section 2.2.

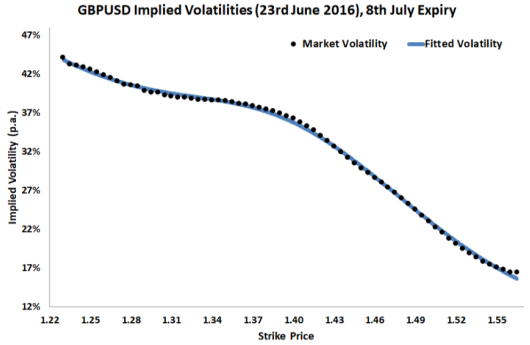

Panel A

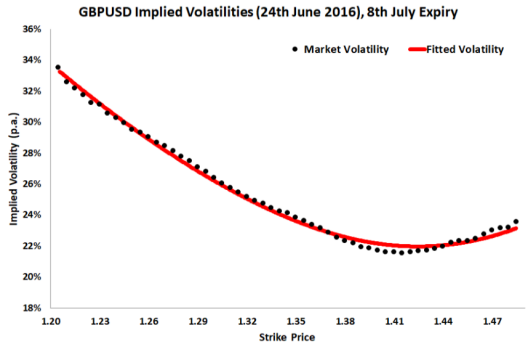

Panel B

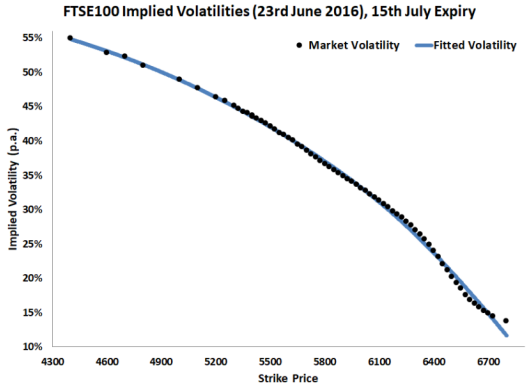

Panel C

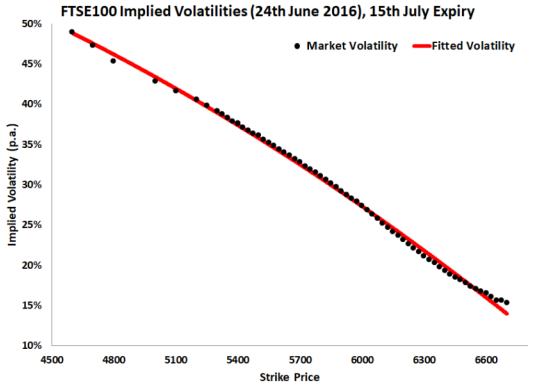

Panel D

Figure 2.5:
This Figure shows Risk-Neutral Distributions (RNDs) extracted on days in the run up to the Brexit Referendum date (23rd June, 2016). In Panels A and B, RNDs are extracted from options on GBPUSD futures with expiry on 8th July 2016. Specifically, Panel A shows RNDs extracted on 3rd June (blue) and 10th June 2016 (red), Panel B shows RNDs extracted on 17th June (blue), 22nd June (red), and 23rd June 2016 (green). In Panels C and D, RNDs are extracted from options on FTSE100 Index with expiry on 15th July 2016. Specifically, Panel C shows RNDs extracted on 3rd June (blue) and 10th June 2016 (red), whereas Panel D shows RNDs extracted on 17th June (blue), 22nd June (red), and 23rd June 2016 (green). In all Panels, the mode(s) of the RNDs are indicated.

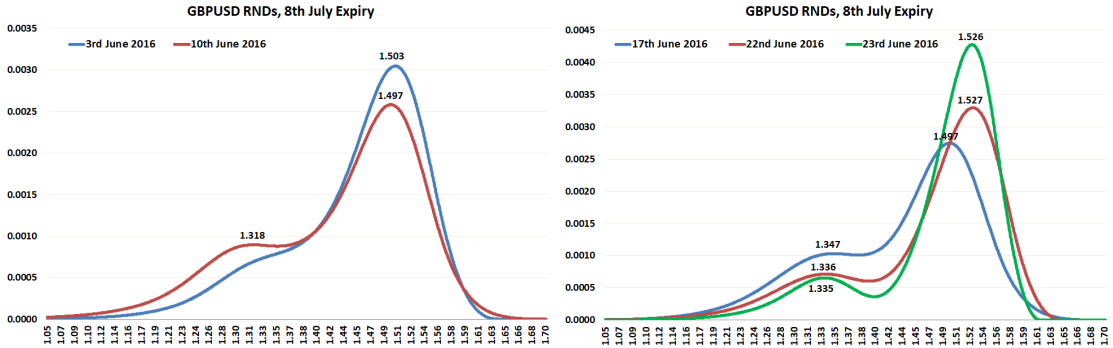

Panel A

Panel B

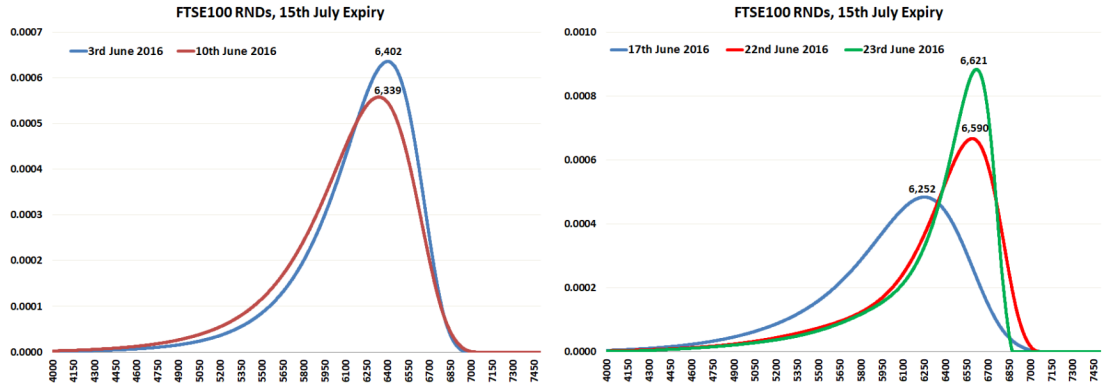

Panel C

Panel D

Figure 2.6:
This Figure shows the evolution of Risk-Neutral Volatility (RNV) (p.a.), which is computed from the corresponding Risk-Neutral Distribution, extracted from 9th May until 5th July 2016. Panel A shows RNVs extracted from options on GBPUSD futures with expiry on 3rd June (blue), 8th July (red), and 5th August 2016 (green). Panel B shows RNVs extracted from options on FTSE100 Index with expiry on 17th June (blue), 15th July (red), and 19th August 2016 (green). The vertical black line indicates the Brexit Referendum date (23rd June, 2016).

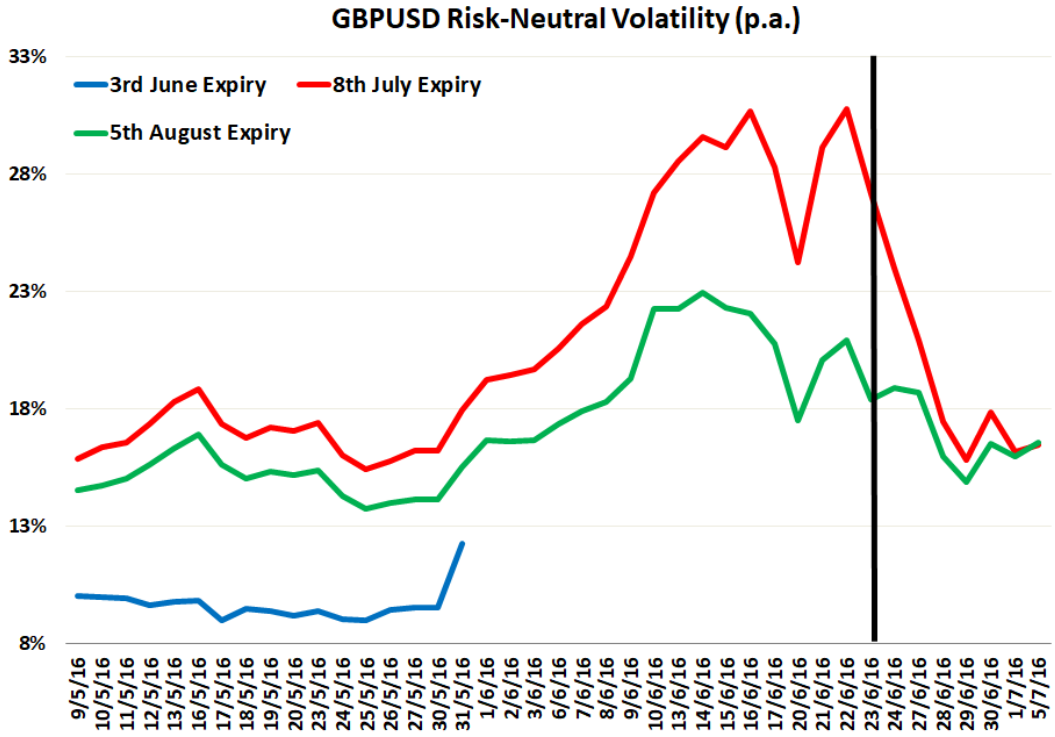

Panel A

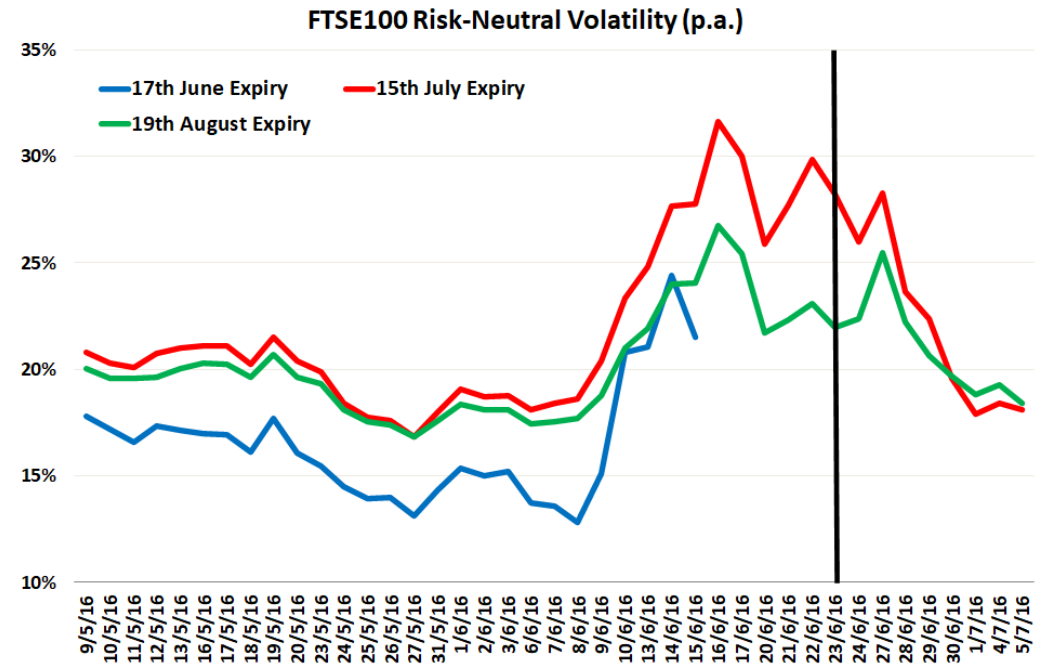

Panel B

Figure 2.7:
This Figure shows the evolution of Risk-Neutral Skewness (RNS) (p.a.), which is computed from the corresponding Risk-Neutral Distribution, extracted from 9th May until 5th July 2016. Panel A shows RNSs extracted from options on GBPUSD futures with expiry on 3rd June (blue), 8th July (red), and 5th August 2016 (green). Panel B shows RNSs extracted from options on FTSE100 Index with expiry on 17th June (blue), 15th July (red), and 19th August 2016 (green). The vertical black line indicates the Brexit Referendum date (23rd June, 2016).

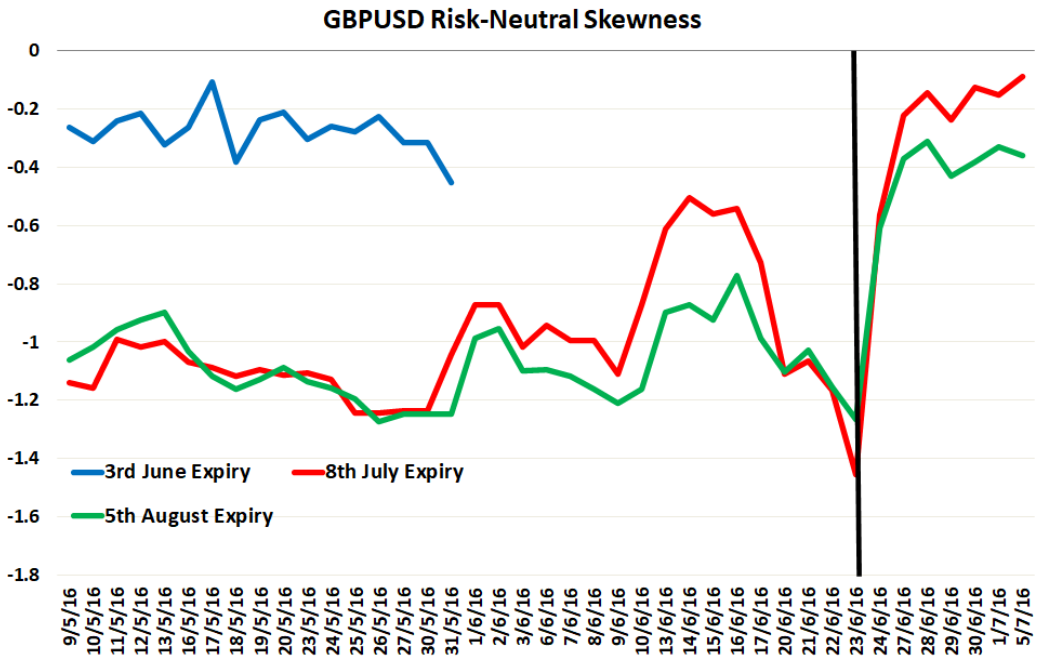

Panel A

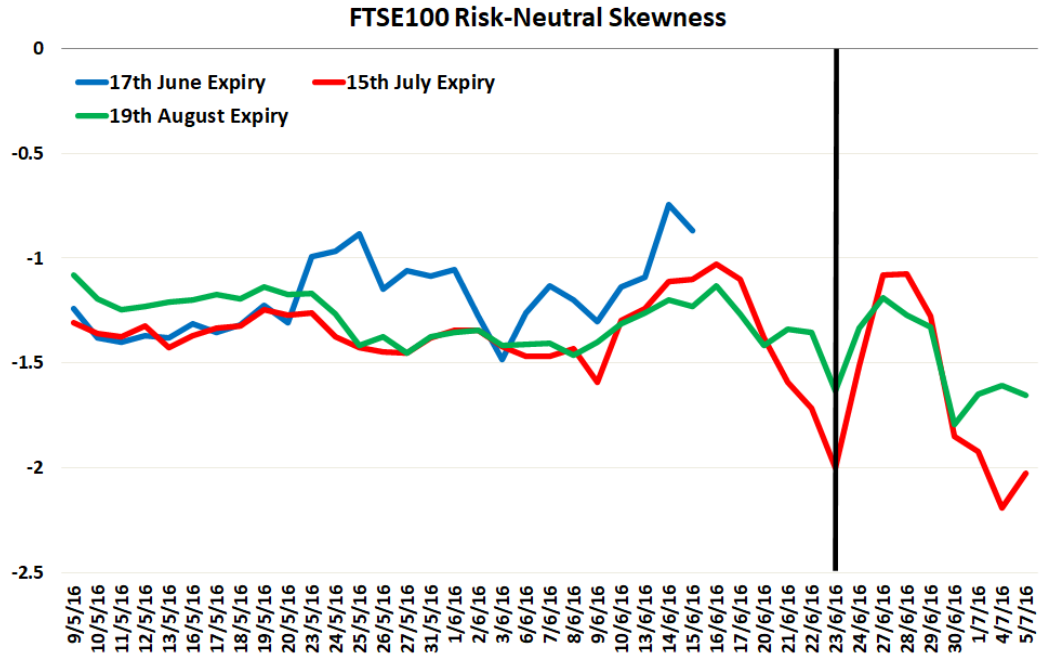

Panel B

Figure 2.8:
This Figure shows the evolution of the Bimodality Coefficient of the corresponding Risk-Neutral Distribution (RND), extracted from 9th May until 5th July 2016. Panel A shows the Bimodality Coefficient of the RND extracted from options on GBPUSD futures with expiry on 3rd June (blue), 8th July (red), and 5th August 2016 (green). Panel B shows the Bimodality Coefficient of the RND extracted from options on FTSE100 Index with expiry on 17th June (blue), 15th July (red), and 19th August 2016 (green). The vertical black line indicates the Brexit Referendum date (23rd June, 2016).

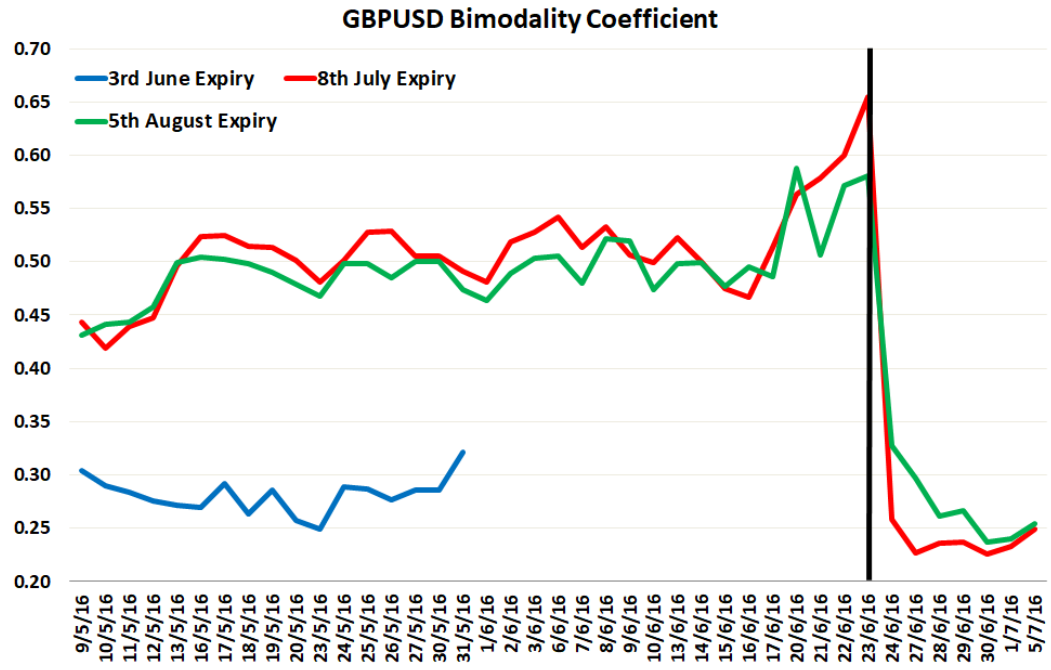

Panel A

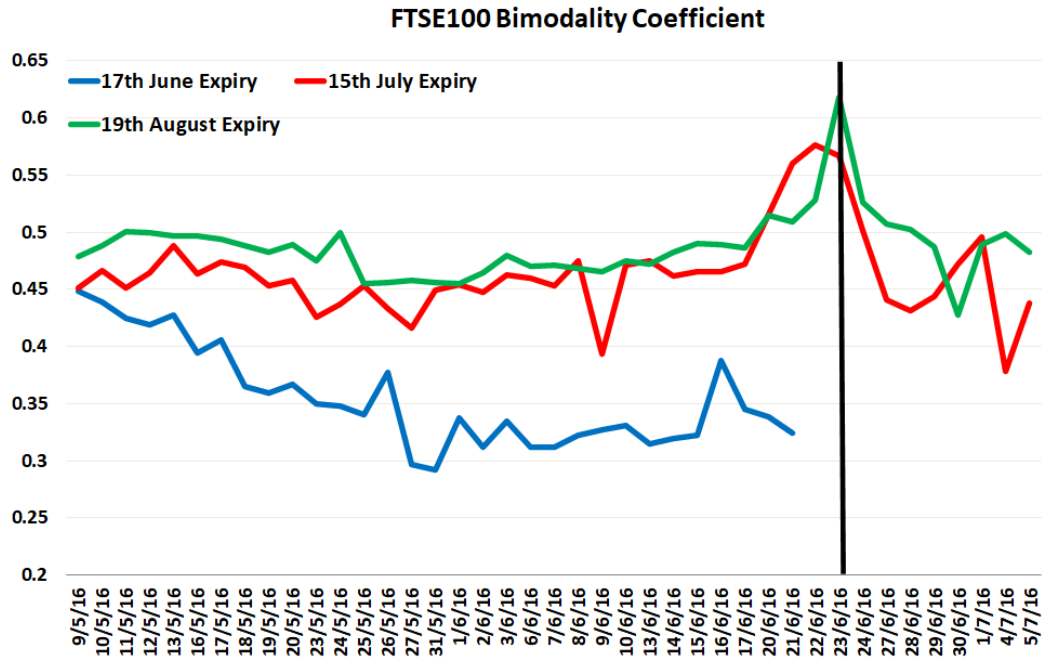

Panel B

Figure 2.9:
This Figure shows GBPUSD Risk-Neutral Distributions (RNDs) extracted on the Brexit Referendum night (23rd to 24th June, 2016). The blue curve illustrates the RND extracted at settlement (20:00 BST) on 23rd June from CME options on GBPUSD futures with expiry on 8th July. The red curve illustrates the RND extracted on 23rd June at 23:00 BST from options on GBPUSD with 1-month maturity, sourced from Bloomberg. The green curve illustrates the corresponding RND extracted on 24th June at 05:30 BST from options on GBPUSD with 1-month maturity, sourced from Bloomberg. In all cases, the mode(s) of the RNDs are indicated.

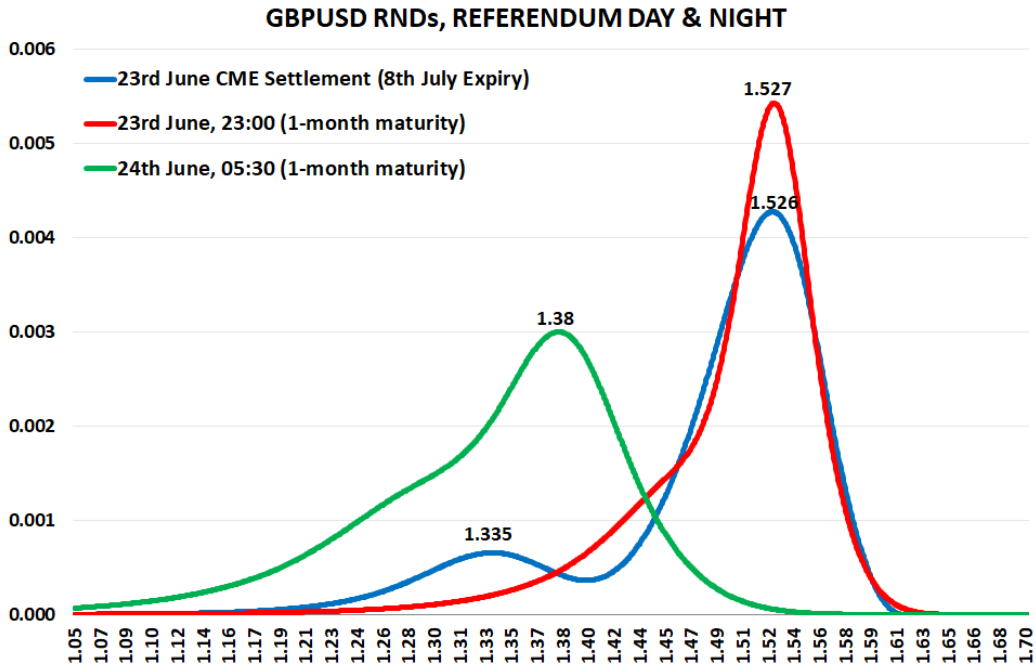

Figure 2.10:
This Figure shows GBPUSD Risk-Neutral Distributions (RNDs) extracted on the Brexit Referendum night (23rd to 24th June, 2016). In Panel A, the blue curve presents the RND extracted at settlement (20:00 BST) on 23rd June from CME options on GBPUSD futures with expiry on 8th July. The green curve presents the RND extracted on 23rd June at 22:10 BST from options on GBPUSD with 1-month maturity, sourced from Bloomberg, whereas the red curve presents the corresponding RND extracted at 22:30 BST. Panel B presents the corresponding RNDs at 23:30 (blue), 00:10 (red), and 01:00 BST (green). Panel C presents the corresponding RNDs at 02:00 (blue), 03:30 (red), and 04:00 BST (green). Panel D presents the corresponding RNDs at 04:40 (blue), 05:30 (red), and 08:50 (green). In all cases, the mode(s) of the RNDs are indicated.

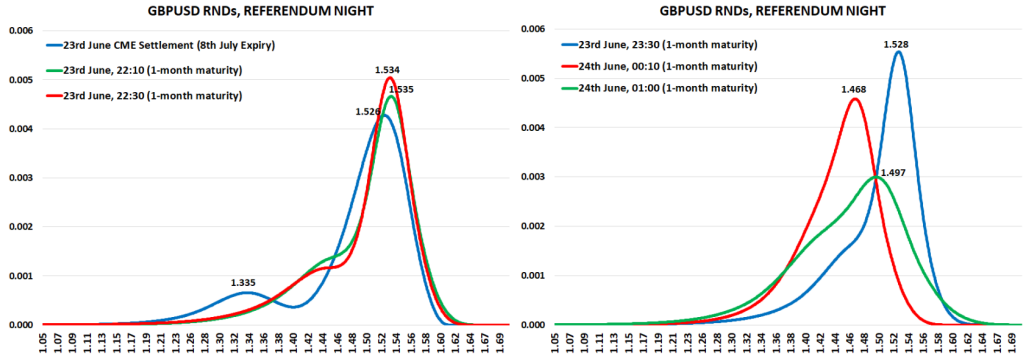

Panel A Panel B

Panel C Panel D

Figure 2.11:
This Figure shows the GBPUSD futures price and Risk-Neutral Volatility on the Brexit Referendum night from 22:00 BST on 23rd June to 06:00 BST on 24th June 2016. Panel A presents the evolution of the GBPUSD futures price (blue, left axis) together with the probability of a Leave Vote outcome implied by betting odds (red, right axis), provided by Betfair. Panel B presents the evolution of the Risk-Neutral Volatility (p.a.) (blue, left axis), extracted from options on GBPUSD with 1-month maturity, sourced from Bloomberg, together with the probability of a Leave Vote outcome implied by betting odds (red, right axis), provided by Betfair.

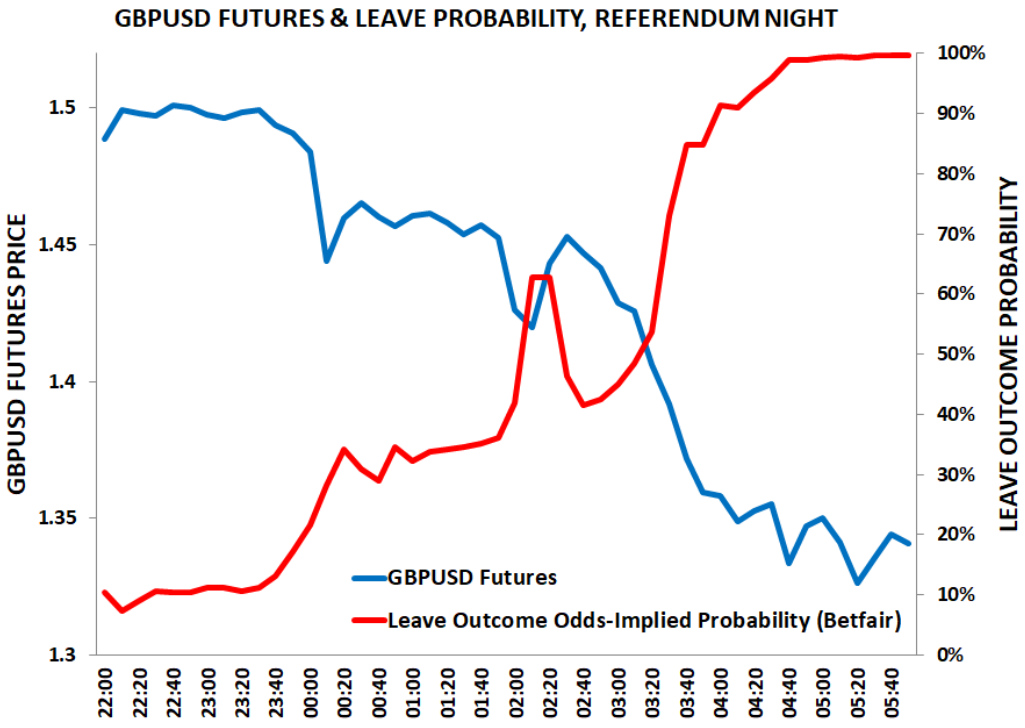

Panel A

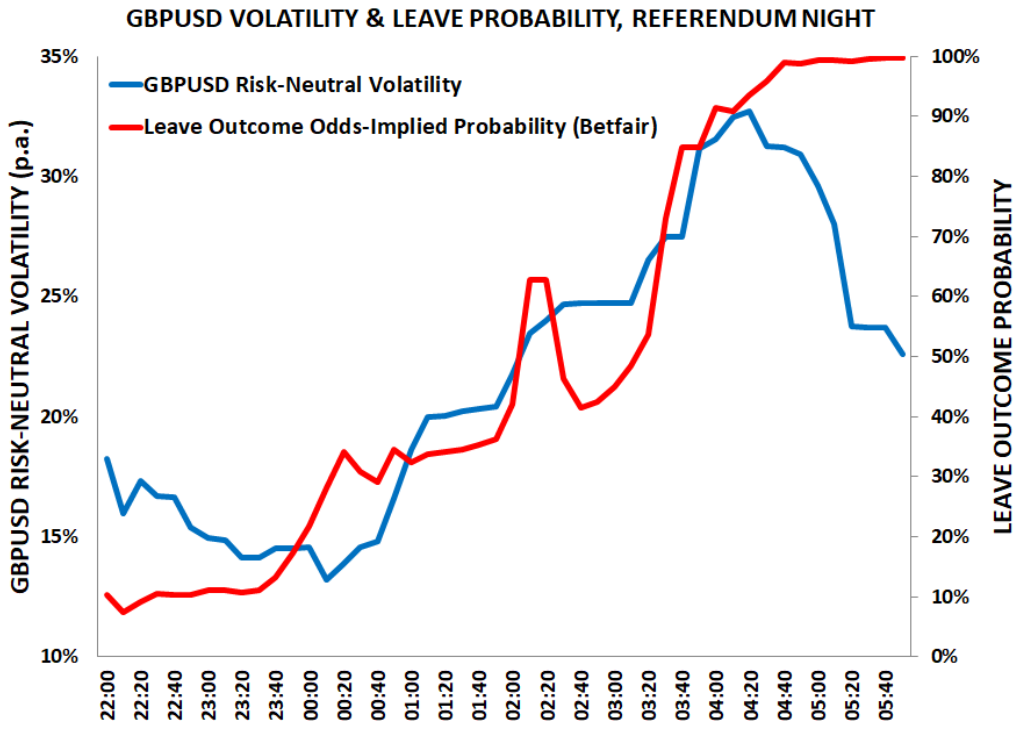

Panel B

Figure 2.12:
This Figure shows two sets of probabilities of a Leave Vote outcome, computed on a daily basis in the run up to the Brexit Referendum date (23rd June, 2016). The blue line indicates the probability of a Leave Vote outcome implied by the prices of options on GBPUSD futures with expiry on 8th July 2016. The red line indicates the corresponding probability implied by betting odds provided by Betfair. The vertical black line indicates the date of the murder of MP Jo Cox (16th June, 2016).

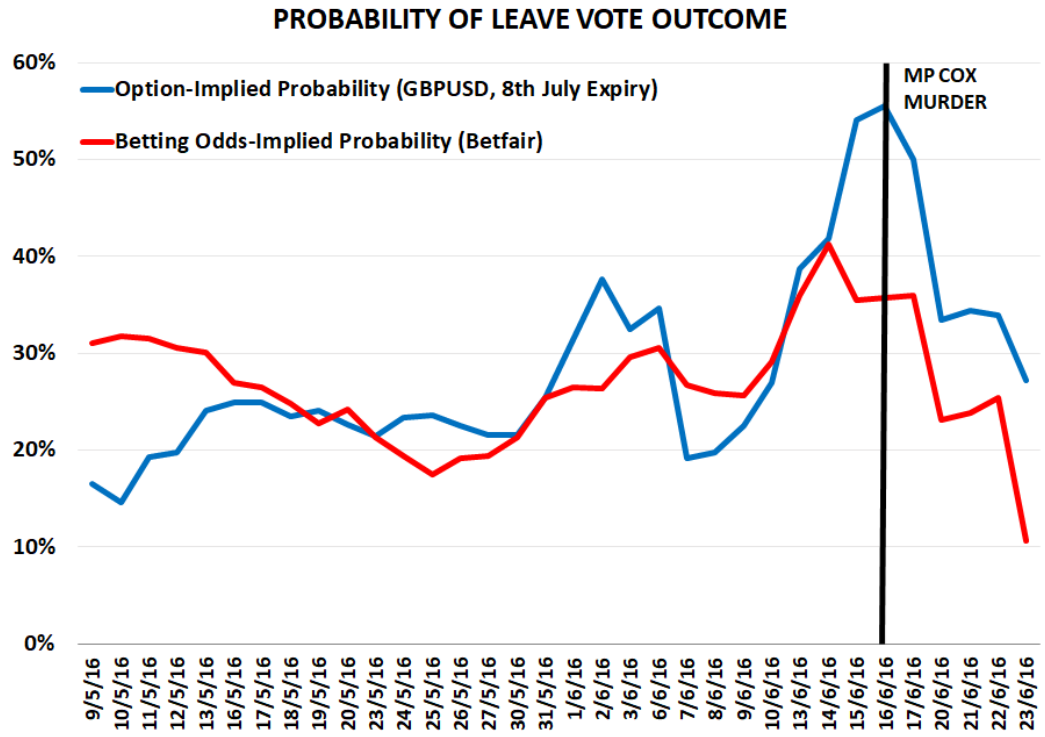

Figure 2.13:
This Figure illustrates the GBPUSD futures price (Panel A) and Implied Volatility (Panel B) in the run up to the Brexit Referendum date (23rd June, 2016), corresponding to the event of a Remain or a Leave Vote outcome, respectively, as computed from options on GBPUSD futures with expiry on 8th July 2016. Panel A shows the GBPUSD futures price in the event of a Remain (red) or a Leave (blue) Vote outcome, together with the actual futures price (green). Panel B shows the GBPUSD futures Implied Volatility (p.a.) in the event of a Remain (red) or a Leave (blue) Vote outcome, together with the realized volatility (p.a.) computed on a daily basis from intraday 1-min GBPUSD futures log returns (yellow). The vertical black line indicates the date of the murder of MP Jo Cox (16th June, 2016).

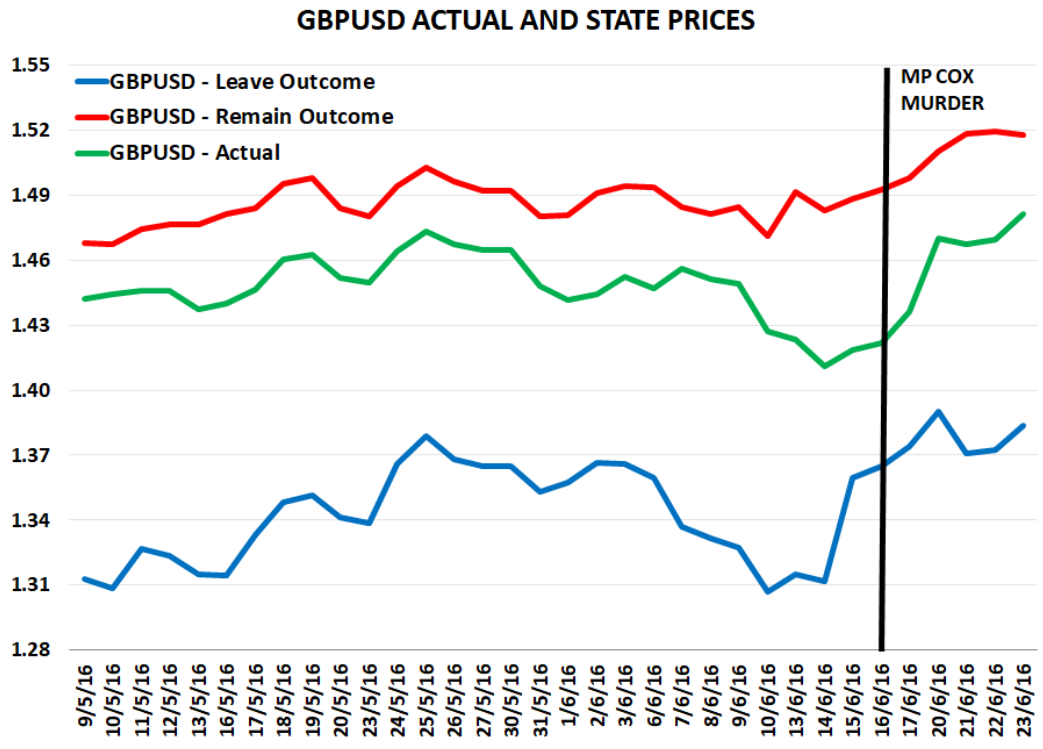

Panel A

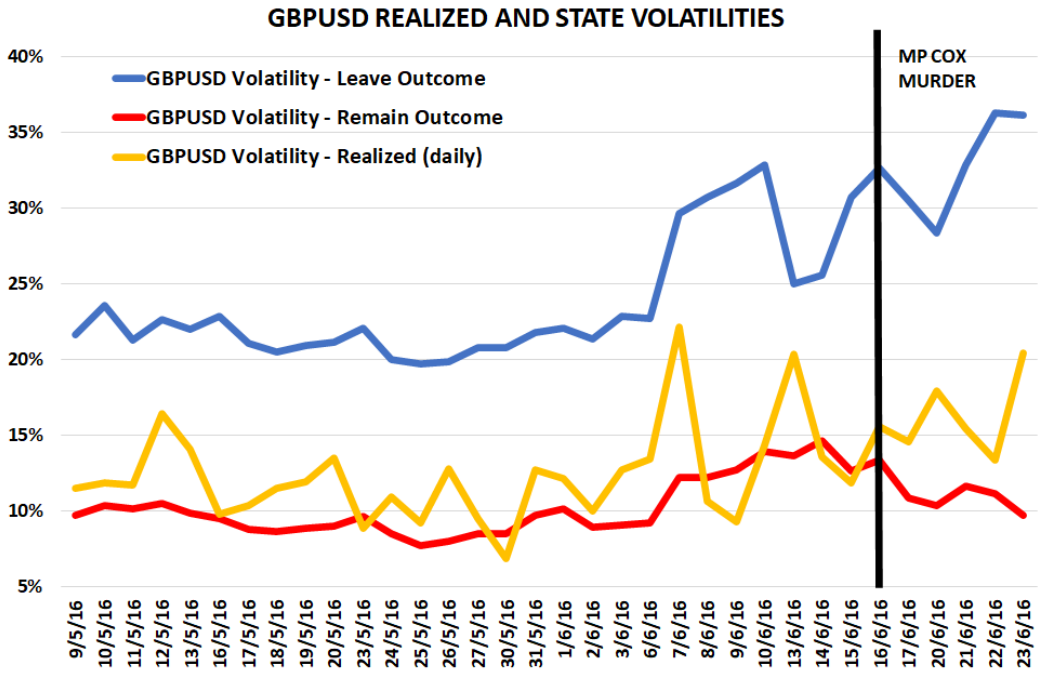

Panel B

Table 2.1: This Table presents an outline of key political events leading to and associated with the Brexit 2016 Referendum.

Date	Event
23rd January, 2013	Bloomberg Speech: Prime Minister (PM) David Cameron calls for fundamental reform of the EU and promises an in-out referendum on UK membership should the Conservatives win a parliamentary majority at the 2015 General Election
May, 2013	The Conservatives publish a draft EU Referendum Bill, which would be held no later than 31st December, 2017
22nd May, 2014	UK Independence Party (UKIP) tops the polls for the European Parliament elections
7th May, 2015	UK General Election: Conservatives win absolute majority in the House of Commons. Their electoral manifesto included Cameron's commitment to hold an inout referendum on UK membership of the EU by the end of 2017
27th May, 2015	Planned referendum is included in the Queen's speech
9th June, 2015	The European Union Referendum Act 2015 passes the second reading in the House of Commons, voted by 544 to 53 in favour
17th December, 2015	The European Union Referendum Act receives Royal Assent. Voters will be asked whether the UK should Remain a member of EU or Leave the EU
20th February, 2016	PM Cameron announces that the referendum will be held on 23rd June, 2016
21st February, 2016	Former Mayor of London and Member of Parliament (MP) Boris Johnson announces that he will campaign for Vote Leave
16th June, 2016	Pro-Remain Labour MP, Jo Cox, is murdered by an allegedly far-right supporter. Official campaigning is suspended for three days
21st June, 2016	The final "Great Debate" is broadcasted by BBC from Wembley Arena
23rd June, 2016	Referendum is held
24th June, 2016	Referendum result is announced. Leave wins, receiving 51.89% of valid votes. Cameron announces that he will resign as PM
13th July, 2016	Theresa May succeeds Cameron as PM

Table 2.2: This Table reports descriptive statistics for the options used to extract Risk-Neutral Densities for GBPUSD futures and the FTSE100 Index, respectively, during the period from 9th May until 5th July 2016. Descriptive statistics are shown separately for each expiry.

	GBPUSD			FTSE100		
Expiry	3rd June	8th July	5th August	17th June	15th July	19th August
Average number of strikes used per day	18	69	83	54	67	64
Average total trading volume across strikes per day	-	-	-	8,026	6,754	2,660
Average total open interest across strikes per day	-	-	-	277,115	243,969	61,899
Number of trading days	17	41	41	27	41	41

Table 2.3: This Table presents the key events and announcements related to the Brexit Referendum during the night of 23rd June and the early morning of 24th June, 2016. All time stamps are in British Summer Time (BST) and correspond to BBC's election night broadcasting.

Time (BST)	Event/Announcement
22:00	Polls Close. No "public" Exit Poll was conducted
22:07	BBC quotes the leader of UKIP, MEP Nigel Farage, saying that "Remain has just edged it"
22:23	BBC psephologist says that the YouGov poll conducted on the same day indicates a Remain lead by 52% to 48%
22:54	BBC quotes that Farage has "unconceded" the Remain victory
23:59	Result for Newcastle is announced. Marginal victory for Remain (50.7% to 49.3%). Much lower vote share for Remain than the one anticipated for this area
00:16	Result for Sunderland is announced. Very strong victory for Leave (61% to 39%). A marginal victory for Leave was anticipated.
00:44	BBC quotes sources from Lewisham (London borough) that Remain may have gained 83% of the vote in this area
00:53	Result for Swindon is announced. Victory for Leave (55% to 45%). Anticipated result if national vote was split 50%-50%
01:18	Result for South Tyneside is announced. Bigger than anticipated victory for Leave (62% to 38%)
01:42	Result for Hartlepool is announced. Bigger than anticipated victory for Leave (70% to 30%)
01:54	Result for City of London is announced. Remain victory by 75% to 25%
02:01	Result for Swansea is announced. Victory for Leave by 52% to 48%, whereas a Remain victory was anticipated
02:04	BBC presenter quotes a leading figure in Labour party saying that they believe it will be a Leave win
02:14	Arron Banks, a donor and co-founder of Leave.EU campaign, says that Leave has won. He states that their own poll showed a Leave win by 52% to 48%
02:19	Result for Lambeth. Bigger than anticipated victory for Remain (79% to 21%). First big London borough to declare result
02:28	Result for Wandsworth (London borough). Bigger than anticipated victory for Remain (75% to 25%)
03:14	BBC psephologist states that London outperformance for Remain does not seem sufficient to offset the outperformance of Leave in other places

03:22	Leave vote has surpassed 51% with 159/382 counting authorities declared
03:46	BBC quotes Farage saying that he “now dares to dream of an independent UK at dawn”
04:01	Farage claims that Leave has won
04:39	BBC calls the Referendum for Leave, projecting a 52% share of the vote
07:01	Final result: Leave 17,410,742 votes (51.9%) – Remain 16,141,241 votes (48.1%)
08:22	Cameron announces that he will resign as PM
08:46	Statement by the Bank of England Governor, Mark Carney, that the Bank is ready to provide liquidity and take further policy actions

Supplementary Appendix

Figure SA.1:
This Figure shows Risk-Neutral Distributions (RNDs) extracted around the Brexit Referendum date (23rd June, 2016) from options with same expiry. In Panel A, RNDs are extracted on 23rd June (blue) and 24th June 2016 (red) from options on AstraZeneca (AZN) with expiry on 15th July 2016. In Panel B, RNDs are extracted on 23rd June (blue) and 24th June (red) from options on GlaxoSmithKline (GSK) with expiry on 15th July 2016. In both Panels, the mode(s) of the RNDs are indicated.

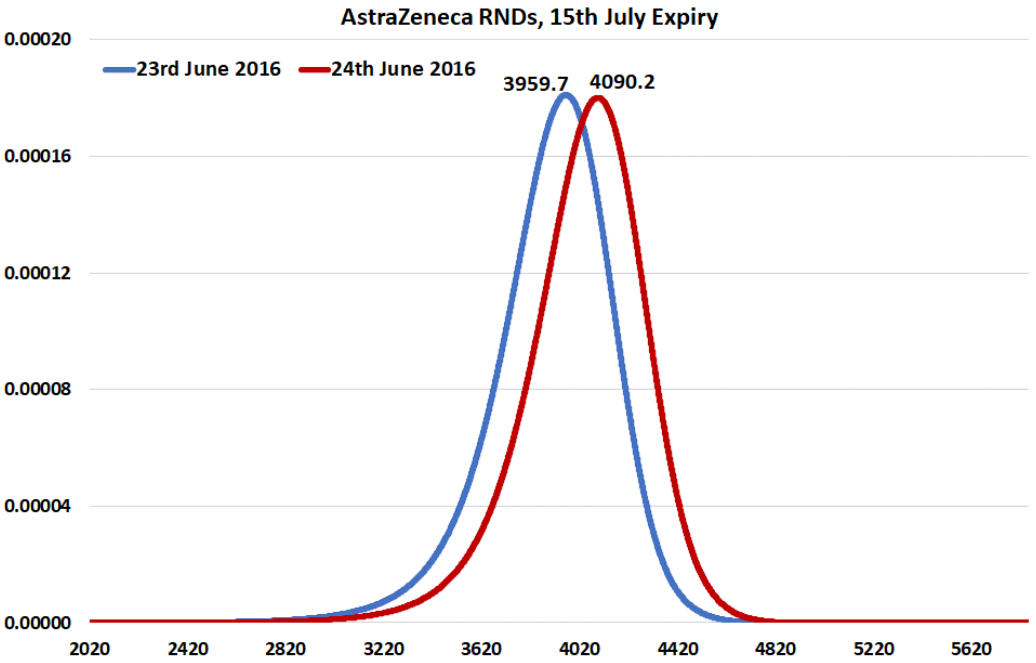

Panel A

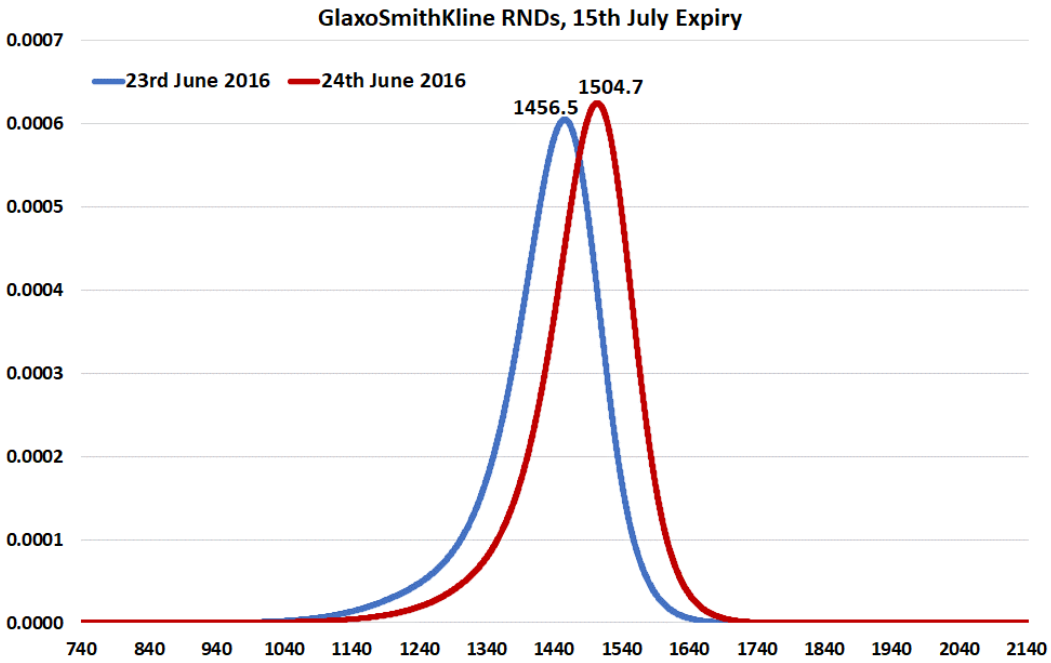

Panel B

Figure SA.2:
This Figure shows Risk-Neutral Distributions (RNDs) extracted around the Brexit Referendum date (23rd June, 2016) from options with same expiry. In Panel A, RNDs are extracted on 23rd June (blue) and 24th June 2016 (red) from options on British Telecom (BT) with expiry on 15th July 2016. In Panel B, RNDs are extracted on 23rd June (blue) and 24th June (red) from options on Sainsbury's (SBRY) with expiry on 15th July 2016. In both Panels, the mode(s) of the RNDs are indicated.

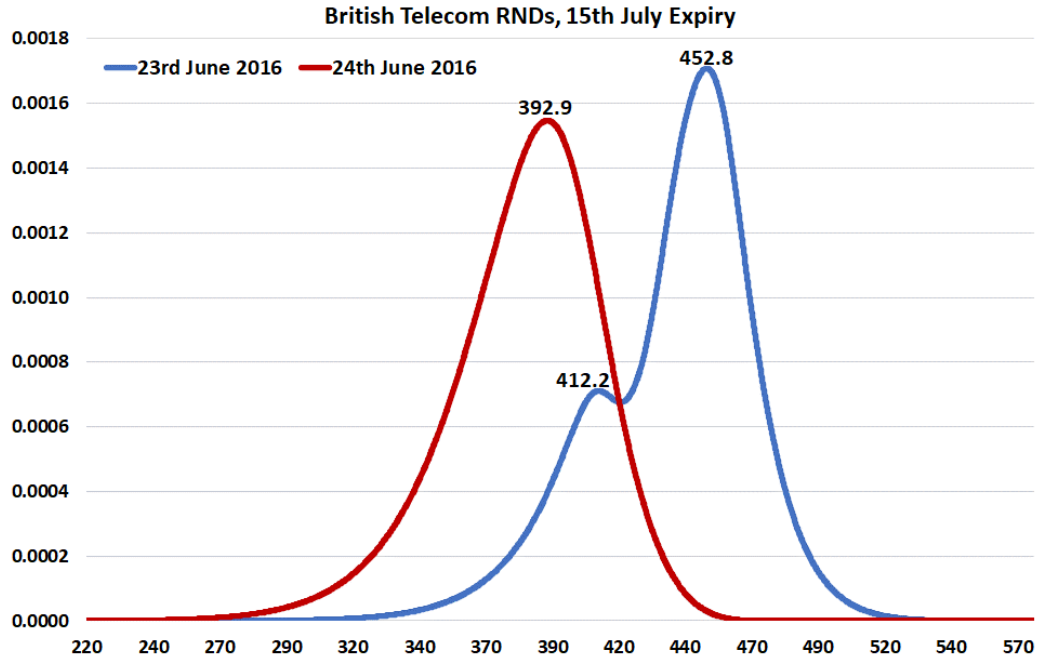

Panel A

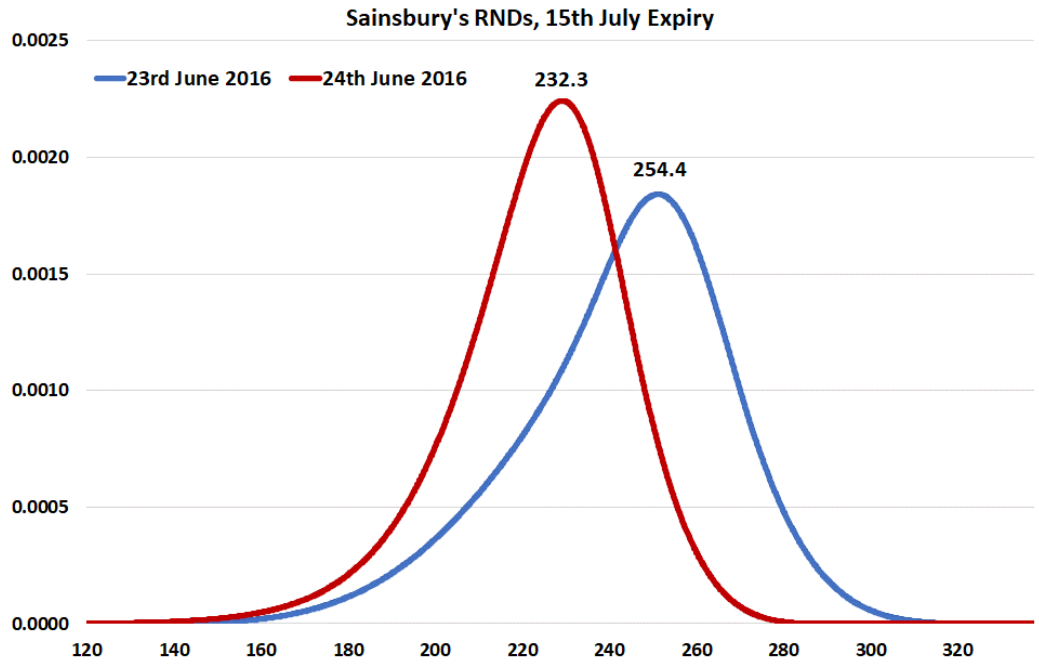

Panel B

Figure SA.3:
This Figure shows risk-adjusted distributions extracted on 23rd June 2016, for different degrees of risk aversion (γ) of the representative agent, using the methodology of Bliss and Panigirtzoglou (2004). Panel A illustrates risk-adjusted distributions for GBPUSD futures using γ=1 (red) and γ=3 (green), together with the RND (blue) extracted from options with expiry on 8th July. Panel B illustrates risk-adjusted distributions for FTSE100 Index using γ=2 (red) and γ=4 (green), together with the RND (blue) extracted from options with expiry on 15th July.

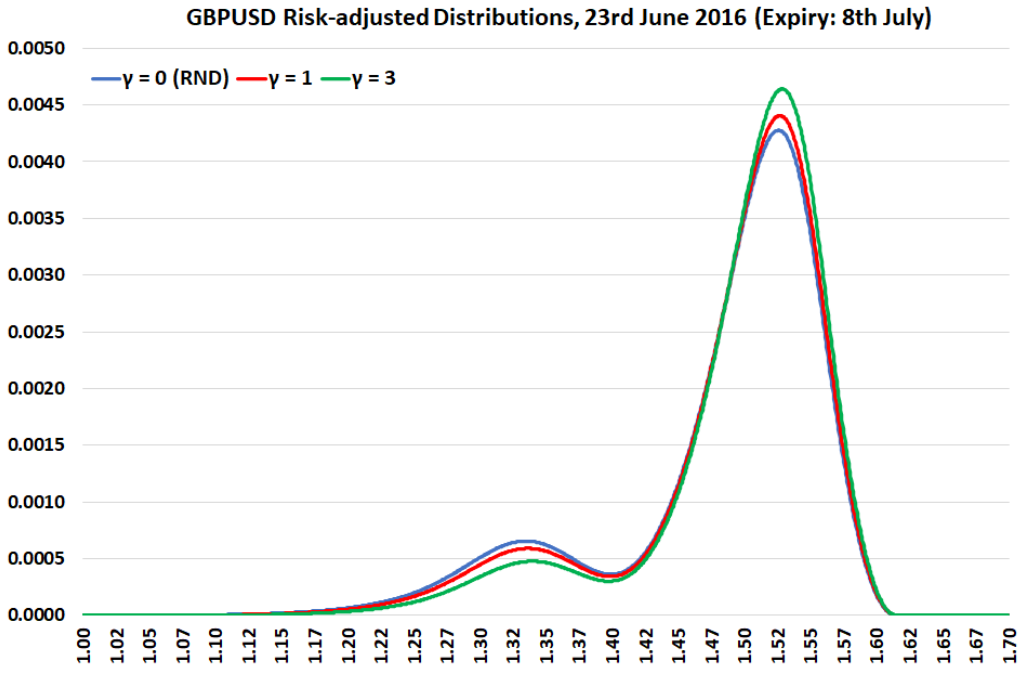

Panel A

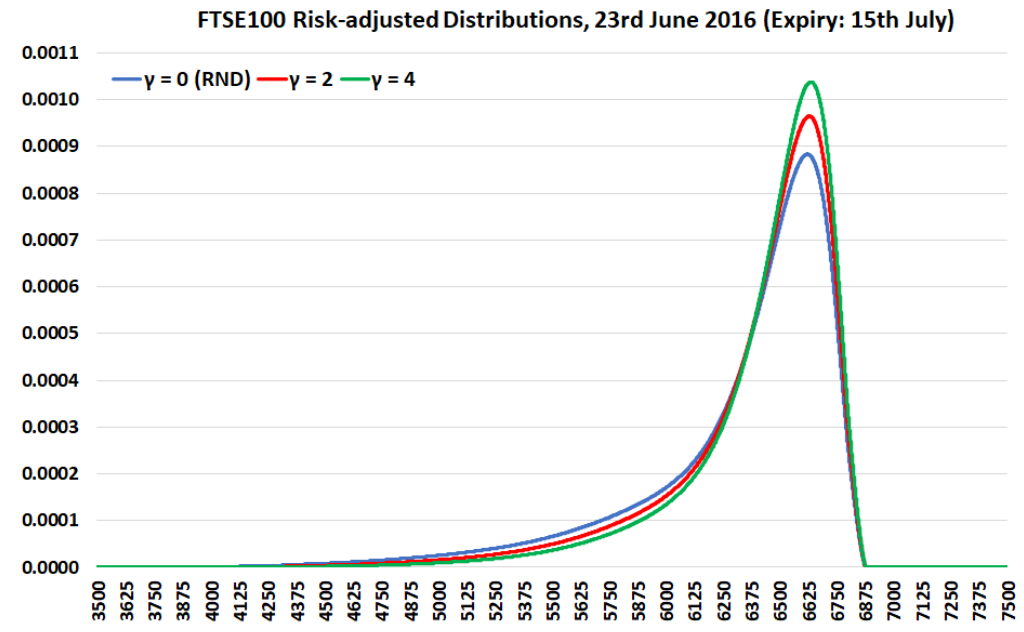

Panel B

Figure SA.4:
This Figure shows the evolution of the Slope of the IV curve, which is estimated on a daily basis by regressing the implied volatilities of out-of-the-money puts on their deltas and an intercept, from 9th May until 5th July 2016. Panel A shows the Slope estimated from options on GBPUSD futures with expiry on 3rd June (blue), 8th July (red), and 5th August 2016 (green). Panel B shows the corresponding Slope estimated from options on FTSE100 Index with expiry on 17th June (blue), 15th July (red), and 19th August 2016 (green). The vertical black line indicates the Brexit Referendum date (23rd June, 2016).

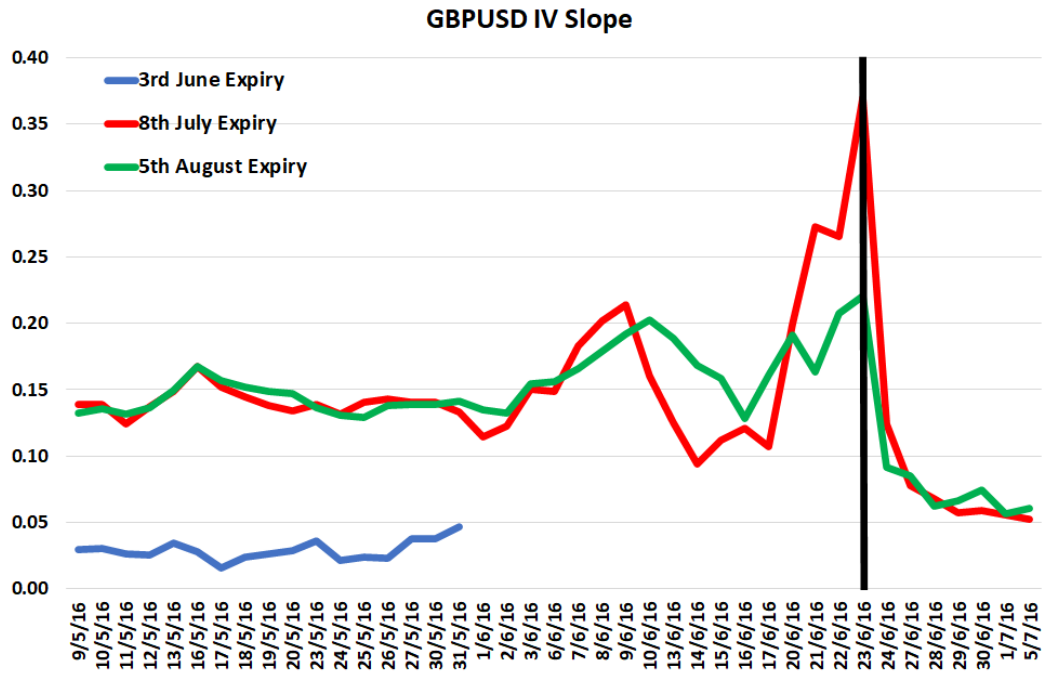

Panel A

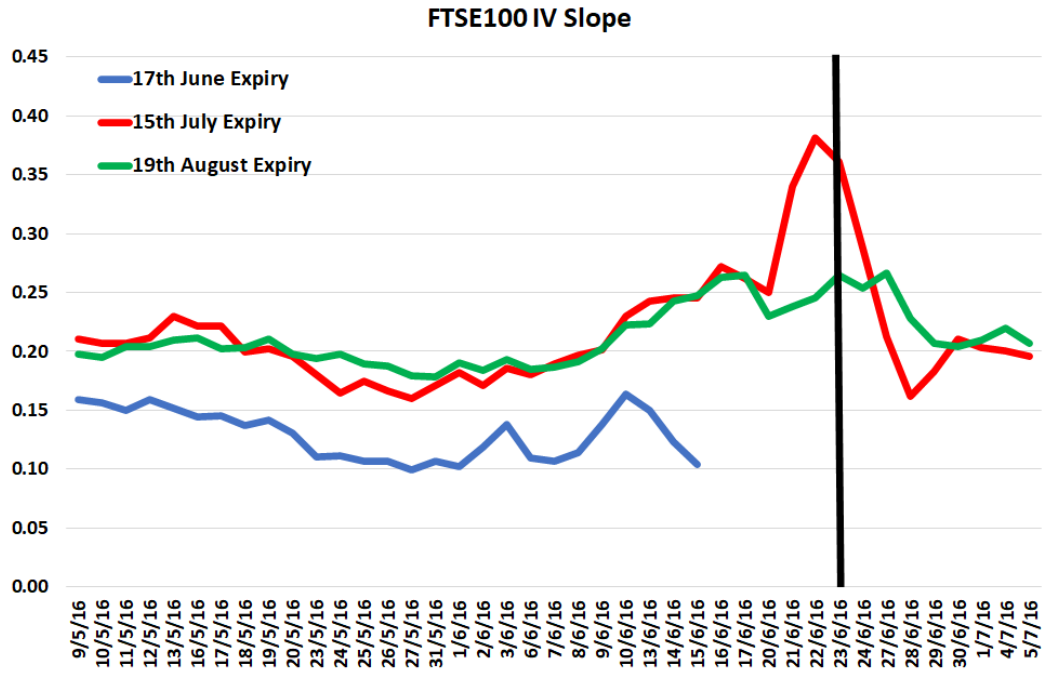

Panel B

Figure SA.5:
This Figure shows the evolution of the SKEW of the IV curve from 9th May until 5th July 2016. SKEW is computed on a daily basis as the difference between the annualized implied volatility of a deep out-of-the-money put, with delta closest to -0.25, and the annualized implied volatility of an at-the-money call, with delta closest to 0.5. Panel A shows the SKEW computed from options on GBPUSD futures with expiry on 3rd June (blue), 8th July (red), and 5th August 2016 (green). Panel B shows the corresponding SKEW computed from options on FTSE100 Index with expiry on 17th June (blue), 15th July (red), and 19th August 2016 (green). The vertical black line indicates the Brexit Referendum date (23rd June, 2016).

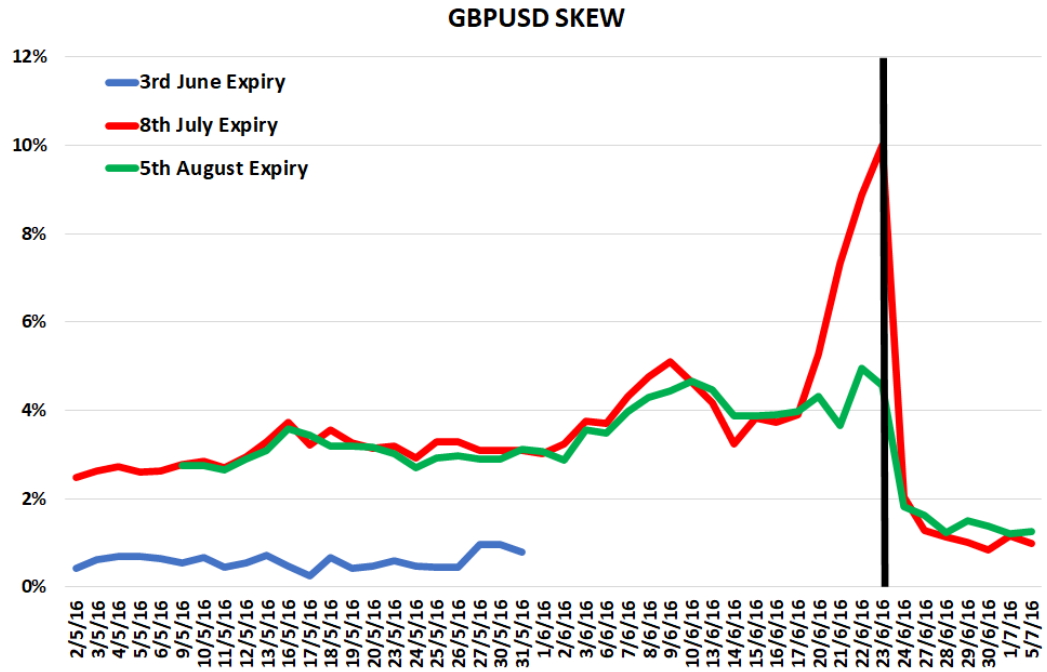

Panel A

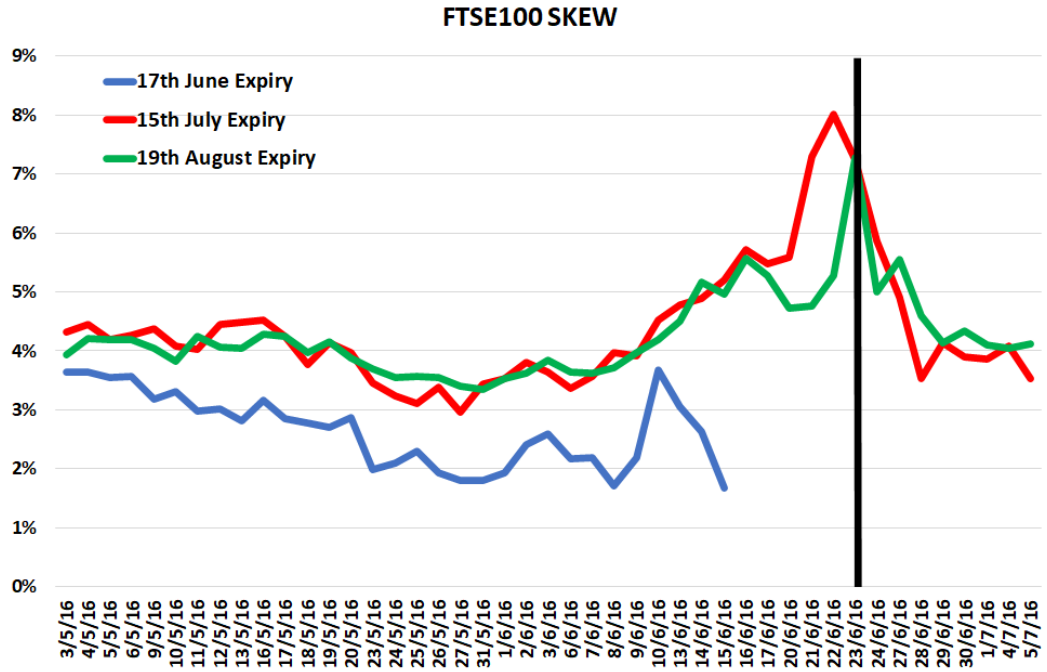

Panel B

Figure SA.6:
This Figure shows Risk-Neutral Distributions (RNDs) extracted on 23rd June (blue) and 24th June 2016 (red) from options on EuroStoxx50 Index with expiry on 15th July 2016. The mode of the RNDs is indicated on the Figure.

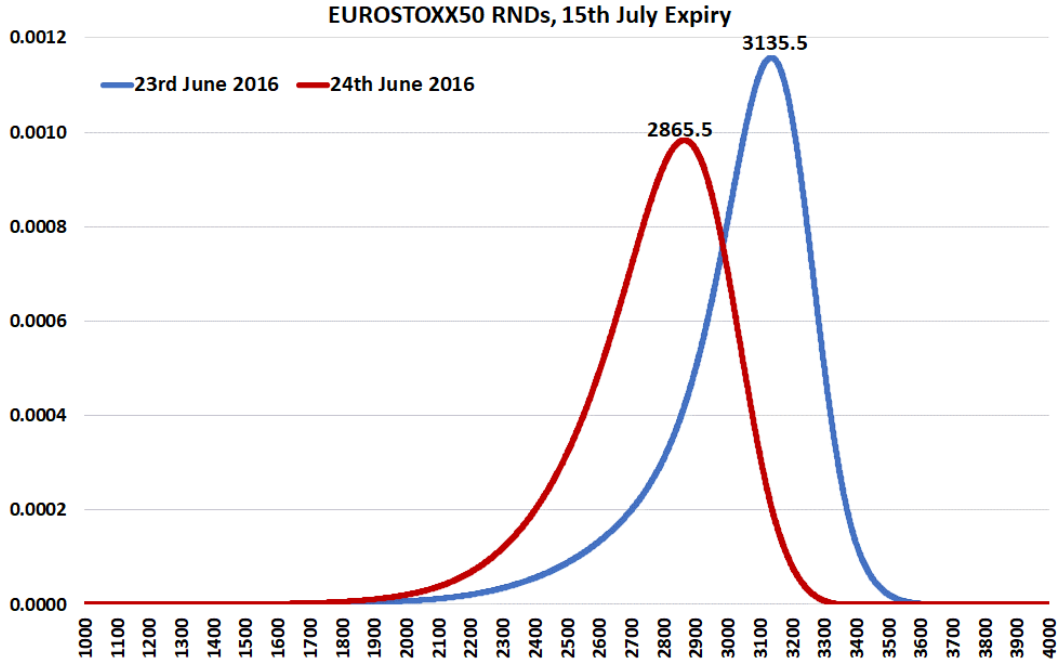

Panel A

Chapter 3

Market Quality and Price Informativeness: Evidence from Extended Trading Hours

3.1. Introduction

Understanding after-hours trading is important for market design as the development of technology has changed the structure of financial markets. There are growing interests in presenting characteristics and examining finance theories of after-hours markets (Barclay and Hendershott, 2003, 2004; Chen, Yu, and Zivot, 2012; Dungey, Fakhrutdinova, and Goodhart, 2009; Jiang, Likitapiwat, and Mcinish, 2012; Tsai, 2010). Traditional financial markets have formal opening and closing times, such as 09:30–16:00 U.S. Eastern Time[1] for core trading sessions in the New York Stock Exchange (NYSE) and the National Association of Securities Dealers Automated Quotations Exchange (NASDAQ). Electronic systems extend traditional financial markets towards trading around the clock. Since 1999 in equity markets, electronic communication networks have allowed retail investors to trade stocks when the core trading session is closed. The Chicago Mercantile Exchange provides Standard and Poor (S&P) 500 futures contract that trades from 18:00 to 17:00 (next day). In 2015, Chicago Board Options Exchange (CBOE) launched Extended Trading Hours[2] from 03:00 to 09:15 for S&P 500 options before the opening of Regular Trading Hours[3] from 09:30 to 16:15. We aim to present the features of intraday option trading and examine the impact of extended trading hours on regular trading hours.

The S&P 500 option market has certain advantages in after-hours market quality analysis. Previous literature evaluates the market quality in either after hours or regular hours. However, the direct impact of after-hours trading on regular hours trading is not clear. The S&P 500 index option market provides a quasi-natural experiment to examine the impact on market quality from the introduction of extended trading hours which is a unique event and not available in previous after-hours equity or futures markets. Moreover, the option market has different features in comparison to the equity and futures markets. Unlike the equity and futures markets, exchange designated market makers provide most liquidity in the option market. After-hours trading has been applied to the equity and futures markets for a long time while the extended trading hours option market is newly introduced and understudied. The lack of empirical evidence raises concerns about extending trading hours in other index and stock options. Finally, some forward looking information, such as implied higher moments of future asset returns, can be only estimated from the option market. The option market provides a chance to examine the relationship between the after-hours market expectation and the realized outcomes in regular trading hours.

We examine the market quality of the index option market with relatively new tick-by-tick option data. By comparing the market quality between extended and regular trading hours, we illustrate an extremely illiquid option market with lower trading activities and higher transaction costs in extended trading hours. It documents time of day market microstructure patterns in extended trading hours. Trading activities are higher and bid-ask spreads are wider at the beginning and the end of extended trading hours. Most importantly, we present a new

[1] Unless otherwise specified, all timestamps in this chapter are U.S. Eastern Time.

[2] CBOE also refers to Extended Trading Hours as Global Trading Hours.

[3] Regular Trading Hours and Core Trading Session are used interchangeably in this chapter.

intraday phenomenon that there are significant peaks of bid-ask spread after macroeconomic news announcements.

This study contributes to the literature by using CBOE's introduction of extended trading hours into the option market as a quasi-natural experiment to study the impact of incorporating extended trading hours on market quality in regular trading hours. Extended trading hours are introduced to S&P 500 index options meanwhile S&P 500 Depositary Receipts ETF options have no extended trading hours. Difference-in-differences analyses between these two option markets provide evidence of enhanced market quality from the introduction of extended trading hours in terms of bid-ask spread and information asymmetry while minimizing the impact from exogenous variables.

We explore the possible mechanisms for the changes in market quality as a consequence of the intertemporally strategic decisions of liquidity suppliers and demanders following the discussion of network effect (Madhavan, 2000) and liquidity externality (Barclay and Hendershott, 2004). Network effect and liquidity externality arise from the heterogeneously intertemporal choices of uninformed liquidity traders and informed traders. The overall outcome of the interaction of concentrated-trading liquidity traders (Admati and Pfleiderer, 1988) and aggressively competed informed traders (Holden and Subrahmanyam, 1992) is that there are little liquidity trading and substantial informed trading in extended trading hours with a reduction of informed trading in regular trading hours. As a result, market quality in extended trading hours is expected to be relatively low while market quality in regular trading hours is enhanced. It provides new evidence for the negative liquidity externality between liquidity suppliers and demanders with high adverse selection as discussed by Tham, Sojli, and Skjeltorp (2018).

This research about extended trading hours complements studies about price informativeness with liquidity conditions. Price formation is one of the most important financial market functions. On one hand, low liquidity conditions may restrict the price informativeness as a limit to arbitrage and hedging (Kerr, Sadka, and Sadka, 2020). The generally extreme illiquidity in extended trading hours may result in stale and uninformative prices, which may further indicate potential market failure. However, on the other hand, exchange designated market makers, such as Prime Market Makers in the option market, have the obligation to continuously provide bid and ask quotes and some informed traders, such as volatility information traders, may allocate their trading to extended trading hours. The participation of market makers and informed traders may be beneficial to price formation. This contrast is worth researching to what extent the extreme illiquid market in extended trading hours incorporates market information. Price informativeness is tested by comparing the option implied information in extended trading hours with realized values in regular trading hours, such as option implied index level at the close of extended trading hours vs. at the opening of the regular trading hours, and option implied volatility vs. realized volatility respectively. We present that, despite the poor market quality in extended trading hours, the option market in extended trading hours is important for incorporating market news and contains accurate expectations for the following regular trading hours.

Market participants may have a better understanding of the trading risk in the extended

trading hours option market, including low liquidity and a high probability of trading against informed traders. They may also have better trading performance by utilizing the implied information from the option market in extended trading hours, given the identified relationship between option implied index level and volatility in extended trading hours with realized values in regular trading hours.

The rest of this chapter is organized as seven parts. Section 3.2 reviews previous literature and brings the hypotheses for this study. Section 3.3 describes the data and institutional background. Section 3.4 compares the option market both in extended and regular trading hours with summary statistics. Section 3.5 tests market quality around the introduction of extended trading hours through a difference-in-differences analysis on quoted and effective spreads. Section 3.6 explores the components that explain differences in market quality by applying the spread decomposition models. Section 3.7 examines whether the option prices in extended trading hours incorporate overnight information and are informative for the following regular trading hours. Section 3.8 concludes.

3.2. Literature Review and Hypotheses Development

In classic market microstructure theory, market participants are categorized as liquidity suppliers and demanders. Liquidity demanders include uninformed liquidity traders and informed traders (Huang and Stoll, 1997; Lin, Sanger, and Booth, 1995; Madhavan, Richardson, and Roomans, 1997). On one hand, there is no strong barrier that prevents order flows between extended and regular trading hours[4]. The market structures in extended trading hours and regular trading hours are similar. In equilibrium, the trading activities and trading costs across the day should also be similar. However, on the other hand, intertemporal liquidity externality theory argues that by bringing liquidity providers and demanders together across time the trading costs will be reduced for all investors. First, intraday discretionary liquidity trading is concentrated in equilibrium (Admati and Pfleiderer, 1988, Barclay and Hendershott, 2004). If a market is already in equilibrium, as liquidity providers and suppliers congregate in regular trading hours so that the trading costs for all investors are reduced, liquidity demanders will have no incentive to move their trades out of regular trading hours as they may bear higher transaction costs. Thus, extended trading hours have a reduction in liquidity trading. Second, although informed traders may participate more actively with the concentrated liquidity trading (Admati and Pfleiderer, 1988), informed traders may still prefer immediate trading in extended trading hours rather than waiting until regular trading hours as a result of competition among informed traders (Holden and Subrahmanyam, 1992). Consequently, some informed trading may be endogenously shifted from regular trading hours to extended trading hours resulting in high adverse selection in extended trading hours. The liquidity externality between liquidity suppliers and demanders is negative when adverse selection is high (Tham, Sojli, and Skjeltorp, 2018), i.e. the increment of informed traders cannot attract more liquidity suppliers. If this

[4]Brokers need to apply for Trading Permit in extended trading hours which is independent of Trading Permit in regular trading hours. Retail investors need to be aware of the material trading risks in extended trading hours before placing orders (Rules of Cboe Exchange).

classic theory about market microstructure is correct, extremely low market quality in extended trading hours and enhanced market quality in regular trading hours will be expected.

Low market quality after hours is documented in both the equity and futures markets. After-hours market quality in terms of trading volume, transaction costs, and information asymmetry is lower in NASDAQ (Barclay and Hendershott, 2003, 2004). McInish and Wood (1992) also find similar conclusions with trading volume and transaction costs in NYSE. In the futures market, thinly traded S&P 500 and NASDAQ 100 futures also confirm the intraday concentration of trading in regular trading hours (Dungey, Fakhrutdinova, and Goodhart, 2009). What is more, Mishra and Daigler (2014) examine intraday market microstructure characteristics only in regular trading hours. We firstly extend the interest of the market microstructure characteristics in both extended and regular trading hours. Based on the theory and documented patterns in the equity and futures markets, we address the first hypothesis as

Hypothesis 1 (H1)**.** *In equilibrium, market quality and trading activity are extremely low in extended trading hours.*

Although the after-hours stock market has low trading volume, it is important for price discovery. Trades before the opening of regular hours are possibly the most informed as information asymmetry is high before markets open and low after markets close (Barclay and Hendershott, 2003). Past literature on option market quality and market design about liquidity externality mainly focuses on the impact from the spatial dimension, such as intermarket competition (Mayhew, 2002), evolution of the equity option market to a national market system (Battalio, Hatch, and Jennings, 2004). However, intertemporal liquidity externality is still under discussion (Barclay and Hendershott, 2004). The impact of after-hours trading on the following regular trading hours market quality is not examined in previous literature. The introduction of extended trading hours raises a new issue in intertemporal market design literature whether the introduction of extended trading hours has a positive impact on the existing market liquidity. Based on the classic market microstructure theory, we address the second hypothesis as

Hypothesis 2 (H2)**.** *The introduction of extended trading hours enhances the market quality in regular trading hours.*

Besides, if Hypothesis 1 is true, arbitrage and hedging may be limited as a lack of liquidity in the extended trading hours option market. Liquidity condition is one of the determinants for price informativeness, such as liquid stock prices are more informative than illiquid stock prices considering future firm earnings (Kerr, Sadka, and Sadka, 2020). It is unclear whether information is still aggregated into the option market and whether option prices contain the latest aggregate expectation in extremely illiquid markets. Previous literature provides some evidence of the price informativeness in extended trading hours. The stock prices in the pre-open session increase the efficiency of the opening prices (Barclay and Hendershott, 2008). After-hours stock realized volatility improves the predictability of stock volatility in the next day (Chen, Yu, and Zivot, 2012). According to previous evidence between after-hours trading and regular hours trading, we address the third hypothesis as

Hypothesis 3 (H3)**.** *Despite low liquidity conditions, the option prices in extended trading hours are informative for the following regular trading hours.*

The results of price informativeness also connect and contribute to the literature on volatility forecasting. We suggest the relevance of option implied volatility in one-day realized volatility forecasting. Widely used volatility forecasting models, such as Heterogeneous Autoregressive (HAR) Model (Corsi, 2009) and HAR Model with Realized Quarticity (HARQ) (Bollerslev, Patton, and Quaedvlieg, 2016), use estimates based on past intraday returns to forecast future realized volatility. Implied volatility contains additional information for future realized volatility and is an unbiased forecast in stock markets (Busch, Christensen, and Nielsen, 2011). Macroeconomic news and global trading in other economies overnight may change the expectation for future asset volatility. We test whether the index option market in extended trading hours incorporates the latest information and provides better volatility forecasts than models based on information before extended trading hours.

3.3. Data and Institutional Details

This section describes the background of CBOE's introduction of extended trading hours in the option market, the data, and the measures of market quality.

3.3.1. CBOE's S&P 500 Index Option Market

As Table 3.1 shows, CBOE provides four types of options with underlying assets related to the S&P 500 index: S&P 500 index traditional options (SPX), S&P 500 index weekly non-traditional options (SPXW)[5], S&P 500 index mini-options (XSP), and Standard & Poor's Depositary Receipts ETF options (SPY). These options share similar impacts from economic variables. CME also provides index options with underlying as S&P 500 futures which is traded in both extended and regular trading hours. As the CBOE S&P 500 index options are the most widely recognized by the market considering the trading volume, we only focus on the S&P 500 index options in CBOE.

-Table 3.1 here-

SPXW and SPY options are the treatment and the control groups respectively to minimize the impact from exogenous variables. First, since March 9, 2015, SPX and SPXW options have been traded in both extended and regular trading hours while SPY and XSP options are only traded in regular trading hours. Second, XSP options' underlying asset is at 1/10th of the S&P 500 index level. They may be less preferred by institutional investors, as reflected by their extremely low trading volume among S&P 500 options. Accordingly, XSP is excluded from

[5]CBOE added expiry dates into SPXW options over time. SPXW firstly included options with expiry dates on non-third Friday and end of the month. On August 15, 2016, CBOE launched S&P 500 Monday Weeklys for SPXW. On February 23, 2016, CBOE launched S&P 500 Wednesday Weeklys for SPXW. On May 1, 2017, CBOE changed the symbol for the existing S&P 500 third Friday PM-settled option series (SPXPM) to option symbol SPXW

this study. Third, SPXW and SPY options were traded on the same system, Hybrid Trading Platform, while SPX options were traded on Hybrid 3.0 Platform around the introduction of extended trading hours[6]. SPX options are excluded from this study as they may be affected by other market structure factors.

In the CBOE SPXW option market, trading participants are clearing trading permit holders, Electronic Access Permit (EAP) brokers, EAP customers, Lead Market Makers (LMMs), and proprietary traders[7]. Non-public and public customers trade though EAP brokers and EAP customers respectively. Based on market microstructure theory, trading participants are categorized into two groups, liquidity suppliers and liquidity demanders. Liquidity suppliers are LMMs and discretionary market makers who can be EAP brokers, EAP customers, or proprietary traders. LMMs are appointed by CBOE and have the obligation to submit continuous bid and ask quotes to the exchange[8] while discretionary market makers are other participants who act as market makers and provide liquidity based on their own circumstances. In the limit order book, the best bid and ask quotes reflect the competition outcomes of all LMMs and discretionary market makers. The main market structure difference between extended and regular trading hours is that there are only three LMMs in extended trading hours but multiple LMMs in regular trading hours.

Liquidity demanders are uninformed liquidity traders and informed traders from EAP brokers, EAP customers, and proprietary traders. Uninformed liquidity traders implement their liquidity demand by taking transaction costs, i.e. bid-ask spread, which is the profit for liquidity suppliers. While liquidity suppliers have a loss when they trade against informed traders.

Moreover, the matching algorithm for both extended and regular trading hours is the same as Price-Time Priority. The regular and extended trading hours are connected by the queuing order book for the opening process of regular trading hours. Active orders at the end of extended trading hours join the queuing order book. The opening price of the regular trading hours is determined by an open auction with the queuing order book[9].

The SPY and SPXW options have a similar market structure. Instead of LMMs, CBOE appoints one Designated Primary Market Maker (DPM) for SPY options. DPM has similar obligations like LMMs that they have to provide continuous bid and ask quotes. The difference between LMMs in SPXW market and DPM in SPY market has only limited impacts on our analysis.

3.3.2. Data and Sample

We use the trades, best bid and best ask data of SPXW and SPY options in Refinitiv DataScope Tick History Time and Sales to examine the market quality around the introduction of extended trading hours. It contains nanosecond timestamped quotes and trades for all

[6]CBOE Regulatory Circular RG17-136

[7]CBOE GTH Participants Providing Partial Access

[8]Rules of Cboe Exchange

[9]CBOE US Options opening Process

SPXW and SPY options and tick-by-tick last for the S&P 500 index. The analyses of market quality and information asymmetry (Hypothesis 1 and Hypothesis 2) are based on six months SPXW and SPY option data around CBOE's introduction of extended trading hours, from December 1, 2014 to May 31, 2015 when the S&P 500 index level was relatively stable[10] and there was no major change in option market structures (see Table 3.2).

-Table 3.2 here-

Because CBOE options are mainly electronically traded and the execution time of the trades is reliable. Trades are matched with the latest quotes. Trade direction is determined by Lee and Ready (1991) original algorithm with the most recent bid-ask quote to determine buyer- or seller-initiated trades, as Savickas and Wilson (2003) compare four classification rules for option trades: quote rule, tick rule, Lee and Ready (1991) rule, and the Ellis, Michaely, and O'Hara (2000) (EMO) rule and conclude Lee and Ready (1991) rule is slightly more accurate than EMO rule in the option market. A recent study by Li, French, and Chen (2017) also uses Lee and Ready (1991) rule with the most recent midquote. If the transaction price is higher (lower) than the midquote, the trade is buyer- (seller-) initiated. If the transaction price is equal to the midquote, the tick direction is applied: an upward (downward) tick direction indicates a buyer- (seller-) initiated trade. The moneyness of the option contract is calculated as the strike price divided by the previous day close level of the underlying index.

U.S. risk-free rate is the zero-coupon rate from OptionMetrics. Cubic spline interpolation[11] is applied to the zero-coupon rate curve to get the risk-free rate with the same time to maturity as the option contract. Daily S&P 500 dividend rate is extracted from OptionMetrics. To estimate realized volatility in extended trading hours, S&P 500 E-mini futures tick-by-tick trade data is extracted from Refinitiv DataScope.

We also use one-minute frequency SPX index level to estimate daily realized volatility and SPXW option data at 09:15, 09:30, and 16:15 in Refinitiv DataScope Tick History Intraday Summaries from the March 9, 2015 to December 31, 2018 to examine the price informativeness in extended trading hours.

SPXW and SPY option data used in this study originate from Options Price Reporting Authority (OPRA) Best-Bid-Offer (BBO). We delete records with a quote size of zero. We also delete records with the same bid and ask quotes with the same timestamp.

3.3.3. Measures of Market Quality

We use OPRA BBO data to calculate bid-ask spread as the main market quality measure, as wide (narrow) quoted and effective spreads indicate low (high) market quality. The dollar quoted spread ($) is the difference between the best bid and best ask quotes. The dollar effective spread ($) is double the difference between the midquote of BBO and the transaction price.

[10]The average daily close S&P 500 index level was 2054.41 from December 1, 2014 to February 28, 2015 and 2094.74 from March 9, 2015 to May 31, 2015. While from October 15, 2014 to November 30, 2014, the S&P 500 index level increased from 1862.49 to 2067.56 with a return as 11.01%. U.S. equity market may be in different regimes before and after December 2014.

[11]Cubic spline interpolation is conducted by MATLAB built-in function *spaps*.

The proportional quoted spread (%) and the proportional effective spread (%) are the dollar quoted spread ($) and the dollar effective spread ($) divided by midquote of BBO respectively. The average quoted spread is equally weighted by quote updates. The average effective spread is weighted by trade volume.

To adjust for the cross-sectional differences of option contracts with different strike prices and time to maturities, and present the relative changes of bid-ask spread with the same option contract in a day, we transform quoted and effective bid-ask spreads into normalized spreads as an additional market quality measure. The intraday bid-ask spread is divided by the average bid-ask spread of the day for the same option contract in the intraday analysis. It captures the intraday seasonality of bid-ask spread and minimizes the impact from the cross-section of strike prices and time to maturities.

3.4. Trading Characteristics of the S&P 500 Index Options

This section documents and compares the descriptive statistics of trading activities and liquidity in extended and regular trading hours from December 1, 2014 to May 31, 2015. It presents an initial analysis of the intraday intertemporal choices of liquidity and informed traders in the S&P 500 index option market, and examines the Hypothesis **1** that market quality and trading activity are extremely low in extended trading hours.

3.4.1. Trading Activities

Table 3.3 compares the trading activities between extended and regular trading hours for SPXW options. The summary of SPXW option trading volume is grouped by option moneyness. Realized volatility of the S&P 500 index is calculated as the annualized realized volatility from S&P 500 E-mini futures one-minute returns. Table 3.3 shows that after the introduction of extended trading hours, trading activities are extremely low in extended trading hours. Extended and regular trading hours have a similar length of trading hours, 6.25 hours vs. 6.45 hours respectively, while more than 99% volume and trades are concentrated in regular trading hours. Trading volume categorized by moneyness presents similar preferences across the day, highest trading volume with at-the-money options and little trading volume with in-the-money options. In the rest of this chapter, only out-of-money and at-the-money options are focused on. The frequency of quote changes and realized volatility are also significantly lower in extended trading hours at 1% significance level, as the frequency of quote changes is 248 vs. 821 and realized volatility is 6.64% vs. 9.97% for extended and regular trading hours respectively. However, French and Roll (1986) document that the variance of stock returns in regular trading hours is five times larger than the variance overnight. It is possible that the trading of S&P 500 E-mini futures increases the realized volatility in extended trading hours. The average trade sizes in regular trading hours are significantly larger with a large standard deviation, indicating a higher potential for large transactions in regular trading hours. In conclusion, the extremely low trading activity in extended trading hours is consistent with liquidity externality theory and the expectation of intraday decisions of liquidity and informed

traders.

-Table 3.3 here-

Figure 3.1 shows the intraday patterns of trading volume, the frequency of quote changes, and realized volatility. In panel A, during regular trading hours, they all exhibit a well-documented U-shaped pattern. Half-hour interval summary across the day confirms that the trading activities are much lower in extended trading hours. In panel B, in extended trading hours, the frequency of quote changes presents a U-shaped pattern while the realized volatility resents a J-shaped pattern. Trading activities are much higher at the end and at the beginning relative to the middle of extended trading hours. The beginning of extended trading hours in the SPXW option market is also the beginning of regular trading hours in European stock exchanges[12]. Extended trading hours connect European financial markets and the US option markets. Moreover, the high trading activities at the end of extended trading hours may be explained by two reasons. First, the macroeconomic news announcements at 08:30 are at the end of extended trading hours and may have a strong influence on the S&P 500 index. Second, the end of extended trading hours can be also regarded as the pre-open session for regular trading hours. Some trading may be shifted from the opening of regular trading hours to the pre-open session. However, this shift is relatively limited in comparison to the enormous amount of trading in regular hours.

-Figure 3.1 here-

3.4.2. Trading Costs

This part compares the dollar, proportional, and intraday normalized quoted and effective spreads between extended and regular trading hours.

Table 3.4 shows that trading costs are significantly higher in extended trading hours. Both quoted and effective spreads in extended trading hours are about twice wider in comparison to them in regular trading hours. Dollar, proportional, and intraday normalized quoted spreads decline at 1% significance level from extended trading hours to regular trading hours by $1.02, 5.97%, and 72.31% respectively. Dollar effective spread declines from extended trading hours to regular trading hours by $1.1 at 5% significance level. Proportional and intraday normalized effective spreads also decline from extended trading hours to regular trading hours by 3.23% and 117.43% at 1% significance level respectively. High trading costs in extended trading hours confirm that most liquidity traders congregate in regular trading hours as the concentration of liquidity trading can reduce overall trading costs. Moreover, high standard deviations relative to the averages of dollar and proportional spreads present the problem that direct comparison among bid-ask spreads with different moneyness and time to maturities may incorporate the information in the cross-section of option bid-ask spread.

-Table 3.4 here-

[12]There may be some small variations as the Daylight Savings Time (DST) is applied differently across countries.

Figure 3.2 shows the intraday patterns of normalized quoted spread in five-minute intervals. Panel A confirms the results in Table 3.4 that trading costs are approximately twice higher in extended trading hours after considering the intraday variations of bid-ask spread. In panel B, news announcements are scheduled macroeconomic announcements at 08:30 in U.S. Bureau of Labor Statistics Release Calendar[13] and U.S. Bureau of Economic Analysis 2014 and 2015 News Release Schedule[14]. Quoted spread is wide at the beginning and at the end relative to the rest of extended trading hours. Besides, there is a significant peak of quoted spread around 08:30 when scheduled macroeconomic announcements are released. Quoted spread increases by 60% around macroeconomic announcements on news dates while there is no such peak on non-news dates. As there is no peak in trading volume or volatility around 08:30 (see Figure 3.1), the order processing costs and inventory holding costs for market makers are not noticeably different around the macroeconomic news announcements. Thus, the temporally increased bid-ask spread is probably a result of information asymmetry as some investors may have better pricing skills for the news announcements. In panel C, the news is the Federal Open Market Committee (FOMC) Minutes at 14:00[15]. In regular trading hours option quoted spread is approximately L-shaped. Quoted spread is wider when the market opens and decreases to a relatively stable level in the rest of regular hours. When there is an FOMC Minutes announcement, quoted spread is twice wider than a regular level which is a similar pattern as 08:30 macroeconomic announcements. At 10:00, which is also the time of some macroeconomic news announcements, there is a small peak in quoted spread. The intraday peaks of quoted spread suggest the importance of macroeconomic news announcements as one determinant of market quality and imply the possible temporally increased information asymmetry in the option market.

The documented patterns in this chapter bring a new phenomenon that there are peaks of bid-ask spread around the macroeconomic announcements which is not documented in previous papers (see Chan, Chung, and Johnson, 1995, Mishra and Daigler, 2014). One main reason is that previous papers use average dollar quoted spread and we use intraday normalized quoted spread. As presented in Table 3.4, dollar quoted spread has a large standard deviation across different moneyness and time to maturities. However, intraday normalized spread controls the cross-sectional differences and compares bid-ask spread for the same option contract and therefore provides more accurate results in describing intraday dynamics.

-Figure 3.2 here-

3.4.3. Probability of Informed Trading

As discussed in Section 3.2, the theory predicts a high probability of informed trading and high adverse selection costs in extended trading hours as a result of heterogeneous preferences

[13] https://www.bls.gov/schedule/2014/home.htm; https://www.bls.gov/schedule/2015/home.htm

[14] https://www.bea.gov/news/archive?field_related_product_target_id=All&created_1=All&title=

[15] https://www.federalreserve.gov/monetarypolicy/fomchistorical2014.htm; https://www.federalreserve.gov/monetarypolicy/fomchistorical2015.htm

of liquidity and informed traders. This part tries to explain the difference in market quality between extended and regular trading hours using the Probability of Informed Trading (PIN) model (Easley, Hvidkjaer, and O' Hara, 2002). Because SPXW options are not frequently traded in extended trading hours, it is not possible to extract adverse selection costs by spread decomposition models directly. The estimated PIN is a proxy for adverse selection costs. A high PIN may explain the wide quoted and effective spreads in the extended trading hours option market, as liquidity providers require more compensation to trade against potential informed traders.

Following the PIN model, buying a call option and selling a put option are both driven by the 'good-news' in the market. Buyer-initiated call option trades and seller-initiated put option trades are regarded as buy trades for the PIN model in this study. Conversely, selling a call option and buying a put option are both driven by 'bad-news' in the market. Seller-initiated call option trades and buyer-initiated put option trades are regarded as sell trades in the PIN model. Trades are categorized into buy trades and sell trades in half-hour intervals for all SPXW options.

In each half hour interval, PIN is estimated with the extended PIN model. Assuming a Poisson arrival process, the likelihood function for each half hour is specified as:

$$\begin{aligned} L((B,S)|\theta) = (1-\alpha)e^{-\epsilon_b T}\frac{(\epsilon_b T)^B}{B!}e^{-\epsilon_s T}\frac{(\epsilon_s T)^S}{S!} \\ + \alpha\delta e^{-\epsilon_b T}\frac{(\epsilon_b T)^B}{B!}e^{-(\mu+\epsilon_s)T}\frac{((\mu+\epsilon_s)T)^S}{S!} \\ + \alpha(1-\delta)e^{-\epsilon_s T}\frac{(\epsilon_s T)^S}{S!}e^{-(\mu+\epsilon_b)T}\frac{((\mu+\epsilon_b)T)^B}{B!} \end{aligned} \tag{3.1}$$

where B and S are total buy trades and sell trades during the period, α is the probability of an information event, δ is the probability of a 'bad-news' day, ϵ_b is the arrival rate of uninformed buy orders, ϵ_s is the arrival order of uninformed sell orders, and μ is the arrival rate of informed orders, T is the length of the period, assuming that every trading day the process is independent, the parameters are estimated by Maximum Likelihood Estimation (MLE).

The probability of informed trading is the expected number of private information-based transactions to the expected total number of trades:

$$PIN = \frac{\alpha\mu}{\epsilon_b + \epsilon_s + \alpha\mu} \tag{3.2}$$

The PIN and parameters in the PIN model are estimated by pin_test function and confidence intervals are estimated by $pin\_confint$ function in R package $pinbasic$ (version 1.2.2) respectively. Table 3.5 presents empirical estimations of the PIN from December 1, 2014 to May 31, 2015. In Table 3.5 the last column shows the PIN with aggregated trades in extended and regular trading hours as 19.66% and 11.19% respectively. We further use a non-parametric bootstrap resampling to compare the PINs in ETH and RTH. Based on 10000 simulations of bootstrap, the PIN in ETH is significantly higher than the PIN in RTH at 1% significance level, which is consistent with the theoretical expectation that most liquidity traders stay in

regular trading hours and some informed traders shift their trades from regular trading hours to extended trading hours. Wide quoted and effective spreads in extended trading hours can be explained by a much higher probability of informed trading. Besides, the PIN in half-hour intervals shows the same conclusion that the PIN is significantly higher in extended trading hours.

However, Gan, Wei, and Johnstone (2017) criticize that the PIN model only weakly fits actual trade data, and suggest that using the PIN as an explanatory variable may result in unreliable results. Duarte, Hu, and Young (2020) show that the PIN fails to match the changes of noise trade. In this chapter, the PIN estimated in this section is not the sole explanatory variable for the characteristics in extended trading hours. The rest of the chapter provides other consistent evidence that the information asymmetry is higher in extended trading hours in comparison to regular trading hours based on the intraday choices of liquidity and informed traders.

-Table 3.5 here-

3.5. Market Quality around CBOE's Introduction of Extended Trading Hours

The previous section presents an illiquid option market in extended trading hours that demonstrates the difficulties of introducing extended trading hours to existing markets. It also brings the question in market design whether it is necessary to have the extended trading hours option market with low market quality. This section aims to test whether the introduction of extended trading hours enhances market quality in regular trading hours as discussed in Hypothesis 2. CBOE launched extended trading hours for SPXW and SPX options on March 9, 2015. There is no other market structure change around this event. Before the introduction of extended trading hours in the option market, private information, such as expectations of future volatility, in extended trading hours is aggregated until the opening of regular trading hours. Informed traders have to wait until the opening of regular trading hours although they may want to exploit the trading opportunities in extended trading hours. In regular trading hours, information asymmetry and adverse selection costs may be high due to the accumulated information. Liquidity providers require high compensation given the high level of information asymmetry. Therefore, relatively high quoted and effective spreads are expected before the introduction of extended trading hours. After the introduction of extended trading hours, private information in extended trading hours can be immediately incorporated into the market. Informed traders compete with each other and take an immediate transaction in extended trading hours. Information asymmetry and adverse selection costs decrease as a result of reduced informed trading in the following regular trading hours. Liquidity providers require less compensation when information asymmetry is low, resulting in relatively low quoted and effective spreads that are indications of enhanced market quality.

3.5.1. Determinants of Bid-Ask Spread

To identify the impact of the introduction of extended trading hours on bid-ask spread, variables with fixed effects have to be controlled first. Option price, trading volume, and time to maturity are the three most relevant control variables in this study.

Mayhew (2002) asserts that option price, option trading volume, and the volatility of the underlying stock are the most important control variables for bid-ask spread analysis. Anand, Hua, and McCormick (2016) also use these control variables in their panel regression. Moreover, option price is related to not only the dollar quoted spread but also the percentage quoted spread.

The underlying assets of SPXW and SPY options have similar volatility as they are proportional to the S&P 500 index level. Also, the daily differences in underlying volatility can be captured by the date fixed effect. Therefore, underlying volatility is not incorporated in our analysis.

Besides the variables described above, there is a maturity effect in implied volatility spread, as discussed by Chong, Ding, and Tan (2003) and Hsieh and Jarrow (2019). As maturity nears, the implied volatility spread increases. Anand and Weaver (2006) also use time to maturity as a control variable in their regression for bid-ask spread. Therefore, we incorporate time to maturity as the third control variable.

3.5.2. Bid-Ask Spread around the Introduction of Extended Trading Hours

Previous literature uses matched samples (Mayhew, 2002), regressions (Anand and Weaver, 2006), and categorized difference-in-differences (Anand, Hua, and McCormick, 2016) to study the impact of market structure changes on option market quality. Mayhew (2002) uses a matched sample method to control variables affecting option market quality other than multi-listing and Designated Primary Market Maker (DPM) structures. Option contracts are matched by price, volume, and volatility for all stock options in CBOE. The differences in paired option bid-ask spreads show the impact of market structure changes. Anand and Weaver (2006) use regression to analyze the impact of the DPM system. They control for the effects of maturity, moneyness, and option price with multiple-listed options. As CBOE has introduced the DPM system whereas other exchanges have not, the interaction variable between CBOE/non-CBOE and Before DPM/Post DPM presents the DPM system's impact on the option market. Anand, Hua, and McCormick (2016) categorize option contracts by their prices and conduct a difference-in-differences analysis within each option price group. They also apply panel regression with fixed entity effect and fixed date effect to confirm the results from the difference-in-differences method.

Following Anand, Hua, and McCormick (2016), and using the introduction of the extended trading hours option market as an event, we conduct a difference-in-differences analysis with controlled variables between SPXW and SPY options to analyze the impact of extended trading hours on the option market. SPY options cannot be traded in extended hours but are affected by the same information as SPXW options. Moreover, the SPDR ETF price is 1/10th

of the S&P 500 index level; hence, ten SPY option contracts are approximately the same as one SPXW option contract plus the early exercise opportunity in American options. The midquote and bid-ask spread of SPY options are multiplied by 10 to match the notional value of SPXW options.

Following Anand, Hua, and McCormick (2016), we categorize option contracts by their prices. Option midquote is the approximation for intraday updated option price. As bid-ask spread is not linearly related to option price, the difference-in-differences regression is conducted in each price category and specified as

$$\begin{aligned} Spread_{i,t,m} = \beta_0 + \beta_1 TTM_{i,t,m} + \beta_2 Mid_{i,t,m} + \beta_3 Volume_{i,t,m} \\ + \beta_4 D_t + \beta_5 D_s + \beta_6 (D_t \cdot D_s) + \varepsilon \end{aligned} \tag{3.3}$$

where $Spread_{i,t,m}$ is the average bid-ask spread (dollar quoted spread, proportional quoted spread, dollar effective spread, and proportional effective spread are separately estimated) of option contract i on day t in midquote category m; D_t is period dummy variable, which equals 1 if after March 9, 2015, and 0 if before February 28, 2015; D_s is the sample dummy variable, which equals 0 for SPY options, and 1 for SPXW options; TTM,Mid,and $Volume$ are the control variables in this study; TTM is the logarithm of days to maturity, Mid is the midquote for the corresponding bid-ask spread; and $Volume$ is the logarithm of trading volume, it is set to 0 if the trading volume is 0; β_0 is the intercept; β_1, β_2, and β_3 are the fixed effects of the control variables; β_4 is the fixed effect of time; β_5 is the fixed effect of option class; β_6 is the impact of the introduction of extended trading hours on option market quality.

If the theory about intraday decisions of liquidity and informed traders is valid and consequently the introduction of extended trading hours in the option market improves market quality as discussed in Hypothesis 2, the bid-ask spread will be reduced in the SPXW option market after the introduction of extended trading hours in comparison to the bid-ask spread changes of SPY options. The null hypothesis for bid-ask spread is $H_0 : \beta_6 = 0$. If market quality improves with extended trading hours, the null hypothesis will be rejected and β_6 will be significantly negative. Significance tests use standard errors clustered on option class, which is categorized by the underlying asset and date.

3.5.3. Empirical Results of Bid-Ask Spread

To explore the impact on bid-ask spread, this section uses five filters for sample data. First, options with midquote less than \$3 are excluded because SPXW options have a different minimum tick size from SPY options below \$3. The minimum price increments for SPXW are \$0.05 under \$3 and \$0.10 above \$3[16]. The minimum price increment for all SPY option series is \$0.01[17]. As ten SPY option contracts have approximately the same notional value as one SPXW option contract, the minimum price increments are the same only for SPY and SPXW options with prices above \$3. Also, options with prices below \$3 are far deep

[16]CBOE Regulatory Circular RG15-029

[17]CBOE Regulatory Circular RG10-051

out-of-the-money options, which are not frequently traded. Second, options with midquote greater than \$100 are also excluded. In this sample, the average one SPXW at-the-money option price is \$41 and the average price of ten SPY at-the-money options is \$53. Options with prices greater than \$100 are deep in-the-money options or long time-to-maturity options that are not liquid in the option market. Third, options with time to maturity greater than 252 business days are excluded as long time to maturity options are not active. Fourth, only at-the-money and out-of-the-money options are included in this analysis, call options with moneyness greater than 0.995 and put options with moneyness smaller than 1.005 are included in the analysis. Fifth, in the calculation of aggregate average effective spread in regular trading hours, options with volume under five contracts in a day are excluded. Such inactive options often have stale quotes that make the effective spread measure inaccurate.

Panels A, B, C, and D of Table 3.6 present the impact of CBOE's introduction of extended trading hours (the coefficient β_6 of $D_t \cdot D_s$ in equation (3.3)) on dollar quoted spread (\$), proportional quoted spread (%), dollar effective spread (\$), and proportional effective spread (%) in regular trading hours. Panels A and B of Table 3.6 show the introduction of extended trading hours reduces quoted spread by \$0.15 or 0.92% at 1% significance. The \$0.15 decrease in dollar quoted spread is economically significant as the minimum tick size is \$0.1 and the average dollar quoted spread is \$0.66 (see Table 3.4). The sample includes options with prices from \$3 to \$100, 0.92% change in proportional quoted spread is also economically significant for trading as the average percentage quoted spread is 7.07% (see Table 3.4). What is more, the bid-ask spread analysis in different option price groups confirms the overall results. The impact of the introduction of extended trading hours on dollar quoted spread increases with option prices while the impact on proportional quoted spread is higher for low price options.

Panels C and D of Table 3.6 show that the introduction of extended trading hours reduces effective spread by \$0.06 or 0.47% at 1% significance. The decreases in effective spreads are economically significant as the average dollar and percentage effective spreads are \$0.17 and 8.69% respectively. As with quoted spread, the dollar impact increases with option prices and the proportional impact is lower for options with high prices.

The adjusted R^2 in effective spread analysis is much lower than that with quoted spread, 0.41 and 0.49 for dollar and percentage quoted spreads while 0.08 for dollar and percentage effective spreads. First, the bid-ask spread analysis in this study only has two types of options, SPXW and SPY. A successful control variable in previous research, underlying asset volatility, is not able to contribute explanatory power among different S&P 500 based options. Second, the calculation of volume-weighted average effective spread in this study may be still affected by the low liquidity and stale quote. Although we require that the trading volume of one option is at least five contracts in a day to filter outliers, however, some illiquid options are still included in the study. Third, effective spread is affected by inside spread liquidity. Inside spread liquidity, such as immediate-or-cancel limit order, resulting in a lower bid-ask spread in comparison to quoted spread. Current literature has not fully researched the inside spread liquidity which makes the control variable for quoted spread hard to explain the variations of effective spread. Low adjusted R^2 for effective spread suggests the importance of further research on the inside spread liquidity.

Overall, as the empirical results in Table 3.6 show, market quality in terms of bid-ask spread is enhanced after the introduction of extended trading hours, providing direct evidence for the hypothesis that the introduction of extended trading hours enhances the market quality in regular trading hours and indirect evidence for the intraday decisions of liquidity and informed traders. Quoted and effective spreads in both dollars and percentages decrease from the pre-introduction period to the post-introduction period. The impact of the introduction of extended trading hours on bid-ask spread is both statistically significant and economically large. The null hypothesis that market quality is not enhanced with extended trading hours is, thus, rejected. It shows the importance of introducing extended trading hours into financial markets although market quality in extended trading hours is low. Market information can be incorporated into the option market immediately in extended trading hours as some informed traders move from regular trading hours to extended trading hours, information asymmetry is lower after the introduction of extended trading hours in the option market. Transaction costs are reduced as market makers require lower compensation for providing liquidity with lower information asymmetry.

-Table 3.6 here-

3.5.4. Intraday Impact on Bid-Ask Spread

Figure 3.2 in section 3.4 shows that quoted spread presents a U-shaped pattern in regular trading hours. To incorporate intraday seasonality of bid-ask spread, Table 3.7 applies the same estimations of Table 3.6 into intraday analysis, showing the impact of introducing extended trading hours (the coefficient β_6 of $D_t \cdot D_s$ in equation (3.3)) every half hour from 09:30 to 16:00.

The intraday estimations confirm extended trading hours consistently decrease quoted spread at 1% significance level across different intervals of the day. The impact on effective spread is especially high in the first half hour interval as a reduction of \$0.14 in comparison to an average reduction of \$0.06 in regular trading hours which is consistent with the theory that overnight accumulated information results in the highest information asymmetry at the beginning of regular trading hours. Moreover, the price sub-samples of intraday estimations basically support the conclusion that the introduction of extended trading hours enhances market quality.

However, there are some exceptions to Hypothesis 2. First, some results with low option prices in 09:30-10:00 interval are not significant. This is probably due to the high market volatility and initiation of quoting from market makers when markets open in regular trading hours. Second, in 14:00-14:30 interval the estimated impact from extended trading hours is not significant. As section 3.4 shows, macroeconomic news has a significant impact on quoted spread and FOMC announcements are released during 14:00 - 14:30. The exogenous shocks from FOMC announcements decrease the significance of the test. Third, the high option price sub-samples of effective spread analysis are not statistically significant or have contradicted conclusions. Trading volume with high option prices is much lower. Grouping by both option

price and time of the day results in an extreme small sample size which makes the effective spread analysis with high option price less reliable.

-Table 3.7 here-

3.5.5. Robustness Check with Bid-Ask Spread Analysis

One of the most important assumptions in difference-in-differences analysis is the parallel trend assumption. Under the assumption, before the event day, the treatment group and the control group should have a parallel trend movement when fixed effects are controlled.

We examine the parallel trend assumption with a placebo test. The only difference between the placebo test and the market quality analysis in Table 3.6 and 3.7 is the sample period. In the placebo test, the Pre-event and Post-event are both before the introduction of extended trading hours, March 9, 2015. Pre-event is from December 1, 2014 to January 14, 2015. Post-event is from January 15, 2015 to February 28, 2015. Because the placebo test contains 6-week in Pre/Post-event period rather than 3-month. Another 6-week impact is conducted in a similar way as Table 3.6 with a 6-week sample.

Table 3.8 shows the coefficient β_6 of $D_t \cdot D_s$ in equation (3.3) with placebo and 6-week tests. The placebo tests confirm there is no economically large or statistically significant change before the introduction of extended trading hours in dollar and percentage quoted spreads as the null hypothesis of $\beta_6 = 0$ is not rejected. Dollar effective spread also follows the parallel trend assumption except for the option price group from \$50 to \$100. Dollar effective spread with option price higher than \$50 are relatively less frequently traded considering the average at-the-money option prices are \$41 and \$53 for SPXW and SPY options. Percentage effective spread presents a statistically significant trend before the introduction of extended trading hours. But the effect is smaller than 6-week test as -0.18% and -0.34% for placebo and 6-week tests respectively. Overall, the 6-week tests confirm the conclusions with 3-month sample periods in Table 3.6. Dollar and percentage quoted spreads decrease by \$0.09 and 0.67% respectively in 6 weeks at 1% significance level. Dollar and percentage effective spreads decrease by \$0.06 at 10% significance level and 0.34% at 5% significance level respectively. Market quality tests with option price sub-samples also support the conclusion that market quality is improved after the introduction of extended trading hours except for the effective spread sub-samples with option prices of \$5 to \$10 and \$30 to \$50 that have smaller sample size because of the shorter sample period.

-Table 3.8 here-

3.6. Information Asymmetry around the Introduction of Extended Trading Hours

Although the decreased bid-ask spread after the introduction of extended trading hours is consistent with intraday intertemporal choices of liquidity and informed traders, other explanations may be still possible, such as heterogeneous effects on SPXW and SPY options

from the same exogenous change. This part directly examines the components of bid-ask spread around the introduction of extended trading hours using spread decomposition models. In the structure spread decomposition models, bid-ask spread is decomposed into asymmetric information costs, inventory holding costs, and order processing costs. As extended trading hours allow market information to be immediately incorporated into the market, asymmetric information costs are expected to be lower in the regular trading hours while order processing costs and inventory holding costs may remain unchanged.

3.6.1. Huang and Stoll (1997) Spread Decomposition Model

Quoted spread decomposition model (Huang and Stoll, 1997) decomposes quoted spread into order processing, adverse selection, and inventory holding components. The change in midquote reflects the private information and inventory holding costs from last trade with non-surprise information deducted and the public information component. It is specified as

$$\begin{aligned} E(x_{t-1}|x_{t-2}) &= (1-2\varphi)x_{t-2} \\ \Delta M_t &= (\alpha+\beta)\frac{s_{t-1}}{2}x_{t-1} - \alpha(1-2\varphi)\frac{s_{t-2}}{2}x_{t-2} + \varepsilon_t \end{aligned} \tag{3.4}$$

where t denotes the trade time, x_t is the trade direction, s_t is the dollar quoted spread, ΔM_t is the midquote change from time $t-1$ to time t, α measures adverse selection costs, β measures inventory holding costs, and φ is the probability that trade price reverses from time $t-1$ to time t, $1-\alpha-\beta$ measures the order processing costs.

The parameters in model (3.4) are estimated by a generalized method of moments (GMM) as GMM has very weak assumptions about the distribution and accounts for the conditional heteroscedasticity. The moments conditions of model (3.4) for GMM estimation are specified as

$$E\begin{pmatrix} (x_{t-1}-(1-2\varphi)x_{t-2}))x_{t-2} \\ (\Delta M_t - (\alpha-\beta)\frac{s_{t-1}}{2}x_{t-1} - \alpha(1-2\varphi)\frac{s_{t-2}}{2}x_{t-2})x_{t-1} \\ (\Delta M_t - (\alpha-\beta)\frac{s_{t-1}}{2}x_{t-1} - \alpha(1-2\varphi)\frac{s_{t-2}}{2}x_{t-2})x_{t-2} \end{pmatrix} = 0 \tag{3.5}$$

where α and β are estimated with boundary from 0 to 1, φ is estimated with boundary from 0.5 to 1.

In applying the quoted spread decomposition model, we use two data filters. First, for a reliable estimation of the model, the option contract needs to be traded frequently. Following Madhavan, Richardson, and Roomans (1997), only options with at least 250 trades from 09:30 to 16:00 are considered in this study. Second, following the adjustment of bunching related data (Huang and Stoll, 1997), sequential trades with the same trade price and same bid-ask quote within 3 seconds are considered as one order.

3.6.2. Lin, Sanger, and Booth (1995) Spread Decomposition Model

This part briefly reviews the spread decomposition model developed by Lin, Sanger, and Booth (1995). The effective spread can be decomposed into adverse selection and order processing components. It assumes a buy order only occurs at ask quote and a sell order only

occurs at bid quote. A sell order at time t indicates that the transaction price P_t equals bid quote B_t. With the probability of order continuation δ, the expected transaction price $E_t(P_{t+1})$ at time $t+1$ is calculated from bid quote B_{t+1} and ask quote A_{t+1} as $\delta B_{t+1} + (1-\delta)A_{t+1}$. Therefore, the conditional profit for the liquidity supplier after a sell order is specified as

$$E_t(P_{t+1}) - P_t = \delta B_{t+1} + (1-\delta)A_{t+1} - B_t \tag{3.6}$$

where P_t is the trade price, A_{t+1} and B_{t+1} are the ask quote and bid quote respectively.

Besides, as midquote is the average of bid and ask quotes $M_t = (A_t + B_t)/2$, one half of effective spread for a sell order is the difference between transaction price and midquote $z_t = P_t - M_t$. The quote revisions are assumed to be $B_{t+1} = B_t + \lambda z_t$ and $A_{t+1} = A_t + \lambda z_t$ where λ is the proportion of spread due to adverse selection. The liquidity providers' profit (equation (3.6)) is represented by effective spread as

$$\begin{aligned} E_t(P_{t+1}) - P_t &= \delta B_{t+1} + (1-\delta)A_{t+1} - B_t \\ &= \lambda z_t + (1-2\delta)[M_t - B_t] + M_t - P_t \\ &= -(1-\lambda-\theta)z_t \end{aligned} \tag{3.7}$$

where the persistence of order flow $\theta = 2\delta - 1$, the order processing costs $\gamma = 1 - \lambda - \theta$.

Since λ is the proportion of quote revision of effective spread and θ is the extent of order persistence, together with equation (3.7), parameters in effective spread decomposition model can be estimated with the regressions as follows:

$$\begin{aligned} M_{t+1} - M_t &= \lambda z_t + e_{t+1} \\ z_{t+1} &= \theta z_t + \eta_{t+1} \\ P_{t+1} - P_t &= -\gamma z_t + u_{t+1} \end{aligned} \tag{3.8}$$

where e_{t+1}, η_{t+1}, and u_{t+1} are uncorrelated, parameters λ, θ, γ are estimated by ordinary least squares (OLS) with boundary from 0 to 1. We apply the same data filters for effective spread decomposition model as specified in Huang and Stoll (1997) quoted spread decomposition model.

3.6.3. Components of Bid-Ask Spread around the Introduction

Following the theory about the intertemporal choices of liquidity and informed traders, the adverse selection costs will be reduced after the introduction of extended trading hours. In the absence of extended trading hours, asymmetric information accumulates during extended trading hours which results in high adverse selection costs in regular trading hours. With extended trading hours, the option market can incorporate information immediately and therefore reduce the information asymmetry in the following regular trading hours.

As with the analysis of bid-ask spread in section 3.5, a difference-in-differences regression for the components of bid-ask spread with control variables as with equation (3.3) is conducted

as

$$y_{i,t} = \beta_0 + \beta_1 TTM_{i,t} + \beta_2 Mid_{i,t} + \beta_3 Volume_{i,t} + \beta_4 D_t + \beta_5 D_s + \beta_6 (D_t \cdot D_s) + \varepsilon \tag{3.9}$$

where $y_{i,t}$ is α, β, $1-\alpha-\beta$, φ from model (3.4) and λ, θ, γ from model (3.8), for each difference-in-differences estimation respectively, of option contract i on day t, other variables are the same as defined for equation (3.3). Significant tests of coefficients use clustered errors on Date.

The components estimated from spread decomposition models are presented as percentages of quoted and effective spreads. We also examine the components of spreads in dollars by multiplying the components in percentages with the average quoted spread or effective spread of the day respectively. Then, the difference-in-differences regression of equation (3.9) is applied to $y_{i,t}$ in dollars.

As with bid-ask spread analysis in the previous section, if the theory of intraday decisions of liquidity and informed traders is correct and the hypothesis that market quality is enhanced with extended trading hours, information asymmetry will be reduced after the introduction of extended trading hours. Therefore, the hypothesis expects that the estimated β_6 in regression (3.9) for adverse selection costs in percentages and dollars are significantly negative.

3.6.4. Empirical Results

The last column in Table 3.9 reports the coefficient β_6 of $D_t \cdot D_s$ in equation (3.9), showing economically large and statistically significant reduction in adverse selection costs after the introduction of extended trading hours for both quoted and effective spreads. After the introduction of extended trading hours, proportional adverse selection costs decrease by 5.13% and 8.38% for quoted and effective spread respectively at 1% significance level. Similarly, adverse selection costs in dollars decrease by 0.75¢ and 0.47¢ for quoted and effective spread respectively at 5% significance level. Meanwhile, order processing costs increase by 10.28% at 1% significance level and 4.27% at 5% significance level for quoted and effective spread respectively. Order processing costs in dollars are not significantly different around the introduction of extended trading hours.

Therefore, enhanced market quality is due to declined adverse selection costs. Both bid-ask spread and information asymmetry confirm the hypothesis that market quality is enhanced by incorporating extended trading hours, indicating the benefits of after-hours trading for the core trading sessions.

However, the dollar changes in the components of bid-ask spread are much smaller than the bid-ask spread changes estimated in the previous section. First, to have reliable estimations from spread decomposition models, we only focus on the options with at least 250 trades per day which are only liquid options. The sample in information asymmetry analysis is only a portion of the sample in bid-ask spread analysis. Second, the BBO data only contains the best bid and ask quotes in the limit order book while in markets there are inside spread liquidity, e.g. immediate-or-cancel limit order may be executed inside bid-ask spread but this order will

not enter the order book if it is not executed. The inside spread liquidity is not considered in the spread decomposition models.

-Table 3.9 here-

3.7. Predictability and Price Informativeness

This section tests the price informativeness in the extended trading hours option market and examines the Hypothesis 3 that the option prices in extended trading hours are informative for the following regular trading hours. It presents that in the extreme illiquid condition, the put-call parity implied index level and the option implied volatility still update efficiently and predict the index opening level and realized volatility in the following regular trading hours respectively.

3.7.1. Put-Call Parity Implied Index Level

The underlying asset of S&P 500 weekly options is the S&P 500 index which is not available in extended trading hours. Traded S&P 500 derivatives in extended trading hours include S&P 500 futures and S&P 500 Emini futures. However, the expiry dates of S&P 500 futures and S&P 500 E-mini futures are different from the expiry dates of S&P 500 weekly options. The option implied index from put-call parity may provide independent information about the S&P 500 index level.

Because there may be deviations from put-call parity (Cremers and Weinbaum, 2010) and other market microstructure effects, intraday option implied index level is not necessarily the same as the index levels in regular trading hours. Option implied index level at the close of extended trading hours $S_{ETH,t}$, at the opening of regular trading hours $S_{Open,t}$, and at the end of regular trading hours $S_{Close,t}$ on day t from put-call parity are specified as option implied futures with the shortest time to maturity

$$S_{i,t} = c_t + Xe^{-rT} - p_t \tag{3.10}$$

where c_t and p_t are call and put option last midquote at 09:15, 09:30, 16:15 on day t for option implied index level $S_{ETH,t}$, $S_{Open,t}$, and $S_{Close,t}$ respectively, X is the strike price, r is risk-free rate, T is the time to maturity. The average of put-call parity implied index levels across different moneyness with the shortest time to maturity is used as the option implied index level. Option implied index overnight return, extended trading hours return, opening return are calculated as the log return of option implied index level respectively.

3.7.2. Option Implied Volatility and Realized Volatility

We follow Bakshi, Kapadia, and Madan (2003) model free implied volatility to extract option implied volatility. Before applying model free implied volatility, option data is filtered by no-arbitrage rule and minimum number of contracts rule. First, if call (put) options with

higher (lower) strike prices have higher or the same prices for the same time to maturity, they will be excluded from this study. Second, after no-arbitrage rule, an option expiry date with no more than 10 option contracts is excluded. Then, the model free implied volatility with discrete out-of-the-money strike prices is approximated as

$$\begin{aligned} M_1 &= e^{rT} - 1 \\ M_2 &= \frac{2}{S_0^2}[\sum_{XP_i} p_i(XP_i - XP_{i-1}) + \sum_{XC_i} c_i(XC_i - XC_{i-1})] \\ IV &= [e^{rT}M_2 - M_1^2]^{\frac{1}{2}} \end{aligned} \tag{3.11}$$

where S_0 is the corresponding option implied index level estimated from formula (3.10), XP_i and p_i are out-of-the-money put option strike price and option price, XC_i and c_i are out-of-the-money call option strike price and option price.

Daily realized volatility is estimated as

$$RV_t = \sqrt{(\sum_{i=1}^{M} r_{t,i}^2)} \tag{3.12}$$

where M is 390 for one-minute return and 78 for five-minute return, $r_{t,i}$ is the logarithm return of the S&P 500 index last level in regular trading hours.

3.7.3. Overnight Changes in the Option Market

In the absence of extended trading hours, the opening process of the option market from 09:15 to 09:30 plays an important role in incorporating overnight information. Overnight changes between the close in previous day and the open in regular trading hours in the option market is fully determined by the opening process. However, extended trading hours provide an opportunity to timely update overnight information. It is not clear whether the opening process still contribute to price discovery with extended trading hours. We compare the option implied index level and implied volatility at 16:15 previous day, 09:15, and 09:30. The opening process is trivial if overnight changes from 16:15 previous day to 09:15 fully explain extended trading hours changes from 16:15 previous day to 09:30. Table (3.10) describes the summary statistics of overnight returns/changes from 16:15 previous day to 09:30, extended trading hours returns/changes from 16:15 previous day to 09:15, opening returns/changes from 09:15 to 09:30 for option implied index level and implied volatility respectively. The average overnight option implied index return is economically and statistically close to zero. Most overnight standard deviation is reflected in extended trading hours. The extended trading hours determine the option implied index level at the opening. Similar to option implied index level, option implied volatility mainly changes in extended trading hours. However, option implied volatility presents a significant negative overnight change as -2.32% and the opening process shows a non-trivial change in option implied volatility. The information incorporation process may be limited as a result of illiquid option market in extended trading hours. Unlike S&P 500 index level, the opening process of the open market still play an important role in

determining the opening value of option prices.

-Table 3.10 here-

This part further quantifies how much overnight changes are explained by extended trading hours. If the option market is efficient in extended trading hours, overnight information will be timely updated in the option market. Extended trading hours changes will reflect most overnight changes.

Option implied index level and implied volatility at the close of extended trading hours is compared with option implied index level and implied volatility at the opening of regular trading hours respectively as

$$r_{o,t} = \alpha_r + (\beta_r - 1) r_{e,t} + \epsilon_{r,t} \tag{3.13a}$$

$$\Delta IV_{o,t} = \alpha_{IV} + (\beta_{IV} - 1) \Delta IV_{e,t} + \epsilon_{IV,t} \tag{3.13b}$$

where $r_{o,t}$ and $r_{e,t}$ are the log returns of option implied index level from 16:15 on day $t-1$ to 09:30 and 09:15 on day t respectively, $IV_{o,t}$ and $IV_{e,t}$ are the differences between option implied volatility from 16:15 on day $t-1$ to 09:30 and 09:15 on day t respectively, the null hypothesis is that the extended trading hours option market incorporates the information about the underlying index level and implied volatility, α and β are close to zero and insignificant, the adjusted R^2 is close to 100%.

Put-call parity implied index level and option implied volatility are estimated from March 9, 2015 to December 31, 2018. Table 3.11 shows the estimation of regression equation (3.13). Panel A proves put-call parity implied S&P 500 index level estimated at 09:15 is consistent with the opening level of the S&P 500 index at 09:30. Overnight information about the index level is fully incorporated into the option market. As the adjusted R^2 is 0.97, α and β are statistically and economically zero, extended trading hours update all information related to the S&P 500 index overnight and the opening process of regular trading hours from 09:15 to 09:30 provides little contribution to price discovery.

Panel B of Table 3.11 shows information about option implied volatility is not fully incorporated into the option market during extended trading hours as the adjusted R^2 is 0.88, α and β are statistically different from zero. It is consistent with the overnight implied volatility changes summary statistics. The opening process of option market is still important for the opening level of S&P 500 index implied volatility which may be a result of the extremely low liquidity in extended trading hours. The results support the hypothesis that option prices timely incorporate market information in extended trading hours and are informative for the following regular trading hours.

-Table 3.11 here-

3.7.4. Realized Volatility Forecasting

Previous part shows extended trading hours reflect most overnight changes of implied volatility. This part explores whether the implied volatility at the end of extended trading

hours provides additional information about the realized volatility in regular trading hours in comparison to the implied volatility at the close of regular trading hours on the previous day.

We apply two widely realized volatility forecasting models, Heterogeneous Autoregressive model (HAR) (Corsi, 2009) and Heterogeneous Autoregressive with Realized Quarticity model (HARQ) (Bollerslev, Patton, and Quaedvlieg, 2016) models, and Implied Volatility for one-day Realized Volatility (RV) forecasting. Besides, following the idea of Busch, Christensen, and Nielsen (2011), implied volatility is incorporated into HAR and HARQ models to examine whether implied volatility in extended trading hours has additional information for the realized volatility in the following regular trading hours. Realized volatility forecasting models with implied volatility at the close of previous trading day (IV_{t-1}^{RTH}) are benchmarks while models with implied volatility at the end of extended trading hours (IV_t^{ETH}) are the tested models. The stardard HAR model is

$$RV_t = \alpha + \gamma_1 RV_{t-1} + \gamma_2 RV_{t-5,t-1} + \gamma_3 RV_{t-22,t-1} + \varepsilon_t \tag{3.14}$$

and HAR models with implied volatility are specified as

$$RV_t = \alpha + \gamma_1 RV_{t-1} + \gamma_2 RV_{t-5,t-1} + \gamma_3 RV_{t-22,t-1} + \beta_1 IV_{t-1}^{RTH} + \varepsilon_t \tag{3.15a}$$

$$RV_t = \alpha + \gamma_1 RV_{t-1} + \gamma_2 RV_{t-5,t-1} + \gamma_3 RV_{t-22,t-1} + \beta_1 IV_t^{ETH} + \varepsilon_t \tag{3.15b}$$

where RV_t and RV_{t-1} are the realized volatilities on day t and $t-1$, $RV_{t-5,t-1}$ and $RV_{t-22,t-1}$ are average realized volatilities in previous 5 days and 22 days respectively, IV_{t-1}^{RTH} IV_t^{ETH} are the model free implied volatility from formula (3.11) at 16:15 on day $t-1$ and at 09:15 on day t respectively.

The standard HARQ model is

$$RV_t = \alpha + \gamma_1 RV_{t-1} + \gamma_2 RV_{t-5,t-1} + \gamma_3 RV_{t-22,t-1} + \gamma_4 RV_{t-1} RQ_{t-1}^{1/2} + \varepsilon_t \tag{3.16}$$

and HARQ models with implied volatility are specified as

$$RV_t = \alpha + \gamma_1 RV_{t-1} + \gamma_2 RV_{t-5,t-1} + \gamma_3 RV_{t-22,t-1} + \gamma_4 RV_{t-1} RQ_{t-1}^{1/2} + \beta_1 IV_{t-1}^{RTH} + \varepsilon_t \tag{3.17a}$$

$$RV_t = \alpha + \gamma_1 RV_{t-1} + \gamma_2 RV_{t-5,t-1} + \gamma_3 RV_{t-22,t-1} + \gamma_4 RV_{t-1} RQ_{t-1}^{1/2} + \beta_1 IV_t^{ETH} + \varepsilon_t \tag{3.17b}$$

where $RQ_{t-1} \equiv \frac{M}{3} \sum_{i=1}^{M} r_{t,i}^4$, and other variables are the same as formula 3.15.

Besides, we also compare the predictability of IV as a sole explanatory variable. Assuming RV is linearly related to IV, implied volatility models are specified as

$$RV_t = \alpha + \beta_1 IV_{t-1}^{RTH} + \varepsilon_t \tag{3.18a}$$

$$RV_t = \alpha + \beta_1 IV_t^{ETH} + \varepsilon_t \tag{3.18b}$$

where all variables are the same as formula 3.15.

Following Patton (2011), Mean Squared Error (MSE) and QLIKE loss function (formula 3.19) with Diebold-Mariano Test are used to evaluate out-of-sample realized volatility forecasting performance.

$$QLIKE = \frac{\hat{\sigma}^2}{\sigma^2} - log\frac{\hat{\sigma}^2}{\sigma^2} - 1 \tag{3.19}$$

where $\hat{\sigma}$ is the market realized volatility, σ is the model forecasted realized volatility.

The null hypothesis for volatility forecasting is that the option market in extended trading hours contains no additional information for the realized volatility in the following regular trading hours. MSE and QLIKE of models with implied volatility in extended trading hours are not significantly lower than those measures of models with implied volatility at previous market close.

Figure 3.3 shows the time series of implied volatility at 09:15 and realized volatility in the following regular trading hours. Panels A and B present that daily movements of realized volatility based on one-minute and five-minute returns are similar. Extended trading hours implied volatility is highly correlated with the following regular trading hours realized volatility, especially from a low volatility regime to a high volatility regime, which is hardly captured by historical realized volatility models.

-Figure 3.3 here-

Table 3.12 examines whether extended trading hours incorporates updated expectation for realized volatility forecasting. After the incorporation of implied volatility at the end of extended trading hours, in-sample and out-of-sample predictability of HAR and HARQ models are improved. With implied volatility, the in-sample adjusted R^2 increases from 75.44% to 82.15% for HAR model, from 75.41% to 82.16% for HARQ model, respectively. The out-of-sample MSE decreases from 2.81×10^{-6} to 2.14×10^{-6} for HAR model, from 3.07×10^{-6} to 2.26×10^{-6} for HARQ model. The improvement of out-of-sample predictability is significant at 1% significance level.

Implied volatility at the end of extended trading hours also provides additional information in comparison to implied volatility at the end of previous trading day. The in-sample adjusted R^2 increases from 77.78% to 82.15% for HAR-IV model, from 77.79% to 82.16% for HARQ-IV model, and from 67.3% to 72% for IV model respectively. The out-of-sample MSE decreases from 2.74×10^{-6} to 2.14×10^{-6} for HAR-IV model, from 2.96×10^{-6} to 2.26×10^{-6} for HARQ-IV model, and from 4.12×10^{-6} to 2.9×10^{-6} for IV model respectively. QLIKE decreases from 0.033 to 0.027 for HAR model, from 0.034 to 0.028 for HARQ model, and from 0.055 to 0.038 for IV model respectively. The improvement of out-of-sample predictability is significant at 1% significance level for all models based on Diebold-Mariano test. Implied volatility as the sole explanatory is less accurate as HAR-IV or HARQ-IV models.

-Table 3.12 here-

Overall, the extended trading hours option market provides informative prices for the following regular trading hours despite the extremely low trading activity in extended trading hours, indicating a strong price formation function. The overnight index return and implied volatility changes are mainly reflected in extended trading hours. Option implied volatility in extended trading hours contains additional information for realized volatility forecasting in the regular trading hours.

3.8. Conclusions

We examine extended trading hours in the option market by comparing extended trading hours vs. regular trading hours, SPXW options vs. SPY options, and pre-introduction vs. post-introduction. We present the intraday market quality, discusses the intertemporal decisions of liquidity and informed traders, and shows the option implied information in the option market.

On one hand, despite potential impacts from global financial markets in extended trading hours and intertemporal liquidity externality from regular trading hours, market quality and trading activity are significantly lower in extended trading hours. The discretionary liquidity traders are still concentrated in regular trading hours while a few informed traders prefer immediate trading in extended trading hours. High trading risk suggests the difficulties for policymakers and exchange owners to provide extended trading hours.

On the other hand, the introduction of extended trading hours in the option market improves market quality in regular trading hours, according to the difference-in-differences analysis between SPXW and SPY options around CBOE's introduction of extended trading hours. Market quality measures in terms of quoted and effective spreads show the enhanced market quality across different option categories during regular trading hours as a result of a reduced accumulation of asymmetric information overnight.

Extended trading hours also change the price formation process overnight and provide informative option prices for the following regular trading hours. Although the liquidity of the option market is extremely low, the option market successfully incorporates updated information in extended trading hours. The opening process of regular trading hours plays a relatively small part in determining the option pricing factors after introducing extended trading hours, including the put-call parity implied index level and implied volatility. What is more, implied volatility in extended trading hours contains incremental information in comparison to models based on information in the previous day for one-day realized volatility forecasting.

References

Admati, A. R. and Pfleiderer, P. (1988) A theory of intraday patterns: Volume and price variability. *Review of Financial Studies* 1.1, pp. 3–40.

Anand, A., Hua, J., and McCormick, T. (2016) Make-take structure and market quality: Evidence from the U.S. options markets. *Management Science* 62.11, pp. 3271–3290.

Anand, A. and Weaver, D. G. (2006) The value of the specialist: Empirical evidence from the CBOE. *Journal of Financial Markets* 9.2, pp. 100–118.

Bakshi, G., Kapadia, N., and Madan, D. (2003) Stock Return Characteristics, Skew Laws, and the Differential Pricing of Individual Equity Options. *Review of Financial Studies* 16.1, pp. 101–143.

Barclay, M. J. and Hendershott, T. (2003) Price Discovery and Trading After Hours. *Review of Financial Studies* 16.4, pp. 1041–1073.

Barclay, M. J. and Hendershott, T. (2004) Liquidity Externalities and Adverse Selection: Evidence from Trading after Hours. *Journal of Finance* 59.2, pp. 681–710.

Barclay, M. J. and Hendershott, T. (2008) A comparison of trading and non-trading mechanisms for price discovery. *Journal of Empirical Finance* 15.5, pp. 839–849.

Battalio, R., Hatch, B., and Jennings, R. (2004) Toward a National Market System for U.S. Exchange–listed Equity Options. *Journal of Finance* 59.2, pp. 933–962.

Bollerslev, T., Patton, A. J., and Quaedvlieg, R. (2016) Exploiting the errors: A simple approach for improved volatility forecasting. *Journal of Econometrics* 192.1, pp. 1–18.

Busch, T., Christensen, B. J., and Nielsen, M. Ø. (2011) The role of implied volatility in forecasting future realized volatility and jumps in foreign exchange, stock, and bond markets. *Journal of Econometrics* 160.1, pp. 48–57.

Chan, K., Chung, Y. P., and Johnson, H. (1995) The Intraday Behavior of Bid-Ask Spreads for NYSE Stocks and CBOE Options. *Journal of Financial and Quantitative Analysis* 30.3, pp. 329–346.

Chen, C.-H., Yu, W.-C., and Zivot, E. (2012) Predicting stock volatility using after-hours information: Evidence from the NASDAQ actively traded stocks. *International Journal of Forecasting* 28.2, pp. 366–383.

Chong, B.-S., Ding, D., and Tan, K.-H. (2003) Maturity Effect on Bid-Ask Spreads of OTC Currency Options. *Review of Quantitative Finance and Accounting* 21.1, pp. 5–15.

Corsi, F. (2009) A Simple Approximate Long-Memory Model of Realized Volatility. *Journal of Financial Econometrics* 7.2, pp. 174–196.

Cremers, M. and Weinbaum, D. (2010) Deviations from Put-Call Parity and Stock Return Predictability. *Journal of Financial and Quantitative Analysis* 45.2, pp. 335–367.

Duarte, J., Hu, E., and Young, L. (2020) A comparison of some structural models of private information arrival. *Journal of Financial Economics* 135.3, pp. 795–815.

Dungey, M., Fakhrutdinova, L., and Goodhart, C. (2009) After-hours trading in equity futures markets. *Journal of Futures Markets* 29.2, pp. 114–136.

Easley, D., Hvidkjaer, S., and O' Hara, M. (2002) Is Information Risk a Determinant of Asset Returns? *Journal of Finance* 57.5, pp. 2185–2221.

Ellis, K., Michaely, R., and O'Hara, M. (2000) The Accuracy of Trade Classification Rules: Evidence from Nasdaq. *Journal of Financial and Quantitative Analysis* 35.4, pp. 529–551.

French, K. R. and Roll, R. (1986) Stock return variances: The arrival of information and the reaction of traders. *Journal of Financial Economics* 17.1, pp. 5–26.

Gan, Q., Wei, W. C., and Johnstone, D. (2017) Does the Probability of Informed Trading Model Fit Empirical Data? *Financial Review* 52.1, pp. 5–35.

Holden, C. W. and Subrahmanyam, A. (1992) Long-Lived Private Information and Imperfect Competition. *Journal of Finance* 47.1, pp. 247–270.

Hsieh, P. and Jarrow, R. (2019) Volatility Uncertainty, Time Decay, and Option Bid-Ask Spreads in an Incomplete Market. *Management Science* 65.4, p. 1833.

Huang, R. D. and Stoll, H. R. (1997) The Components of the Bid-Ask Spread: A General Approach. *Review of Financial Studies* 10.4, pp. 995–1034.

Jiang, C. X., Likitapiwat, T., and Mcinish, T. H. (2012) Information Content of Earnings Announcements: Evidence from After-Hours Trading. *Journal of Financial and Quantitative Analysis* 47.6, pp. 1303–1330.

Kerr, J., Sadka, G., and Sadka, R. (2020) Illiquidity and Price Informativeness. *Management Science* 66.1, pp. 334–351.

Lee, C. M. C. and Ready, M. J. (1991) Inferring Trade Direction from Intraday Data. *Journal of Finance* 46.2, pp. 733–746.

Li, W.-X., French, J. J., and Chen, C. C.-S. (2017) Informed trading in S&P index options? Evidence from the 2008 financial crisis. *Journal of Empirical Finance* 42, pp. 40–65.

Lin, J.-C., Sanger, G., and Booth, G. (1995) Trade size and components of the bid-ask spread. *Review of financial studies* 8.4, pp. 1153–1183.

Madhavan, A. (2000) Market microstructure: A survey. *Journal of Financial Markets* 3.3, pp. 205–258.

Madhavan, A., Richardson, M., and Roomans, M. (1997) Why Do Security Prices Change? A Transaction-Level Analysis of NYSE Stocks. *Review of Financial Studies* 10.4, pp. 1035–1064.

Mayhew, S. (2002) Competition, Market Structure, and Bid-Ask Spreads in Stock Option Markets. *Journal of Finance* 57.2, pp. 931–958.

McInish, T. H. and Wood, R. A. (1992) An Analysis of Intraday Patterns in Bid/Ask Spreads for NYSE Stocks. *Journal of Finance* 47.2, pp. 753–764.

Mishra, S. and Daigler, R. T. (2014) Intraday Trading and Bid–Ask Spread Characteristics for SPX and SPY Options. *Journal of Derivatives* 21.3, p. 70.

Patton, A. J. (2011) Volatility forecast comparison using imperfect volatility proxies. *Journal of Econometrics* 160.1, pp. 246–256.

Savickas, R. and Wilson, A. J. (2003) On Inferring the Direction of Option Trades. *Journal of Financial and Quantitative Analysis* 38.4, pp. 881–902.

Tham, W. W., Sojli, E., and Skjeltorp, J. A. (2018) Cross-sided liquidity externalities. *Management Science* 64.6, pp. 2901–2929.

Tsai, I.-C. (2010) Order imbalances from after-hours trading. *Applied Financial Economics* 20.12, pp. 983–987.

Table 3.1: Comparison of S&P 500 options.

This table compares options directly or indirectly related to the S&P 500 index provided by CBOE. The information is extracted from the CBOE website.

S&P 500 Options	S&P 500 PM-settled Traditional	S&P 500 3rd Fridays Options	S&P 500 weeklys options	S&P 500 Mini options	SPDR ETF options
Option Root Ticker	SPX	SPXPM	SPXW	XSP	SPY
Underlying	S&P 500 index	S&P 500 index	S&P 500 index	0.1× S&P 500 index	SPDR ETF
Settlement Type	AM-settled	PM-settled	PM-settled	PM-settled	PM-settled
Settlement Date	3rd Fridays	3rd Fridays	Monday, Wednesday, Friday weeklys. End of the month	Fridays	Fridays or End of Quarters
Settlement Type	Cash	Cash	Cash	Cash	Physical ETF
Exercise Style	European	European	European	European	American
Extended Hours Trading	Yes	Yes	Yes	No	No
Note		SPXPM ticker merged to SPXW on May 1st, 2017	SPX Monday Weeklys - Launched August 15th, 2016 SPX Wednesday Weeklys - Launched February 23rd, 2016		

Table 3.2: Market structure changes of S&P 500 options.
This table shows the market structure changes of S&P 500 weeklys and S&P 500 ETF options from 2014 to 2015.

Effective Date	Regulatory Circular	Applicable on SPXW/SPY	Content
January 30, 2014	RG14-010	SPXW	· Expansion of Number of Expirations
February 1, 2014	RG13-158	SPXW	· Changes to the Fees Schedule for CBOE
September 5, 2014	RG14-130	SPY	· Amendment to Increase $1 Strikes
November 1, 2014	RG14-125	SPXW	· Implementation of SPX Combo Order Indicator
November 14, 2014	RG14-158	SPXW/SPY	· Bid-Ask Differentials and Minimum Quote Size
December 1, 2014	RG14-170	SPXW	· Changes to the Fees Schedule for CBOE
January 26, 2015	RG15-006	SPXW/SPY	· New Quote Risk Monitor (QRM) Features
October 9, 2015	RG15-142	SPY/SPXW	· Multi-Class Broad-Based Index Spread Orders
From September 27, 2012 to July 12, 2015	RG12-132, RG13-148, RG15-009	SPY	· A pilot program that eliminates position and exercise limits for physically-settled options
November 2, 2015	RG15-154	SPXW	· Changes to the Fees Schedule for CBOE

Table 3.3: Summary statistics of trading activities in extended and regular trading hours. This table shows the averages and standard deviations of daily trading volume[18], trade size, number of trade, and frequency of quote changes per contract of SPXW options. S&P 500 index volatility is proxied by realized volatility of S&P 500 E-mini futures. The last column shows the average differences between extended and regular trading hours with the two-sample t-test. The sample period is from December 1, 2014 to May 31, 2015. ***, **, and * indicate statistical significance at 1%, 5%, and 10% levels, respectively.

	Extended Hours		Regular Hours		Diff
	Mean	Std. Dev.	Mean	Std. Dev.	
Aggregate Volume	227	520	377523	140538	-377296***
ATM Volume	182	421	241676	92790	-241493***
Near OTM Volume	42	175	99709	47528	-99667***
Deep OTM Volume	2	15	35446	27904	-35444***
Near ITM Volume	0	1	437	539	-437***
Deep ITM Volume	1	6	307	1691	-306*
Trade Size	11	56	27	132	-16***
Number of Trades	43	37	13987	5006	-13945***
Number of Quote Changes	248	473	821	623	-574***
Realized Volatility	6.64%	2.80%	9.97%	3.53%	-3.33%***

[18]ATM options have moneyness from 0.95 to 1.05. Near ITM (OTM) options are call (put) options with moneyness from 0.85 to 0.95 and put (call) options with moneyness from 1.05 to 1.15. Deep ITM (OTM) options are call (put) options with moneyness smaller than 0.85 and put (call) options with moneyness greater than 1.15.

Table 3.4: Summary statistics of trading costs in extended and regular trading hours.

This table compares the averages and standard deviations of SPXW option trading costs. The last column shows the average differences between extended and regular trading hours with the two-sample t-test. Quoted spread excludes in-the-money options that are call (put) options with moneyness smaller (greater) than 0.95 (1.05). Effective spread uses all traded option contracts. Dollar quoted/effected spread is expressed in dollars. Proportional quoted/effected spread and normalized quoted/effective spread are expressed in percentages. The sample period is from December 1, 2014 to May 31, 2015. ***, **, and * indicate statistical significance at 1%, 5%, and 10% levels, respectively.

	Extended Hours		Regular Hours		Diff
	Mean	Std. Dev.	Mean	Std. Dev.	
Dollar Quoted Spread ($)	2.03	2.44	1.01	0.98	1.02***
Proportional Quoted Spread (%)	18.00	22.73	12.03	15.93	5.97***
Normalized Qutoed Spread (%)	166.12	109.74	93.81	15.42	72.31***
Nobs (per day)	2440		2454		
Dollar Effective Spread ($)	1.4	18.7	0.3	3.05	1.1**
Proportional Effective Spread (%)	18.43	36.65	15.20	37.52	3.23***
Normalized Effective Spread (%)	217.35	454.65	99.92	3.46	117.43***
Nobs (per day)	24		863		

Table 3.5: The probability of informed trading (PIN).

This table shows the PIN (Easley, Hvidkjaer, and O' Hara, 2002) of SPXW options. The PIN is estimated in half-hour intervals from 03:00 to 16:00. The last column shows the PIN estimated with aggregate trades in extended and regular trading hours. 95% confidence intervals are simulated with function $pin\_confint$ in R $pinbasic$ package. Values are expressed in percentages. The sample period is from December 1, 2014 to May 31, 2015.

PIN (%) in extended trading hours														
	03:30	04:00	04:30	05:00	05:30	06:00	06:30	07:00	07:30	08:00	08:30	09:00	09:30[19]	Extended Hours
PIN	40.77	47.38	38.59	33.1	50.5	42.03	59.73	47.96	39.96	29.56	48.76	39.67	55.19	19.66
2.5%	29.70	27.14	12.60	0.00	26.89	16.10	38.62	29.20	19.67	12.33	29.92	21.36	41.69	10.66
97.5%	50.02	62.61	57.89	67.84	66.16	76.99	72.93	70.82	59.89	49.70	66.13	53.38	66.44	27.93
PIN (%) in regular trading hours														
	10:00	10:30	11:00	11:30	12:00	12:30	13:00	13:30	14:00	14:30	15:00	15:30	16:00	Regular Hours
PIN	10.3	13.23	11.42	10.45	16.62	12.01	15.15	16.84	12.55	17.21	14.04	11.5	13.67	11.19
2.5%	7.92	10.76	8.47	7.63	13.25	8.51	11.66	13.74	9.09	13.75	10.79	8.32	10.41	9.01
97.5%	12.66	15.61	14.32	13.31	19.90	15.41	18.48	19.80	16.13	20.48	17.15	14.64	16.70	13.24

[19] In 09:00 to 09:30 interval, the trading period is from 09:00 to 09:15.

Table 3.6: Impact of CBOE's introduction of extended trading hours in the option market on bid-ask spread.

This table reports the results of the difference-in-differences analysis (see equation 3.3) about the impact of CBOE's introduction of extended trading hours estimated by the coefficient β_6 of $D_t \cdot D_s$ on dollar quoted spread ($), proportional quoted spread (%), dollar effective spread ($), and proportional effective spread (%) respectively. Standard errors are in parentheses. The treatment group is SPXW options; the control group is SPY options. The pre-introduction sample period is three months before the introduction of extended trading hours, from December 1, 2014 to February 28, 2015. The post-introduction sample period is three months after the introduction of extended trading hours, from March 9, 2015 to May 31, 2015. The whole sample is categorized by option prices. Significance tests use standard errors clustered on option class and date. Coefficient β_6 of $D_t \cdot D_s$ in panels A and C are expressed in U.S. dollars. Coefficient β_6 of $D_t \cdot D_s$ in panels B and D are expressed in percentages. ***, **, and * indicate statistical significance at 1%, 5%, and 10% levels, respectively.

	Overall	3<Price≤5	5<Price≤10	10<Price≤30	30<Price≤50	50<Price≤100
Panel A: Quoted spread($)						
$D_t \cdot D_s$	-0.15***	-0.04***	-0.06***	-0.17***	-0.25***	-0.37***
	(0.02)	(0.01)	(0.01)	(0.03)	(0.03)	(0.05)
N	217417	31513	45519	80214	34959	25212
Adjusted R^2	0.41	0.56	0.58	0.22	0.40	0.35
Panel B: Percentage quoted spread (%)						
$D_t \cdot D_s$	-0.92***	-0.82***	-0.85***	-0.92***	-0.64***	-0.57***
	(0.16)	(0.29)	(0.2)	(0.14)	(0.08)	(0.08)
N	217417	31513	45519	80214	34959	25212
Adjusted R^2	0.49	0.57	0.59	0.36	0.41	0.36
Panel C: Effective spread($)						
$D_t \cdot D_s$	-0.06***	-0.04**	-0.02**	-0.09***	-0.07***	-0.12***
	(0.02)	(0.02)	(0.01)	(0.02)	(0.02)	(0.02)
N	80306	11189	17992	33014	11401	6710
Adjusted R^2	0.08	0.01	0.03	0.06	0.03	0.04
Panel D: Percentage effective spread(%)						
$D_t \cdot D_s$	-0.47***	-0.56***	-0.33***	-0.53***	-0.20***	-0.25***
	(0.09)	(0.14)	(0.12)	(0.12)	(0.06)	(0.03)
N	80306	11189	17992	33014	11401	6710
Adjusted R^2	0.08	0.04	0.04	0.05	0.04	0.04

Table 3.7: Intraday impact of CBOE's introduction of extended trading hours in the option market on bid-ask spread.

This table reports the results of the difference-in-differences analysis (see equation 3.3) about the impact of CBOE's introduction of extended trading hours estimated by the coefficient β_6 of $D_t \cdot D_s$ on dollar quoted spread ($), proportional quoted spread (%), dollar effective spread ($), and proportional effective spread (%) respectively in 30-minute intervals. The treatment group is SPXW options; the control group is SPY options. The pre-introduction sample period is three months before the introduction of extended trading hours, from December 1, 2014 to February 28, 2015. The post-introduction sample period is three months after the introduction of extended trading hours, from March 9, 2015 to May 31, 2015. The whole sample is categorized by option prices and 30-minute intervals. Significance tests use standard errors clustered on option class and date. Values in panel A and C are expressed in U.S. dollars. Values in panel B and D are expressed in percentages. ***, **, and * indicate statistical significance at 1%, 5%, and 10% levels, respectively.

Panel A: Quoted spreads ($)													
	10:00	10:30	11:00	11:30	12:00	12:30	13:00	13:30	14:00	14:30	15:00	15:30	16:00
Overall	-0.13 ***	-0.16 ***	-0.15 ***	-0.16 ***	-0.14 ***	-0.14 ***	-0.13 ***	-0.13 ***	-0.12 ***	-0.17	-0.18 ***	-0.14 ***	-0.14 ***
3<Price≤5	-0.02	-0.04 ***	-0.04 ***	-0.05 ***	-0.04 ***	-0.04 ***	-0.03 ***	-0.03 **	-0.06 *	-0.04 *	-0.05 **	-0.04 ***	-0.04 ***
5<Price≤10	-0.03	-0.07 ***	-0.06 ***	-0.08 ***	-0.07 ***	-0.07 ***	-0.06 ***	-0.06 ***	-0.09 ***	-0.09 ***	-0.09 ***	-0.07 ***	-0.08 ***
10<Price≤30	-0.12 **	-0.15 ***	-0.14 ***	-0.16 ***	-0.15 ***	-0.14 ***	-0.12 ***	-0.13 ***	-0.11 **	-0.22 *	-0.17 ***	-0.14 ***	-0.5 ***
30<Price≤50	-0.27 ***	-0.28 ***	-0.28 ***	-0.26 ***	-0.24 ***	-0.23 ***	-0.22 ***	-0.23 ***	-0.21 ***	-0.29 *	-0.30 ***	-0.25 ***	-0.24 ***
50<Price≤100	-0.42 ***	-0.45 ***	-0.45 ***	-0.40 ***	-0.37 ***	-0.36 ***	-0.36 ***	-0.35 ***	-0.31 ***	-0.29	-0.43 ***	-0.35 ***	-0.331 ***
Panel B: Percentage quoted spreads (%)													
	10:00	10:30	11:00	11:30	12:00	12:30	13:00	13:30	14:00	14:30	15:00	15:30	16:00
Overall	-0.63 ***	-0.98 ***	-0.94 ***	-1.01 ***	-0.93 ***	-0.90 ***	-0.78 ***	-0.80 ***	-1.01 ***	-0.98 ***	-1.08 ***	-0.84 ***	-0.93 ***
3<Price≤5	-0.40	-1.04 ***	-1.04 ***	-1.12 ***	-0.98 ***	-1.02 ***	-0.73 ***	-0.67 **	-1.42 *	-0.79	-1.23 **	-0.93 ***	-1.11 ***
5<Price≤10	-0.29	-0.92 ***	-0.91 ***	-1.16 ***	-0.99 ***	-0.96 ***	-0.83 ***	-0.84 ***	-1.23 ***	-1.19 ***	-1.20 ***	-0.91 ***	-1.06 ***
10<Price≤30	-0.59 **	-0.80 ***	-0.76 ***	-0.91 ***	-0.82 ***	-0.79 ***	-0.68 ***	-0.73 ***	-0.59 ***	-1.12 **	-0.95 ***	-0.74 ***	-0.82 ***
30<Price≤50	-0.71 ***	-0.74 ***	-0.74 ***	-0.68 ***	-0.62 ***	-0.60 ***	-0.56 ***	-0.58 ***	-0.52 ***	-0.74 *	-0.78 ***	-0.65 ***	-0.61 ***
50<Price≤100	-0.62 ***	-0.68 ***	-0.68 ***	-0.62 ***	-0.57 ***	-0.55 ***	-0.56 ***	-0.54 ***	-0.48 ***	-0.46	-0.67 ***	-0.54 ***	-0.51 ***

Panel C: Effective spreads ($)													
	10:00	10:30	11:00	11:30	12:00	12:30	13:00	13:30	14:00	14:30	15:00	15:30	16:00
Overall	-0.14 **	-0.05 ***	-0.04 ***	-0.04 ***	-0.03 ***	-0.03 ***	-0.03 ***	-0.04 ***	-0.04 ***	-0.08 ***	-0.04 ***	-0.04 ***	-0.05 ***
3<Price≤5	-0.01	-0.03 ***	-0.03 ***	-0.02 ***	-0.02 ***	-0.02 **	-0.03 ***	-0.02 ***	-0.04 ***	-0.00	-0.02 ***	-0.02 ***	-0.02 ***
5<Price≤10	-0.01	-0.03 ***	-0.02 ***	-0.03 ***	-0.03 ***	0.00	-0.02 **	-0.04 ***	-0.03 ***	-0.04	-0.03 ***	-0.02 **	-0.03 ***
10<Price≤30	-0.30 *	-0.07 ***	-0.04 ***	-0.04 ***	-0.04 ***	-0.04 ***	-0.03 ***	-0.06 ***	-0.03 ***	-0.12 ***	-0.04 ***	-0.05 ***	-0.06 ***
30<Price≤50	-0.05 *	-0.03	-0.06 **	-0.07 ***	-0.05 **	-0.03	-0.02	-0.03	-0.09 ***	-0.09	-0.09 ***	0	-0.03
50<Price≤100	-0.07	-0.02	-0.20 ***	-0.06	0.24 ***	0.17 **	0.08	0.02	0.03	-0.12	0.09	-0.11	-0.13
Panel D: Percentage effective spreads (%)													
	10:00	10:30	11:00	11:30	12:00	12:30	13:00	13:30	14:00	14:30	15:00	15:30	16:00
Overall	-0.27 ***	-0.45 ***	-0.34 ***	-0.3 ***	-0.35 ***	-0.15 *	-0.28 ***	-0.45 ***	-0.37 ***	-0.27	-0.34 ***	-0.33 ***	-0.37 ***
3<Price≤5	-0.34 *	-0.72 ***	-0.79 ***	-0.54 ***	-0.57 ***	-0.41 ***	-0.64 ***	-0.58 ***	-0.92 ***	0.72 ***	-0.58 ***	-0.60 ***	-0.58 ***
5<Price≤10	-0.13	-0.41 ***	-0.31 ***	-0.37 ***	-0.47 ***	0.00	-0.20	-0.62 ***	-0.43 ***	-0.40	-0.41 ***	-0.25 ***	-0.41 ***
10<Price≤30	-0.33 ***	-0.43 ***	-0.26 ***	-0.24 ***	-0.26 ***	-0.20 **	-0.18 ***	-0.31 ***	-0.16 **	-0.58	-0.23 ***	-0.27 ***	-0.29 ***
30<Price≤50	-0.12 *	-0.13 *	-0.17 **	-0.19 ***	-0.12 ***	-0.09 ***	-0.05	-0.11 ***	-0.22 ***	-0.15 ***	-0.27 ***	0.01	-0.11 ***
50<Price≤100	-0.13	-0.02	-0.33 ***	-0.10 **	0.33 *	0.20 ***	0.14	0.01 ***	-0.02	-0.26 ***	0.13 ***	-0.21 ***	-0.21 ***

Table 3.8: Robustness check of the impact of CBOE's introduction of extended trading hours in the option market on bid-ask spread.

This table reports the results of the difference-in-differences analysis (see equation 3.3) about the impact of CBOE's introduction of extended trading hours estimated by the coefficient β_6 of $D_t \cdot D_s$ on dollar quoted spread ($), proportional quoted spread (%), dollar effective spread ($), and proportional effective spread (%) respectively. Standard errors are in parentheses. The treatment group is SPXW options; the control group is SPY options. In Panel A of the placebo test, the pre-introduction sample period is from December 1, 2014 to January 14, 2015. The post-introduction sample period is from January 15, 2015 to February 28, 2015. In Panel B of 6-week analysis, the pre-introduction sample period is from January 15, 2015 to February 28, 2015. The post-introduction sample period is from March 9, 2015 to April 17, 2015. The whole sample is categorized by option prices. Significance tests use standard errors clustered on option class and date. Values with quoted spread ($) and effective spread ($) are expressed in U.S. dollars. Values with percentage quoted spread (%) and percentage effective spread (%) are expressed in percentages. ***, **, and * indicate statistical significance at 1%, 5%, and 10% levels, respectively.

Panel A: Placebo Tests						
	Overall	3<Price≤5	5<Price≤10	10<Price≤30	30<Price≤50	50<Price≤100
Quoted Spread ($)	0.01	0.02	0.02	0.03	0.02	-0.06
	(0.03)	(0.02)	(0.02)	(0.03)	(0.04)	(0.07)
Percentage Quoted Spread (%)	-0.08	0.61	0.2	0.14	0.04	-0.05
	(0.24)	(0.47)	(0.29)	(0.17)	(0.11)	(0.1)
Effective Spread ($)	-0.01	-0.01	-0.02	-0.02	-0.03	-0.01***
	(0.01)	(0.01)	(0.01)	(0.01)	(0.03)	(0)[+20]
Percentage Effective Spread (%)	-0.18**	-0.08	-0.29*	-0.23***	-0.08	-0.03***
	(0.09)	(0.18)	(0.15)	(0.08)	(0.08)	(0)[+]
Panel B: 6-week impact of the introduction						
Quoted Spread ($)	-0.09***	-0.05***	-0.04**	-0.17***	-0.16***	-0.12**
	(0.03)	(0.01)	(0.02)	(0.06)	(0.03)	(0.06)
Percentage Quoted Spread (%)	-0.67***	-1.10***	-0.51*	-0.85***	-0.41***	-0.23**
	(0.17)	(0.35)	(0.26)	(0.23)	(0.08)	(0.09)
Effective Spread ($)	-0.06*	-0.05	-0.01	-0.08***	-0.05	-0.05***
	(0.03)	(0.03)	(0.02)	(0.03)	(0.04)	(0)
Percentage Effective Spread (%)	-0.34**	-0.49*	-0.16	-0.44**	-0.15	-0.13***
	(0.16)	(0.28)	(0.2)	(0.19)	(0.12)	(0.02)

[20]+ denotes the adjustment by Cameron (n.d.) that set negative variance as zero in two-way clustered errors

Table 3.9: The components of bid-ask spread around the introduction of extended trading hours.

This table reports the components of quoted and effective spreads estimated by the models of Huang and Stoll (1997) and Lin et al. (1995), respectively. Quoted spread is decomposed into adverse selection costs (α), inventory holding costs (β), and order processing costs ($1-\alpha-\beta$). φ is the probability that trade direction reverses. Effective spread is decomposed into adverse selection costs (λ) and order processing costs (γ). θ is the persistence of order flow. Column Diff-in-Diffs shows the impact of the introduction of extended trading hours on the components of spreads by difference-in-differences analysis, the coefficient β_6 of $D_t \cdot D_s$ in equation (3.9). The treatment group is SPXW options; the control group is SPY options. The pre-introduction ("Pre") sample is defined as three months before the introduction of extended trading hours from December 1, 2014 to February 28. The post-introduction ("Post") sample is defined as three months after the introduction of extended trading hours from March 9, 2015 to May 31, 2015. All options with over 250 trades during regular trading hours in a day are considered. Significant tests of coefficients in difference-in-differences use clustered errors on Date. Columns Pre and Post show the average of each component. Column Difference shows the results of two-sample t-test comparing the averages of Pre sample and Post sample. ***, **, and * indicate statistical significance at 1%, 5%, and 10% levels, respectively.

Components		SPXW Options Pre	SPXW Options Post	SPXW Options Difference	SPY Options Pre	SPY Options Post	SPY Options Difference	Diff-in-diffs
Panel A: The decomposition of quoted spread								
α	¢	3.62	2.37	-1.25***	4.43	4.31	-0.12	-0.75*
	%	10.35	7.63	-2.72***	19.2	21.39	2.2***	-5.13***
β	¢	3.42	2.19	-1.23**	4.46	4.38	-0.08	-0.69*
	%	10.1	7.75	-2.35**	18.91	21.52	2.61***	-5.15***
$1-\alpha-\beta$	¢	26.13	20.51	-5.63***	15.41	12.32	-3.09***	-0.43
	%	79.55	84.61	5.07***	61.89	57.08	-4.81***	10.28***
φ	%	50.12	50.16	0.04	50.11	50.12	0.01	0.01
Panel B: The decomposition of effective spread								
λ	¢	2.47	1.74	-0.73***	3.04	3.14	0.1	-0.47**
	%	33.67	28.99	-4.68**	36.29	40.5	4.21***	-8.38***
γ	¢	3.36	2.45	-0.91***	3.81	3.39	-0.42***	0.37
	%	52.43	55.14	2.71	48.24	45.93	-2.3***	4.27**
θ	%	14.6	16.7	2.1*	16.23	14.2	-2.03***	4.37***

Table 3.10: Summary Statistics of overnight changes of S&P 500 implied index level and volatility.

Column Mean is tested by one sample t-test with a null hypothesis as mean zero. ***, **, and * indicate statistical significance at 1%, 5%, and 10% levels, respectively. The sample period is from March 9, 2015 to December 31, 2018.

SPXW		Mean (%)	Std (%)	Skewness	Kurtosis	Sample Size
Implied Index Return	Overnight	0.01	0.52	-0.55	9.26	953
	ETH	0.01	0.51	-0.61	9.26	
	Opening	0.01*	0.09	-0.01	9.68	
Implied Volatility Change	Overnight	-2.32***	3.0	-1.73	13.18	953
	ETH	-1.9***	3.11	-0.6	16.02	
	Opening	-0.41***	1.08	-7.25	77.45	

Table 3.11: Overnight option implied index level and volatility.

This table presents the results of regression analysis equations 3.13a and 3.13b, examining the relationship between changes in extended trading hours and overnight changes of implied index levels and volatility. The sample period is from March 9, 2015 to December 31, 2018.

	Coefficient	Std	t	p
Panel A: Option Implied Index Level				
α	5.34E-05	2.86E-05	1.87	0.06
β	-1.23E-03	5.63E-03	-0.22	0.83
Adjusted R^2		0.97		
Panel B: Option Implied Volatility				
α	-5.95E-03	3.94E-04	-15.11	0
β	-9.59E-02	1.08E-02	-8.88	0
Adjusted R^2		0.88		

Table 3.12: Realized volatility forecasting with implied volatility.

This table compares one-day realized volatility forecasting models with implied volatilities at the end of previous trading day (IV_{t-1}^{RTH}) and at the end extended trading hours (IV_{t}^{ETH}). Realized volatility is calculated with one-minute log returns. Models are estimated by OLS. Standard errors are in parentheses. Adj. R^2 is the adjusted R^2 for the in-sample regression. MSE and QLIKE are measures for out-of-sample prediction accuracy with 252-day rolling window. Significance tests for MSE and QLIKE use Diebold-Mariano Test with benchmarks as the standard HAR and HARQ models in Panels A and B respectively. In Panel C, the bench mark is implied volatility at the end of previous trading day (IV_{t-1}^{RTH}). ***, **, and * indicate statistical significance at 1%, 5%, and 10% levels, respectively.

Model	Intercept ($\times 10^{-4}$)	$RV_{t-22,t-1}$ ($\times 10^{-1}$)	$RV_{t-5,t-1}$ ($\times 10^{-1}$)	RV_{t-1} ($\times 10^{-1}$)	$RQ_{t-1}^{1/2} \cdot RV_{t-1}$	IV_t^{ETH} ($\times 10^{-1}$)	IV_{t-1}^{RTH} ($\times 10^{-1}$)	Adj. R^2 (%)	MSE ($\times 10^{-6}$)	QLIKE ($\times 10^{-1}$)
Panel A: HAR Model										
HAR	2.72	-0.63	8.14	2.01				75.44	2.81	0.31
	(1.34)	(0.40)	(0.54)	(0.39)						
HAR-IV_{t-1}^{RTH}	-2.61	-0.51	6.68	0.51			2.44	77.78	2.74	0.33
	(1.38)	(0.38)	(0.53)	(0.4)			(0.25)			
HAR-IV_{t}^{ETH}	-2.47	-0.93	5.56	0.86		3.71		82.15	2.14***	0.27***
	(1.17)	(0.34)	(0.48)	(0.34)		(0.2)				
Panel B: HARQ Model										
HARQ	2.70	-0.64	8.12	2.05	-6.98			75.41	3.07	0.33
	(1.36)	(0.41)	(0.55)	(0.49)	(59.52)					
HARQ-IV_{t-1}^{RTH}	-2.98	-0.6	6.51	0.82	-68.39		2.48	77.79	2.96**	0.34
	(1.41)	(0.39)	(0.55)	(0.48)	(56.89)		(0.25)			
HARQ-IV_{t}^{ETH}	-2.75	-1	5.42	1.14	-58.75	3.72		82.16	2.26***	0.28***
	(1.19)	(0.35)	(0.49)	(0.42)	(50.77)	(0.2)				

Model	Intercept ($\times 10^{-4}$)	$RV_{t-22,t-1}$ ($\times 10^{-1}$)	$RV_{t-5,t-1}$ ($\times 10^{-1}$)	RV_{t-1} ($\times 10^{-1}$)	$RQ_{t-1}^{1/2} \cdot RV_{t-1}$	IV_t^{ETH} ($\times 10^{-1}$)	IV_{t-1}^{RTH} ($\times 10^{-1}$)	Adj. R^2 (%)	MSE ($\times 10^{-6}$)	QLIKE ($\times 10^{-1}$)
Panel C: IV Model										
IV_{t-1}^{RTH}	-1.42						6.53	67.3	4.12	0.55
	(1.39)						(0.15)			
IV_t^{ETH}	1.65					7.19		72	2.9***	0.38***
	(1.19)					(0.15)				

Figure 3.1: Trading volume, realized volatility, and the frequency of quote changes in half-hour intervals.

Panel A and B show the averages of aggregate trading volume of all SPXW options, the frequency of SPXW quote changes, realized volatility of S&P 500 E-mini futures in half-hour intervals. The sample period is from December 1, 2014 to May 31, 2015.

Panel A: Extended and regular trading hours.

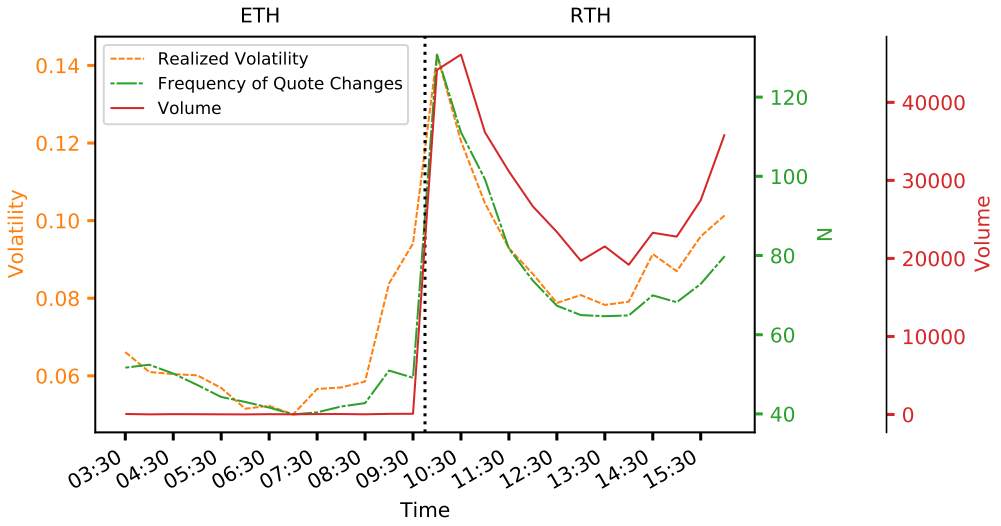

Panel B: Extended trading hours.

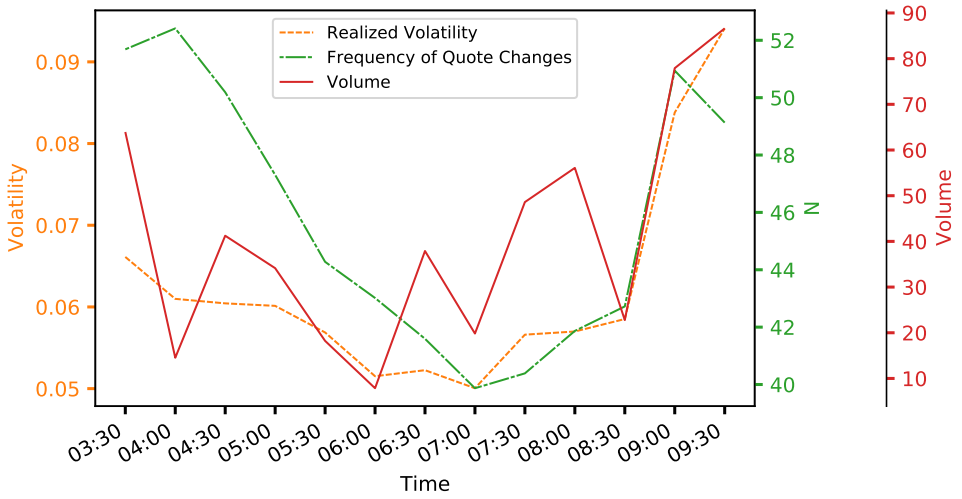

Figure 3.2: Intraday normalized quoted spread.

This figure shows the intraday average normalized quoted spread pattern in five-minute intervals for SPXW options. In-the-money options are excluded. In panel B, news (non-news) dates are dates with (without) macroeconomic news announcements at 08:30. In panel C, news (non-news) dates are dates with (without) FOMC announcements after 14:00. The sample period is from December 1, 2014 to May 31, 2015.

Panel A: Intraday normalized quoted spread.

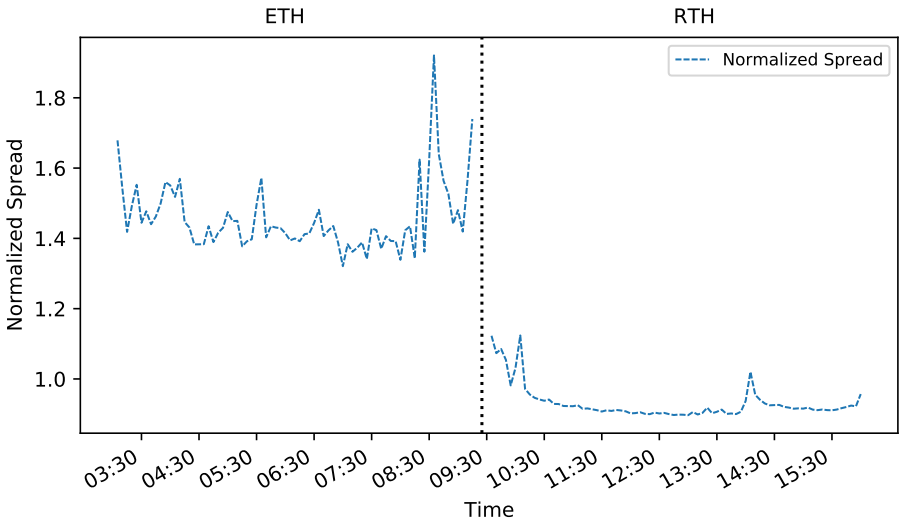

Panel B: Normalized quoted spread in extended trading hours

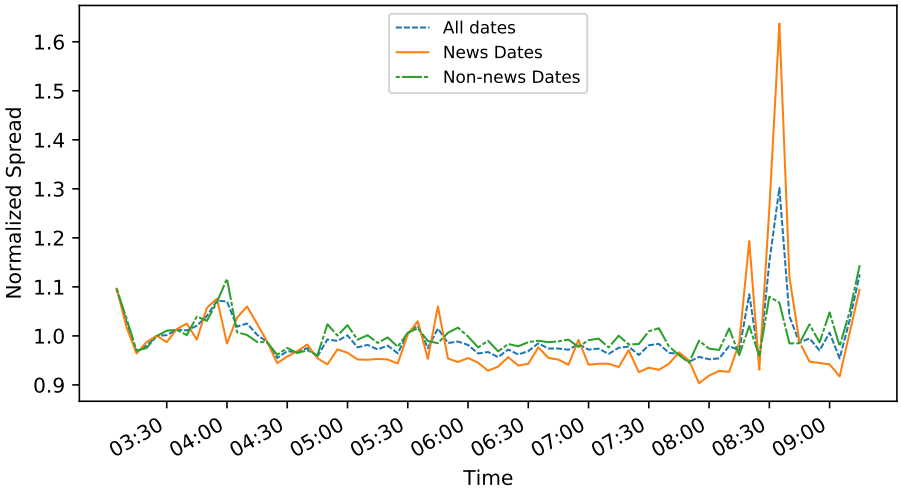

Panel C: Normalized quoted spread in regular trading hours

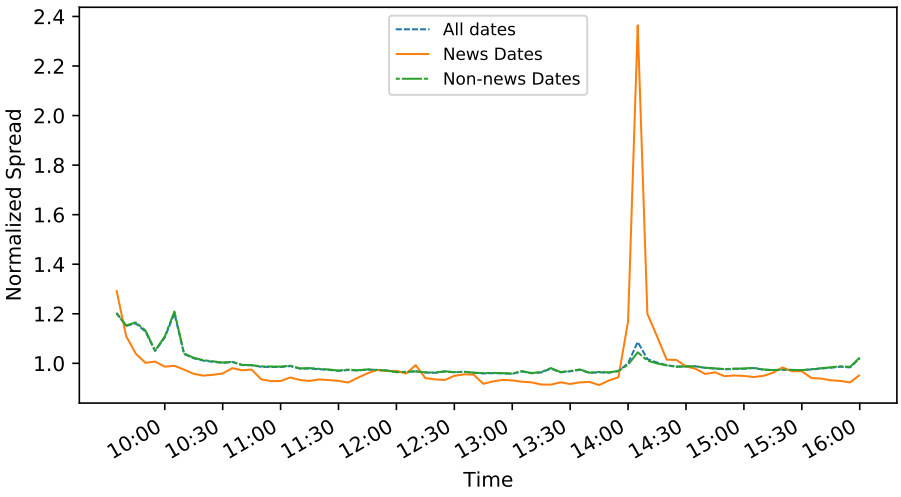

Figure 3.3: Daily dynamics of realized volatility and implied volatility.

Panel A and B plot the realized volatility estimated from one-minute and five-minute returns respectively. Implied volatility is estimated by model free volatility (Bakshi, Kapadia, and Madan, 2003) with the last midquote at 09:15. The sample period is from March 9, 2015 to December 31, 2018.

Panel A: One-minute Realized Volatility (RV) with Implied Volatility(IV)

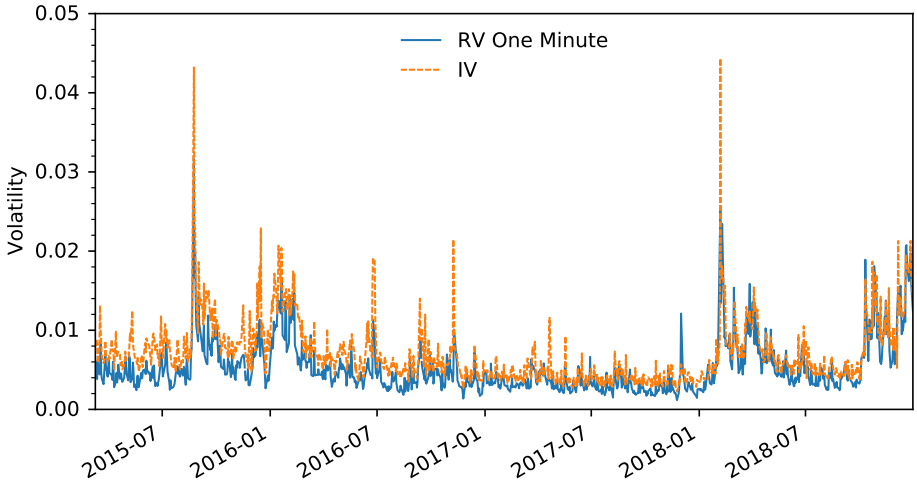

Panel B: Five-minute Realized Volatility (RV) with Implied Volatility(IV)

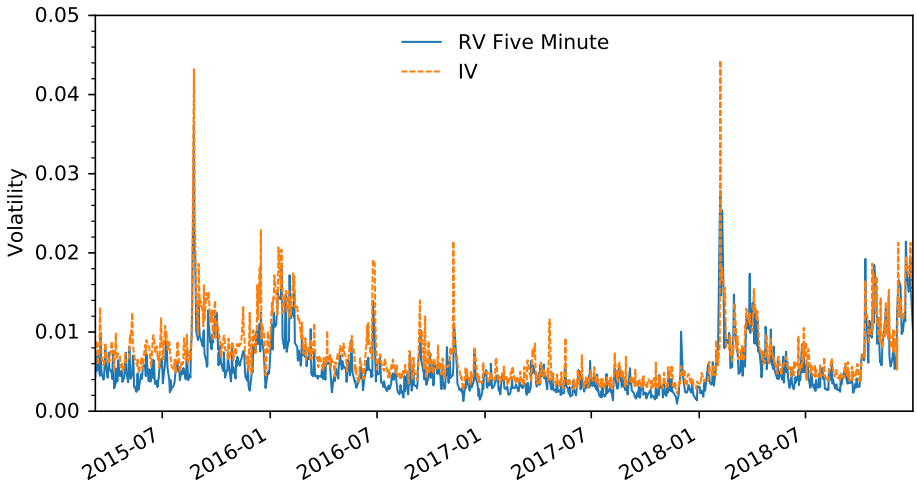

Chapter 4

The Ross Recovery Theorem and the Term Structure of Interest Rates

4.1. Introduction

Computing the physical probability distribution of future asset prices is important for all aspects of finance. Estimation methods of risk-neutral probability distribution have already been well developed (see Jackwerth, 2004 and Figlewski, 2018 for an overview). Empirical analysis shows the risk-neutral probability distribution contains important market information (Figlewski, 2018). However, risk-neutral probabilities are adjusted by market investors' risk preferences. It is still difficult to recover the physical probabilities from the risk-neutral probabilities without specifying a representative agent's utility function. Ross (2015) tries to solve the problem and proposes a theorem to recover the 'physical'[1] probability distribution and the pricing kernel at the same time with just a snapshot of option prices.

A list of literature has been developed around Ross recovery. First, the Ross recovery theorem is limited by discrete and bounded states. Dillschneider and Maurer (2019) and Golec, Xu, and Yao (2022) extend the original discrete Ross recovery to continuous states. Walden (2017) extends Ross recovery with unbounded diffusion processes. Second, empirical applications try to identify the information in Ross recovered probabilities but with contradicted conclusions. On one hand, Audrino, Huitema, and Ludwig (2021) show Ross recovered moments yield additional predictive information to risk-neutral moments. And Ross recovered probabilities can be distinctly different from risk-neutral probabilities. On the other hand, extensions of Ross recovery, Ross stable (Jackwerth and Menner, 2020) and generalized recovery (Jensen, Lando, and Pedersen, 2019)[2] yield a relatively stable pricing kernel, indicating only a small difference between the risk-neutral measure and the Ross recovery measure. They present that Ross recovered probability distributions fail to predict future returns or realized volatility. In addition, based on different estimation approaches to Ross recovery, Jackwerth and Menner (2020) present completely different recovered probabilities from the same spot state prices. A reliable and consistent Ross recovery estimation process is needed in empirical studies. Third, some literature examines the explicit and implicit assumptions in Ross recovery. Theoretically, Borovička, Hansen, and Scheinkman (2016) argue that instead of recovering physical probabilities, Ross recovery implicitly assumes the martingale component of stochastic discount factors as identical to unity and recovers long-term risk-neutral probabilities. Empirical evidence also shows that the implicit assumption of the martingale component in Ross recovery is not correct for recovering physical probabilities (Bakshi, Chabi-Yo, and Gao, 2018). Qin, Linetsky, and Nie (2018) further show that the bond market evidence is against one of Ross recovery assumptions that the transition is independent over time.

Although Ross recovered probabilities may be not physical probabilities, it is still unclear whether Ross recovered probabilities provide additional information in comparison to risk-neutral probabilities. Existing literature provides no explanation why different approaches to Ross recovery yield substantially different recovered probabilities while the assumptions are

[1] We use 'physical' with apostrophes to indicate that Ross (2015) recovered probabilities may be different from the true physical probabilities as Bakshi, Chabi-Yo, and Gao (2018) and Borovička, Hansen, and Scheinkman (2016) argue.

[2] We use generalized recovery by Jensen, Lando, and Pedersen (2019) and Ross Stable by Jackwerth and Menner (2020) interchangeably as they independently propose this recovery estimation.

the same. Martin and Ross (2019) theoretically present an important relationship between Ross recovery and the term structure of interest rates. This chapter contributes to the literature of Ross recovery by proposing an implied condition of interest rates and presents that Ross recovered probabilities are heavily affected by the term structure of interest rates.

We show that existing Ross recovery estimations omit an interest rate condition. As a result, Ross recovery implied term structure of interest rates substantially deviates from the market term structure and Ross recovered probabilities are not correctly estimated. This methodological explanation contributes to the understanding of the empirical differences between the original Ross recovery estimation and generalized recovery.

Incorporating the interest rate condition provides a reliable and consistent estimation process for Ross recovery. Ross recovered probabilities are the same as the risk-neutral probabilities when the term structure of interest rates is flat. In reality, when the term structure is not flat, Ross recovery with an interest rate condition yields recovered probabilities close to the risk-neutral probabilities as with generalized recovery.

In addition, we contribute to the literature by presenting three other challenges in Ross recovery estimations. First, different choices of the period length regarding transition matrix are not equivalent. The transition matrix with a short period implies the existence of a nonnegative n^{th} root of a transition matrix with a long period. Thus, the recovered probabilities may be considerably different depending on the choice of the period length. Second, different least squares representations are not equivalent when there is no unique and exact transition matrix for the spot state prices. Linear and nonlinear representations of Ross recovery imply substantially different term structures of interest rates. Third, the number of states in the transition matrix also plays an important role in Ross recovery estimation. Ross recovery results in more stable and well-behaved recovered probabilities with sparse states in comparison to dense states for the same number of expiries.

We further propose a multi-period Ross recovery estimation so that both the fitted state price surface in Ross recovery is correctly represented and the implied term structure of interest rates is consistent with the market term structure. This new Ross recovery estimation addresses the difference between the original Ross recovery and generalized recovery that Ross recovery requires a time-homogeneous transition matrix or a Markov chain process for the spot state price surface. With this empirical approach, we find that there is only small difference between Ross recovered probabilities comparing to both risk-neutral and generalized recovered probabilities with a market example.

This chapter also relates to the non-parametric Risk-Neutral Distribution (RND) estimation developed by Figlewski (2010). The non-parametric method provides an unbiased spot state price surface in comparison to other parametric risk-neutral distribution methods. We extend Figlewski's non-parametric estimation into different horizons and make the term structure of interest rates correctly captured in the risk-neutral probability surface. An accurate risk-neutral probability surface is the prerequisite for Ross recovery.

The rest of this chapter is organized as eight parts. Section 4.2 reviews the Ross recovery theorem and presents the implied term structure of interest rates. Section 4.3 shows the spot state price surface estimation. Section 4.4 reviews existing approaches to Ross recovery, labeled

Ross Basic and Ross Stable. It addresses that the term structure of interest rates is omitted in existing literature if we intend to extract information from Ross recovered probabilities. Section 4.5 is the main discussion of this chapter. By incorporating the term structure into Ross recovery, recovered probabilities are stable and close to risk-neutral probabilities. Section 4.6 discusses the nonlinear multi-period Ross recovery estimation. Section 4.7 presents our proposed Ross Root estimation to discuss the choice of transition period length. Section 4.8 compares the Ross recovery implied information from different approaches. Section 4.9 concludes.

4.2. Ross recovery theorem

This section reviews the Ross recovery theorem and its implied term structure of interest rates. Based on a spot state price matrix, Ross proposes a recovery method to extract the transition matrix, 'physical' probability distributions, and the pricing kernel at the same time. This section summarizes the existing and our proposed empirical approaches to Ross recovery.

4.2.1. Original Ross Recovery Theorem

We focus on Ross recovery with finite discrete states. The Ross recovery theorem explicitly makes three assumptions. First, it assumes a time-homogeneous one-period transition matrix that links the state prices at time t and state prices at time $t+h$ as a Markov chain process. A state price $\pi(t, t+h, i, j)$ with $t > 0$ is the transition price from time t to $t+h$ and from state i to state j. Transition state prices are not directly observable in the market. Ross recovery assumes the one-period transition matrix is time-homogeneous, independent from time t. As a result, the one-period transition state price , $\pi(t, t+h, i, j) = a(i, j) \forall t$, is only determined by the start state i and end state j given a transition period h. Based on spot state prices at time t and the transition matrix, each state j at time $t+h$ is calculated as:

$$\pi_0(t+h, j) = \sum_{i \in N} \pi_0(t, i) a(i, j), \forall j \in N \tag{4.1}$$

where N is the set of all states. $a(i, j)$ is the transition state price from state i to state j during any one-period time h and is the entry in the transition matrix $\mathbf{A} = [a(i, j), i, j \in N]$. The spot state prices with horizon $t = 0$ is determined by the current state as Π_0. The one-period state price transition matrix implies spot state prices at any time $n \cdot h (n \in \mathbb{N})$ as

$$\Pi_n = \Pi_0 \times \boldsymbol{A}^n \tag{4.2}$$

where $\Pi_n = [\pi_0(n \cdot h, j)]$ is a row vector indicating the spot state prices from current state to state j at time $n \cdot h$, Π_0 and Π_n are the 0^{th} and n^{th} row in the spot state price surface $\mathbf{\Pi}$.

Second, the Ross recovery theorem assumes all transition state prices in $\boldsymbol{A}$ are positive.

Third, as the stochastic discount factor (m) links the physical probability (p) and state price (π) in the form of $p = \pi / m$, Ross further assumes the stochastic discount factor is transition

independent. Then the one-period stochastic discount factor from state i to state j is

$$m_{i,j} = \delta \frac{u_j^{'}}{u_i^{'}} \tag{4.3}$$

where $u^{'}$ and δ can be interpreted as marginal utility and a utility discount factor, respectively.

Based on the above stochastic discount factors, we can derive that the one-period state price transition matrix $\mathbf{A}$ corresponds to a one-period Ross recovered probability transition matrix $\mathbf{S}$. Each row in the matrix $\mathbf{S}$ indicates all possible outcomes from a state during one period. Therefore, the sum of each row in the matrix $\mathbf{S}$ equals one. Based on this idea, the state price transition matrix satisfies the following equation:

$$\mathbf{A} \times Z = \delta Z \tag{4.4}$$

where Z is a vector of the inverse $u_i^{'}$, i.e. $z_i = 1/u_i^{'}$.

Equation (4.4) is an eigenvalue problem. By using the Perron-Frobenius theorem, the largest eigenvalue corresponds to the only eigenvector with strictly positive z_i. Therefore, given the state price transition matrix, based on the solution of equation (4.4), the stochastic discount factors and Ross recovered probabilities are uniquely determined. The spot state price surface $\mathbf{\Pi}$ can be transformed to a Ross recovered probability surface $\boldsymbol{P}$ with the stochastic discount factors. Ross recovered probabilities at time $n \cdot h$ in the Ross recovered probability surface $\boldsymbol{P}$ is calculated in a similar way as equation (4.2)

$$P_n = P_0 \times \boldsymbol{S}^n \tag{4.5}$$

where P_0, P_n are the 0^{th} and n^{th} row in the Ross recovered probability surface $\boldsymbol{P}$. As the state price transition matrix directly implies the recovered probability transition matrix, Ross recovery only needs to extract the state price transition matrix from the spot state price matrix.

4.2.2. Ross Recovery Implied Interest Rate

In an economy that follows the Ross recovery theorem, the transition matrix fully determines interest rates, including the state interest rate, the spot rate curve, and the forward rate curve.

The sum of each row in the state price transition matrix is the one-period interest rate discount factor in the corresponding state. The state interest rate vector is

$$R = [r_i], \text{and } r_i = -log(\sum_j a(i,j)) \tag{4.6}$$

where r_i stands for the one-period interest rate if the economy is at state i, and $a(i,j)$ is the one-period transition state price from Ross recovery. Because the transition matrix is time-homogeneous, state interest rates R are also independent of time.

Martin and Ross (2019) and Ross (2015) are especially interested in the long end interest rate because of the convergence of the transition matrix with an infinite horizon. However, the

long end interest rate is not directly observable in the market. We use the current state and the transition matrix to calculate the Ross recovery implied interest rates. Based on the current spot state price vector Π_0 and the transition matrix $\boldsymbol{A}$, the N-period state prices are calculated as $\Pi_0 \times \mathbf{A}^n$. Then the N-period spot rate is calculated as

$$y_n = -log(\sum_j \pi_0(n \cdot h, j)), \text{and} \quad \Pi_n = [\pi_0(n \cdot h, j)] = \Pi_0 \times \mathbf{A}^n \tag{4.7}$$

where y_n is the N-period spot rate from time 0 to time $n \cdot h$, $\Pi_n = [\pi_0(n \cdot h, j)]$ is the n-period Ross recovery implied spot state prices which is calculated by formula (4.2).

The forward rate b_n is the interest rate from time $n \cdot h$ to time $(n+1) \cdot h$. There are two ways to calculate the forward rate. First, the forward rate can be inferred from the spot rate curve in equation (4.7). Second, the forward rate can be also estimated from the state interest rate in equation (4.6). Moreover, the state price transition matrix uniquely determine a transition Ross recovered probability matrix as equation (4.5). The n^{th} one-period forward rate from time $n \cdot h$ to time $(n+1) \cdot h$ is calculated as

$$b_n = -log(P_n \cdot R) = -log(\sum (P_0 \times \boldsymbol{S}^n) \cdot R) \tag{4.8}$$

where P_n is the n^{th} period Ross recovered probability as formula (4.5), R is the state interest rate as formula (4.6).

4.2.3. A comparison of Ross recovery approaches

We use the original Ross recovery estimation (Ross, 2015), labeled Ross Basic (Jackwerth and Menner, 2020), as the benchmark. Ross (2015) and Jackwerth and Menner (2020) notice the unreasonable state interest rates in Ross Basic. They further propose incorporating extra conditions to Ross Basic estimation, such as imposing upper and lower bounds in the transition matrix implied interest rates (Ross Bounded) or assuming there is only one mode in each row of the transition matrix (Ross Unimodal). However, those conditions and constraints are not implied in the original Ross Recovery theorem. Recovered probabilities may include other information by imposing such conditions. We intend to extract the information only in Ross recovery and therefore exclude Ross recovery approaches with additional assumptions from this study.

Table 1 compares different approaches to Ross recovery. Ross Stable rearranges the original Ross recovery and drops the time-homogeneous transition matrix assumption. However, Ross Stable can only be estimated by a non-linear equation system. As proposed by Jensen, Lando, and Pedersen (2019), Ross Stable Linear uses a linear approximation for the utility discount factor δ in Ross Stable. As a result, Ross Stable Linear can be estimated by a linear least squares estimation. We propose three new approaches to Ross recovery labeled as Ross Spot Rate, Ross Power, and Ross Root. These approaches illustrate how the term structure of interest rates, the representation of least squares estimation, and the choice of transition period affect the recovered probabilities as shown in later sections.

-Table 1 here-

4.3. Spot State Price Surface

A state price $\pi(t_0, t_0 + t, i, j)$, or Arrow-Debreu price[3], is the expected price at time t_0 for a unit payment at time $t_0 + t$ when the economy transforms from one state i to another state j accordingly. Using a cross-section of options with a series of strike prices, the spot state price $\pi_0(t, j)$ is determined by the state j in horizon t given a spot state $i = i_0$ at spot time $t_0 = 0$. The spot state price estimation is independent of the Ross recovery theorem. A reliable spot state price surface is the prerequisite for Ross recovery estimation as the transition matrix in Ross recovery theorem is directly estimated from the spot state price surface.

We use Figlewski (2010) non-parametric risk-neutral distribution to estimate spot state prices at different expiries. We also make some adjustments for Figlewski's method to ensure that the risk-neutral distribution accurately reflects the term structure of interest rates and the state prices are fully extracted in both moneyness and time-to-maturity dimensions.

4.3.1. Data

We use the S&P 500 weekly options (SPXW) on January 4, 2019, as an example for empirical analysis. The estimation process can be easily extended to other assets or dates. S&P 500 weekly European put and call option quotes are extracted from Refinitiv DataScope. The last midquote on each date is used as the option close price. Further studies can be applied to intraday data. S&P 500 weekly option has more expiry dates[4] than the standard S&P 500 options so that a more detailed S&P 500 state price surface is possible. The moneyness of each S&P 500 option contract is the strike price divided by the corresponding S&P 500 index level.

U.S. interest rate is the zero-coupon yield from OptionMetrics. A cubic spline interpolation[5] is applied to the zero-coupon bond price based on the zero-coupon yield. The interest rate with the same time to maturity as the option contract is estimated from the interpolated zero-coupon bond price curve. Daily S&P 500 index dividend yields are also from OptionMetrics. The dividend ratio is the average realized dividend yields from the trading date to the expire date of each option contract.

4.3.2. Risk-Neutral Distribution Surface

We exclude in-the-money option contracts that are call options with moneyness lower than 99.5% and put options with moneyness higher than 100.5%. Based on the standard option pricing model of Black and Scholes (1973), at-the-money and out-of-the-money option prices are transformed into Implied Volatilities (IVs). A discrete IV surface consists of option IVs with their moneyness and time to maturity. A fourth degree spline interpolation on both moneyness and time to maturity[6] is conducted on the discrete IV surface to get a smooth

[3] We uses state price and Arrow-Debreu price interchangeably

[4] SPXW options provide the weekly Monday, Wednesday, Friday expiry dates

[5] The cubic spline interpolation is conducted by MATLAB function *spaps*.

[6] The spline interpolation uses *scipy.interpolate.bisplrep* function in Python package *scipy* version 1.4.1

fitted IV surface $\mathbf{IV} = [IV(X_j, T)]$. The interpolation is from 1 day to 252 days with a 1-day interval and from moneyness 0 to moneyness 2 with an interval of 0.0001. The extrapolated IV beyond the minimum or maximum market moneyness is excluded in the next step to avoid any unreliable shape in the deep tails. The fitted IV surface is transformed back to the call option price surface $\mathbf{C} = [C(X_j, T)]$ by the Black-Scholes model again. The risk-neutral probability density $f(X, T)$ and cumulative risk-neutral probability $F(X, T)$ at strike price X_j and time to maturity T is estimated by the approximation formula of Breeden and Litzenberger (1978)

$$f(X_i, T) \approx e^{rT} \frac{C_{i+1,T} - 2C_{i,T} + C_{i-1,T}}{(\Delta X)^2} \tag{4.9}$$

and the cumulative probability function is

$$F(X_i, T) \approx e^{rT} [\frac{C_{i+1,T} - C_{i-1,T}}{X_{i+1,T} - X_{i-1,T}}] + 1 \tag{4.10}$$

The above procedures provide a central risk-neutral probability distribution from the minimum market strike price to the highest market strike price. The tails of the risk-neutral probability distribution are estimated with Generalized Extreme Value (GEV) distribution in the form of

$$G_(x) = exp[-(1 + \xi \frac{S_T - \mu}{\sigma})^{\frac{1}{\xi}}] \tag{4.11}$$

where ξ determines the shape, μ is the mean, σ is the variance of GEV model.

The six parameters of the left and right tails are estimated together by satisfying the following constraints: i) the density of the GEV tail equals the density of the central RND at the first and the second connection points in both left and right tails. The first connection point of the right tail is the strike at the 97% cumulative risk-neutral probability or the maximum market strike whichever is smaller. The percentile of the first right connection point is α_R The second connection point is the strike that is closest to the percentile $\alpha_R - 3\%$. The first connection point of the left tail is the strike at the 3% cumulative risk-neutral probability or the minimum market strike whichever is greater. The percentile of the first left connection point is α_L. The second left connection point is the strike that is closest to the percentile α_L+3%. ii) The sum of central RND and tail probability equals 100%. iii) The expectation of moneyness based on central density and tail distribution equals corresponding risk-neutral measure, the interest rate return minus the dividend ratio as $exp((r - q)T)$.

The procedures above provide a smooth and well-behaved RND surface. Panel A of Figure 4.1 shows that the RND surface estimated on January 4, 2019 is smooth and reliable. Panel B of Figure 4.1 shows the term structure of RND from short to long horizons. The shorter term RNDs are more concentrated around at-the-money and relatively symmetric. The longer term RNDs are more disperse and negatively skewed.

-Figure 4.1 here-

The expectation of a RND reflects the corresponding interest rate. RND implied interest rates should equal to the market interest rates. Figure 4.2 compares the implied interest rates from the RND surface and market interest rates. The market interest rate is from 2.4% to 2.8% for horizons within one year. It increases sharply in the short term and decreases slowly in the

medium and long terms as the horizon increases. The RND implied interest rate is consistent with the market interest rate indicating a reliable estimation based on the risk-neutral measure.

-Figure 4.2 here-

The number of distinct economy states determines the number of strikes or moneyness in RND that further determines the size of unknown parameters in Ross recovery. To have a relatively good balance between the smoothness of state price surface and the number of unknown parameters in the following Ross recovery, we apply 100 states from moneyness 0 to moneyness 2 with an interval of 0.02. The horizon is from 2 days to 250 days with an interval of 2 days. The RND surface is reduced into a 125×100 RND matrix $\mathbf{Q} = [q(t,i)]$ where t is the horizon of the RND and i is the moneyness. Each row in RND matrix $\mathbf{Q}$ is a RND with time to maturity as t. Each column in the RND matrix $\mathbf{Q}$ shows the risk-neutral probability at state i. In the later part of this chapter, the economy states are further reduced into 20 states with an interval of 0.1 moneyness because of time-consuming nonlinear calculations.

4.3.3. Risk-Neutral Distribution to State Price

The risk-neutral probability matrix $\mathbf{Q}$ and the spot state price matrix $\mathbf{\Pi} = [\pi_0(t,i)]$ are linked via interest rates. Risk neutral probability $q(t,i)$ is transformed to spot state price $\pi_0(t,i)$ directly by the corresponding interest rate r_f^t. With continuous compounding,

$$\pi_0(t,i) = q(t,i)exp(-r_f^t \cdot t) \tag{4.12}$$

Besides, the spot state price with horizon $t = 0$ equals one for the current state and zero for all other states, i.e. a state price vector Π_0 with only one non-zero entry. The $t = 0$ state price vector can be added to the spot state price matrix as the first row to have a complete spot state price matrix $\mathbf{\Pi}$ from time 0 to time T.

4.4. Existing Empirical Approaches to Ross Recovery

This section reviews Ross Basic and Ross Stable. It explores the implied term structure of interest rates in Ross Stable and discusses how small errors in the utility discount factor heavily affect the recovered probabilities in Ross Stable.

4.4.1. Ross Basic Estimation

In the original estimation by Ross (2015) and the Ross Basic estimation labeled by Jackwerth and Menner (2020), the state price transition matrix is estimated by minimizing the one-period transition errors. Following Jackwerth and Menner (2020), we use an overlapping approach to estimate the transition matrix. The spot state price surface $\mathbf{\Pi}$ from day 0 to day 250 with an interval of 2 days as estimated in section 4.3 is rearranged into two subgroups of spot state price surfaces $\mathbf{\Pi}_a$ and $\mathbf{\Pi}_b$. Spot state price surface $\mathbf{\Pi}_a$ is from day 0 to day 230. Spot state price surface $\mathbf{\Pi}_b$ is from day 20 to day 250. The one-period transition is 20 business days (one month). The 20-day state price transition matrix $\boldsymbol{A}$ links the spot state prices at day

t with spot state prices at day t+20 as $\mathbf{\Pi}_b = \mathbf{\Pi}_a \times \boldsymbol{A}$. This equation is solved by minimizing the following least squares estimation

$$\min_{a(i,j)} \sum_{j \in N} \sum_{t=0}^{230} (\pi_0(t+20, j) - \sum_{i \in N} \pi_0(t, i) a(i, j))^2 \quad s.t. \quad a(i, j) \geq 0 \tag{4.13}$$

where $\pi_0(t, i)$ and $\pi_0(t, j)$ are the spot state prices in the spot state price surface $\mathbf{\Pi}$. This least squares problem is estimated by $lsqnonneg$ function in MATLAB[7].

Figure 4.3 shows the state price transition matrix by Ross Basic. Panel A of Figure 4.3 presents that there is an extreme state price in the transition matrix when the moneyness is close to 0. Market spot state prices with moneyness below 0.4 and above 1.4 are close to 0. They correspond to the deep tails of risk-neutral probability distributions. There is little information for the estimation of transition matrix with transition start state below moneyness 0.4 or above moneyness 1.4. Therefore, some extreme values in the rows corresponding to the deep tails of the spot state prices have no obvious impact on the estimation process. Panel B of Figure 4.3 excludes the rows in the transition matrix corresponding to the deep tails and starts from moneyness 0.4 to moneyness 1.4. Similar to the results of Jackwerth and Menner (2020), the main diagonal of the transition matrix has relatively higher state prices because of higher probabilities of the same state at the end of the transition period as the initial of the transition period. However, it is difficult to understand the state prices away from the main diagonal. Especially high state prices are next to state prices close to 0.

-Figure 4.3 here-

Figure 4.4 compares the fitted risk-neutral and recovered probabilities from the market risk-neutral probabilities. The fitted one-period risk-neutral probabilities at time t are calculated by the market risk-neutral probabilities at time $t - h$ and the one-period transition matrix. The multi-period fitted risk-neutral probabilities at time t is based on the spot state prices Π_0 multiply by $(t/h)^{th}$ (20 days per period, 6 periods for 120 days in this example) power function of the transition matrix as formula (4.2). Recovered probabilities are the multi-period risk-neutral probabilities recovered by the transition matrix implied stochastic discount factors. The fitted one-period risk-neutral probabilities are not necessarily the same as the Ross recovery implied multi-period risk-neutral probabilities because of estimation errors.

Ross Basic fits well with the spot state prices. There is no obvious difference between the fitted one-period risk-neutral probabilities and the market risk-neutral probabilities for the 20-day horizon. However, in the long term, there are some differences around the mode of the distributions. 120-day fitted risk-neutral probabilities based on a one-period transition present small differences from the market risk-neutral probabilities while 120-day fitted risk-neutral probabilities based on multi-period transitions show relatively large estimation errors. If you minimize errors in one-period transition and use this as an input for multi-period, it may not be a good fit for multi periods. The Ross Basic least squares problem (4.13) is an overspecified linear equation system with a nonnegativity constraint for transition state prices, an exact

[7]Least squares problem (4.13) can be written in a standard $C \cdot x - d$ form as Appendix A.4.1. $lsqnonneg$ function in MATLAB provides a fast and reliable solution to the standard $C \cdot x - d$ linear least squares problem.

solution is not possible given the spot state prices. The least squares estimation provides a satisfying but not the same fitted spot state price surface as the market spot state price surface.

Despite only small errors in Ross Basic, the recovered probability distribution is not smooth or well-behaved. The recovered probability at moneyness 0.94 is negligible while the risk-neutral probability is substantial at the same moneyness for the 20-day horizon as shown in Panel A of Figure 4.4. 120-day recovered probability distribution has even more kinks. Ross Basic in (4.13) only minimizes the one-period transition errors. Longer term, such as 120-day, recovered probability distribution therefore may have more estimation errors and unreliable shapes.

-Figure 4.4 here-

Figure 4.5 shows the Ross transition matrix implied interest rates. Panel A shows the state interest rates. Panel B compares the implied with market spot rates. First, the state interest rates take extreme values. Ross Basic results in unreasonable large and negative interest rates. Second, the implied spot rate curve is far different from the market spot rate curve. Ross Basic fails to incorporate the market interest rates that determine the sum of spot state prices in each horizon. A spot state price surface provides a solution for least squares problem (4.13). However, such a solution is not necessarily consistent with Ross recovery as Ross implicit assumptions are not addressed. As a result, the recovered probabilities and stochastic discount factors from Ross Basic are not consistent with the Ross recovery theorem.

-Figure 4.5 here-

4.4.2. Ross Stable/ Generalized Recovery

In contrast to imposing additional constraints or assumptions to the Ross recovery theorem, generalized recovery (Jensen, Lando, and Pedersen, 2019) and Ross Stable (Jackwerth and Menner, 2020) only keep the assumption of transition-independent stochastic discount factors. The one-period time-homogeneous transition matrix is excluded from generalized recovery and Ross Stable. With the assumption that the stochastic discount factor is transition-independent as in the equation (4.3), the spot state price surface can be transformed to a surface of recovered probabilities. A set of equations without transition matrix is specified as follows

$$\begin{bmatrix} \pi_0(1,1) & \dots & \pi_0(1,j) & \dots & \pi_0(1,N) \\ \pi_0(2,1) & \dots & \pi_0(2,j) & \dots & \pi_0(2,N) \\ \vdots & \vdots & \dots & \vdots & \\ \pi_0(T,1) & \dots & \pi_0(T,j) & \dots & \pi_0(T,N) \end{bmatrix} \times \begin{bmatrix} z_1/z_1 \\ \vdots \\ z_{k-1}/z_1 \\ z_k/z_1 \\ \vdots \\ z_N/z_1 \end{bmatrix} = \begin{bmatrix} \delta^1 \\ \delta^2 \\ \vdots \\ \delta^{T-1} \\ \delta^T \end{bmatrix} \tag{4.14}$$

where $\pi_0(t,j)$ is the spot state price in the spot state price surface $\mathbf{\Pi}$, z_k and δ are the inverse of marginal utility and the utility discount factor, respectively, each row indicates that the sum of recovered probabilities equals one. This equation system is estimated by minimizing the

squared errors labeled Ross Stable as

$$\min_{z_k,\delta} \sum_{t=1}^{t=250} ((\sum_{k=1}^{N} \pi_0(t,k) z_k/z_1) - \delta^t)^2 \quad s.t. \quad z_k \geq 0, \delta \geq 0 \tag{4.15}$$

Figure 4.6 shows the recovered probability distributions of Ross Stable. Panels A and B show that Ross Stable recovered probabilities are close to the market risk-neutral probabilities for both 20-day and 120-day horizons. This result is consistent with the empirical result of Jackwerth and Menner (2020). They also find that the stochastic discount factor is stable and close to one.

-Figure 4.6 here-

The stable stochastic discount factor suggests that the recovered probabilities are close to risk-neutral probabilities empirically. Ross Basic provides well-fitted risk-neutral probabilities. However, Ross Basic recovered probabilities and Ross Stable recovered probabilities present significant differences while they both have the same form of pricing kernel. It is not clear which approach provides recovered probabilities correctly reflecting the time-homogeneous pricing kernel. The rest of this chapter tries to explain the differences between Ross Basic and Ross Stable mainly as a result of an omitted interest rate condition in Ross Basic.

Ross Stable in the form of equation (4.14) is close to a linear system, but the right hand side is a power function of the utility discount factor δ. Jensen, Lando, and Pedersen (2019) propose a linear approximation $\delta^t \approx \alpha_t + \beta_t \delta$ around $\delta_0 = 0.97$ and Ross Stable becomes a linear system as

$$\begin{bmatrix} -\beta_1 & \pi_0(1,1) & \dots & \pi_0(1,j) & \dots & \pi_0(1,N) \\ -\beta_2 & \pi_0(2,1) & \dots & \pi_0(2,j) & \dots & \pi_0(2,N) \\ \vdots & \dots & \dots & \dots & \dots & \vdots \\ -\beta_T & \pi_0(T,1) & \dots & \pi_0(T,j) & \dots & \pi_0(T,N) \end{bmatrix} \times \begin{bmatrix} \delta \\ z_1/z_1 \\ \vdots \\ z_{k-1}/z_1 \\ z_k/z_1 \\ \vdots \\ z_N/z_1 \end{bmatrix} = \begin{bmatrix} \alpha_1 \\ \alpha_2 \\ \vdots \\ \alpha_{T-1} \\ \alpha_T \end{bmatrix} \tag{4.16}$$

where $\alpha_t = -(t-1)\delta_0^t$ and $\beta_t = t\delta_0^{t-1}$, with other variables being the same as equation (4.14). Jensen, Lando, and Pedersen (2019) present the closed-form solution for this system. However, the closed form solution z_k of this system may be negative. To ensure the nonnegativity of z_k, an additional constraint $z_k \geq 0$ is required for this equation system. With this nonnegativity constraint, there is no closed from solution. Instead, this closed form approach has to be estimated by a least squares estimation similarly as Ross Stable

$$\min_{z_k,\delta} \sum_{t=1}^{t=250} ((\sum_{k=1}^{N} \pi_0(t,k) z_k/z_1) - (\alpha_t + \beta_t \delta))^2 \quad s.t. \quad z_k \geq 0, \delta \geq 0 \tag{4.17}$$

this least squares problem is estimated by $lsqnonneg$ function in MATLAB because it is already in the standard $C \cdot x - d$ form. This estimation is labeled as Ross Stable Linear.

Figure 4.7 compares the linear approximation and the original power function of δ^t. The linear approximation works well as $\alpha_t + \beta_t\delta$ is close to δ^t within one year horizon.

-Figure 4.7 here-

Figure 4.8 shows the Ross Stable Linear recovered probabilities and the market risk-neutral probabilities. Although the linear approximation only has small differences from the original δ^t, the recovered probabilities substantially deviate from the Ross Stable recovered probabilities with many kinks. A small change in the utility discount factor results in a substantial change in the pricing kernel. It suggests the importance of the utility discount factor in transition-independent recovery. The empirical results of Ross Stable Linear are less precise than Ross Stable. Ross recovery implied information may be largely different from Ross Stable Linear recovered information.

-Figure 4.8 here-

The difference between Ross Stable Linear and Ross Stable shows how recovered probabilities are sensitive to time discount factors. As Ross Basic fails to reflect the term structure of interest rates that determine the risk-free discount factors, it will improve the accuracy of recovered probabilities by considering interest rates for Ross recovery estimations as the next section shows.

4.5. Recovery with Interest Rates

In the previous section, Ross Basic and Ross Stable provide different recovered probabilities for the same spot state price surface. This section discusses the omitted condition in Ross Basic and how flat term structure results in a risk-neutral recovery.

4.5.1. A Flat Term Structure

Assume we start our analysis with a flat term structure of interest rates. In an economy following the assumptions in Ross recovery or Ross Stable, no matter the shape of the spot state price surface, the recovered probabilities degenerate to risk-neutral probabilities when the term structure of interest rates is flat.

Based on Ross recovery, there is a recovered probability surface $\boldsymbol{P}$ from spot state price surface $\boldsymbol{\Pi}$ according to formula (4.5). A subgroup probability surface $\hat{\boldsymbol{P}}$ consists of $T = N$ consecutive recovered probability from the original recovered probability surface $\boldsymbol{P}$. The probability surface $\hat{\boldsymbol{P}}$ is a square probability matrix with the sum of each row equals one. Assuming the probability surface $\hat{\boldsymbol{P}}$ is invertible

$$\begin{aligned} \hat{\boldsymbol{P}}\boldsymbol{e} &= \boldsymbol{e} \\ \boldsymbol{e} &= \hat{\boldsymbol{P}}^{-1}\boldsymbol{e} \end{aligned} \tag{4.18}$$

where **e** is a column unit vector.

In a Ross recovery economy, the state interest rate vector R is estimated from the transition matrix shown as formula (4.6). The expected one-period forward rate from any time t is

$E(b_t) = P_t R$. Given a market forward rate curve $\hat{B} = [b_1, b_2, ..., b_N]'$, and time-homogeneous state interest rate vector $R = [r_{t1}, r_{t2}, ..., r_T]'$

$$\hat{\boldsymbol{P}} R = \hat{B} \tag{4.19}$$

If the term structure is flat, i.e. $\hat{B} = [b_1, b_2, ..., b_N]' = b\boldsymbol{e}$,

$$\begin{aligned} \hat{\boldsymbol{P}} R &= \hat{B} \\ R &= \hat{\boldsymbol{P}}^{-1} b\boldsymbol{e} \\ R &= b\boldsymbol{e} \end{aligned} \tag{4.20}$$

i.e. when the forward rates on all trading dates are the same, Ross Recovery transition matrix implied interest rates are state independent and equal to the forward rate. According to the Ross recovery theorem, if the interest rate is state independent, recovered probabilities become risk-neutral probabilities. The flat term structure uniquely determines a stable pricing kernel in the Ross recovery theorem. Therefore, Ross Recovery provides no additional information in comparison to risk-neutral estimation when the term structure is flat.

In Ross Stable, the stochastic discount factor is transition-independent. If the term structure of interest rates is flat, it can be noticed that a unit vector and the interest rate discount factor are always one set of solution for equation system (4.14)

$$z_k = 1, \forall i \in N, and \quad \delta = exp(y_1) \tag{4.21}$$

where y_1 is spot rate.

This solution is independent of the shape of the spot state price surface. As long as the term structure is flat, risk-neutral estimation is always one solution of Ross Stable. This result is similar to Ross recovery, indicating that the assumption of transition-independent stochastic discount factors has an important impact on the recovery estimation. In reality, although the term structure may be not flat, it is unlikely to change substantially. The numerical solution of (4.14) may be still close to formula (4.21) as shown in the empirical result of Ross Stable in previous section. Jensen, Lando, and Pedersen (2019) also point out, in generalized recovery/ Ross stable, the risk-neutral solution may be not unique under a flat term structure.

4.5.2. Ross Recovery Estimation with an Interest Rate Condition

The term structure of interest rates is usually not flat. E.g. the term structure on January 4, 2019 increases with time in the short and medium terms but slightly decreases in the long term (see Figure 4.1). We therefore propose an interest rate condition for Ross recovery. The transition matrix in Ross recovery implies a forward rate curve and a spot rate curve as discussed in section 4.2.2. The expected forward rate under Ross recovery should equal the market one-period forward rate. And the Ross recovery implied spot rate for any horizon should equal the market spot rate.

A. Ross Forward Rate Estimation

We propose a Ross recovery estimation labeled Ross Forward Rate which minimizes the errors between the implied forward rate and the market forward rate in comparison to Ross Basic. Like Ross Basic, we have the following least squares estimation

$$\min_{a(i,j)} \sum_{j\in N} \sum_{t=0}^{230} (\pi_0(t+20,j) - \sum_{i\in N} \pi_0(t,i)a(i,j))^2 + \sum_{t=0}^{230} (b_t - \hat{b}_t)^2 \quad s.t. \quad a(i,j) \geq 0 \quad (4.22)$$

where b_t is the transition matrix implied forward rate as in formula (4.8), $\hat{b}_t$ is the market forward rate from the term structure, other variables are the same as in the Ross Basic.

However, this method has to find the Perron–Frobenius eigenvalue in each iteration during the optimization process. Thus, Ross Forward Rate is a nonlinear equation system. It is computation-intensive to find the local minimum. As a forward rate curve can be transformed to a spot rate curve directly, the following Ross Spot Rate estimation provides an alternative approach to incorporating the term structure of interest rates without imposing a nonlinear constraint to Ross Basic.

B. Ross Spot Rate Estimation

The Ross Spot Rate estimation tries to minimize the errors between implied spot rates and market spot rates. As the sum of spot state prices for any horizon t is the interest rate discount factor, Ross Spot Rate requires that fitted interest rate discount factors equal market interest rate discount factors.

$$\begin{aligned}\min_{a(i,j)} \sum_{j\in N} \sum_{t=0}^{230} (\pi_0(t+20,j) - \sum_{i\in N} \pi_0(t,i)a(i,j))^2 + \omega \sum_{t=0}^{230} (\sum_{j\in N} (\pi_0(t+20,j) \\ - \sum_{j\in N} \sum_{i\in N} \pi_0(t,i)a(i,j))^2 \quad s.t. \quad a(i,j) \geq 0 \end{aligned} \quad (4.23)$$

where ω determines the relative importance of Ross Basic and the interest rate condition, ω is set to a large value 100000 to ensure that the interest rate condition is satisfied, all other variables are the same as Ross Basic. This optimization problem is estimated in a similar way as Ross Basic through $lsqnonneg$ function in MATLAB[8].

Figure 4.9 shows the estimated state price transition matrix by Ross Spot Rate approach. As the spot state prices are close to zero in the deep tails, the Ross Spot Rate transition matrix has some extreme values in the states corresponding to deep tails. Panel B of Figure 4.9 shows the center part of the transition matrix. The state prices on the diagonal are higher than other states in the transition matrix.

-Figure 4.9 here-

Panels A and B of Figure 4.10 are fitted risk-neutral and recovered probabilities for

[8]Least squared problem (4.23) can be written in a standard $C \cdot x - d$ form as Appendix A.4.3.

20-day and 120-day horizons, respectively. 20-day fitted risk-neutral probabilities are not substantially different from market risk-neutral probabilities. Overall, 120-day fitted risk-neutral probabilities are close to the market risk-neutral probabilities. However, the fitted risk-neutral probability distribution deviates from the market risk-neutral probability distribution around its mode. Unlike Ross Basic, the recovered probability distributions are close to the fitted risk-neutral probability distribution, especially for the 20-day horizon. Ross Spot Rate provides similar results as the Ross Stable, indicating a relatively stable pricing kernel. As the additional constraint of Ross Spot Rate in comparison to Ross Basic is implied by the Ross recovery theorem, the strange shape of the Ross Basic recovered probability distribution is a result of the ill-conditioned estimation process. The Ross Spot Rate estimation complements the Ross recovery estimation by taking into account the implied spot rate curve.

-Figure 4.10 here-

Panel A of Figure 4.11 shows one-period state interest rates. It is similar to Ross Basic, Ross Spot Rate still results in states with extreme positive and negative interest rates. However, Ross Spot Rate state interest rates are less volatile comparing to Ross Basic. Panel B of Figure 4.11 shows that Ross Spot Rate implied interest rates are close to market interest rates. The Ross Spot Rate implied interest rates from the one-period calculation are consistent with market interest rates, indicating an accurate estimation for the optimization problem (4.23). However, implied interest rates based on the multi-period calculation for 120-day are not the same as the market interest rates. Ross Spot Rate only minimizes the one-period estimation errors.

-Figure 4.11 here-

4.6. Multi-Period Ross Recovery Estimation

In the above Ross Basic and Ross Spot Rate estimations, the fitted spot state price at time t is represented as the market spot state price at time $t-1$ times the one-period transition matrix. However, based on the equation (4.2), fitted spot state prices at time t are also represented as market spot state prices at time t_0 times the power function of the transition matrix. We propose a new approach termed Ross Power estimation by minimizing the errors between the market spot state prices and the fitted spot state prices calculated through the power function of the transition matrix.

Based on the equation (4.2), the spot state price surface is solely represented by the transition matrix. Following the same idea of overlapping spot state price surface as in Ross Basic, spot state prices are specified as

$$\Pi_{i+20n} = \Pi_i \times \boldsymbol{A}^n, where \quad i = 0, 1, ..., 19, \quad n = 1, 2, ... \tag{4.24}$$

This multi-period representation is not a linear equation. It consists of n^{th} power function of the transition matrix for n^{th} period spot state prices. In addition, a penalty term ω on the error between the market interest rate discount factor and Ross implied interest rate discount factor for each horizon captures the relative importance of fitting the state prices and fitting

the interest rate condition.

$$\min_{a(i,j)} \sum_{j \in N} \sum_{t=20}^{250} (\pi_0(t,j) - \hat{\pi}_0(t,j))^2 + \omega \sum_{t=20}^{250} (\sum \pi_0(t,j) - \sum \hat{\pi}_0(t,j))^2$$
$$\text{where } \hat{\Pi} = [\hat{\pi}_0(t,j)], s.t. \quad a(i,j) \geq 0 \tag{4.25}$$

where $\hat{\Pi}_t = [\hat{\pi}_0(t,j)]$ is the Ross Power method fitted spot state prices at time t calculated as formula (4.24).

If there is an exact and unique Ross recovery transition matrix satisfying the market spot state price surface, different approaches, including Ross Basic, Ross Spot Rate, and Ross Power, will have the same solution for the Ross recovery theorem. However, the market spot state price surface usually implies no exact transition matrix for Ross recovery. Least squares estimations with different representations are not equivalent when there is no exact solution. The least squares solution for Ross Basic or Ross Spot Rate is not necessarily the solution for Ross Power. Ross Power has the advantage of correctly representing the long-term spot state prices and interest rates as a result of the n^{th} power function of the transition matrix.

In previous linear least squares representations of Ross recovery estimation, there are 100 states which result in a transition matrix with $100^2 = 10000$ unknown parameters. To reduce the computational intensity of Ross Power, this section uses a simplified spot state price surface with 20 states from moneyness 0 to moneyness 2 with an interval as moneyness 0.1. Thus, the number of unknown parameters in the nonlinear least squares problem (4.25) decreases from 10000 to 400 which makes the computation feasible. Also, the nonlinear least squares problem (4.25) may have many local minimum values. To compare with Ross Spot Rate, Ross Power uses the output of Ross Spot Rate as the starting guess in the optimization process.

Figure 4.12 shows the estimated state price transition matrix by Ross Power. It is similar to other Ross recovery estimations, the transition matrix has some extreme values in the states corresponding to the deep tails. The state prices at the main diagonal of the transition matrix are much higher than other state prices in the transition matrix.

-Figure 4.12 here-

Panels A and B of Figure 4.13 are the Ross Power fitted risk-neutral and recovered probabilities for 20-day and 120-day horizons. Ross Power fitted risk-neutral probability distribution has more deviations from the market risk-neutral probability distribution than other Ross recovery approaches as a result of more strict constraints from the power function of the transition matrix. This evidence is against Ross's assumption of a time-homogeneous one-period transition matrix. Therefore, Ross recovered probabilities may be different from generalized recovered/ Ross Stable recovered probabilities depending on how market spot state prices deviate from a Markov chain process with a time-homogeneous transition matrix. Given the empirical fact that there is no exact transition matrix for market spot state prices, Ross recovered probabilities incorporate the information of a transition matrix in comparison to generalized recovery.

When a spot state price surface satisfies a time-homogeneous one-period transition matrix

as the Ross Power fitted spot state prices, Ross recovered probabilities are close to the risk-neutral probabilities and provide little additional information. Audrino, Huitema, and Ludwig (2021) find Ross recovered probabilities are informative with an additional stability term but without the interest rate condition. Their recovered probabilities are not Ross recovered probabilities as their estimated transition matrix may be inconsistent with the market term structure of interest rates. However, examining how their estimation process incorporates other informative factors may be useful for future research.

-Figure 4.13 here-

Panel A of Figure 4.14 shows state interest rates. Ross Power implies relatively stable state interest rates around at-the-money states. Only the states corresponding to the deep left tail of the market risk-neutral distribution implies extreme state interest rates. There is no extreme state interest rate around at-the-money states. Panel B of Figure 4.14 shows that Ross Power implies a term structure of interest rates that is almost the same as the market term structure. The nonlinear Ross Power estimation correctly represents the long-term interest rates in comparison to other Ross recovery approaches.

-Figure 4.14 here-

Overall, we suggest that applications of Ross recovery should reflect all implied requirements, such as the term structure of interest rates and the multi-period transition. Ross Power can be a successful approach as it incorporates all known requirements for Ross recovery. The empirical analysis from Ross Power shows when a market term structure is not flat but short-term upward-sloping, Ross recovered probabilities are still close to risk-neutral probabilities.

4.7. Ross Root Estimation

This section addresses another challenge in Ross recovery estimations. Different lengths of transition periods are likely to result in substantially different recovered transition matrices. Transition matrix with a short period implicitly has a condition that the power function of the one-period transition matrix is the multi-period transition matrix. This is equivalent as that the long term transition matrix has a nonnegative k^{th} root.

4.7.1. The One-period Transition

Based on the assumption in the Ross recovery theorem, there is a time-homogeneous one-period transition matrix. Ross makes no further assumption on the period length of transition that can be one day or one month. However, in the empirical estimations, different lengths of transition imply different conditions.

As it is in Ross Basic, the spot state price surface $\mathbf{\Pi}$ can be rearranged into two subgroups $\mathbf{\Pi}_a$ and $\mathbf{\Pi}_b$ with a time lag h. A state price transition matrix $\boldsymbol{A}_h$ with a transition period h links these two subgroups as $\mathbf{\Pi}_b = \mathbf{\Pi}_a \times \boldsymbol{A}_h$. Besides, the transition matrix $\boldsymbol{A}_h$ can be calculated from a state price transition matrix $\boldsymbol{A}_{h/2}$ with a transition period $h/2$ as $\boldsymbol{A}_h = \boldsymbol{A}_{h/2}^2$. Then the two subgroups can be linked by the transition matrix $\boldsymbol{A}_{h/2}$ as $\mathbf{\Pi}_b = \mathbf{\Pi}_a \times \boldsymbol{A}_{h/2}^2$.

Therefore, there are two approaches to estimate the transition matrix given a spot state price surface. The approach of estimating $\boldsymbol{A}_{h/2}$ is equivalent to estimating $\boldsymbol{A}_h$ with a condition that $\boldsymbol{A}_h$ has a nonnegative square root. According to the uniqueness and existence condition of a nonnegative square root of a nonnegative matrix by Tam and Huang (2016), a long period transition matrix $\boldsymbol{A}_h$ directly estimated from Ross Basic approach may have no nonnegative square root.

The above analysis can be easily extended to k^{th} root of the transition matrix. In Ross Recovery estimations, by choosing a relatively long transition period, the estimation process has more flexibility to fit the market spot state prices. By choosing a relatively short transition period, the estimation process implicitly incorporates the existence of a nonnegative k^{th} root of a long period transition matrix.

4.7.2. Transition Period of Two days

In Ross Basic, the transition period is 20 days. We propose a new estimation method labeled Ross Root with a transition period of 2 days. Ross Root implicitly requires the existence of a nonnegative 10^{th} root for a one-month transition matrix while the one-month transition matrix in Ross Basic may have no such nonnegative 10^{th} root.

Spot state price surfaces $\boldsymbol{\Pi}_a$ and $\boldsymbol{\Pi}_b$ are the same as Ross Basic. The 2-day state price transition matrix $\boldsymbol{A}_{2d}$ links the state prices at day t with state prices at day t+20 as $\boldsymbol{\Pi}_b = \boldsymbol{\Pi}_a \times \boldsymbol{A}_{2d}^{10}$. It is difficult to calculate the 10^{th} root of the matrix $\boldsymbol{A}_{2d}^{10}$. Therefore, Ross Root is estimated by the same least squares problem (4.13) but changing the transition time from 20 days to 2 days.

Figure 4.15 shows the state price transition matrix of Ross Root. First, the transition states corresponding to the deep tails of the spot state price surface present extreme values as with other Ross recovery approaches. Second, the state prices are much higher on the main diagonal of the transition matrix as with Ross Basic. However, by changing the transition period h, Ross Root provides a substantially different transition matrix to Ross Basic.

-Figure 4.15 here-

Figure 4.16 shows recovered distributions from Ross Root. Panels A and B show risk-neutral probabilities and recovered probabilities with 20-day and 120-day horizons, respectively. Like Ross Basic, Ross Root fits well with the market spot state prices. For the 20-day horizon, Ross Root fitted risk-neutral probabilities present no obvious difference from the market risk-neutral probabilities. For the 120-day horizon, there are some minor differences between the fitted and the market risk-neutral probabilities around the mode. Unlike Ross Basic, the fitted risk-neutral probability distributions from one-period and multi-period estimations are not different as the one-month transition matrix is calculated by 10^{th} power function of the 2-day transition matrix. The nonlinearity of long-term Ross fitted risk-neutral probability distribution is reflected in Ross Root.

Although Ross Root is similar to Ross Basic with fitted risk-neutral probability distributions, Ross Root recovered probabilities are dramatically different from Ross Basic recovered probabilities. Ross Root recovered probability distribution is not smooth, indicating stochastic

discount factors with dramatic shapes.

-Figure 4.16 here-

Figure 4.17 shows the Ross Root implied interest rates. Ross Root implied interest rates have a similar pattern as Ross Basic implied interest rates. First, there are extreme implied state rates, e.g. over 6000% annualized state interest rate. Second, the implied spot rates, from -10% to 15%, are far different from the market spot rates. Ross Root fails to incorporate the market interest rates. It is not a surprise that Ross Root has similar problems as Ross Basic because they are estimated by the same least squares problem. However, it should be noticed that by changing the transition period to a shorter time, Ross Basic provides substantially different results from the same spot state price surface.

-Figure 4.17 here-

Existing literature provides no guidance to the choice of period length for transition matrix. Following previous literature, we focus on the one-month transition matrix.

4.8. Ross Recovery Implied Information

This section compares the implied information from different approaches of Ross recovery. Because of the computational limitation in Ross Power, this section estimates different Ross recovery approaches using the relatively sparse spot state price surface with 20 states from moneyness 0 to moneyness 2 with an interval as moneyness 0.1.

The accuracy of the transition matrix is estimated as the Sum of Squared Errors (SSE) between the fitted spot state prices and the market spot state prices from 20 days to 250 days. Estimation accuracies of Ross Stable and Ross Stable Linear are estimated as the Sum of Squared Errors between the sum of recovered probability and 100% as there is no transition matrix.

Table 2 shows the estimation accuracies of different Ross recovery approaches. Overall, there are only small errors in all Ross recovery approaches. The estimated one-period transition matrix provides a reliable representation for the whole spot state price surface. The one-period transition matrix yields forecasts about the long-term risk-neutral probability distribution that is not directly observable in the market. SSE of Ross Basic is the smallest among all Ross recovery approaches as Ross Basic ignores some implicit conditions. The largest SSE of Ross Root indicates that by choosing a short transition period, the market spot state prices are not consistent with Ross recovery assumptions. However, the optimal period length of transition still requires further research. Ross Spot Rate and Ross Power have greater SSE than Ross Basic because of an additional interest rate condition. Applications of Ross recovery have to determine the relative importance between fitting the overall spot state price surface and fitting the term structure of interest rates. If the term structure of interest rates is ignored, a linear estimation of Ross recovery is Ross Basic with small SSE. If fitting the interest rate term structure is the priority, such as Ross Spot Rate, relatively large SSE come with the interest rate condition. Because Ross Stable only uses the time-homogeneous stochastic discount factor assumption in Ross recovery without assuming a time-homogeneous transition matrix, the SSE of Ross Stable and Ross Stable Linear are extremely small.

-Table 2 here-

The stochastic discount factors show the pricing kernel between the risk-neutral measure and Ross recovery measure. Figure 4.18 compares the 20-day stochastic discount factors of all approaches to Ross recovery theorem on January 4, 2019 with 20-state spot state price surface. Extreme recovered probabilities and volatile shapes of stochastic discount factors in Ross Basic and Ross Root are probably due to the ill-conditioned estimation process.

Unlike the result of the 100-state state price surface (see the difference of fitted risk-neutral distribution and recovered probability distribution as Figure 4.8), stochastic discount factors of Ross Stable Linear are similar to that of Ross Stable with the 20-state state price surface. Fitting the transition matrix in a dense spot state price surface is more likely to result in a relatively volatile pricing kernel. Ross Spot Rate with a 20-state state price surface also implies a more stable pricing kernel to Ross Spot Rate with a 100-state state price surface.

Ross Stable, Ross Stable Linear, Ross Spot Rate, and Ross Power all have relatively stable pricing kernels, especially around at-the-money. The relatively stable stochastic discount factor suggests similar information between the risk-neutral measure and the long-term risk-neutral measure. Ross Spot Rate and Ross Power require a time-homogeneous transition matrix in comparison to Ross Stable. Empirically, Ross Spot Rate and Ross Power have relatively more volatile pricing kernels.

-Figure 4.18 here-

Based on the transition matrix, Ross recovery has the advantages of calculating spot state prices beyond market horizons of spot state prices. We select a long-term horizon, 10 years, to present the long-term convergence in Ross recovery. The sum of spot state prices reflects the interest rate discount factor that is horizon dependent. Figure 4.19 presents the long-term risk-neutral and recovered probability distributions. The time-homogeneous transition matrix estimated from a one-year spot state price surface implies approximately bimodal risk-neutral distributions in the long term with an upside movement and a downside movement in the underlying asset price. Market option contracts on January 4, 2019 include expiries only within a horizon of 258 days. The transition matrix provides a novel method for long-term expectations. Although Ross recovered probabilities are empirically close to the risk-neutral probabilities, the reasons for the implied long-term bimodal risk-neutral distribution are unclear. Similar to risk-neutral probability distributions, recovered probability distributions also converge to their long-term stationary distributions. Consistent to Figure 4.18 of the stochastic discount factors, the stationary recovered probabilities of Ross Basic and Ross Root indicate strange shapes while the stationary recovered probabilities of Ross Spot Rate and Ross Power are close to the fitted risk-neutral probability distributions.

-Figure 4.19 here-

Table 3 quantifies the differences between fitted risk-neutral probabilities and recovered probabilities of different Ross approaches with their moments. For one-period horizon, moments of fitted risk-neutral distributions are close to moments of market risk-neutral distributions, indicating again a relatively accurate fitting of the transition matrix with the market spot state price surface. The first four moments of recovered probability distributions from Ross Spot Rate and Ross Power are similar to their corresponding fitted risk-neutral

moments while recovered moments of Ross Basic and Ross Root are largely different from their corresponding fitted risk-neutral moments. The first four moments of recovered probability distributions from Ross Stable, and Ross Stable Linear are close to the market risk-neutral moments. This is consistent with the shapes of their stochastic discount factors in Figure 4.18. Table 3 panel B confirms in the long term, moments of both recovered probabilities and fitted risk-neutral probabilities from Ross Spot Rate and Ross Power are close to each other while moments of recovered probabilities from Ross Basic and Ross Root are different from other approaches.

-Table 3 here-

4.9. Conclusions

We propose the importance of the term structure of interest rates in Ross recovery. When the term structure of interest rates is flat, Ross recovery and generalized recovery are always the same as a risk-neutral estimation. When the term structure of market interest rates is not constant across different horizons, an interest condition is necessary for Ross recovery. Using market interest rates on January 4, 2019 as an example, empirical Ross recovered probabilities are still close to risk-neutral probabilities. Previous literature omits this interest rate condition in Ross recovery. By incorporating the interest rate condition into Ross recovery, we explain the difference between the Ross Basic and generalized recovery/ Ross Stable.

In addition, we examine that the period length of transition and the specification of least squares estimation affect the recovered probabilities. A short one-period transition period in Ross recovery implies the requirement for a nonnegative root of the long-term transition matrix which is a strong extra constraint in Ross recovery estimation. Selecting a longer period of transition would fit better with the market spot state price surface all else equal.

Linear least squares representation of Ross recovery is a fast estimation. However, when there is no exact transition matrix satisfying the spot state price surface, the linear representation is not accurate in representing the term structure of Ross recovery implied interest rate. A nonlinear representation of Ross recovery solves this problem. Further research about the optimization calculation of the nonlinear representation of Ross recovery may provide a more accurate estimation of Ross recovery.

References

Audrino, F., Huitema, R., and Ludwig, M. (2021) An Empirical Implementation of the Ross Recovery Theorem as a Prediction Device. *Journal of Financial Econometrics* 19.2, pp. 291–312.

Bakshi, G., Chabi-Yo, F., and Gao, X. (2018) A Recovery that We Can Trust? Deducing and Testing the Restrictions of the Recovery Theorem. *Review of Financial Studies* 31.2, pp. 532–555.

Black, F. and Scholes, M. (1973) The Pricing of Options and Corporate Liabilities. *Journal of Political Economy* 81.3, pp. 637–654.

Borovička, J., Hansen, L. P., and Scheinkman, J. A. (2016) Misspecified Recovery. *Journal of Finance* 71.6, pp. 2493–2544.

Breeden, D. T. and Litzenberger, R. H. (1978) Prices of State-Contingent Claims Implicit in Option Prices. *Journal of Business* 51.4, pp. 621–651.

Dillschneider, Y. and Maurer, R. (2019) Functional Ross recovery: Theoretical results and empirical tests. *Journal of Economic Dynamics and Control* 108, p. 103750.

Figlewski, S. (2010) Estimating the Implied Risk-Neutral Density for the US Market Portfolio. *Volatility and Time Series Econometrics*. Oxford: Oxford University Press.

Figlewski, S. (2018) Risk-Neutral Densities: A Review. *Annual Review of Financial Economics* 10.1, pp. 329–359.

Golec, J., Xu, Y., and Yao, X. (2022) Empirical Ross recovery without discretization. *Financial review* 57.2, pp. 345–367.

Jackwerth, J. C. (2004) *Option-implied Risk-neutral Distributions and Risk Aversion*. Charlotteville: Research Foundation of AIMR.

Jackwerth, J. C. and Menner, M. (2020) Does the Ross recovery theorem work empirically? *Journal of Financial Economics* 137.3, pp. 723–739.

Jensen, C. S., Lando, D., and Pedersen, L. H. (2019) Generalized recovery. *Journal of Financial Economics* 133.1, pp. 154–174.

Martin, I. W. R. and Ross, S. A. (2019) Notes on the yield curve. *Journal of Financial Economics* 134.3, pp. 689–702.

Qin, L., Linetsky, V., and Nie, Y. (2018) Long Forward Probabilities, Recovery, and the Term Structure of Bond Risk Premiums. *Review of Financial Studies* 31.12, pp. 4863–4883.

Ross, S. (2015) The Recovery Theorem. *Journal of Finance* 70.2, pp. 615–648.

Tam, B.-S. and Huang, P.-R. (2016) Nonnegative square roots of matrices. *Special Issue: Legacy of Hans Schneider* 498, pp. 404–440.

Walden, J. (2017) Recovery with Unbounded Diffusion Processes. *Review of Finance* 21.4, pp. 1403–1444.

Table 1: A comparison between different approaches to Ross recovery.
This table compares different approaches to Ross recovery approaches in this study. ”Yes” (”No”) indicates whether this assumption/condition is (not) included in the approach. ”Na” presents that this assumption/condition is not related in the approach. Ross assumption 1 is the time-homogeneous transition matrix assumption.

	Ross Basic	Ross Stable	Ross Stable Linear	Ross Spot Rate	Ross Power	Ross Root
Ross assumption 1	Yes	**No**	**No**	Yes	Yes	Yes
Linear least squares representation	Yes	**No**	Yes	Yes	**No**	Yes
Interest rate condition	No	Na	Na	Yes	Yes	No
Transition period (days)	20	Na	Na	20	20	**2**

Table 2: Estimation Accuracy.
This table shows the Sum of Squared Errors (SSE) of different Ross recovery approaches with the S&P 500 weekly option data on January 4, 2019. SSE of Ross Basic, Ross Spot Rate, Ross Power, and Ross Root show the difference between Ross fitted spot state price surface and the market spot state price surface. SSE of Ross Stable and Ross Stable Linear show the difference between the sum of the recovered probability and 100%.

	SSE
Ross Basic	2.64e-02
Ross Spot Rate	3.14e-02
Ross Power	3.14e-02
Ross Root	6.74e-02
Ross Stable	2.40e-30
Ross Stable Linear	2.40e-30

Table 3: Moments.
This table shows the moments of fitted and recovered probability distributions from different Ross recovery estimations with the S&P 500 weekly option data on January 4, 2019. In panel A, mean and standard deviation are annualized.

Panel A: One Period					
		Mean (%)	Std (%)	Skewness	Kurtosis
Market Risk-neutral probability		0.85	20.36	-0.95	4.37
Ross Basic	Fitted	1.00	20.16	-0.87	4.27
	Recovered	-1.53	27.14	-0.64	3.80
Ross Spot Rate	Fitted	0.87	20.37	-0.96	4.40
	Recovered	0.85	20.39	-0.96	4.41
Ross Power	Fitted	1.17	19.97	-0.85	4.30
	Recovered	1.06	20.02	-0.84	4.30
Ross Root	Fitted	0.92	19.87	-0.82	4.18
	Recovered	-19.32	31.55	-0.08	2.92
Ross Stable		1.17	19.97	-0.85	4.30
Ross Stable Linear		1.06	20.02	-0.84	4.30
Panel B: Long Term					
		Mean (%)	Std (%)	Skewness	Kurtosis
Ross Basic	Fitted	1.23	22.05	-0.32	2.01
	Recovered	9.14	26.00	-0.85	2.53
Ross Spot Rate	Fitted	0.93	21.08	-0.37	2.12
	Recovered	0.83	21.15	-0.37	2.14
Ross Power	Fitted	0.93	21.08	-0.37	2.12
	Recovered	0.83	21.15	-0.37	2.14
Ross Root	Fitted	1.74	19.83	-0.48	2.78
	Recovered	0.83	31.03	-0.49	2.15

Figure 4.1: RND surface of SPXW options on January 4, 2019.
Panel A shows the risk-neutral distribution surface. Panel B selects four RNDs from the surface.

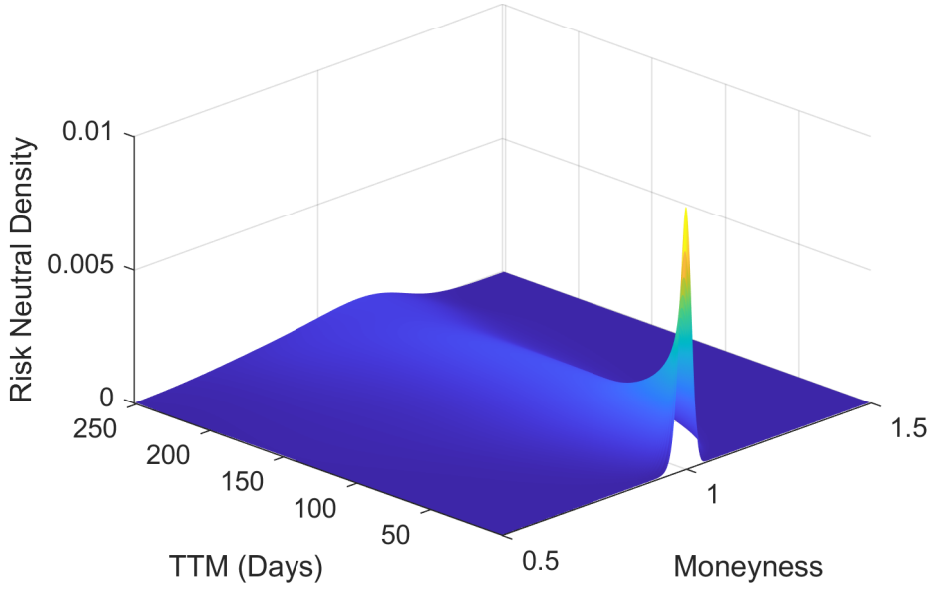

Panel A: RND Surface.

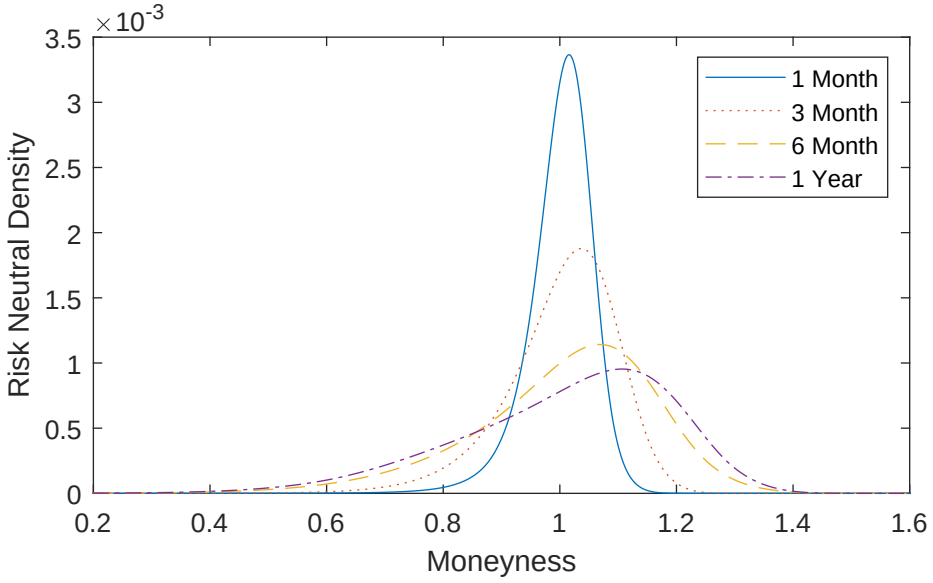

Panel B: Term Structure of RNDs

Figure 4.2: A comparison between RND implied interest rates and the market interest rates. Market interest rates are based on the US zero-coupon yield. Fitted interest rates are interpolated interest rates. RND implied interest rates are the expected returns of the RND plus the corresponding dividend yields for each horizon. Sample date is on January 4, 2019.

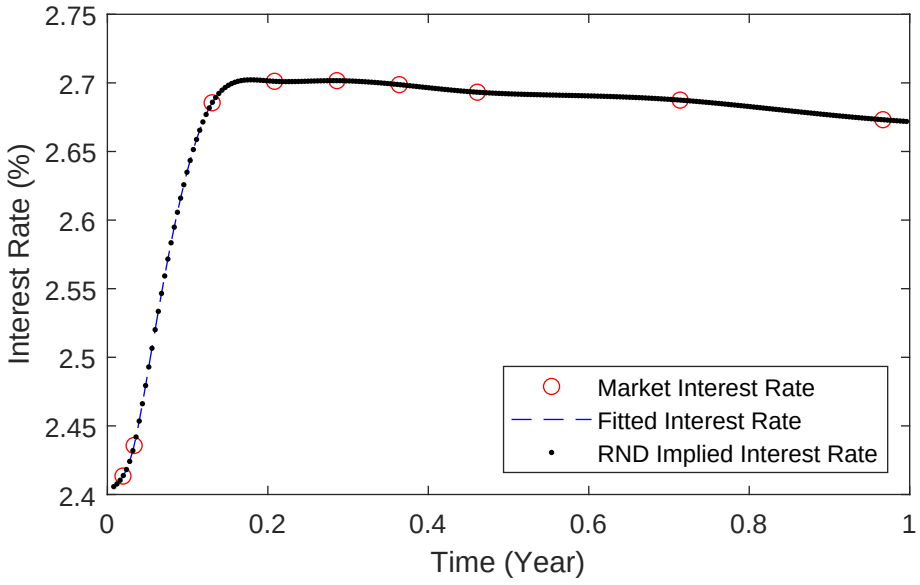

Figure 4.3: Ross Basic Transition Matrix.
This figure shows the one-period state price transition matrix based on Ross Basic with SPXW options on January 4, 2019. Panel B focuses on the states with moneyness from 0.4 to 1.4. State i is the state at time t. State j is the state at time $t+1$.

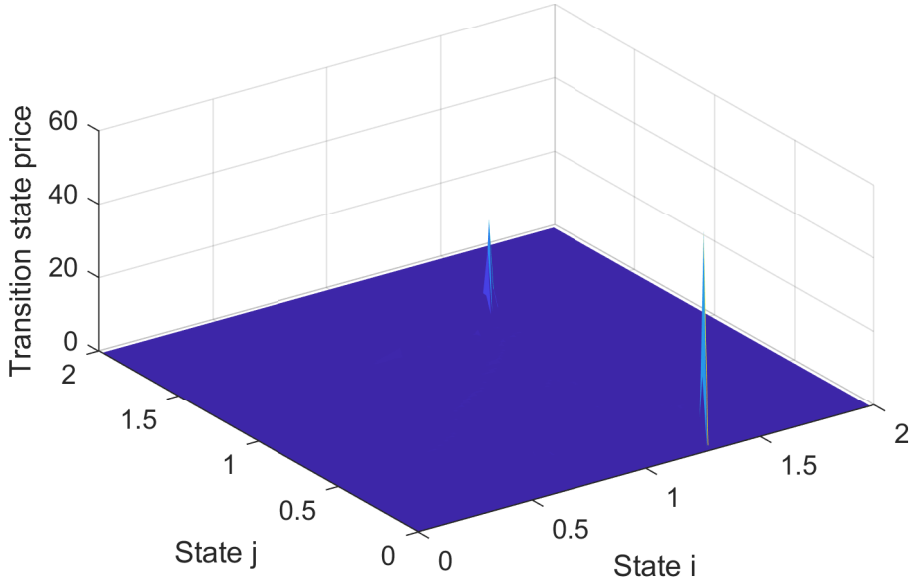

Panel A: Transition Matrix

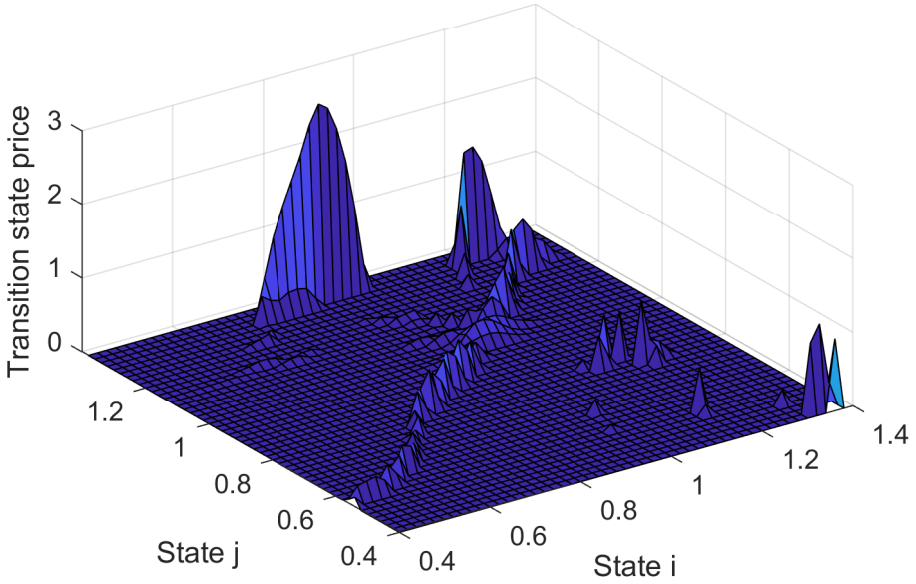

Panel B: Transition Matrix Center

Figure 4.4: Recovered Ross Basic Probability Distributions.
This figure shows fitted risk-neutral (RN) probabilities and recovered probabilities based on Ross Basic with SPXW options on January 4, 2019. Fitted RN Probabilities (One Period) are calculated with the market spot state prices at time $t-1$ and the transition matrix. Fitted RN Probabilities (Multi Periods) are calculated with the market spot state prices at t_0 and the n^{th} power of the transition matrix.

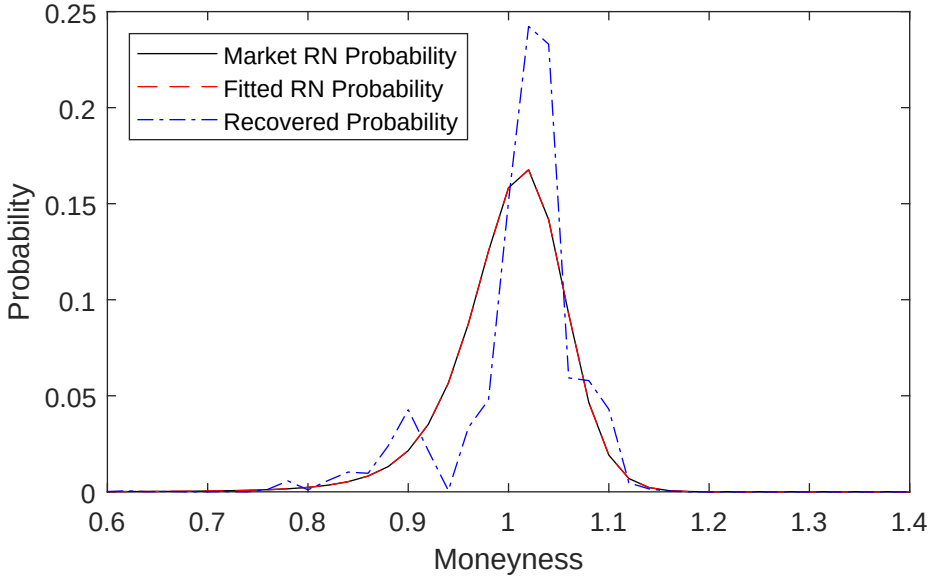

Panel A: 20-day

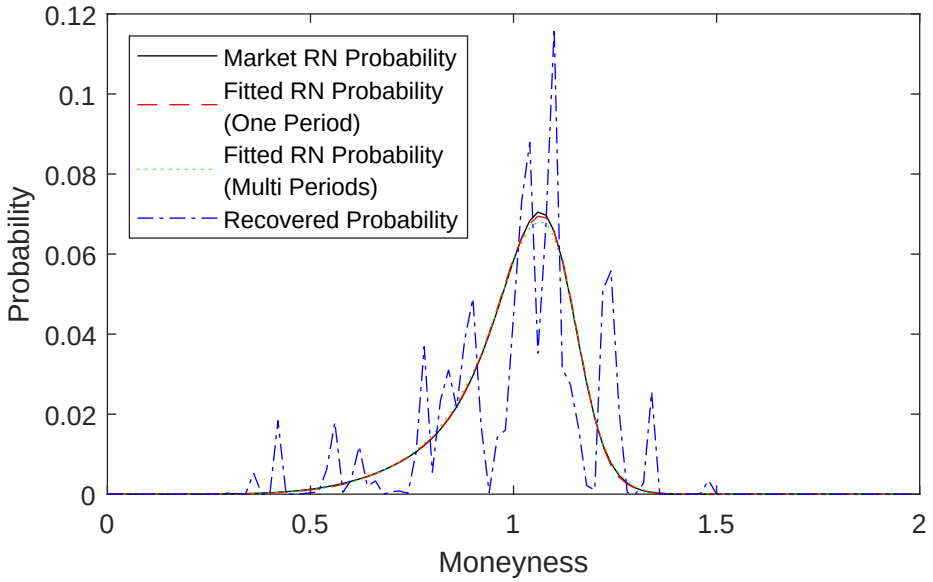

Panel B: 120-day

Figure 4.5: Ross Basic Implied Interest Rates.
This figure shows the implied interest rates based on Ross Basic with SPXW options on January 4, 2019. Panel A shows the one-period state interest rates. In Panel B, Recovery implied spot rates (One Period) are calculated with the market spot state prices at time $t-1$ and the transition matrix. Recovery implied spot rates (Multi Periods) are calculated with the market spot state prices at t_0 and the n^{th} power of the transition matrix.

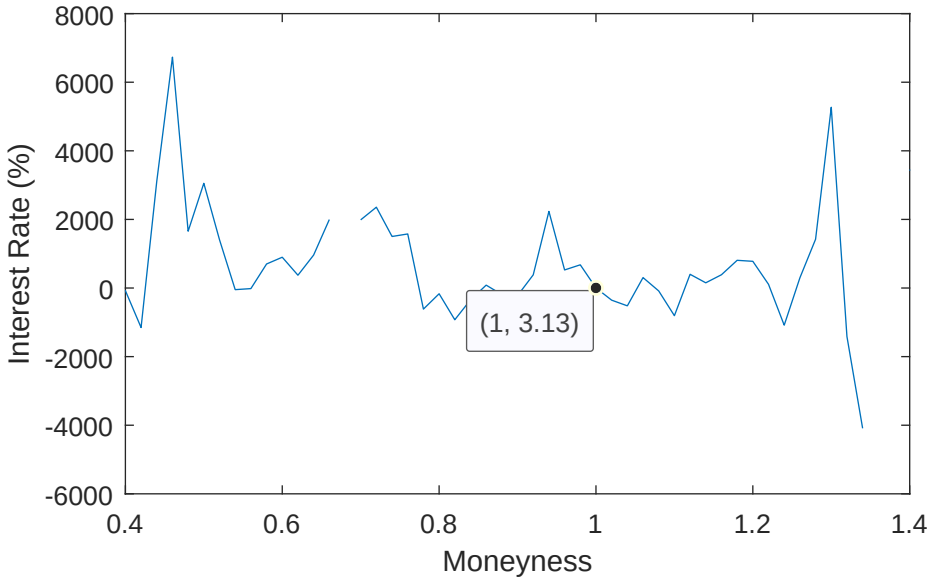

Panel A: State Interest Rate

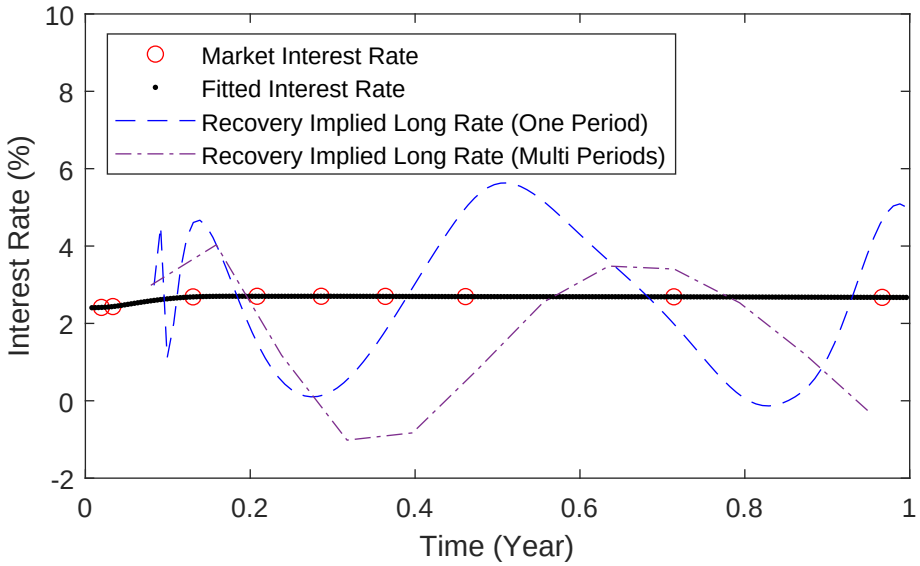

Panel B: Spot rate Curve

Figure 4.6: Recovered Ross Stable Probability Distributions.
This figure shows market risk-neutral (RN) probabilities and recovered probabilities based on Ross Stable with SPXW options on January 4, 2019.

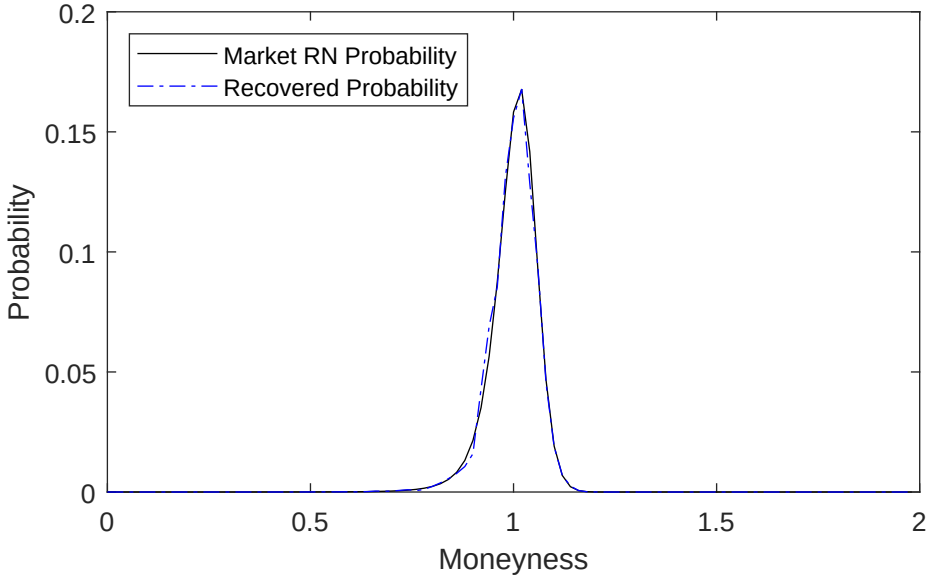

Panel A: 20-day

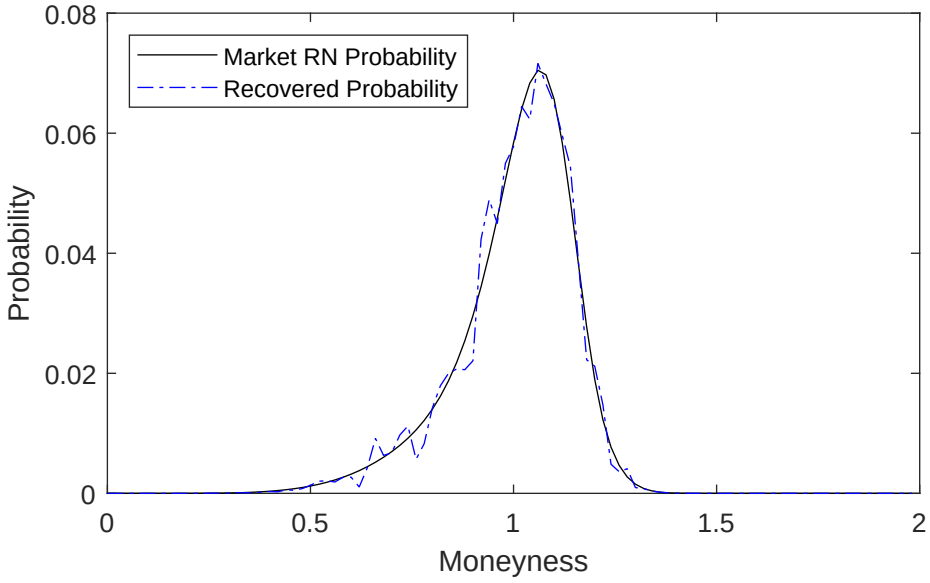

Panel B: 120-day

Figure 4.7: The Linear Approximation of Time Discount Factor. This figure shows the linear approximation of the utility discount factor as $\alpha_t + \beta_t \delta$ and the original utility discount factor δ^t based on Ross Stable Linear with SPXW options on January 4, 2019.

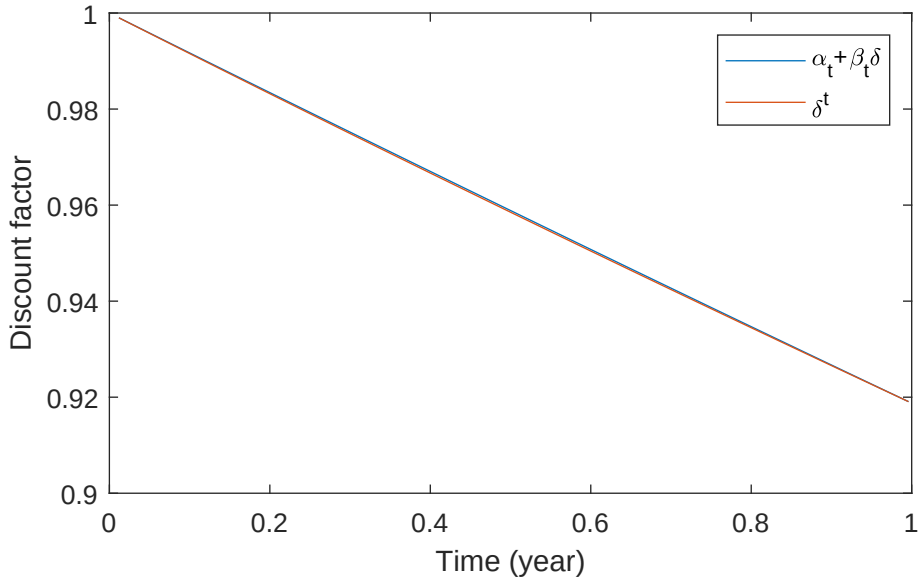

Figure 4.8: Recovered Ross Stable Linear Probability Distributions.
This figure shows market risk-neutral (RN) probabilities and recovered probabilities based on Ross Stable Linear with SPXW options on January 4, 2019.

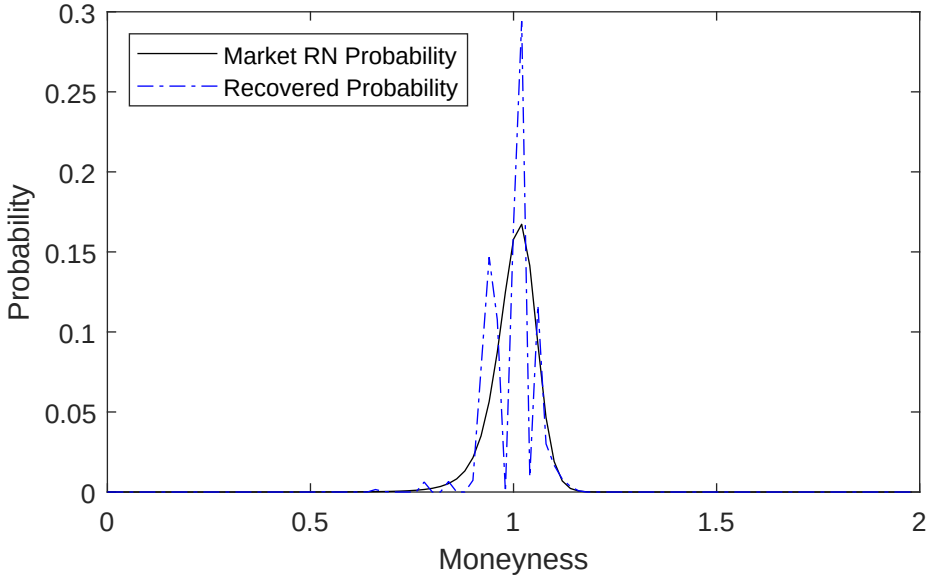

Panel A: 20-day

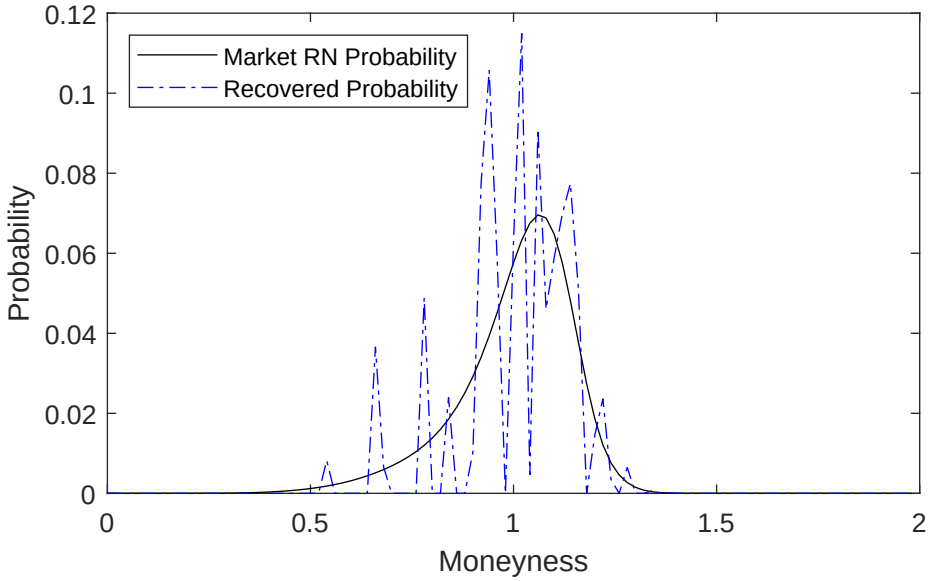

Panel B: 120-day

Figure 4.9: Ross Spot Rate Transition Matrix.
This figure shows the one-period state price transition matrix based on Ross Spot Rate with SPXW options on January 4, 2019. Panel B focuses on the states with moneyness from 0.4 to 1.4. State i is the state at time t. State j is the state at time $t+1$.

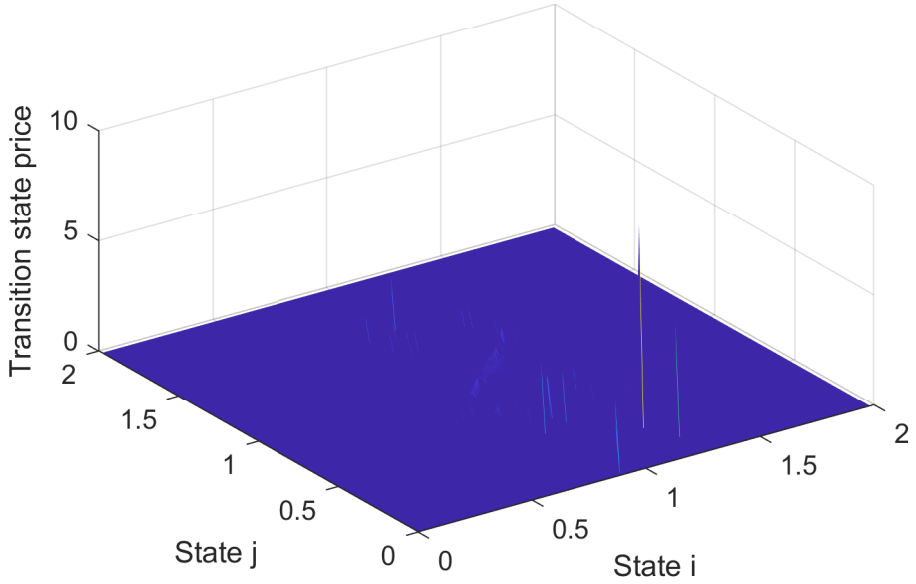

Panel A: Transition Matrix

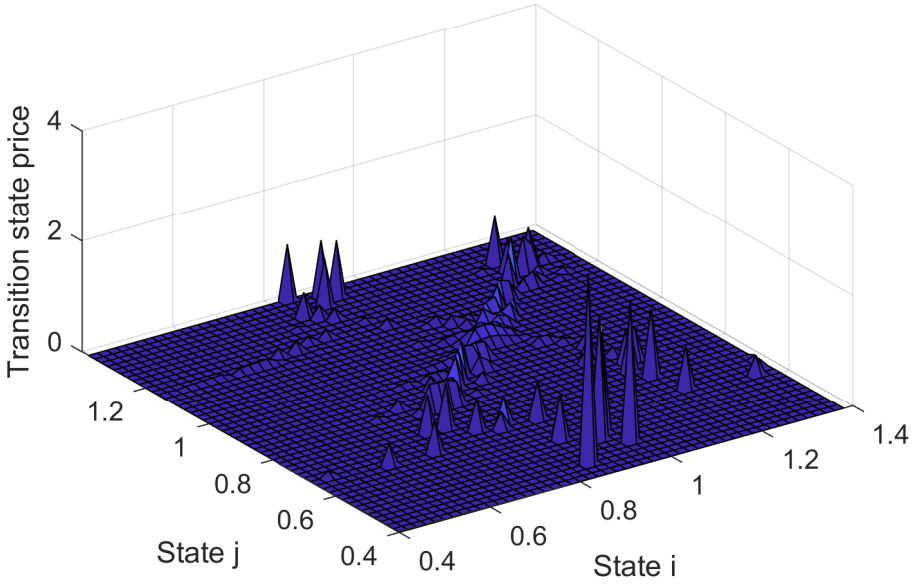

Panel B: Transition Matrix Center

Figure 4.10: Recovered Ross Spot Rate Probability Distributions.
This figure shows fitted risk-neutral (RN) probabilities and recovered probabilities based on Ross Spot Rate with SPXW options on January 4, 2019. Fitted RN Probabilities (One Period) are calculated with the market spot state prices at time $t-1$ and the transition matrix. Fitted RN Probabilities (Multi Periods) are calculated with the market spot state prices at t_0 and the n^{th} power of the transition matrix.

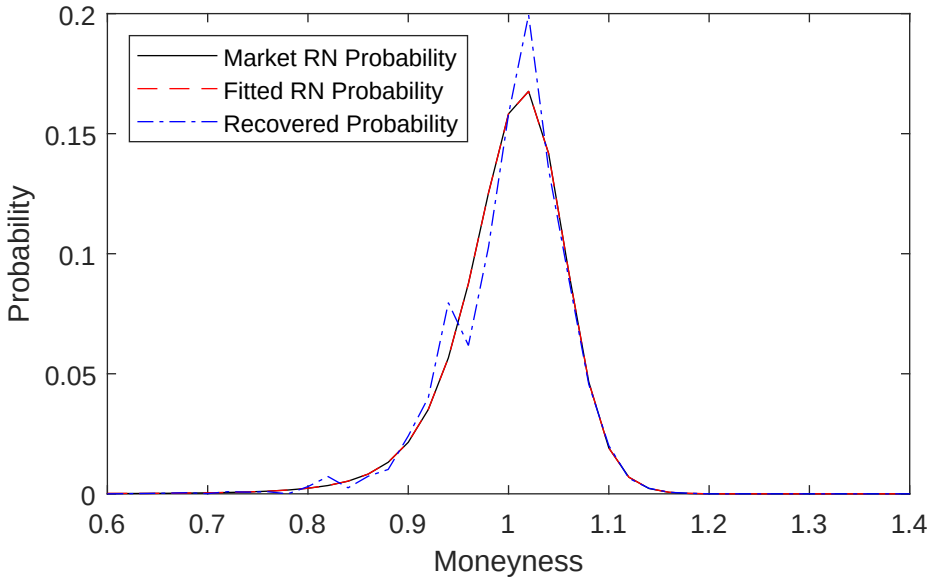

Panel A: 20-day

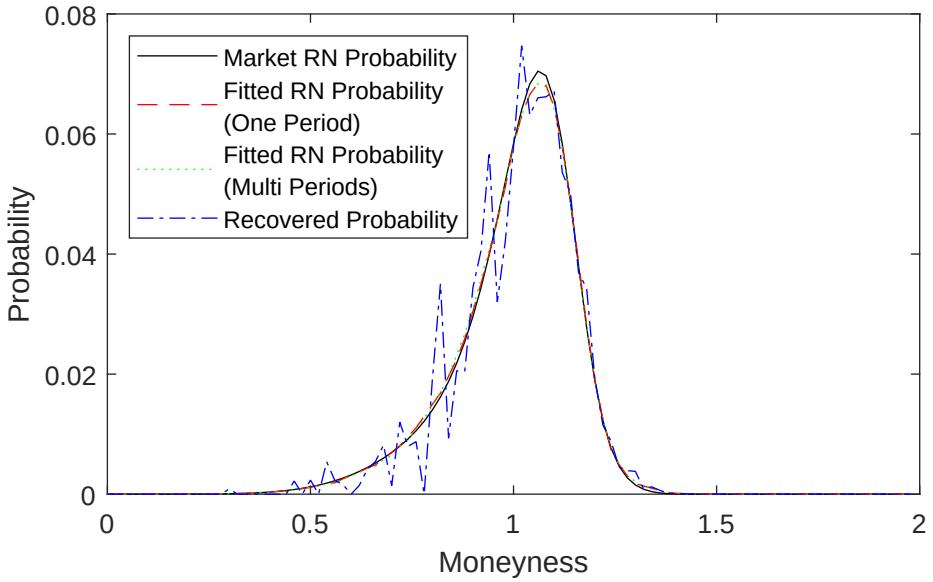

Panel B: 120-day

Figure 4.11: Ross Spot Rate Implied Interest Rates.
This figure shows the implied interest rates based on Ross Spot Rate with SPXW options on January 4, 2019. Panel A shows the one-period state interest rates. In Panel B, Recovery implied spot rates (One Period) are calculated with the market spot state prices at time $t-1$ and the transition matrix. Recovery implied spot rates (Multi Periods) are calculated with the market spot state prices at t_0 and the n^{th} power of the transition matrix.

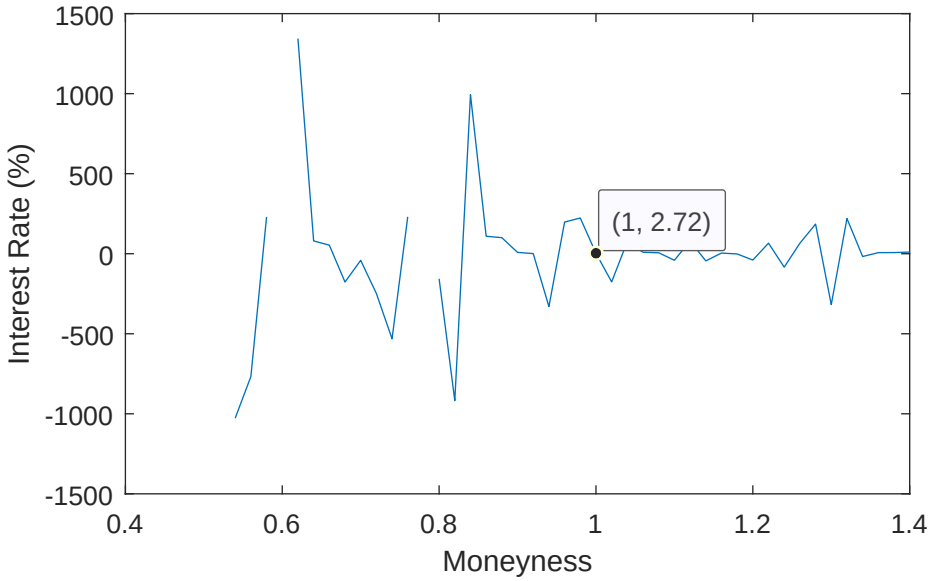

Panel A: State Interest Rate.

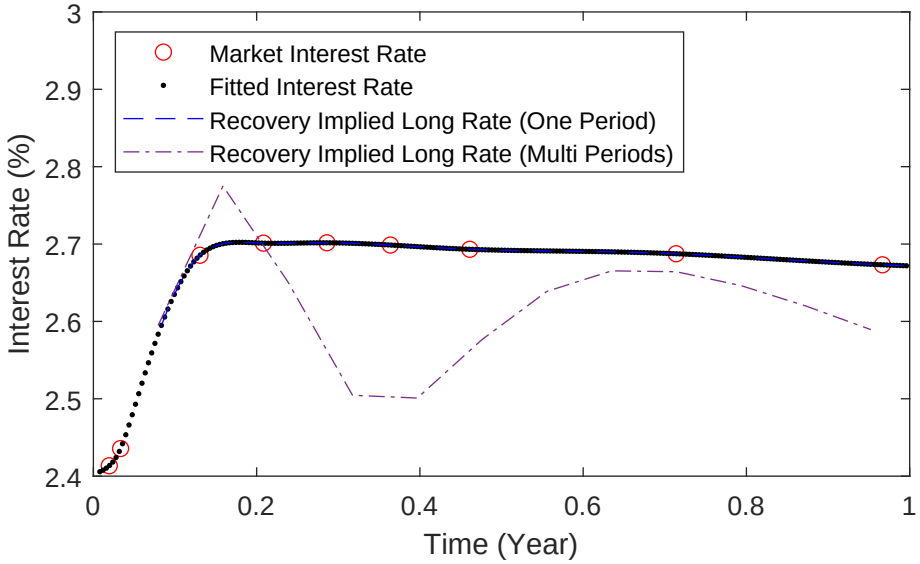

Panel B: Spot rate Curve

Figure 4.12: Ross Power Transition Matrix.
This figure shows the one-period state price transition matrix based on Ross Power with SPXW options on January 4, 2019.

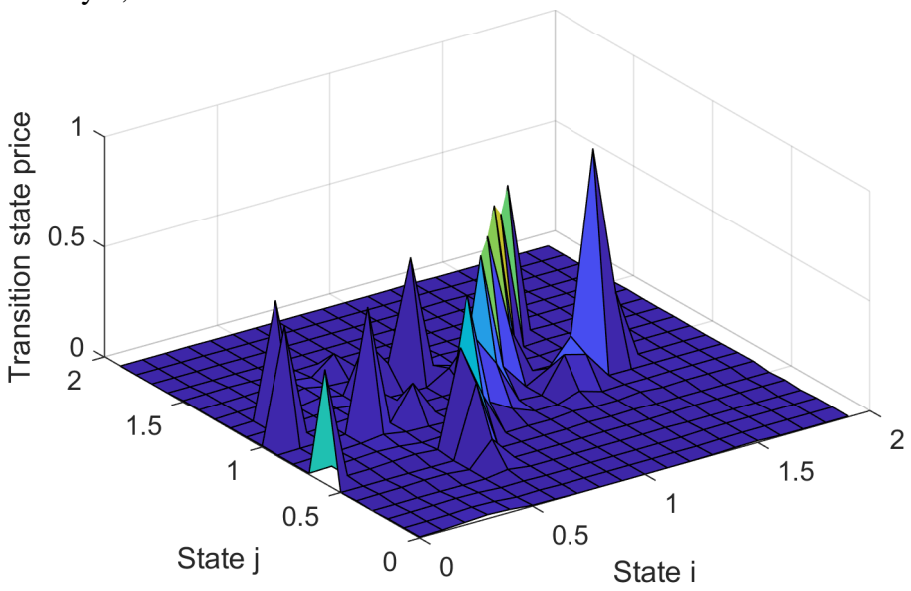

Figure 4.13: Recovered Ross Power Probability Distributions.
This figure shows fitted risk-neutral (RN) probabilities and recovered probabilities based on Ross Power with SPXW options on January 4, 2019. Fitted RN Probabilities (One Period) are calculated with the market spot state prices at time $t-1$ and the transition matrix. Fitted RN Probabilities (Multi Periods) are calculated with the market spot state prices at t_0 and the n^{th} power of the transition matrix.

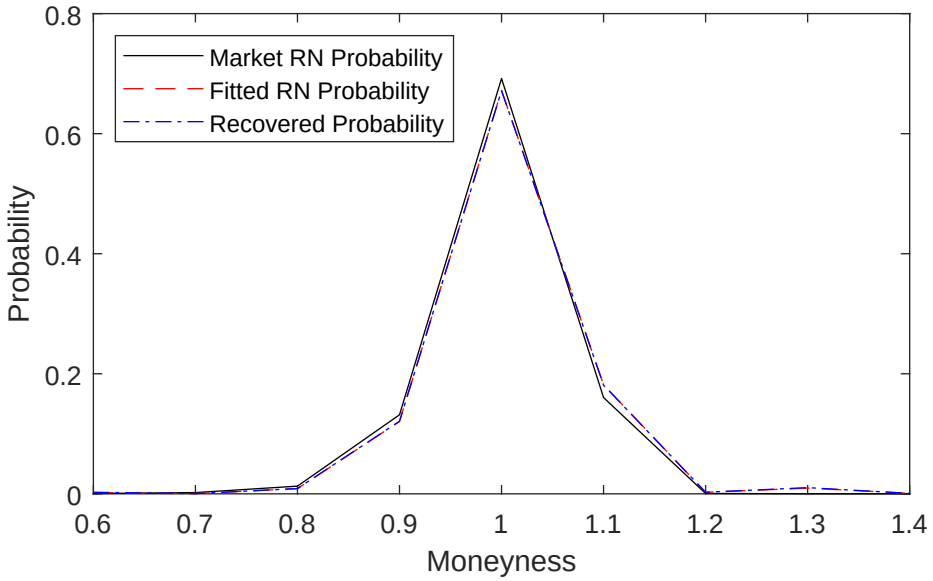

Panel A: 20-day

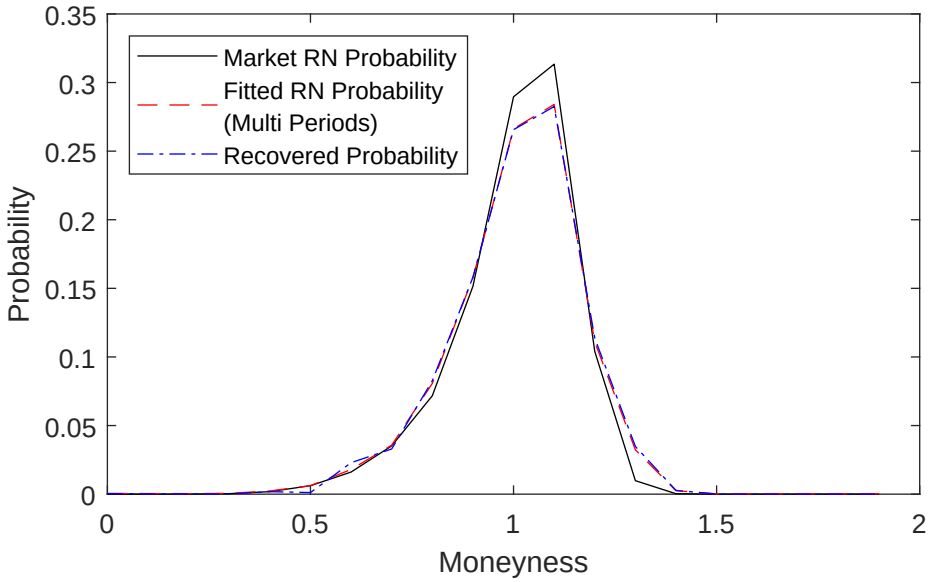

Panel B: 120-day

Figure 4.14: Ross Power Implied Interest Rate.
This figure shows the implied interest rate based on Ross Power with SPXW options on January 4, 2019. Panel A shows the one-period state interest rates. In Panel B, Recovery implied spot rates (One Period) are calculated with the market spot state prices at time $t-1$ and the transition matrix. Recovery implied spot rates (Multi Periods) are calculated with the market spot state prices at t_0 and the n^{th} power of the transition matrix.

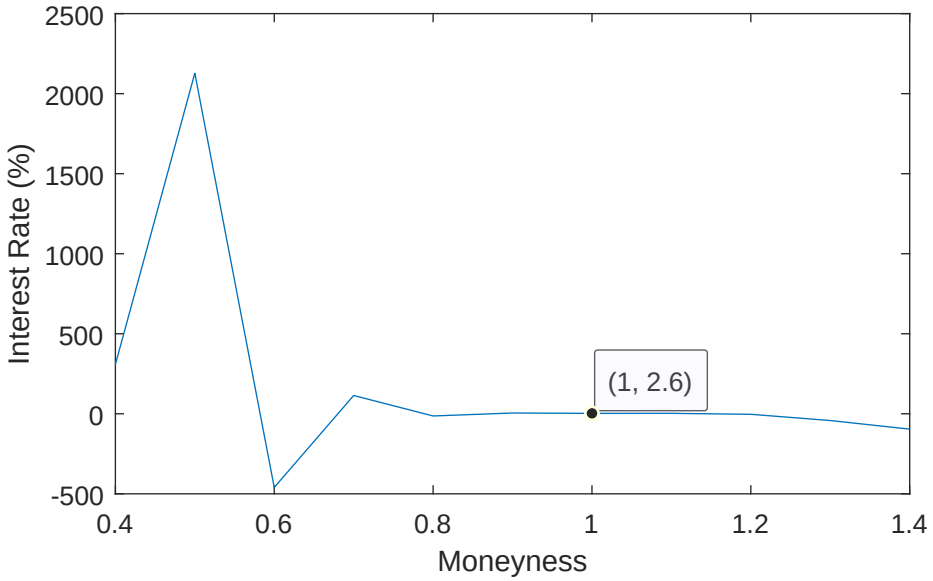

Panel A: State Interest Rate

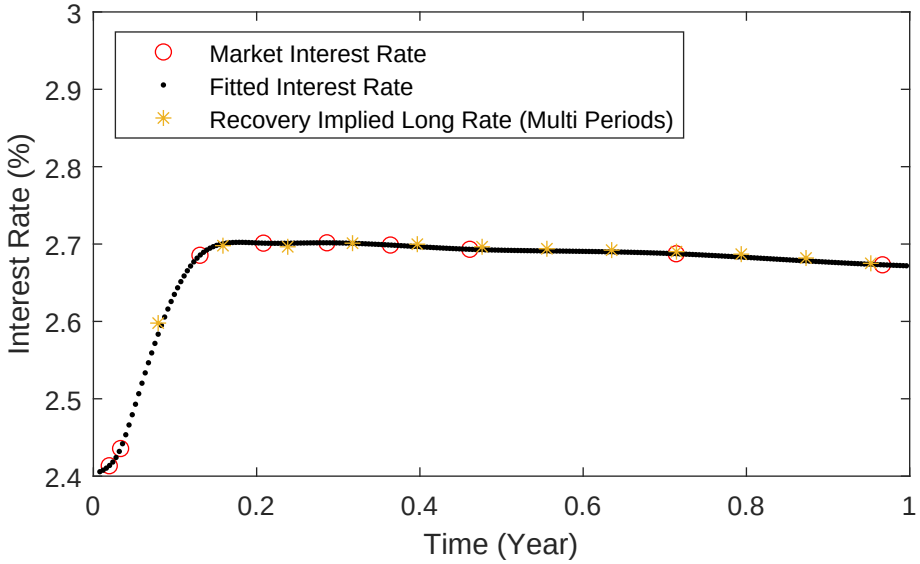

Panel B: Spot Rate Curve

Figure 4.15: Ross Root Transition Matrix.
This figure shows the one-period state price transition matrix based on Ross Basic with SPXW options on January 4, 2019. Panel B focuses on the states with moneyness from 0.4 to 1.4. State i is the state at time t. State j is the state at time $t+1$.

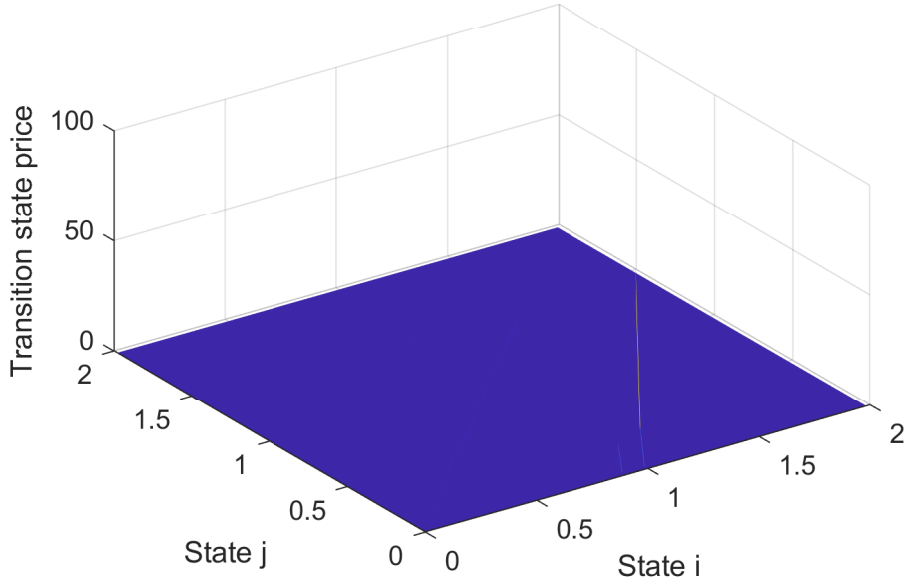

Panel A: Transition Matrix

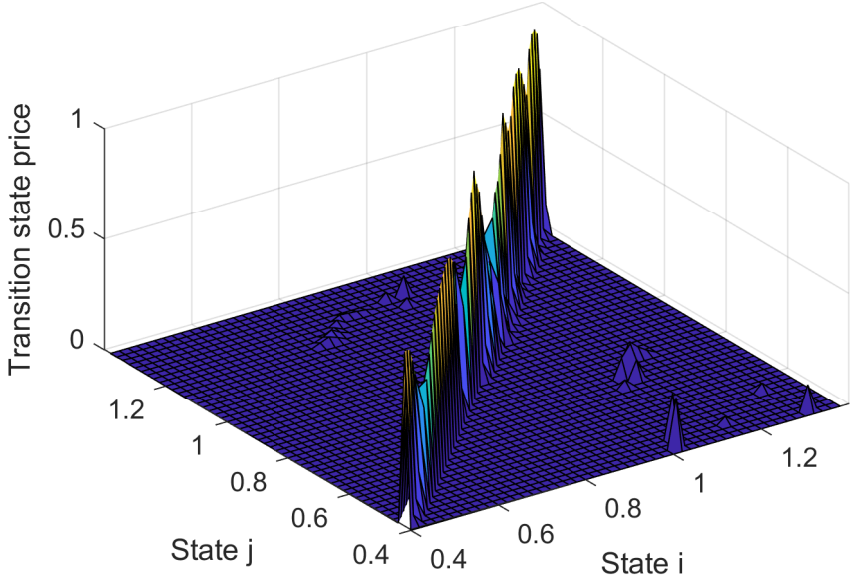

Panel B: Transition Matrix Center

Figure 4.16: Recovered Ross Root Probability Distributions.
This figure shows fitted risk-neutral (RN) probabilities and recovered probabilities based on Ross Root with SPXW options on January 4, 2019. Fitted RN Probabilities (One Period) are calculated with the market spot state prices at time $t-1$ and the transition matrix. Fitted RN Probabilities (Multi Periods) are calculated with the market spot state prices at t_0 and the n^{th} power of the transition matrix.

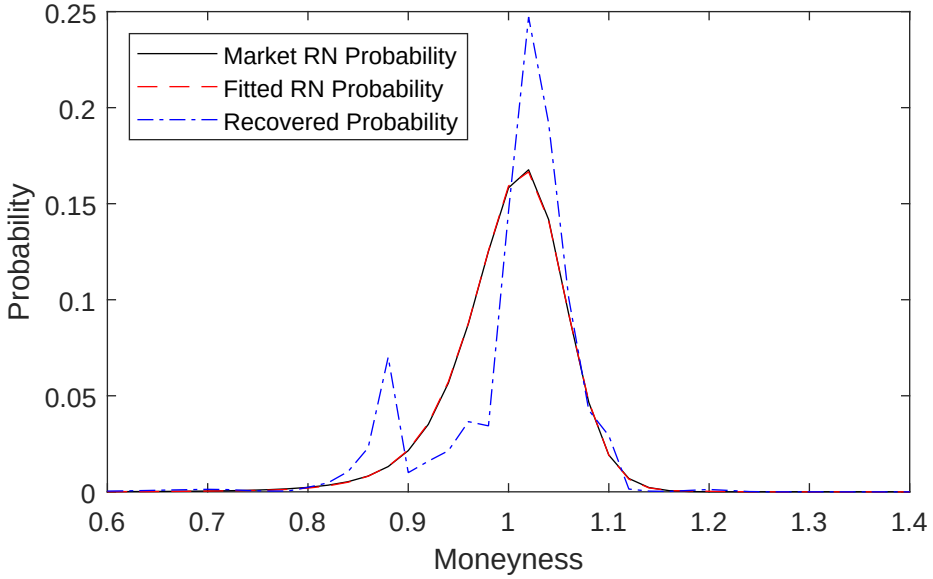

Panel A: 20-day

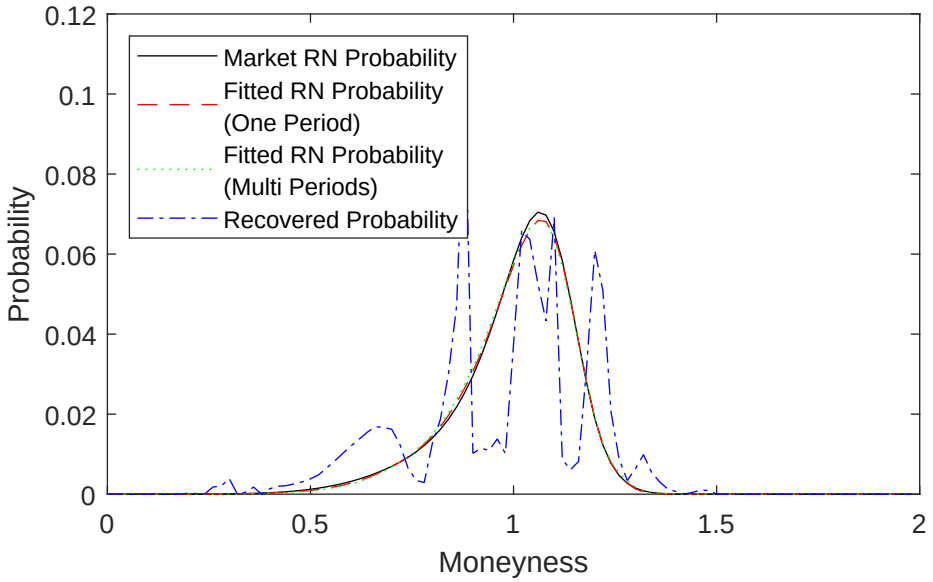

Panel B: 120-day

Figure 4.17: Ross Root Implied Interest Rates.
This figure shows the implied interest rates based on Ross Root with SPXW options on January 4, 2019. Panel A shows the one-period state interest rates. In Panel B, Recovery implied spot rates (One Period) are calculated with the market spot state prices at time $t-1$ and the transition matrix. Recovery implied spot rates (Multi Periods) are calculated with the market spot state prices at t_0 and the n^{th} power of the transition matrix.

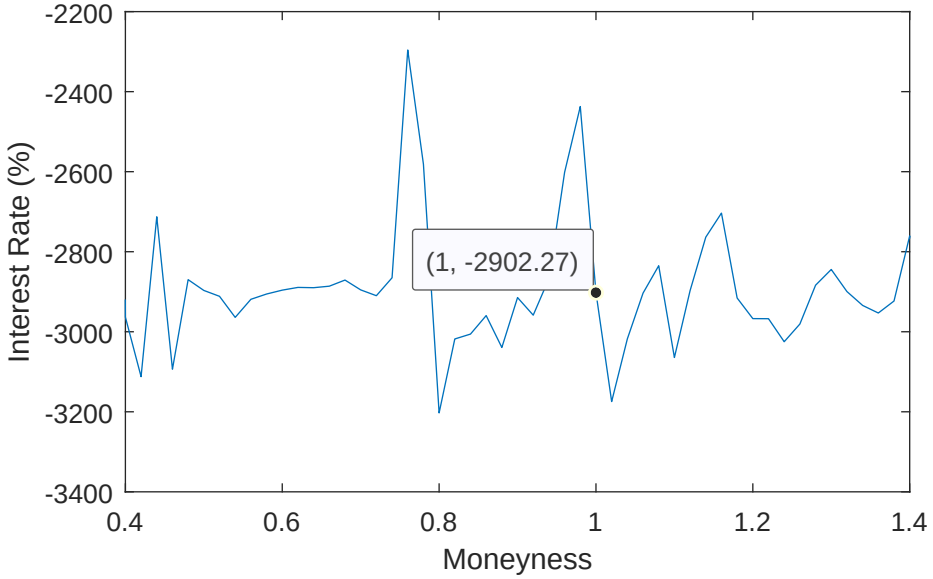

Panel A: State Interest Rate

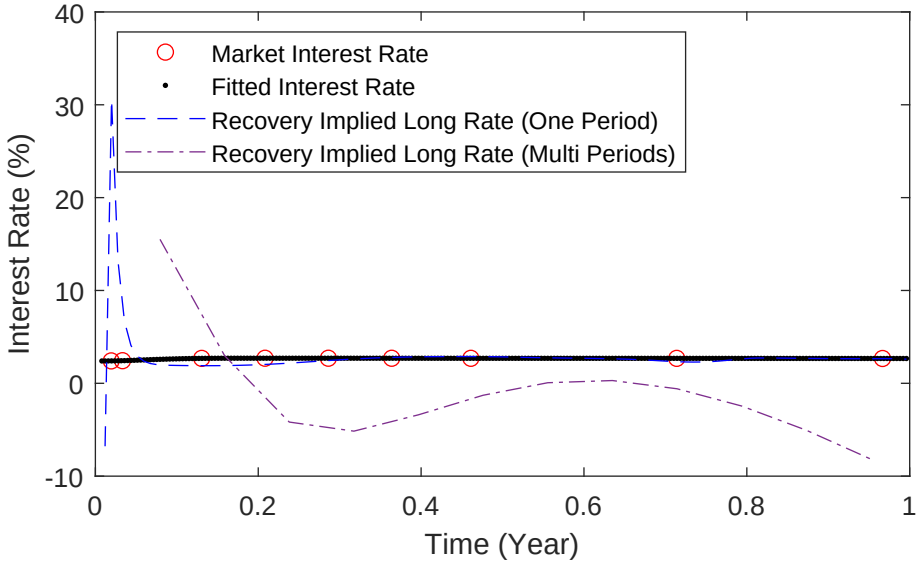

Panel B: Spot rate Curve

Figure 4.18: Stochastic Discount Factors.
This figure compares the inverse of stochastic discount factor $m^{-1} = z_j/(z_0\delta)$. The horizontal line is the stochastic discount factor of a constant one.

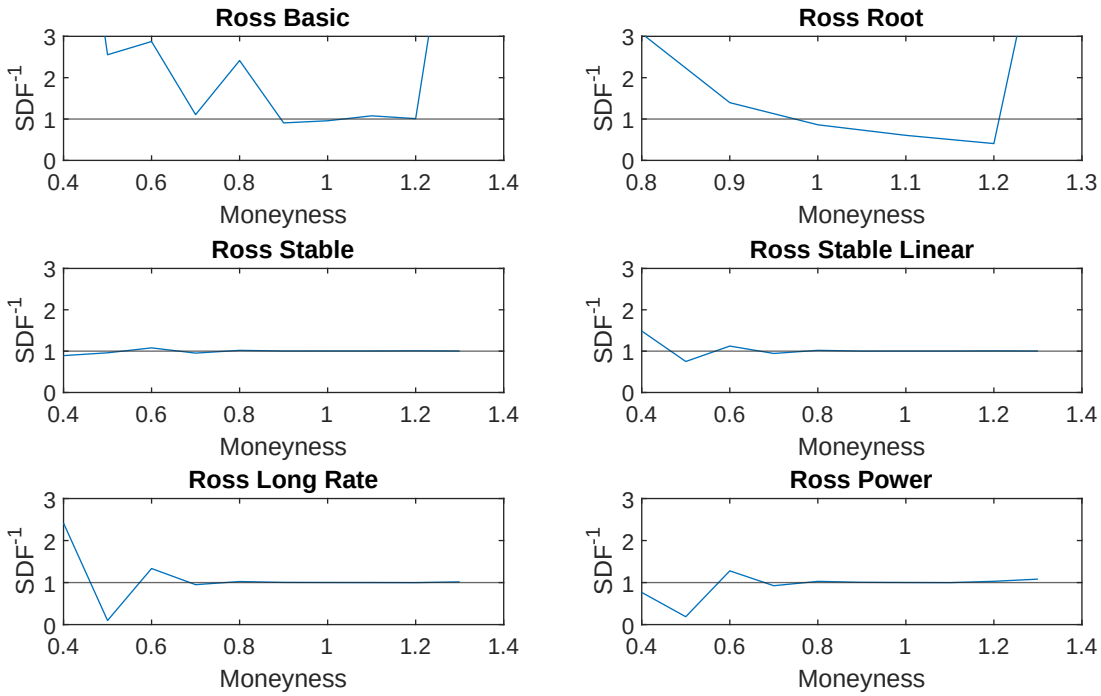

Figure 4.19: Long-Term Probability Distributions.
This figure compares the long-term (10 years) probability distributions from different Ross recovery approaches. The dash lines are fitted risk-neutral probability distributions. The solid lines are recovered probability distributions.

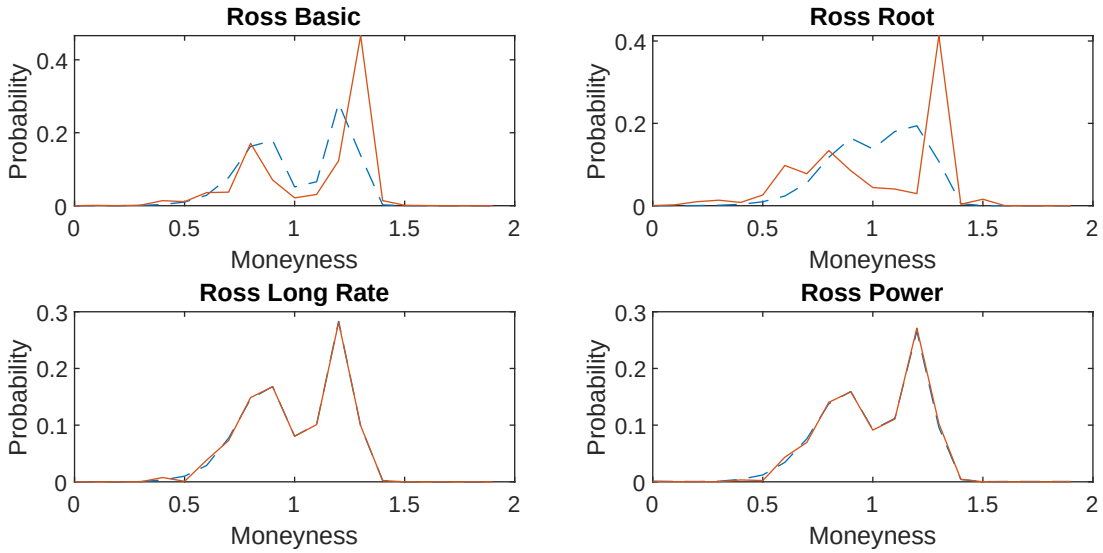

Appendix: Least Squares Estimation for Ross recovery

This section explicitly provides the standard $C \cdot x - d$ form linear equation system for Ross recoveryn. In a standard $C \cdot x - d$ form linear equation system, x is a column vector with n unknown variables, C is a matrix with n columns, d is a column vector with the same length as the rows of matrix C. The MATLAB function $lsqnonneg$ provides a fast and reliable solution to a Standard $C \cdot x - d$ form linear equation system.

Least Squares Estimation for Ross Basic

Given the market spot state price surfaces $\mathbf{\Pi}_a = [\Pi'_{a1}, ..., \Pi'_{ai}, ..., \Pi'_{aT}]'$, where Π_{ai} is the row vector in $\mathbf{\Pi}_a$, $\mathbf{\Pi}_b = [\Pi'_{b1}, ..., \Pi'_{bi}, ..., \Pi'_{bT}]'$, where Π_{bi} is the row vector in $\mathbf{\Pi}_b$, and the state price transition matrix $\boldsymbol{A} = [A_1, A_2, ..., A_N]$, where A_j is the column vector in the transition matrix. A row vector with all zero entries $\mathbf{0}_N = [0, ..., 0]_N$ has the same length as the number of states N in transition matrix A. The original matrix equation $\mathbf{\Pi}_b = \mathbf{\Pi}_a \times \boldsymbol{A}$ is equivalent to a new equation system as

$$\begin{bmatrix} C_1 \\ C_2 \\ \vdots \\ C_i \\ \vdots \\ C_T \end{bmatrix} \times \begin{bmatrix} A_1 \\ A_2 \\ \vdots \\ A_j \\ \vdots \\ A_{N-1} \\ A_N \end{bmatrix} = \begin{bmatrix} \Pi'_{b1} \\ \Pi'_{b2} \\ \vdots \\ \Pi'_{bi} \\ \vdots \\ \Pi'_{bT} \end{bmatrix}, \text{where} \quad C_i = \begin{bmatrix} \Pi_{ai} & \mathbf{0}_N & ... & \mathbf{0}_N & ... & \mathbf{0}_N \\ \mathbf{0}_N & \Pi_{ai} & ... & \mathbf{0}_N & ... & \mathbf{0}_N \\ \vdots & ... & ... & ... & ... & \vdots \\ \mathbf{0}_N & \mathbf{0}_N & ... & \Pi_{ai} & ... & \mathbf{0}_N \\ \vdots & ... & ... & ... & ... & \vdots \\ \mathbf{0}_N & \mathbf{0}_N & ... & \mathbf{0}_N & ... & \Pi_{ai} \end{bmatrix} \tag{A.4.1}$$

such that the new equation system follows the standard $C \cdot x - d$ form.

Similarly, Ross Root also has a standard $C \cdot x - d$ form by replacing the transition period in Ross Basic to a shorter period.

Least Squares Estimation for Ross Spot Rate

Ross Spot Rate has an additional interest rate condition in comparison to Ross Basic estimation. The sum of fitted spot state prices equals the sum of market spot state prices for any horizons. With a unit row vector $\boldsymbol{e} = [1, ..., 1]_N$, the interest rate condition is

$$\begin{bmatrix} \boldsymbol{e}C_1 \\ \boldsymbol{e}C_2 \\ \vdots \\ \boldsymbol{e}C_i \\ \vdots \\ \boldsymbol{e}C_T \end{bmatrix} \times \begin{bmatrix} A_1 \\ A_2 \\ \vdots \\ A_j \\ \vdots \\ A_{N-1} \\ A_N \end{bmatrix} = \begin{bmatrix} \sum \Pi_{b1} \\ \sum \Pi_{b2} \\ \vdots \\ \sum \Pi_{bi} \\ \vdots \\ \sum \Pi_{bT} \end{bmatrix}, \text{where} \quad C_i = \begin{bmatrix} \Pi_{ai} & \mathbf{0}_N & ... & \mathbf{0}_N & ... & \mathbf{0}_N \\ \mathbf{0}_N & \Pi_{ai} & ... & \mathbf{0}_N & ... & \mathbf{0}_N \\ \vdots & ... & ... & ... & ... & \vdots \\ \mathbf{0}_N & \mathbf{0}_N & ... & \Pi_{ai} & ... & \mathbf{0}_N \\ \vdots & ... & ... & ... & ... & \vdots \\ \mathbf{0}_N & \mathbf{0}_N & ... & \mathbf{0}_N & ... & \Pi_{ai} \end{bmatrix} \tag{A.4.2}$$

This interest rate condition is applied to Ross Basic estimation,

$$\begin{bmatrix} C_1 \\ C_2 \\ \vdots \\ C_i \\ \vdots \\ C_T \\ \omega\boldsymbol{e}C_1 \\ \omega\boldsymbol{e}C_2 \\ \vdots \\ \omega\boldsymbol{e}C_i \\ \vdots \\ \omega\boldsymbol{e}C_T \end{bmatrix} \times \begin{bmatrix} A_1 \\ A_2 \\ \vdots \\ A_j \\ \vdots \\ A_{N-1} \\ A_N \end{bmatrix} = \begin{bmatrix} \Pi'_{b1} \\ \Pi'_{b2} \\ \vdots \\ \Pi'_{bi} \\ \vdots \\ \Pi'_{bT} \\ \omega \sum \Pi_{b1} \\ \omega \sum \Pi_{b2} \\ \vdots \\ \omega \sum \Pi_{bi} \\ \vdots \\ \omega \sum \Pi_{bT} \end{bmatrix} whereC_i = \begin{bmatrix} \Pi_{ai} & \mathbf{0}_N & ... & \mathbf{0}_N & ... & \mathbf{0}_N \\ \mathbf{0}_N & \Pi_{ai} & ... & \mathbf{0}_N & ... & \mathbf{0}_N \\ \vdots & ... & ... & ... & ... & \vdots \\ \mathbf{0}_N & \mathbf{0}_N & ... & \Pi_{ai} & ... & \mathbf{0}_N \\ \vdots & ... & ... & ... & ... & \vdots \\ \mathbf{0}_N & \mathbf{0}_N & ... & \mathbf{0}_N & ... & \Pi_{ai} \end{bmatrix} \tag{A.4.3}$$

where the weight parameter ω (ω is 100000 in this chapter to guarantee the interest rate condition is satisfied) determines the relative importance between Ross Basic and the interest rate condition. Therefore, Ross Spot Rate as (A.4.3) is a standard form $C \cdot x - d$ least square problem.

Chapter 5

Conclusions and Suggestions for Future Research

This thesis is an effort to understand the option implied information. It consists of three essays on political risk, extended trading hours, and Ross (2015) recovered probability respectively.

In the first essay, we examine the Brexit referendum that took place on 23rd June 2016. The option market can ex ante detect and quantify the political risk due to a scheduled political event. Risk-Neutral Densities estimated by the non-parametric method developed by Figlewski (2010) present bimodal distributions with a left mode indicating large potential downside movement from the Leave outcome of the Brexit referendum. The unusual bimodal Risk-Neutral Distribution is associated with an Implied Volatility curve with local concavity. Option implied event probabilities following the method by Borochin and Golec (2016) show an independent source of expected probability for the outcome of the Brexit referendum besides public media polls and betting implied odds. Based on the large swings in outcome probabilities during the counting process of the Brexit referendum, the impacts of the Brexit referendum on financial markets with both Leave and Remain outcomes are consistent with the ex ante expectations in the option markets. Besides, the option markets distinguish the differential impacts of a political event on different financial markets. The option markets show significant political risk with GBPUSD and less pronounced risk with FTSE 100. GBPUSD rates and FTSE 100 index movements after the Brexit referendum validate the ex ante expectation from the option market.

In the second essay, we compare the market quality around the introduction of extended trading hours for S&P 500 options. This essay contributes to the literature about after-hours financial markets (see Barclay and Hendershott, 2003, 2004; Chen, Yu, and Zivot, 2012; Dungey, Fakhrutdinova, and Goodhart, 2009; Jiang, Likitapiwat, and Mcinish, 2012; Tsai, 2010) by using the introduction of extended trading hours as a quasi-natural experiment. After controlling the fixed effects from other variables by using S&P 500 SPDR ETF options, we present evidence that the introduction of extended trading hours has enhanced market quality in the following regular trading hours in terms of bid-ask spreads and asymmetric information costs. Extended trading hours play an important role in determining the opening price in the option market. The opening process of S&P 500 options from 09:15 to 09:30 contributes little to the opening level of S&P 500 index options after introducing the extended trading hours. The put-call parity implied index level and the Implied Volatility at the opening of regular trading hours are close to the values at the close of extended trading hours compared to the values at the close of the previous trading day. The extended trading hours are also informative for future asset prices despite extreme illiquidity in the extended trading hours. The Implied Volatility at the end of extended trading hours provides significantly additional information for the realized volatility in the following regular trading hours in comparison to models based on information from the previous day.

In the third chapter, we present the importance of the term structure of interest rates for Ross recovered probabilities (Ross, 2015) and generalized recovery (Jensen, Lando, and Pedersen, 2019). Previous applications of Ross recovery (such as Audrino, Huitema, and Ludwig, 2021; Jackwerth and Menner, 2020; Ross, 2015) omit a interest rate condition and result in significantly different recovered probabilities. After incorporating the interest rate

condition, Ross recovered probability is identical to risk-neutral probability when the term structure of interest rate is flat and is close to risk-neutral probability when the term structure of interest rate is upward sloping with a market example. The link between risk-neutral probability and Ross recovered probability through the term structure of interest rates supports that Ross recovered probabilities are long-term risk-neutral probabilities (Borovička, Hansen, and Scheinkman, 2016) instead of physical probabilities. Besides, although Ross recovery Theorem allows a flexible shape of a pricing kernel, hidden constraints in Ross recovery, including the length of transition period and the Linear least squares representation, restrict the shape of the pricing kernel and should be noticed before any empirical conclusions.

This thesis can be further studied in different directions based on the analysis in each essay. The first essay can be easily extended to an analysis of political, or more general analysis of any risk due to scheduled polarised events. The quasi-natural experiment analysis between different options with the same underlying asset in the second essay can be applied to other market structure changes. The third essay empirically points out the limitation of Ross recovered probability. However, the time homogeneous transition matrix assumption in Ross recovery theorem may still be applied for further studies. With the help of the Markov chain, the term structure of risk-neutral distribution is connected across periods and can to applied to study the horizon effect in the option market. As Ross recovery requires only a snapshot of option prices, the time homogeneous transition matrix can be applied to high frequency data for intraday analysis.

References

Audrino, F., Huitema, R., and Ludwig, M. (2021) An Empirical Implementation of the Ross Recovery Theorem as a Prediction Device. *Journal of Financial Econometrics* 19.2, pp. 291–312.

Barclay, M. J. and Hendershott, T. (2003) Price Discovery and Trading After Hours. *Review of Financial Studies* 16.4, pp. 1041–1073.

Barclay, M. J. and Hendershott, T. (2004) Liquidity Externalities and Adverse Selection: Evidence from Trading after Hours. *Journal of Finance* 59.2, pp. 681–710.

Borochin, P. and Golec, J. (2016) Using options to measure the full value-effect of an event: Application to Obamacare. *Journal of Financial Economics* 120.1, pp. 169–193.

Borovička, J., Hansen, L. P., and Scheinkman, J. A. (2016) Misspecified Recovery. *Journal of Finance* 71.6, pp. 2493–2544.

Chen, C.-H., Yu, W.-C., and Zivot, E. (2012) Predicting stock volatility using after-hours information: Evidence from the NASDAQ actively traded stocks. *International Journal of Forecasting* 28.2, pp. 366–383.

Dungey, M., Fakhrutdinova, L., and Goodhart, C. (2009) After-hours trading in equity futures markets. *Journal of Futures Markets* 29.2, pp. 114–136.

Figlewski, S. (2010) Estimating the Implied Risk-Neutral Density for the US Market Portfolio. *Volatility and Time Series Econometrics*. Oxford: Oxford University Press.

Jackwerth, J. C. and Menner, M. (2020) Does the Ross recovery theorem work empirically? *Journal of Financial Economics* 137.3, pp. 723–739.

Jensen, C. S., Lando, D., and Pedersen, L. H. (2019) Generalized recovery. *Journal of Financial Economics* 133.1, pp. 154–174.

Jiang, C. X., Likitapiwat, T., and Mcinish, T. H. (2012) Information Content of Earnings Announcements: Evidence from After-Hours Trading. *Journal of Financial and Quantitative Analysis* 47.6, pp. 1303–1330.

Ross, S. (2015) The Recovery Theorem. *Journal of Finance* 70.2, pp. 615–648.

Tsai, I.-C. (2010) Order imbalances from after-hours trading. *Applied Financial Economics* 20.12, pp. 983–987.